

University of Southampton

*Biosynthesis of 4-methyl-5-(β -hydroxyethyl)thiazole
phosphate in *Escherichia coli**

by

Roberta Leonardi

A thesis presented for the degree of Doctor of Philosophy

School of Chemistry
University of Southampton
UK

January 2004

UNIVERSITY OF SOUTHAMPTON

ABSTRACT

FACULTY OF SCIENCE

CHEMISTRY

Doctor of Philosophy

Biosynthesis of 4-methyl-5-(β -hydroxyethyl)thiazole phosphate in *Escherichia coli*

by Roberta Leonardi

Escherichia coli assembles thiamine (vitamin B₁) by coupling 4-amino-5-hydroxymethyl-2-methylpyrimidine pyrophosphate (Hmp-PP) and 4-methyl-5-(β -hydroxyethyl)thiazole phosphate (Thz-P). These two heterocycles are independently synthesised through pathways that are currently poorly understood. At least six structural proteins, IscS, ThiI and ThiFSGH, participate in the biosynthesis of the intermediate thiazole from tyrosine, 1-deoxy-D-xylulose-5-phosphate (Dxp) and cysteine. As a prerequisite to studying the mechanism of Thz-P biosynthesis, the soluble expression of ThiH, a protein characterised by a marked tendency to form inclusion bodies, was investigated. A C-terminal hexahistidine tagged ThiH (ThiH-His) was successfully expressed in a soluble form from thiGH-His-tag and thiFSGH-His-tag bearing plasmids. Under anaerobic conditions, ThiG and ThiH-His co-purified and were shown to form a large multimeric non-covalent complex. Electron paramagnetic resonance and UV-visible spectroscopies, together with iron and sulphide analyses revealed the presence of an iron-sulphur cluster within this complex. In vitro reconstitution of thiazole synthase activity was also achieved, for the first time, by using cell-free extracts and proteins derived from adenosine-treated *E. coli* 83-1 cells. The addition of adenosine or adenine to growing cultures of *A. aerogenes*, *S. typhimurium* and *E. coli* has previously been shown to relieve thiamine's repression of its own biosynthesis and increase the expression levels of the thiamine biosynthetic enzymes. By exploiting this effect, in vitro thiazole synthase activity of cleared lysates or desalted proteins from *E. coli* 83-1 was shown to be dependent upon the addition of purified ThiGH-His complex, tyrosine (but not cysteine or Dxp) and an as yet unidentified intermediate present in the protein fraction from these cells. The activity was strongly stimulated by the addition of S-adenosylmethionine and NADPH.

List of Contents

<i>List of Figures, Schemes and Tables</i>	<i>VII</i>
<i>Acknowledgements</i>	<i>XVI</i>
<i>Abbreviations</i>	<i>XVII</i>
<i>Chapter 1. Introduction</i>	1
1.1 Thiamine and its Discovery	1
1.2. Reactivity and Biochemical Functions of Thiamine Pyrophosphate	2
1.3. Thiamine Biosynthesis	7
1.3.1. Thiamine Precursors	8
1.3.2. Gene Organization, Function and Regulation in <i>E. coli</i>	12
1.3.3. Enzymes Involved in the Thiazole Biosynthesis in <i>E. coli</i>	16
<i>Chapter 2. Expression Studies on ThiH</i>	26
2.1. Introduction	26
2.2. Results and Discussion	30
2.2.1. pRL200 and pRL220: T7 Compared with araBAD Promoter	30
2.2.2. pRL221 and pRL222: Co-expression of ThiH with GroEL/GroES and TrxA	33
2.2.3. Mutations in thiH: Assembling of pRL220*	36
2.2.4. pRL400: Co-expression of ThiH with ThiG	37
2.2.5. pRL800/820 and pRL1000/1020: Co-expression of Hexahistidine-tagged ThiH with ThiG and ThiFSG	39
2.2.6. pRL821: Co-expression of ThiGH-His with the Isc Proteins	43
2.2.7 pRL1021: Co-expression of ThiFSGH-His with the Isc Proteins	45
2.2.8. pRL1300 and pRL1500: Expression of ThiCEFSGH-His and ThiEFSGH-His.	48

2.3. Summary and Conclusions	49
-------------------------------------	-----------

<i>Chapter 3. Isolation and Initial Characterization of the ThiGH-His Complex</i>	51
3.1. Introduction	51
3.2. Results and Discussion	51
3.2.1. Aerobic Purification of ThiH from pRL400	51
3.2.2. Anaerobic Purifications of ThiGH-His	55
3.2.3. Analytical Gel Filtration Chromatography	63
3.2.4. Metal and Sulphide Analyses	68
3.2.5. Spectroscopic Properties of the Complex	70
3.2.6. <i>In Vivo</i> Activity of the ThiH-His expressed from pRL1020/BL21(DE3)	76
3.2.7. Chemical and Enzymatic Reconstitution Experiments	77
3.3. Summary and Conclusions	79

<i>Chapter 4. Expression of Thiamine Biosynthetic Enzymes and Synthesis of Thiamine Precursors</i>	81
4.1. Introduction	81
4.2. Results and Discussion	82
4.2.1. Expression of ThiI	82
4.2.2. Expression of ThiE	83
4.2.3. Expression of ThiD	85
4.2.4. Expression and Purification of ThiFS from pRL1800/BL21(DE3)	87
4.2.5. Expression and Purification of Dxs-His	91
4.2.6. Enzymatic Synthesis of 1-deoxy-D-xylulose-5-phosphate (Dxp)	92
4.2.7. Synthesis of 4-amino-5-hydroxymethyl-2-methylpyrimidine (Hmp)	93
4.2.8. Synthesis of 4-methyl-5-(β -hydroxyethyl)thiazole phosphate (Thz-P)	94
4.3. Summary and Conclusions	94

Chapter 5. In Vivo Studies on Thiamine Biosynthesis	95
5.1. Introduction	95
5.2. Results and Discussion	99
5.2.1. Effect of the Adenosine Treatment on the Production of TPP by <i>E. coli</i> 83-1	99
5.2.2. Comparison between Adenosine Treated 83-1 and pRL1020/83-1 Cells in the Presence of β-L-arabinose	103
5.2.3. De-repression Experiments on <i>E. coli</i> KG33 Cells	106
5.3. Summary and Conclusions	110
Chapter 6. In Vitro Reconstitution of the Thiazole Synthase Activity Using <i>E. coli</i> Cell-free Extracts	111
6.1. Introduction	111
6.2. Results and Discussion	112
6.2.1. <i>In Vitro</i> Assay Strategy and Conditions	112
6.2.2. Thiazole Synthase Activity in <i>E. coli</i> Cleared Cell Lysates	116
6.2.3. Comparing the Effect of the ThiGH-Enriched Protein Fraction and Purified ThiFS and ThiGH-His	118
6.2.4. Thiazole Synthase Activity Dependency on the Concentration of the Precursors	120
6.2.5. Thiazole Synthase Activity: Effect of ThiF and ThiS	124
6.2.6. Effect of the Concentration of ThiGH-His and Time Course	127
6.2.7. Preliminary Fractionation Experiments on the De-repressed pRL1020/83-1 Cleared Lysate	130
6.2.8. Thiazole Synthase Activity: Preliminary Experiments on the Effect of SAM and Reducing Agents	134
6.2.9. Proposed Mechanisms for Thz-P Biosynthesis	138
6.3. Summary and Conclusions	142

Chapter 7. Experimental Methods	144
7.1. Materials	144
7.2. Equipment	145
7.3. General Experimental Methods	146
7.4. Experimental for Chapter 2	158
7.4.1. pRL200 and pRL220: T7 Compared with araBAD Promoter	159
7.4.2. pRL221 and pRL222: Co-expression of ThiH with GroEL/GroES and TrxA	160
7.4.3. Mutations in <i>thiH</i> : Assembling of pRL220*	160
7.4.4. pRL400: Co-expression of ThiH with ThiG	161
7.4.5. pRL800/820 and pRL1000/1020: Co-expression of Hexahistidine-tagged ThiH with ThiG and ThiFSG	161
7.4.6. pRL821: Co-expression of ThiGH-His with the Isc Proteins	162
7.4.7. pRL1021: Co-expression of ThiFSGH-His with the Isc Proteins	162
7.4.8. pRL1300 and pRL1500: Expression of ThiCEFSGH-His and ThiEFSGH-His	163
7.5. Experimental for Chapter 3	165
7.5.1. Aerobic Purification of ThiH from pRL400	165
7.5.2. Anaerobic Purifications of ThiGH-His	167
7.5.3. Analytical and Preparative Gel Filtration Chromatography Under Anaerobic Conditions	168
7.5.4. Iron and Sulphide Analyses	169
7.5.5. UV-visible and EPR spectra	173
7.5.6. <i>In Vivo</i> Activity of the ThiH-His expressed from pRL1020/BL21(DE3)	174
7.5.7. Chemical and Enzymatic Reconstitution Experiments	174
7.6. Experimental for Chapter 4	176
7.6.1. Expression of ThiI	176
7.6.2. Expression of ThiE	177
7.6.3. Expression of ThiD	177
7.6.4. Expression and Purification of ThiFS from pRL1800/BL21(DE3)	179
7.6.5. Expression and Purification of Dxs-His	180

7.6.6. Enzymatic Synthesis of 1-deoxy-D-xylulose-5-phosphate (Dxp)	182
7.6.7. Synthesis of 4-amino-5-hydroxymethyl-2-methylpyrimidine (Hmp)	184
7.6.8. Synthesis of 4-methyl-5-(β -hydroxyethyl)thiazole phosphate (Thz-P)	186
7.7. Experimental for Chapter 5	187
7.7.1. Effect of the Adenosine Treatment on the Production of TPP by <i>E. coli</i> 83-1	187
7.7.2. Comparison between Adenosine Treated 83-1 and pRL1020/83-1Cells in the Presence of β -L-arabinose	188
7.7.3. De-repression Experiments on <i>E. coli</i> KG33 Cells	189
7.8. Experimental for Chapter 6	191
7.8.1. Large Scale Growth of <i>E. coli</i> pRL1020/83-1 in the Presence of Adenosine	191
7.8.2. General Conditions for the <i>In Vitro</i> Assay	191
7.8.3. Thiazole Synthase Activity in <i>E. coli</i> Cleared Cell Lysates	194
7.8.4. Comparing the Effect of the ThiGH-Enriched Protein Fraction and Purified ThiFS and ThiGH-His	194
7.8.5. Thiazole Synthase Activity Dependency on the Concentration of the Precursors	195
7.8.6. Thiazole Synthase Activity: Effect of ThiF and ThiS	196
7.8.7. ThiGH-His Time Course and Dosage	197
7.8.8. Preliminary Fractionation Experiments on the De-repressed pRL1020/83-1 Cleared Lysate	197
7.8.9. Thiazole Synthase Activity: Preliminary Experiments on the Effect of SAM and Reducing Agents	198
Appendix A	200
List of Assembled Plasmids	200
Maps of Cloning Plasmids (pBAD-TOPO Derivatives)	201

<i>Appendix B</i>	204
B.1. Agarose gel electrophoresis	204
B.2. Sodium Dodecyl Sulphate Polyacrylamide Gel Electrophoresis (SDS-PAGE)	205
B.3. Bradford Assay	207
B.4. Growth Media	207
<i>Bibliography</i>	210

List of Figures, Schemes and Tables

Figure 1.1. Structure of thiamine	1
Figure 1.2. Schematic representation of the TPP-induced change in the mRNA secondary structure	15
Figure 1.3. Alignment of <i>E. coli</i> ThiH with sequences from BioB, LipA, ArrAE and PflAE from <i>E. coli</i> and Kam from <i>Bacillus halodurans</i>	22
Figure 1.4. Model of the interaction of SAM with the [4Fe-4S] ^{2+/+} cluster of PflAE	24
Figure 2.1. Schematic representation of the cylindrical cavity created by the GroEL/ES complex, and inside which newly synthesised polypeptide chains can complete their folding	27
Figure 2.2. Genes constituting the isc operon	29
Figure 2.3. Maps of pRL200 and pRL220, not to scale	31
Figure 2.4. Coomassie Blue stained 15 % SDS-PAGE gel of soluble proteins produced by pRL220/LMG194 and pRL200/BL21(DE3) after induction with increasing concentrations of L-arabinose or IPTG	32
Figure 2.5. Coomassie Blue stained 15 % SDS-PAGE gel of insoluble proteins produced by pRL220/LMG194 and pRL200/BL21(DE3) after induction with increasing concentrations of L-arabinose or IPTG	33
Figure 2.6. Maps of pRL221 and pRL222	34
Figure 2.7. Coomassie Blue stained 15 % SDS-PAGE gel of soluble and insoluble proteins produced at 15 °C by pRL220/LMG194, pRL220/BL21(DE3), pRL221/LMG194, pRL221/BL21(DE3), pRL222/LMG194 and pRL222/BL21(DE3)	35
Figure 2.8. Coomassie Blue stained 15 % SDS-PAGE gel of soluble and insoluble proteins produced at 37 °C by pRL220/LMG194, pRL220/BL21(DE3), pRL221/LMG194, pRL221/BL21(DE3), pRL222/LMG194 and pRL222/BL21(DE3)	36
Figure 2.9. Map of pRL400	37

Figure 2.10. Coomassie Blue stained 15 % SDS-PAGE gel of soluble proteins expressed at 22 °C and 37 °C from pRL220*/LMG194, pRL200/BL21(DE3) and pRL400/BL21(DE3)	38
Figure 2.11. Coomassie Blue stained 15 % SDS-PAGE gel of insoluble proteins expressed at 22 °C and 37 °C from pRL220*/LMG194, pRL200/BL21(DE3) and pRL400/BL21(DE3)	39
Figure 2.12. Maps of pRL800, pRL1000 and the respective derivatives pRL820 and pRL1020	40
Figure 2.13. Coomassie Blue stained 15 % SDS-PAGE gel of soluble and insoluble proteins expressed from pRL400/BL21(DE3), pRL800/BL21(DE3) and pRL1000/BL21(DE3) at 28 °C	41
Figure 2.14. Coomassie Blue stained 15 % SDS-PAGE gel of soluble proteins expressed from pET-24d(+)/BL21(DE3), pBAD/HisA/BL21(DE3), pRL200/BL21(DE3), pRL220*/BL21(DE3), pRL800/BL21(DE3), pRL820/BL21(DE3), pRL1000/BL21(DE3) and pRL1020/BL21(DE3) at 28 °C	43
Figure 2.15. Map of pRL821	44
Figure 2.16. Coomassie Blue stained 15 % SDS-PAGE gel of soluble and insoluble proteins expressed from pRL800/BL21(DE3) and pRL821/BL21(DE3) at 28 °C	44
Figure 2.17. Map of pRL1021	45
Figure 2.18. Coomassie Blue stained 15 % SDS-PAGE gel of soluble and insoluble proteins expressed from pRL1021/BL21(DE3) at 28 °C	46
Figure 2.19. Maps of pRL1300 and pRL1500	47
Figure 2.20. Coomassie Blue stained 15 % SDS-PAGE gel of soluble and insoluble proteins expressed from pRL1020/BL21(DE3), pRL1300/BL21(DE3) and pRL1500/BL21(DE3) at 28 °C	48
Figure 3.1. Ion exchange chromatography. Coomassie Blue stained 15 % SDS-PAGE gels of proteins eluted from the Q-Sepharose column	52
Figure 3.2. Gel filtration chromatography. Coomassie Blue stained 15 % SDS-PAGE gels of proteins eluted from the Superdex 200 (S-200) column	53
Figure 3.3. Hydrophobic interaction chromatography. Coomassie Blue stained 15 % SDS-PAGE gels of fractions eluted from the column Source Phe column	53

Figure 3.4. Affinity chromatography. Coomassie Blue stained 15 % SDS-PAGE gels of fractions eluted from the Blue Sepharose column	54
Figure 3.5. Purification of ThiGH-His from pRL800/BL21(DE3). Coomassie Blue stained 15 % SDS-PAGE gels of proteins eluted from A: Ni-chelating column and B: gel filtration column	56
Figure 3.6. ESI-MS of ThiGH-His isolated from pRL1020/BL21(DE3)	57
Figure 3.7. Purification of ThiGH-His from pRL821/BL21(DE3). Coomassie Blue stained 15 % SDS-PAGE gels of proteins eluted from A: Ni-chelating column and B: gel filtration column	58
Figure 3.8. Purification of ThiGH-His from pRL1021/BL21(DE3). Coomassie Blue stained 15 % SDS-PAGE gels of proteins eluted from A: Ni-chelating column and B: gel filtration column	59
Figure 3.9. Purification of ThiGH-His from pRL820/BL21(DE3). Coomassie Blue stained 15 % SDS-PAGE gels of proteins eluted from A: Ni-chelating column and B: gel filtration column	60
Figure 3.10. Purification of ThiGH-His from pRL1000/BL21(DE3). Coomassie Blue stained 15 % SDS-PAGE gels of proteins eluted from A: Ni-chelating column and B: gel filtration column	61
Figure 3.11. Purification of ThiGH-His from pRL1020/BL21(DE3). Coomassie Blue stained 15 % SDS-PAGE gels of proteins eluted from A: Ni-chelating column and B: gel filtration column	62
Figure 3.12. Coomassie Blue stained 15 % SDS-PAGE gel of purified ThiGH-His samples isolated from pRL800/BL21(DE3), pRL1000/BL21(DE3) and pRL1020/BL21(DE3)	63
Figure 3.13. Analysis of ThiGH-His isolated from pRL800/BL21(DE3) by analytical gel filtration chromatography	64
Figure 3.14. Analysis of ThiGH-His isolated from pRL1000/BL21(DE3) by analytical gel filtration chromatography	65
Figure 3.15. Analysis of ThiGH-His isolated from pRL821/BL21(DE3), batch A, by analytical gel filtration chromatography	67
Figure 3.16. UV-visible spectra of ThiGH-His samples and ThiGH-His complex	71
Figure 3.17. UV-visible spectrum of ThiH-His monomer	71

Figure 3.18. Interconversion between Fe-S clusters	72
Figure 3.19. UV-visible spectra of ThiGH-His (4-5 mg/ml in ThiH-His) from pRL800/BL21(DE3) before and after exposure to air	73
Figure 3.20. UV-visible spectra of ThiGH-His from pRL1020/BL21(DE3) (6 mg/ml in ThiH-His) in 50 mM Tris-HCl, 5 mM DTT, 25 % (w/v) glycerol. The sample was anaerobically incubated with 5-deazaflavin (33 mM) and irradiated for 45 min with a light projector	74
Figure 3.21. X-band EPR spectra of ThiGH-His (5 mg/ml in ThiH-His) isolated from pRL1020/BL21(DE3). A: as isolated. B: after reduction with dithionite (1 mM, 30 min)	75
Figure 3.22. Complementation experiment	77
Figure 4.1. Map of pRL600	82
Figure 4.2. Coomassie Blue stained 15 % SDS-PAGE gel of soluble and insoluble proteins produced by two colonies of pRL600/BL21(DE3)	83
Figure 4.3. Map of pRL2030	84
Figure 4.4. Coomassie Blue stained 15 % SDS-PAGE gel of soluble and insoluble proteins produced by pRL2030/BL21(DE3) and pRL2030/C43(DE3)	84
Figure 4.5. Maps of pRL2200 (left hand side) and of pRL2220 (right hand side)	86
Figure 4.6. Coomassie Blue stained 15 % SDS-PAGE gels. A: proteins expressed from pRL2200/BL21(DE3), cleared lysate and pellet. B: proteins expressed from pRL2220/BL21(DE3), cleared lysate and pellet	86
Figure 4.7. Coomassie Blue stained 18 % SDS-PAGE gel of proteins expressed from pRL1800/BL21(DE3) at 27 and 37 °C	88
Figure 4.8. First step in the ThiFS purification. Coomassie Blue stained 18 % SDS-PAGE gel of pellets and supernatant from the $(\text{NH}_4)_2\text{SO}_4$ precipitation, and fractions eluted from the ion exchange column (Q-Sepharose).	89
Figure 4.9. ThiS purification. Coomassie Blue stained 18 % SDS-PAGE of fractions eluted from the gel filtration column (S-75)	89
Figure 4.10. ThiF purification. Coomassie Blue stained 15 % SDS-PAGE gel of fractions eluted from the gel filtration column (S-75)	90
Figure 4.11. Coomassie Blue stained 18 % SDS-PAGE gel of purified ThiF and ThiS	90

Figure 4.12. Coomassie Blue stained 15 % SDS-PAGE gel of soluble and insoluble proteins expressed from 2 colonies of BL21(DE3) transformed with a pET-23b-derived vector encoding Dxs-His	91
Figure 4.13. Dxs-His purification	92
Figure 5.1. TPP content of <i>E. coli</i> 83-1 incubated with (solid line) or without (dashed line) adenosine	100
Figure 5.2. TPP production by washed cell suspensions of <i>E. coli</i> 83-1 previously incubated with (solid lines) or without (dashed lines) adenosine	101
Figure 5.3. TPP content of <i>E. coli</i> 83-1 and pRL1020/83-1 incubated with adenosine in the presence of β -L-arabinose	104
Figure 5.4. TPP production by washed cell suspensions of <i>E. coli</i> 83-1 and pRL1020/83-1, previously incubated with adenosine and β -L-arabinose	105
Figure 5.5. Coomassie Blue stained 15 % SDS-PAGE gel of soluble proteins expressed during the adenosine treatment of <i>E. coli</i> pRL1020/83 and 83-1 in the presence of β -L-arabinose	105
Figure 5.6. Time course of pBAD/HisA/KG33 growth in minimal Davis-Mingoli medium, and consequent depletion in TPP	107
Figure 5.7. Time course of pBAD/HisA/KG33 growth in minimal Davis-Mingoli medium, and consequent depletion in TPP	108
Figure 5.8. Overall TP and TPP production	109
Figure 6.1. HPLC traces of oxidised reaction mixtures containing the de-repressed pRL1020/83-1 proteins, purified ThiGH-His, ATP, Hmp and Tyr	116
Figure 6.2. <i>De novo</i> TP and TPP production from mixtures of ThiGH-His enriched protein fraction and de-repressed pRL1020/83-1 lysate containing increasing amounts (0 to 100 %) of ThiGH-His enriched protein fraction	117
Figure 6.3. <i>De novo</i> TP and TPP production. All samples contained Tyr, Cys, Dxp, ATP and Hmp	119
Figure 6.4. Effect of the concentration of Dxp (A), Cys (B) and Tyr (C) on the overall production of TP and TPP	121
Figure 6.5. HPLC traces of oxidised reaction mixtures incubated with increasing concentrations of Tyr (0-2 mM)	122

Figure 6.6. Proposed structure of an enzyme-bound intermediate and its tautomer for ThiGH-His dependent thiazole biosynthesis	124
Figure 6.7. Effect of ThiFS on the production of TP and TPP by de-repressed pRL1020/83-1 proteins	125
Figure 6.8. Effect of ThiFS on the overall TP and TPP production of de-repressed pRL1020/83-1 proteins	126
Figure 6.9. Time course of the production of TP and TPP. All Samples contained de-repressed pRL1020/83-1 proteins, ATP, Hmp and Tyr	128
Figure 6.10. Effect of ThiGH-His on thiamine biosynthesis	129
Figure 6.11. Coomassie stained 15 % SDS-PAGE gel of proteins eluted from the analytical gel filtration column	131
Figure 6.12. Activity test (overall TP and TPP production) on the fractions eluted from the analytical gel filtration column	132
Figure 6.13. Coomassie stained 15 % SDS-PAGE gel of the de-repressed pRL1020/83-1 proteins eluted from the gel filtration column	133
Figure 6.14. Activity test (overall TP and TPP production) on the fractions eluted from the gel filtration column	134
Figure 6.15. Effect of SAM and reducing agents on the production of TP and TPP	135
Figure 6.16. Effect of SAM (without addition of reductant) on the TP and TPP production of standard assays	136
Figure 6.17. Effect of SAM and reducing agents on the TP and TPP production, expressed as relative activity	136
Figure 7.1. Typical TP and TPP calibration curves; (A) chromatographic systems 1 and (B) chromatographic system 2	157
Figure 7.2. Purified PCR products	164
Figure 7.3. Identification of positive colonies containing pRL221 (A) and pRL222 (B) by plasmid DNA isolation and restriction	164
Figure 7.4. Identification of positive clones containing pRL1021 by plasmid DNA isolation and restriction	165
Figure 7.5. Coomassie Blue stained 15 % SDS-PAGE gel of ThiH-His monomer (lane 1) and ThiGH-His complex (lane 2) isolated from a purified sample of ThiGH-His (lane 3) by gel filtration chromatography	169

Figure 7.6. Typical iron standard curve	172
Figure 7.7. Typical sulphide standard curve	173
Figure 7.8. PCR screening to identify colonies containing pRL500	176
Figure 7.9. Purified thiE (660 bp, lane 1, A) and thiD-His (830 bp, lane 1, B)	178
Figure 7.10. Dxp reaction mixture monitored by thin layer chromatography	184
Figure 7.11. Hmp synthesis monitored by thin layer chromatography	185
Scheme 1.1. Formation of the stabilised ylide-type carbanion	3
Scheme 1.2. Decarboxylation of α -keto acids catalysed by the TPP-dependent E1 components of pyruvate and α -ketoglutarate dehydrogenases	4
Scheme 1.3. General mechanism of the transketolase-catalysed transfer of a 2-carbon unit from xylulose-5-phosphate to an aldose	6
Scheme 1.4. Assembling of thiamine pyrophosphate from Hmp-PP and Thz-P	8
Scheme 1.5. Assembling of the pyrimidine moiety of thiamine pyrophosphate from the respective precursors in enteric bacteria and yeast	9
Scheme 1.6. Assembling of Thz-P in enteric bacteria/plant and aerobic bacteria/yeast from the respective precursors	11
Scheme 1.7. Enzymes involved in the biosynthesis of thiamine pyrophosphate	13
Scheme 1.8. Comparison between the proposed activation of ubiquitin (Ub), ThiS and MoeD by the respective activating enzymes E1, ThiF and MoeB	17
Scheme 1.9. Representation of the sulphur transfer from Cys to a generic substrate, catalysed by IscS and ThiI	18
Scheme 1.10. Mechanism for the biosynthesis of the thiazole moiety of thiamine proposed by Begley	19
Scheme 1.11. Thiazole biosynthesis in <i>B. subtilis</i>	21
Scheme 1.12. Reductive cleavage of SAM to the DOA radical and methionine	22
Scheme 1.13. Proposed mechanism for the BioB catalysed formation of biotin	23
Scheme 2.1. Redox cycle through which TrxB (thioredoxin reductase) and TrxA catalyse the reduction of disulphide bridges formed in cytoplasmic proteins	28
Scheme 4.1. Thiamine pyrophosphate (TPP) biosynthesis in <i>E. coli</i>	81
Scheme 4.2. Assembling of pRL1800 from pRL1000	87

Scheme 4.3. Enzymatic synthesis of 1-deoxy-D-xylulose-5-phosphate	93
Scheme 4.4. Synthesis of 4-amino-5-hydroxymethyl-2-methylpyrimidine (Hmp)	93
Scheme 4.5. Synthesis of 4-methyl-5-(β -hydroxyethyl)thiazole phosphate (Thz-P)	94
Scheme 5.1. Formation of AIR through the first five steps of the <i>de novo</i> purine biosynthesis	96
Scheme 5.2. Pathways of purine interconversion	98
Scheme 6.1. Coupled assay strategy	113
Scheme 6.2. Proposed model for Thz-P formation under the <i>in vitro</i> assay conditions here described	123
Scheme 6.3. Reductive cleavage of SAM by a [4Fe-4S] ⁺ cluster to the DOA radical and methionine, and abstraction of an H atom from the substrate RH. Steps 1, 2 and/or the H atom abstraction may occur in a concerted fashion	138
Scheme 6.4. First proposed mechanism for Thz-P biosynthesis	139
Scheme 6.5. Second proposed mechanism for Thz-P biosynthesis	140

Table 1.1. Position of the genes involved in thiamine biosynthesis in <i>E. coli</i> . Position of <i>thiK</i> from (46)	12
Table 2.1. List of plasmids whose construction is herein described	30
Table 3.1. Cell paste yields obtained from different ThiGH-His expression systems	55
Table 3.2. Sulphide and metal content of ThiGH-His samples isolated from different expression systems	68
Table 5.1. Effect of adenosine treatment on the TPP content (ng/mg wet cells) of washed cell suspensions of <i>E. coli</i> 83-1	102
Table 6.1. TPP and TP content of cleared lysates from pRL1020/BL21(DE3) and de-repressed pRL1020/83-1 cells before and after gel filtration through a NAP-10 column. Data are expressed as pmoles/mg of protein	114
Table 6.2. Components present in a typical assay	115
Table 6.3. Fraction numbers and correspondent retention times of proteins eluted from the analytical gel filtration column	131
Table 7.1. Conditions for PCR reactions	147

Table 7.2. PCR amplification reaction cycle conditions	147
Table 7.3. A-tailing conditions	148
Table 7.4. Compositions of reaction mixtures prepared for PCR screening of positive colonies	149
Table 7.5. Conditions for analytical plasmid DNA restriction digestion	150
Table 7.6. Conditions for preparative plasmid DNA restriction digestion	151
Table 7.7. Conditions for the ligation of a DNA fragment into an expression vector	152
Table 7.8. Dilution series for TP or TPP standards	157
Table 7.9. List of primers used during this project	158
Table 7.10. Dilution series for iron standards	171
Table 7.11. Dilution series for sulphide standards	172
Table 7.12. Enzymes and other components used to reconstitute the Fe-S centre of ThiGH-His samples isolate from pRL800/BL21(DE3)	175
Table 7.13. Components present in the <i>in vitro</i> complementation assays	190
Table 7.14. Mixture of low molecular weight components added to <i>in vitro</i> assays	193
Table 7.15. Conditions for experiment 6.2.2, Chapter 6	194
Table 7.16. Conditions adopted to vary the Dxp concentration in reaction mixtures containing the de-repressed pRL1020/83-1 proteins, purified ThiGH-His, Cys, Tyr, Hmp and ATP in a total volume of 270 µl	195
Table 7.17. Conditions adopted to vary the Cys (or Tyr) concentration in His, reaction mixtures containing the de-repressed pRL1020/83-1 proteins, purified ThiGH-Dxp, Tyr (or Cys), Hmp and ATP in a total volume of 270 µl	196

Acknowledgements

I warmly thank Dr. Peter L. Roach, my supervisor, for the scientific and moral support he has given me during my Ph.D, and for having shared my frustrations and joys of this rather demanding project. I am grateful for the practical help he provided in the laboratory, especially at the beginning, for his untiring ear and contributions to many presentations, and for his proofreading of this thesis.

I thank Dr. M. Kriek, R. Wood and Dr. W. Smith for the proofreading of this thesis and, together with Dr. C. Neylon and the other member of the Roach group, past and present, for making life in the laboratory more enjoyable. I particularly thank Dr. M. Kriek for the amplification of the *thiFSGH-His* operon and Southampton University and Royal Society for funding.

I am grateful to Prof. T. Brown for having allowed the use of his equipment, to Prof. M. Bradley for the generous loan of the HPLC, to Prof. D. Lowe and Dr. S. Fairhurst from the John Innes Centre (Norwich) for EPR spectra, to Dr. N. Shaw for metal analysis and to Dr. J. Langley, Ms. J. Herniman and Mrs J. Street for the outstanding MS and NMR services they provided.

Last but not least, I thank my family in Italy, my loving husband Paolo, my friends and my first chemistry teacher, Dr. E. Annoè, for their support, encouragement and inspiration.

Abbreviations

Abs or A_x	absorbance (at x nm)
AIR	5-iminoimidazole ribotide
<i>amp</i>	ampicillin resistance gene
arabinose	β -(+)-L-arabinose
<i>araC</i>	gene encoding AraC, the arabinose operon regulatory protein
ArrAE	anaerobic ribonucleotide reductase activating enzyme
BioB	biotin synthase
CoA	coenzyme A
Cys	cysteine
DAF	5-deazaflavin
DM	Davis-Mingioli
DMPD	<i>N,N</i> -dimethyl- <i>p</i> -phenylenediamine
DOA	5'-deoxyadenosyl radical
Dxp	1-deoxy-D-xylulose-5-phosphate
Dxs-His	hexahistidine tagged 1-deoxy-D-xylulose-5-phosphate synthase
EPR	Electron Paramagnetic Resonance
ESI-MS	ElectroSpray Ionisation Mass Spectrometry
FPLC	Fast Performance Liquid Chromatography
Gly	glycine
Hmp	4-amino-5-hydroxymethyl-2-methylpyrimidine
Hmp-P	4-amino-5-hydroxymethyl-2-methylpyrimidine monophosphate
Hmp-PP	4-amino-5-hydroxymethyl-2-methylpyrimidine pyrophosphate
I.D.	Internal Diameter
ICP-AES	Inductively Coupled Plasma Atomic Emission Spectroscopy

IPTG	isopropyl- β -D-thiogalactopyranoside
k	kilo
Kam	lysine 2,3-amino mutase
<i>kan</i>	kanamycin resistance gene
kbp	kilo base pairs
l	liter
<i>lacI</i>	gene encoding the Lac repressor
LipA	lipoyl synthase
MCS	Multiple Cloning Site
MWCO	Molecular Weight Cut Off
OD _x	Optical Density at x nm
ORF	Open Reading Frame
PEI	polyethyleneimine
PflAE	pyruvate formate-lyase activating enzyme
P _i	inorganic phosphate
pMK	plasmids assembled by Dr. M. Kriek
PMSF	phenylmethylsulfonyl fluoride
pRL	plasmids assembled by the author
RP-HPLC	Reversed Phase High Performance Liquid Chromatography
S	total spin quantum number
SAM	<i>S</i> -adenosylmethionine
SCE	Saturated Calomel Electrode
SD	Standard Deviation
T	thiamine
TBAH	tetrabutylammonium hydroxide
<i>thiH-His</i>	<i>thiH</i> gene encoding ThiH-His
ThiH-His	ThiH with a C-terminal hexahistidine tag
ThiS-COSH	ThiS thiocarboxylate
Thz-P	4-methyl-5-(β -hydroxyethyl)thiazole phosphate
TP	thiamine monophosphate
TPP	thiamine pyrophosphate

TPPP	thiamine triphosphate
Tyr	tyrosine
U	unit
W	watt

[HPLC\Methods\...] refers to the name of the HPLC file in which the raw data for a specific experiment are stored. The folder 'HPLC' is on a compact disk, which is supporting material for this thesis.

Chapter 1.

Introduction

“There is present in rice polishings a substance different from proteins and salts, which is indispensable to health and the lack of which causes nutritional polyneuritis”

Christian Eijkman and Gerry Grijns, 1906

1.1 Thiamine and its Discovery

Thiamine (**Figure 1.1**), also known as vitamin B₁, is a water soluble vitamin. The biologically active forms of thiamine are the correspondent pyrophosphate (TPP) and triphosphate (TPPP). Thiamine pyrophosphate is the cofactor of several enzymes involved primarily in carbohydrate metabolism. These enzymes participate in the biosynthesis of neurotransmitters, pentoses used as nucleic acid precursors and in the production of reducing equivalents used against oxidative stress and in several biosynthetic pathways (1,2) (section 1.2). Thiamine triphosphate is present in nerves where it has been shown to activate a chloride ion channel. A deficiency of thiamine in humans affects the cardiovascular (wet beriberi) and nervous (dry beriberi) systems. Therefore, besides being used to prevent and treat beriberi, this vitamin is also efficient in the treatment of neurological disorders such as the Wernicke-Korsakoff syndrome and possibly Alzheimer’s disease.

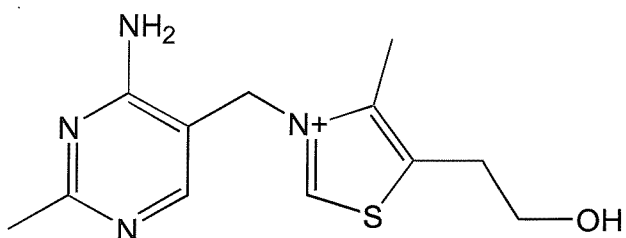


Figure 1.1. Structure of thiamine.

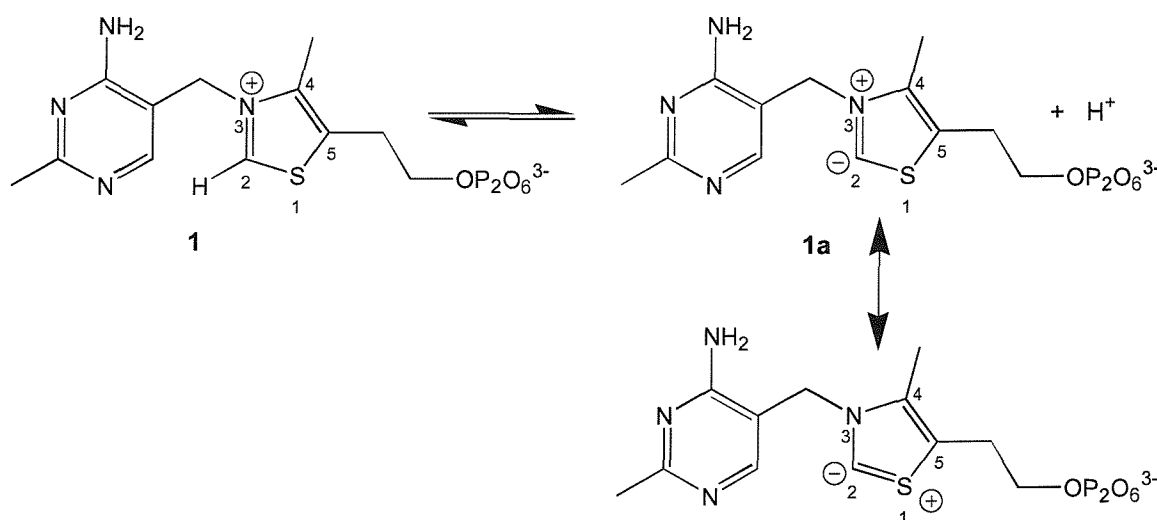
The history of thiamine began with the investigations into the causes of beriberi. This neurological disease was particularly widespread in Asia where a diet essentially

based on polished rice could not supply sufficient vitamin, as this is mainly contained in the rice husk. The early symptoms of beriberi include loss of appetite with subsequent muscle weakness and lassitude; as the disease progresses, affected people develop paresthesia (spontaneous sensations such as burning and tingling), possible swelling of feet and lower legs and also mental confusion and psychosis. Degeneration of the heart muscle causes heart failure, which is generally the cause of death. In the 1880s, as much as 40 % of the Japanese Navy crew might have developed beriberi. Dr. K. Takaki, at the time Director General of the Naval Medical Services, discovered the correlation between the disease and the poor diet of the sailors, and by ordering an increase in the meat, fish and vegetable rations succeeded in dramatically reducing the incidence of beriberi. In the meantime, Dutch medical officers Dr. C. Eijkman and Dr. G. Grijns, working at a military hospital in Java, observed that polyneuritis gallinarum, a beriberi like disease in chickens, could be induced in chickens fed with polished rice and reverted by feeding rice bran. This observation would have eventually led to the revolutionary notion that the absence of a substance in food could cause a disease, which is a founding principle of modern nutrition science. In the first decade of the new century (1911), a young chemist named C. Funk crystallised an amine extracted from the rice bran. He thought he had isolated the anti beriberi factor and coined the word 'vitamin' for 'vital amine'. Although the substance was not thiamine, the name remained. It was much later, in 1926, that vitamin B₁ was finally crystallised, again by two Dutch chemists, B.C.P. Jansen and W. Donath working in Eijkman's old laboratory. Unfortunately, they published the wrong formula and only 10 years later, in 1936, the correct formula was elucidated by R. R. Williams. A chemical synthesis for thiamine was available soon after, and from the 1950's, in the Western world, the vitamin is routinely added to many commercial foods (3-5).

1.2. Reactivity and Biochemical Functions of Thiamine Pyrophosphate

Thiamine pyrophosphate (**1**) is the main biologically active form of vitamin B₁. It is a cofactor for enzymes involved in carbohydrate and branched-chain amino acid metabolisms, and helps catalysing the decarboxylation of α -keto acids and C-C bond formation. In all TPP-dependent enzymes the proton loss from the C2 of the thiazole

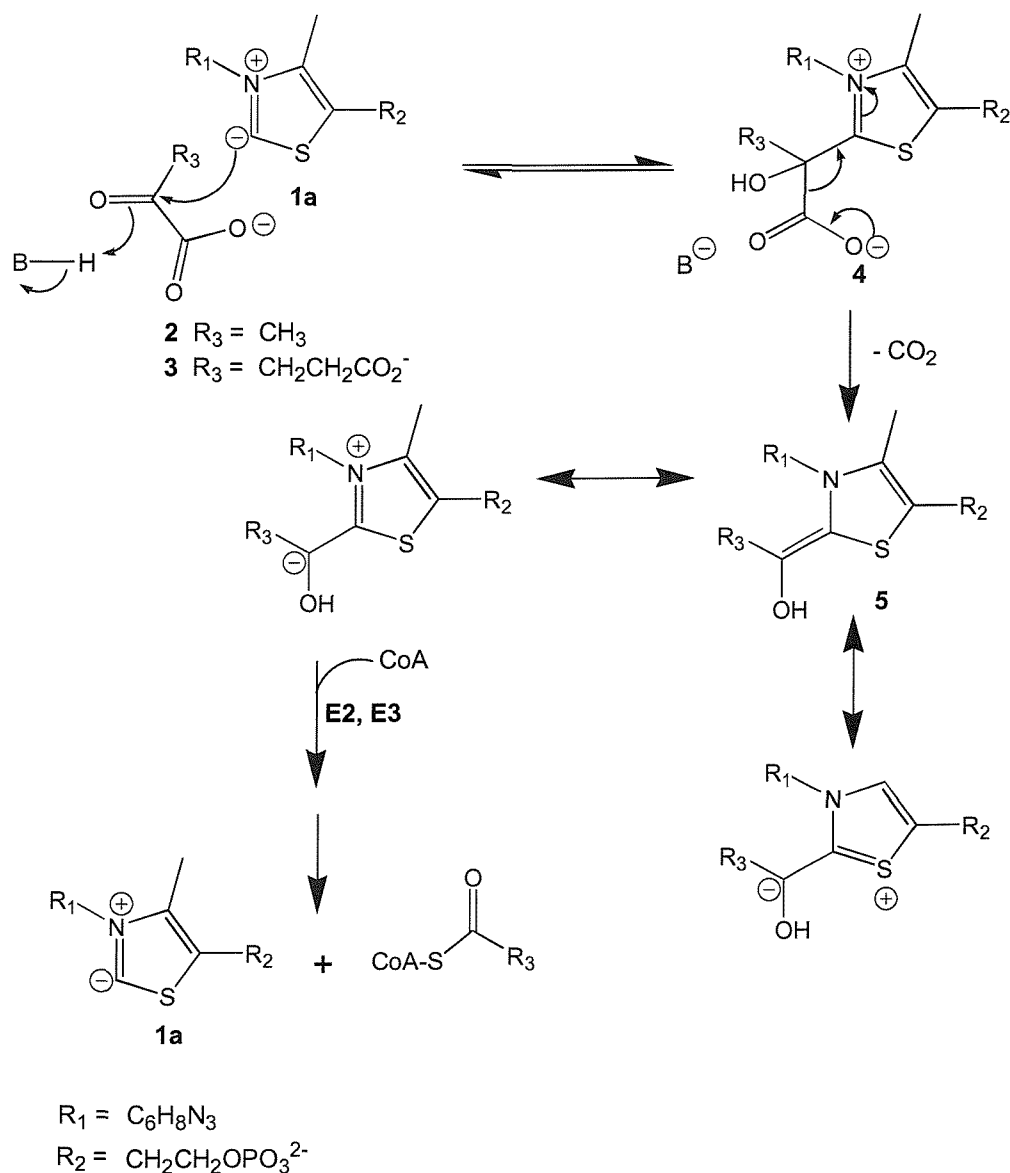
ring is the first step in the catalysis (**Scheme 1.1**). This proton is rather acidic (6) due to the stabilization of the correspondent carbanion (**1a**) by the adjacent sulphur and by the positive charge on the nitrogen (7). This ylide-type carbanion is both a potent nucleophile and a good leaving group. The following catalytic steps are characterised by the nucleophilic attack of **1a** on the substrate, with subsequent cleavage of a C-C bond. This cleavage releases the first product, leaving a second, resonance stabilised carbanion (enamine). Examples of TPP-dependent enzymes are pyruvate and α -ketoglutarate dehydrogenases, transketolase, 1-deoxy-D-xylulose-5-phosphate synthase and α -acetolactate synthase.



Scheme 1.1. Formation of the stabilised ylide-type carbanion.

Pyruvate dehydrogenase and α -ketoglutarate dehydrogenase are two important enzymes in the Kreb's cycle. The E1 components of these complexes, catalyse the decarboxylation of pyruvate (**2**) and α -ketoglutarate (**3**), respectively (8), through the mechanism shown in **Scheme 1.2**. The nucleophilic addition of the resonance stabilised thiazolium carbanion to the carbonyl group of the α -keto acid, followed by protonation, leads to the formation of an α -hydroxyacid (**4**). This adduct readily undergoes decarboxylation producing a hydroxyalkylthiamine pyrophosphate, stabilised by resonance (**5**). This hydroxyalkyl group is then oxidised and transferred to the lipoamidic prosthetic group of the pyruvate dehydrogenase and α -ketoglutarate dehydrogenase E2 components, releasing **1a**. The E2 components of the respective

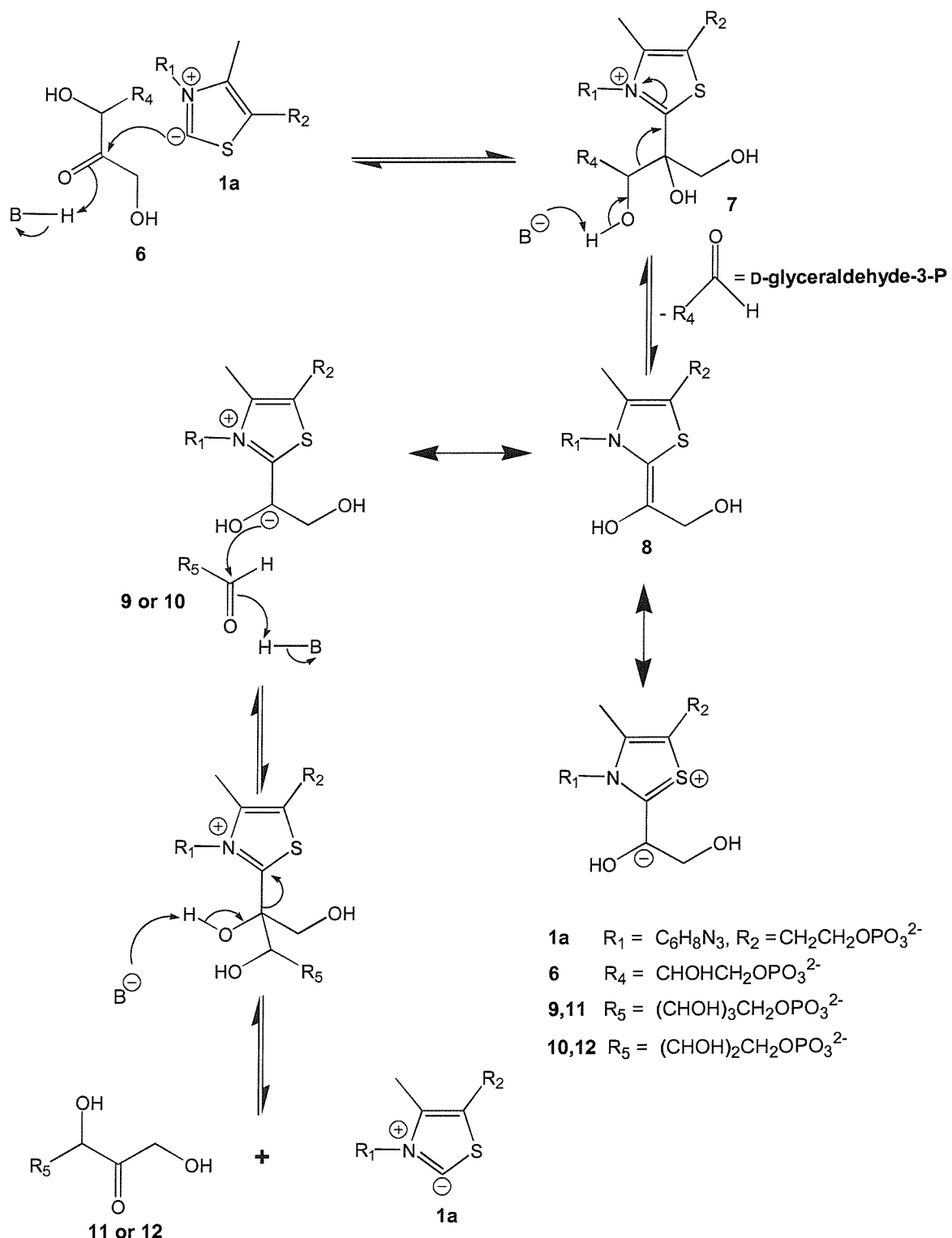
complexes then transfer the acetyl or succinyl groups to coenzyme A, with the oxidised form of the lipoamide being regenerated by the E3 component, which is identical in the two dehydrogenases. Decreased activities of pyruvate dehydrogenase and α -ketoglutarate dehydrogenase cause failure in ATP synthesis, and lower ATP levels have been found in brain regions damaged by thiamine deficiency (2).



Scheme 1.2. Decarboxylation of α -keto acids catalysed by the TPP-dependent E1 components of pyruvate and α -ketoglutarate dehydrogenases. The transfer of the acetyl and succinyl groups to coenzyme A occurs by a multistep mechanism and involves the E2 and E3 components of the respective complexes.

TPP-dependent transketolase is one of the enzymes required in the non-oxidative part of the pentose phosphate pathway (8). This pathway produces NADPH for various biosynthetic reactions, and riboses for the biosynthesis of nucleotides, nucleic acids and coenzymes. All the reactions catalysed in the non-oxidative part of the pathway, which interconverts sugars containing 3-7 carbon atoms, are reversible. In particular, transketolase transfers a 2-carbon unit from the ketose xylulose-5-phosphate (6) to an aldose, ribose-5-phosphate (9) or erythrose-4-phosphate (10). As with the decarboxylation of α -keto acids, the first step is the formation of **1a**, followed by nucleophilic addition to the carbonyl of the ketose and production of **7** (**Scheme 1.3**). The C-C bond adjacent to the carbonyl group of **6** undergoes cleavage, releasing D-glyceraldehyde-3-phosphate and producing the activated glycoaldehyde intermediate **8**. The nucleophilic addition of this intermediate to the carbonyl group of another aldehyde, followed by the elimination of **1a**, leads to the reversible formation of a new ketose: sedoheptulose-5-phosphate (**11**, from **9**) or fructose-6-phosphate (**12**, from **10**). The transketolase-catalysed formation of erythrose 4-phosphate is important for the biosynthesis of aromatic amino acids.

1-deoxy-D-xylulose-5-phosphate synthase (Dxs) is a TPP-dependent enzyme which catalyses the formation of 1-deoxy-D-xylulose-5-phosphate (Dxp) from pyruvate and D-glyceraldehyde-3-phosphate (9,10). Remarkably, besides being a precursor for isoprenoids and vitamin B₆, this sugar is also incorporated in the thiazole moiety of thiamine pyrophosphate, which is therefore implicated in its own biosynthesis. The formation of Dxp is likely to occur through the condensation of the hydroxyethylthiamine pyrophosphate (**5**), derived from the decarboxylation of the pyruvate, with the carbonyl group of D-glyceraldehyde-3-phosphate (**11**), and therefore through a combination of the mechanisms shown in **Schemes 1.2** and **1.3**.

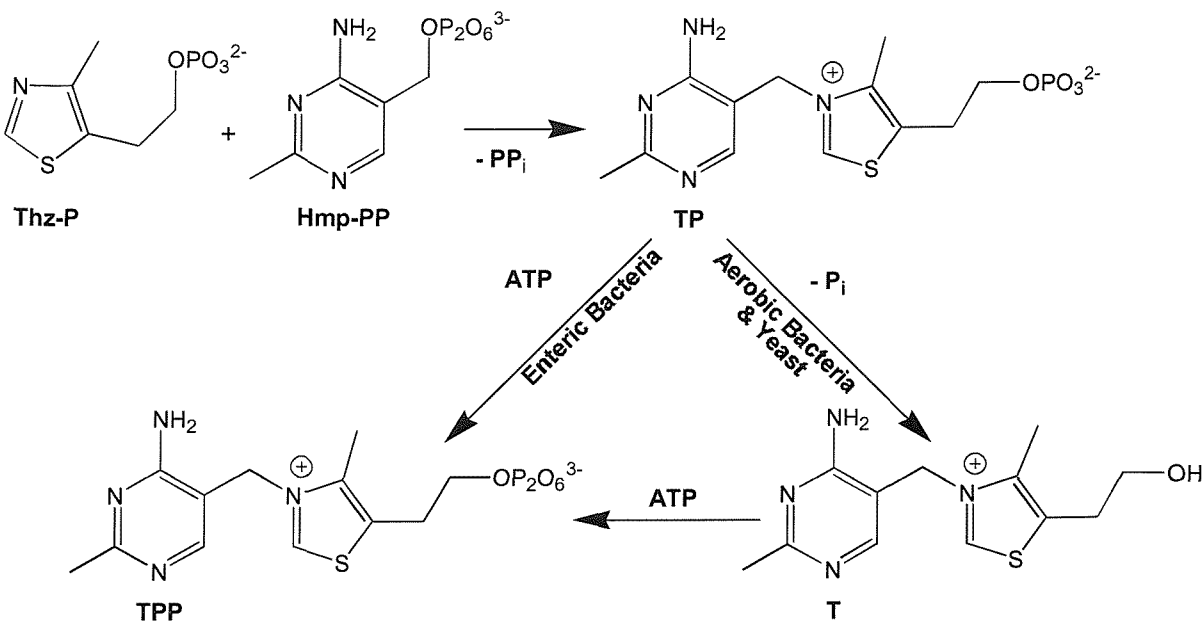


Scheme 1.3. General mechanism of the transketolase-catalysed transfer of a 2-carbon unit from xylulose-5-phosphate to an aldose.

In a similar way, α -acetolactate synthase catalyses the first step in valine and isoleucine biosyntheses. In both cases the enzyme converts pyruvate into the correspondent carbanion **5**, followed by nucleophilic attack either on another pyruvate molecule to form α -acetolactate, an intermediate in the valine biosynthesis, or on α -ketobutyrate to form α -aceto- α -hydroxybutyrate for the biosynthesis of isoleucine (12).

1.3. Thiamine Biosynthesis

Despite the early elucidation of the structure of thiamine and the wealth of information on TPP-dependent enzymes (sections 1.1 and 1.2), the knowledge of the biochemical mechanisms and enzymology of thiamine biosynthesis is still fragmentary. Thiamine biosynthesis occurs in most microorganisms and higher plants. All organisms able to produce the vitamin initially assemble the correspondent monophosphate (TP) by coupling 4-methyl-5-(β -hydroxyethyl)thiazole phosphate (Thz-P) and 4-amino-5-hydroxymethyl-2-methylpyrimidine pyrophosphate (Hmp-PP) (**Scheme 1.4**); TP is then converted to TPP, either by direct phosphorylation (in enteric bacteria) or by de-phosphorylation to thiamine (T) followed by pyrophosphorylation (in aerobic bacteria and yeast) (5,13). The two heterocyclic precursors of thiamine pyrophosphate, Hmp-PP and Thz-P, are biosynthesised through independent pathways. It is now accepted that these pathways differ in enteric bacteria and yeast and that the biosynthesis of thiamine represents a remarkable example of biochemical diversity. The following paragraphs summarise some important findings concerning precursors in thiamine biosynthesis and gene organization, with particular emphasis on the Thz-P biosynthesis in *E. coli*.

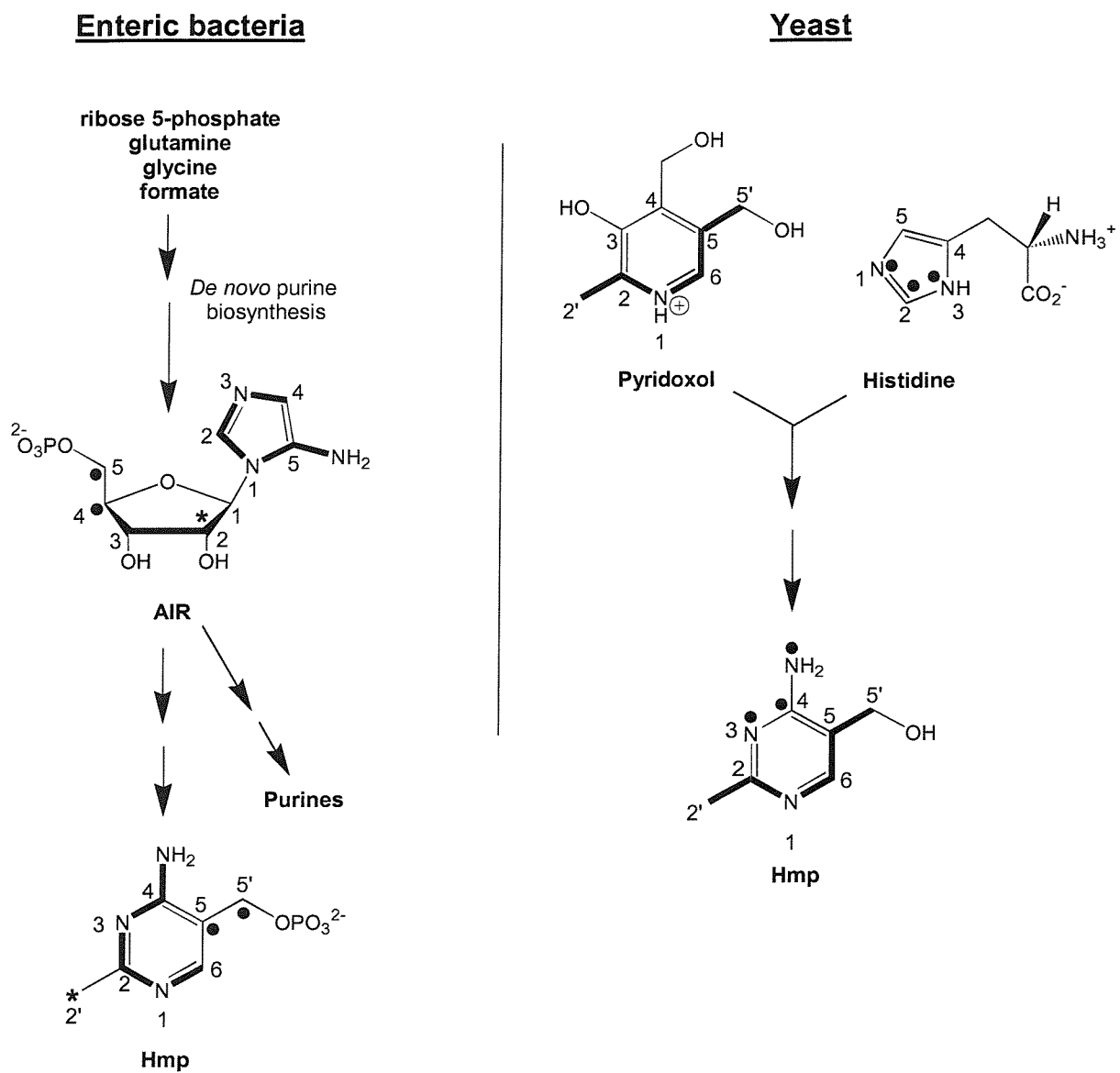


Scheme 1.4. Assembling of thiamine pyrophosphate from Hmp-PP and Thz-P.

1.3.1. Thiamine Precursors

Considerable progress in the identification of the precursors for each heterocyclic moiety of thiamine has been made, especially in the last 2 decades, through the use of isotopic labels. Comprehensive reviews on this topic are those by White and Spenser (5,14). In enteric bacteria such as *E. coli* and *S. typhimurium*, it is now firmly established that all the atoms of 4-amino-5-hydroxymethyl-2-methylpyrimidine (Hmp) derive from 5-aminoimidazole ribotide (AIR) (**Scheme 1.5**) (15,16). In particular, AIR undergoes a complex rearrangement resulting in a ring expansion of the imidazole by insertion of carbon C4 (or C5) from the ribose unit. In fact, C4 and C5 appear to be transferred as an intact unit, and whilst one of these carbon atoms is incorporated into the pyrimidine ring, the other becomes the hydroxymethyl substituent. The final carbon of Hmp, the methyl group, is provided by the C2 of the ribose. Therefore, three of the five carbon atoms of the ribose are incorporated into the imidazole ring of AIR to form the substituted pyrimidine Hmp, while the remaining two atoms, C1 and C3 are lost. AIR is an intermediate in the *de novo* purine biosynthesis, and its imidazole ring derives from glycine, glutamine and formate (17). It was the combined effort of several research groups which made

possible the rationalization of the complex incorporation patterns of radioactive precursors [formate, glycine and glucose, see quoted reviews (5,14)], culminating with the elucidation of the remarkable rearrangement leading from AIR to Hmp, but the credit of the discovery of the AIR intermediacy in both the purine and thiamine biosyntheses belongs to Newell and Tucker (18). Their findings remain one of the milestones in the investigation of thiamine biosynthesis.

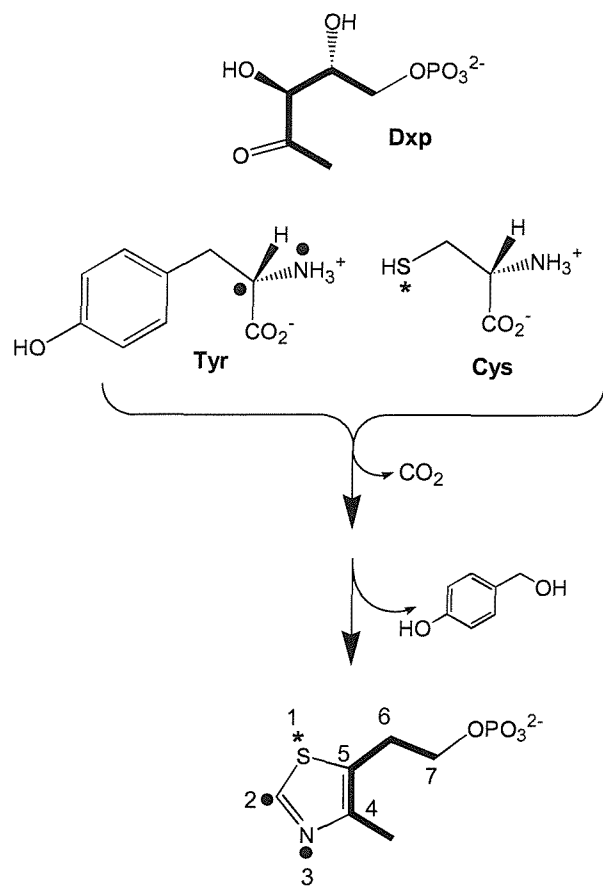


Scheme 1.5. Assembling of the pyrimidine moiety of thiamine pyrophosphate from the respective precursors in enteric bacteria and yeast. Adapted from (5,14).

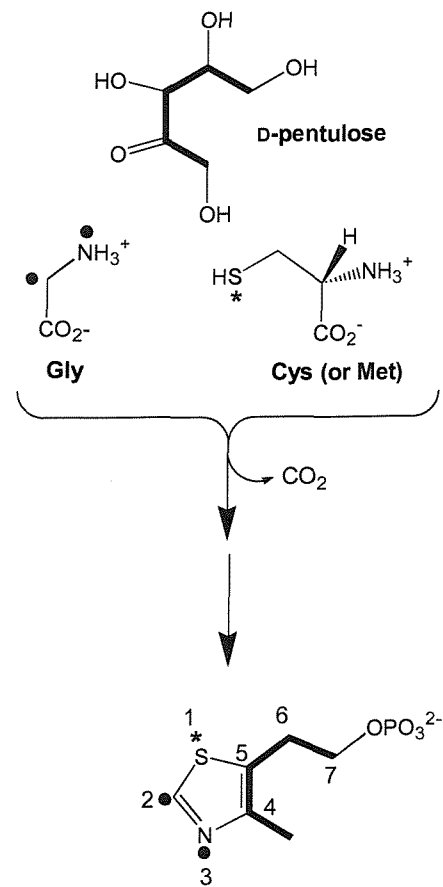
In yeast, whilst AIR is still an intermediate in the *de novo* purine biosynthesis (19), it is not a precursor of the pyrimidine moiety of thiamine. In *S. cerevisiae*, Hmp derives from histidine (20) and pyridoxol (21). In particular, N1, C2 and N3 of histidine become N3, C4 and the NH₂ group of Hmp (**Scheme 1.5**). The remaining atoms derive from pyridoxol or, as more recently discovered, from 2'-hydroxypyridoxol (22). Histidine and pyridoxol in yeast, and AIR in bacteria, are advanced Hmp precursors. More distant, but common precursors in both bacteria (enteric and aerobic) and yeast are formate and glucose. Formate is incorporated in the pyrimidine moiety of thiamine and enters C2 in bacteria (23,24) and C4 in eukaryotes (25,26); glucose, instead, enters different positions in either vitamin moieties [see Himmeldirk *et al*, 1998, for a comprehensive rationalization of all previous findings on the incorporation of radiolabelled glucose (27)].

In enteric bacteria, the thiazole moiety of thiamine derives from 1-deoxy-D-xylulose-5-phosphate (28,29), tyrosine (30-32) and cysteine (33). In particular, the sugar is completely incorporated into the thiazole, as a C₅ unit, whilst cysteine donates the S atom and tyrosine provides the C2 and the nitrogen atoms (**Scheme 1.6**). In *E. coli*, the side chain of tyrosine has been shown to be released as *p*-hydroxybenzyl alcohol during the biosynthesis of thiamine (34). The thiazole ring is assembled from Dxp, Tyr and Cys also in higher plants (35), and whilst enteric bacteria and plants seem to adopt the same route, aerobic bacteria seem to employ the yeast pathway, assembling the thiazole moiety from glycine and a pentulose derived from glucose (27,36). Both the glycine and the pentulose provide the C2-N and the entire carbon backbone, respectively, as intact units. The source of the sulphur atom is still unclear and, in *S. cerevisiae*, both cysteine and methionine have been shown to be sulphur donors (33,37). Interestingly, Tyr and Gly are mutually exclusive in *B. subtilis*, *P. putida*, *E. coli* and *E. aerogenes* (36), supporting the evidence for different pathways to the thiazole between aerobic and anaerobic bacteria. Mechanisms for the intramolecular rearrangement of AIR to yield Hmp, and for the formation of the thiazole from Tyr, Cys and Dxp have been proposed by Spenser and Begley (5,13,38).

Enteric bacteria/Plants



Aerobic bacteria/Yeast



Scheme 1.6. Assembling of Thz-P in enteric bacteria/plant and aerobic bacteria/yeast from the respective precursors. Adapted from (5,14).

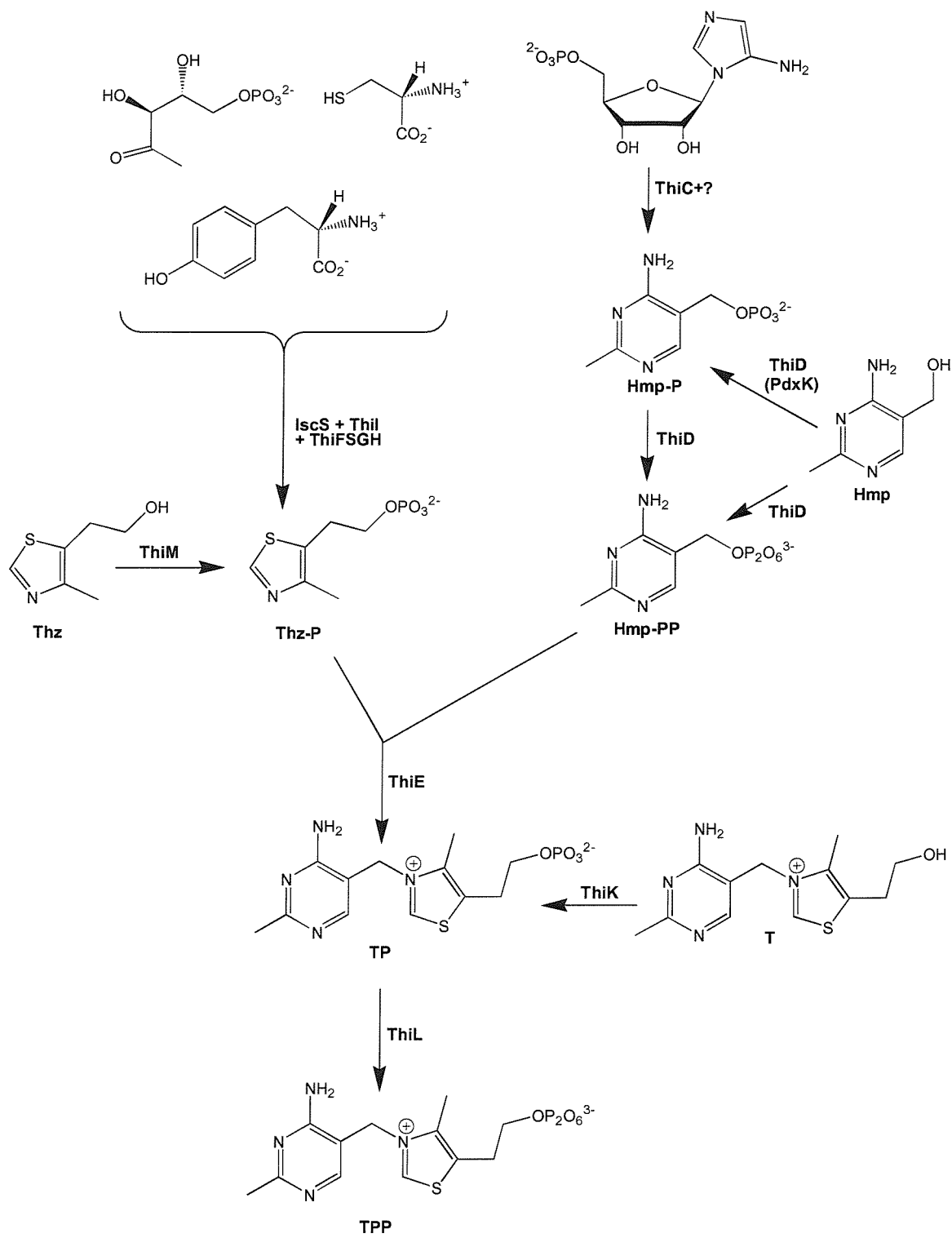
1.3.2. Gene Organization, Function and Regulation in *E. coli*

In *E. coli* and *S. typhimurium* the genes involved in thiamine biosynthesis, transport and salvage have a very similar organization and location on the respective chromosomes (13). Genes that were first discovered in one organism were soon found in the other, and vice versa. These genes (**Table 1**) are organised in three operons, *thiCEFSGH* (39-41), *thiMD* (42,43) and *thiBPQ* (44), and five single loci, *thiI* (45), *thiK* (46), *thiL* (47), *iscS* (48,49) and *dxs* (9,10). A sixth locus, *pdxK*, is not directly related to thiamine biosynthesis but the correspondent gene product, encoding a pyridoxine kinase, is able to phosphorylate Hmp to Hmp-P (13,50). In addition to the role played in thiamine biosynthesis, both the products of the *thiI* and *iscS* genes are involved in the generation of 4-thiouridine (51,52), and *iscS* is also part of an operon essential for the assembling and repairing of Fe-S clusters (53,54).

Gene	Position (min)
<i>thiCEFSGH</i>	90.36-90.28
<i>thiMD</i>	47.05-47.03
<i>thiBPQ</i>	1.61-1.56
<i>thiL</i>	9.37
<i>thiI</i>	9.5
<i>thiK</i>	25
<i>dxs</i>	9.43
<i>iscS</i>	53.3

Table 1.1. Position of the genes involved in thiamine biosynthesis in *E. coli*. Position of *thiK* from (46).

The functions of most of the thiamine biosynthetic enzymes have been deduced and assigned through the characterisation of specific thiamine auxotrophic mutants, and for a few of them, the activities have been reconstituted (**Scheme 1.7**).



Scheme 1.7. Enzymes involved in the biosynthesis of thiamine pyrophosphate.
Adapted from (13).

In particular, it has been shown that ThiD catalyses either the phosphorylation of Hmp-P to Hmp-PP or the direct pyrophosphorylation of Hmp to Hmp-PP (50,55). Whilst mutations in *thiD* result in thiamine auxotrophy, mutations in *thiM* and *thiK*, which encode the thiazole kinase and thiamine kinase, respectively, do not impair the vitamin biosynthesis, suggesting that ThiM and ThiK are involved in salvage processes (43,46). ThiL is a thiamine monophosphate kinase (47), and ThiE, or thiamine phosphate synthase, catalyses the coupling of Thz-P and Hmp-PP (56).

This enzyme has been more extensively characterised in *B. subtilis*, due the higher solubility than the *E. coli* homolog, and the crystal structure solved (57). In addition to the ThiE crystal structure, the analysis of crystal structures of ThiE mutants has provided evidence to support a coupling mechanism in which Hmp-PP dissociates to form a proposed carbocation before being attacked by the N3 of Thz-P (58,59). The *thiBPQ* operon encodes a transport system for both thiamine and thiamine pyrophosphate (44), and the product of the *dxs* gene catalyses the formation of 1-deoxy-D-xylulose-5-phosphate (sections 1.2 and 1.3.1). The reconstituted activities of IscS, ThiI, ThiF and ThiS, which more directly concern this work, are described separately and in more detail in section 1.3.3. The activities of ThiH and ThiG will be the subject of this thesis, and the activity of ThiC, the only enzyme so far found to be required for the conversion of AIR to Hmp (39) has not been, as yet, successfully reconstituted (13).

The *thiCEFSGH*, *thiMD* and *thiBPQ* operons are regulated by thiamine pyrophosphate (41,43,44), whilst ThiI and ThiL are not (45,47). It is not surprising that ThiI, as well as probably IscS and Dxs, are not repressed by the vitamin, since these enzymes are shared with other biosynthetic pathways. The repression exerted by thiamine pyrophosphate on its own biosynthesis had been already investigated in *S. typhimurium* by Newell and Tucker (60) and in *E. coli* by Kawasaki and co-workers (61). The latter, in particular, showed that at least three enzymes (responsible for four enzymatic activities, given the bifunctionality of ThiD) were subjected to this repression: ThiD, ThiM and ThiE. Due to the similar extent of repression it was also proposed that these enzymes could be organised in an operon, which was later confirmed, for the two kinases, by D. Downs and co-workers who also found that not only the *thiMD* but also the *thiCEFSGH* and *thiBPQ* operons were transcriptionally

regulated by the vitamin. They also reported that a mutation in ThiL, and therefore the inability to convert thiamine to the correspondent pyrophosphate, resulted in decreased repression of the TPP-regulated *thiCEFSGH* operon, suggesting that TPP was the actual effector (41). More recent studies have elucidated the regulatory role of RNA sequences upstream of genes involved in thiamine biosynthesis or transport, in prokaryotes (62). These sequences, which contain a highly conserved 38-base *thi* box (63), can fold in a conserved secondary structure called the THI element. It has been proposed that in the presence of thiamine pyrophosphate, a change in this secondary structure could result in either transcriptional or translational attenuation. In *E. coli*, this hypothesis has recently received support from the work of Winkler and co-workers who have shown that the untranslated regions of *thiC* and *thiM* mRNAs, containing the *thi* box, can bind directly to thiamine pyrophosphate and, less efficiently, to thiamine (64). The resultant mRNAs-effector complexes adopt a conformation which sequesters the ribosome-binding site and causes a reduction in gene expression (**Figure 1.2**).

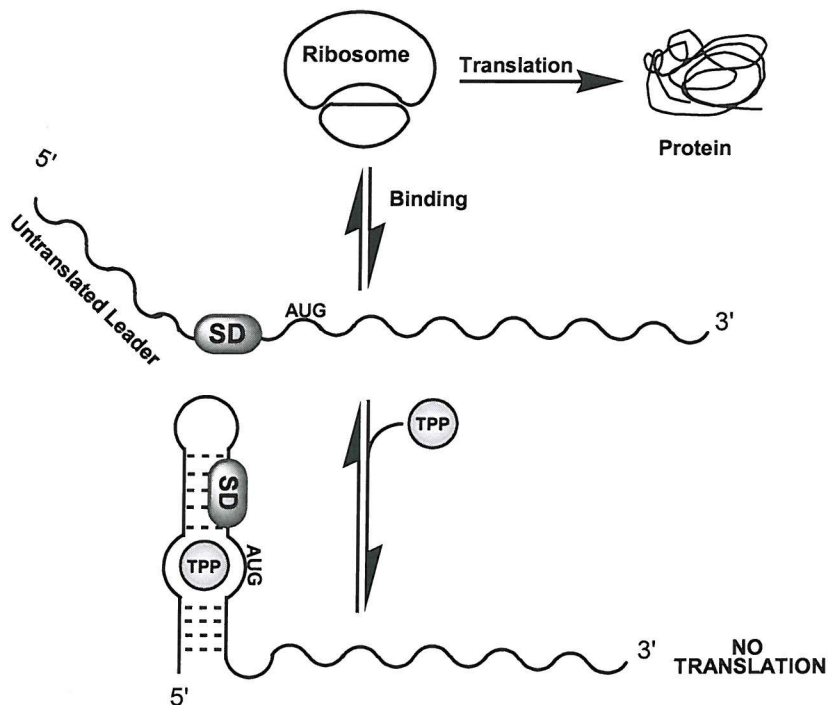


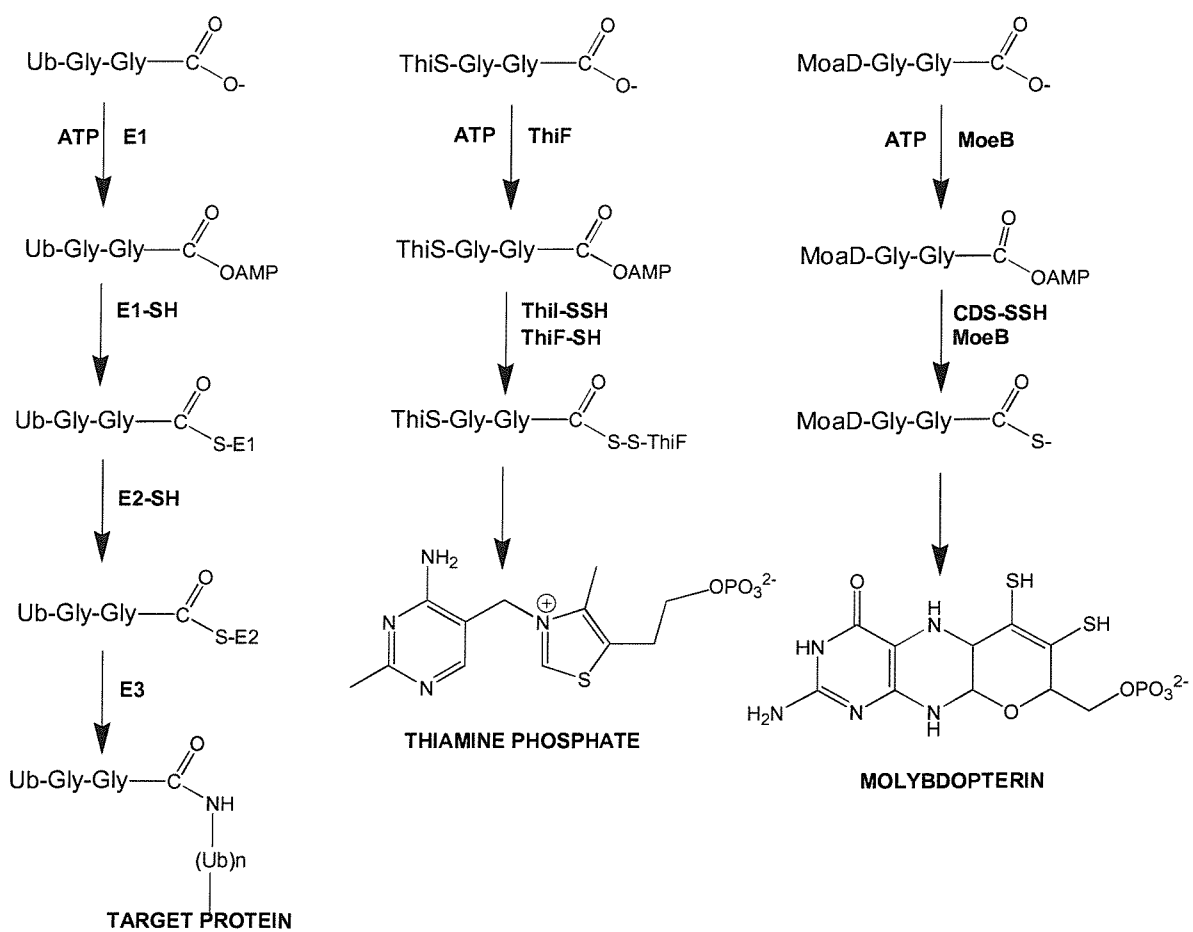
Figure 1.2. Schematic representation of the TPP-induced change in the mRNA secondary structure. The conformation of the mRNA-TPP complex precludes any interaction with the ribosome by sequestering the Shine and Dalgarno (SD) element. Under these conditions no translation occurs. Adapted from (65).

More specifically, *thiM* was shown to be subjected to a TPP-induced translational repression, whilst *thiC* to both translational and transcriptional regulation. This mode of regulation, characterised by small molecules binding directly to the RNA, without the intermediacy of a protein, is rare but not unique. Vitamin B₁₂ has also been shown to interact directly with the mRNA leader sequence of the *btuB* gene, and to regulate its expression in a similar way (64-66). In addition to the repression by TPP, another proposed control mechanism operating on the biosynthesis of the vitamin is the feedback inhibition exerted by the thiazole but, apparently, not by the pyrimidine moiety. This difference was noted by Newell and Tucker during their work on *S. typhimurium* mutants blocked in the biosynthesis of either one or the other heterocycle: whilst mutants impaired in the thiazole biosynthesis accumulated Hmp and excreted it into the medium, no thiazole was accumulated in mutants unable to assemble the pyrimidine (45,60,67). Newell and Tucker also investigated the de-repression effect exerted by adenosine on the biosynthesis of the vitamin. The addition of this purine nucleoside to growing cultures of *S. typhimurium* LT2, was shown to release the repression exerted by TPP on its own biosynthesis, by decreasing the intracellular content of the vitamin (68). This technique was subsequently exploited in labelling experiments with the objective of identifying thiamine precursors (29,30).

1.3.3. Enzymes Involved in the Thiazole Biosynthesis in *E. coli*

Despite the progress made in the identification of enzymes and precursors involved in thiamine biosynthesis, little is known about the biochemical mechanism leading to the formation of the thiazole ring of the vitamin. The assembling of the thiazole from Tyr, Cys and Dxp requires at least six gene products which are ThiFSGH, ThiI and IscS. More specifically, IscS, ThiI and ThiF are involved in the sulphur mobilization from Cys to the C-terminal carboxylate of ThiS, the sulphur carrier in thiamine biosynthesis (13,49). ThiS is a small protein (7 kDa) which, despite the low sequence identity to ubiquitin (14 %), has been recently shown to possess the ubiquitin fold, in addition to the highly conserved C-terminal Gly-Gly sequence (69). In a mechanism clearly related to the activation of ubiquitin, the C-terminal carboxylate of ThiS has to be adenylated before undergoing attack by a nucleophilic sulphur donor.

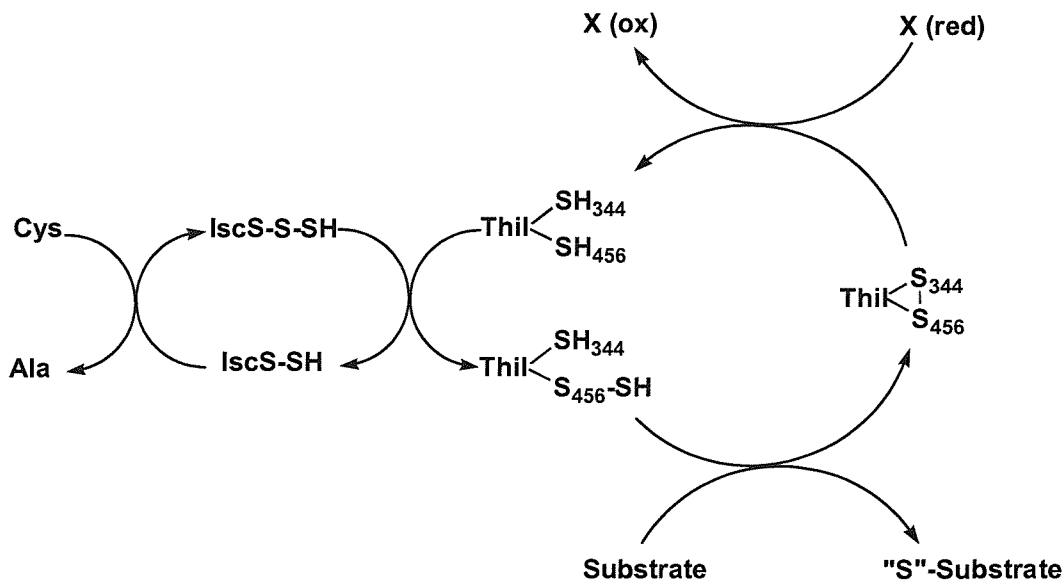
The adenylation is catalysed, in an ATP-dependent reaction, by ThiF, which is homologous in sequence to part of the ubiquitin-activating enzyme, E1 (49,70,71). Besides ThiS and ThiF, two other *E. coli* enzymes involved in sulphur insertion into a cofactor, MoaD and MoeB, share functional and structural similarities with ubiquitin and E1, respectively (**Scheme 1.8**). ThiF and MoeB show a remarkable sequence identity (42 % over 245 residues), which is reflected in analogous functions (70,72,73), and both ThiS and MoaD possess the C-terminal pair of glycine residues, the ubiquitin fold and form thiocarboxylates involved in sulphur insertion (74).



Scheme 1.8. Comparison between the proposed activation of ubiquitin (Ub), ThiS and MoaD by the respective activating enzymes E1, ThiF and MoeB. The sulphur for both thiamine and molybdopterin biosyntheses is provided by a sulphurtransferase, probably ThiI and CDS (cysteine sulphinate desulphinase), respectively. Adapted from (70).

The sulphur atom for the biosynthesis of the thiazole is mobilised from Cys by IscS and ThiI, with IscS catalysing the first step and forming an active site persulphide (49,52). IscS is a pyridoxal phosphate-dependent cysteine desulphurase which, remarkably, is required in thiamine biosynthesis not only because of the direct role played in the sulphur transfer but also for the proposed assembling and/or maintenance of the potential Fe-S cluster in ThiH (48,75,76). From IscS the sulphur atom is subsequently transferred to ThiI, which again forms an active site persulphide (77). This sequence of reactions is common to both thiamine and 4-thiouridine biosyntheses.

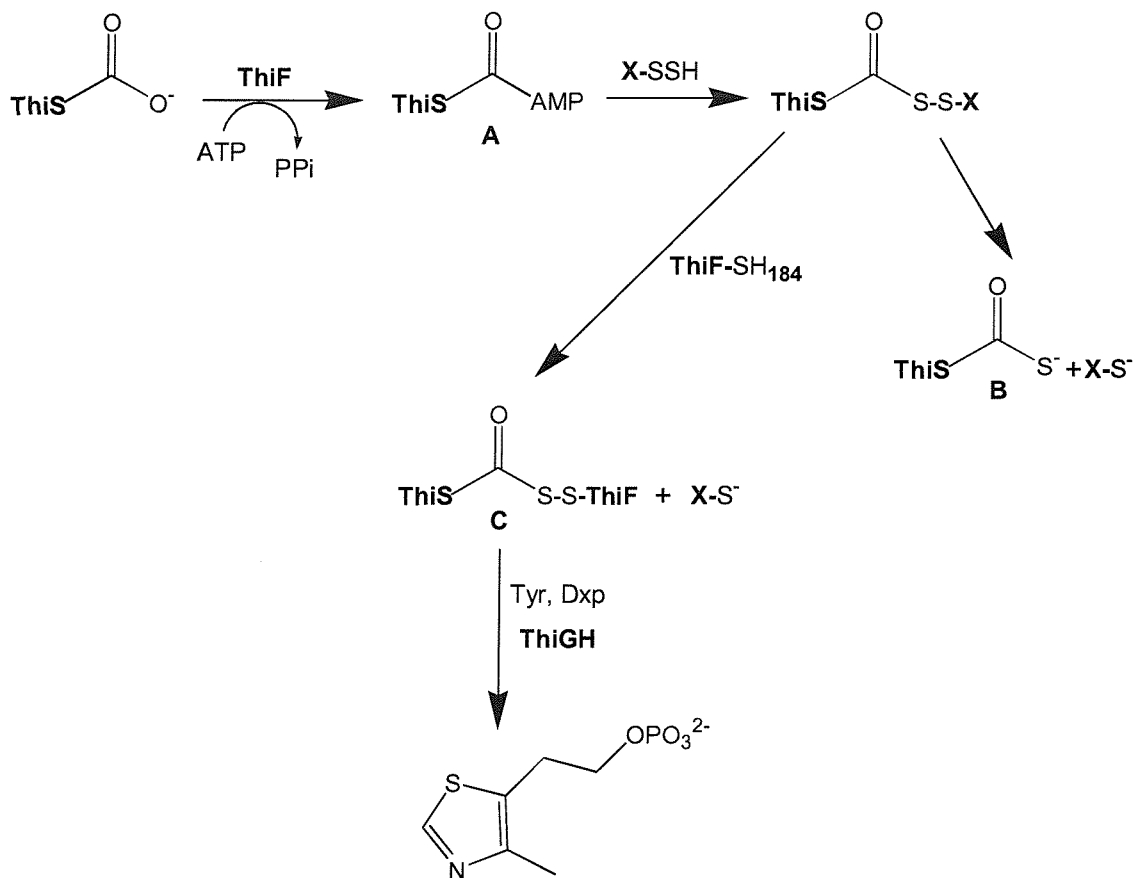
Both the *in vivo* and *in vitro* activities of ThiI have been recently shown to depend on two cysteine residues: Cys-456 and Cys-344 (77,78). Wright and co-workers have elegantly provided evidence that support the sequential sulphur transfer from IscS to Cys-456 of ThiI, and from Cys-456 to 4-thiouridine, via the formation of a disulphide bridge between Cys-456 and Cys-344, which has to be reduced to allow subsequent catalytic cycles (78) (**Scheme 1.9**).



Scheme 1.9. Representation of the sulphur transfer from Cys to a generic substrate, catalysed by IscS and ThiI. The resultant disulphide bridge in ThiI has to be reduced by a reductant (X) to allow subsequent catalytic cycles. The biosynthesis of 4-thiouridine has been shown to occur through this mechanism, and a similar mechanism might be operating in the biosynthesis of the thiazole moiety of thiamine. Adapted from (78).

As the IscS/Thil couple is also involved in thiamine biosynthesis, the sulphur insertion into the vitamin could occur *via* a similar mechanism, perhaps with the formation of a covalent ThiI/ThiS intermediate.

Once the C-terminal carboxylate of ThiS is adenylated by ThiF (**A**, **Scheme 1.10**), the sulphur atom can be transferred to this protein, but neither the donor nor the form of ThiS actually responsible for the sulphur insertion into the forming thiazole, have been conclusively identified. Initial investigations led Begley and co-workers to isolate ThiS thiocarboxylate (**B**), which was thought to be the actual sulphur carrier (71).

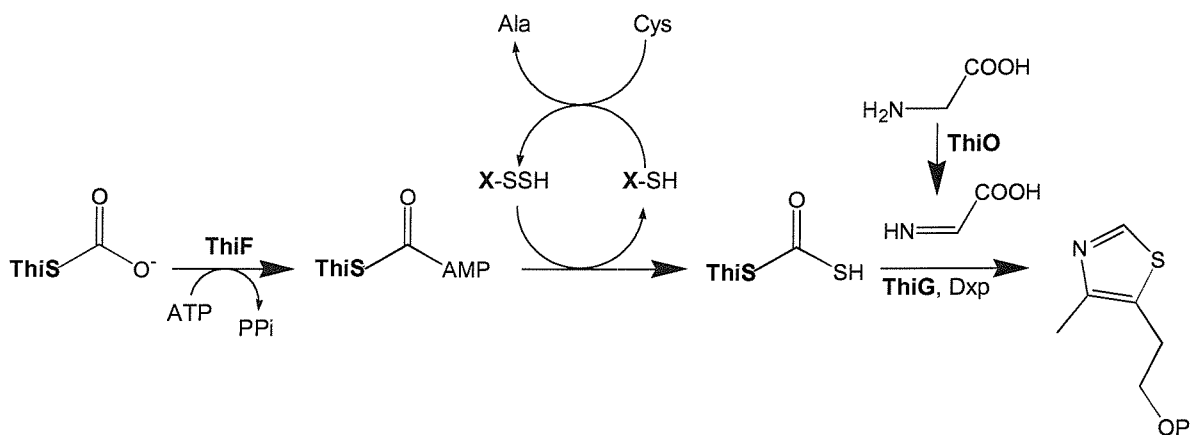


Scheme 1.10. Mechanism for the biosynthesis of the thiazole moiety of thiamine proposed by Begley (38). X was proposed to be IscS, but there is evidence to support a similar role played by ThiI, at least *in vivo*. Adapted by (38).

The formation of this intermediate in the thiazole biosynthesis was found to be conditional, *in vivo*, to the presence of ThiI, since ThiS-COSH could not be detected in a *thiI*⁻ strain. Lauhon and co-workers then successfully reconstituted *in vitro* the formation of ThiS-COSH, but showed that ThiI was not essential, although it stimulated the sulphur transfer from IscS to the activated ThiS (49). More recently, another intermediate in which ThiS thiocarboxylate is crosslinked to ThiF through an acyldisulphide bond has been isolated (38) (C). The ThiF cysteine residue involved in the linkage, Cys-184, is essential for thiazole biosynthesis, since in a *thiF*⁻ background, cells transformed with a plasmid encoding a ThiF(C184S) were unable to grow in the absence of thiazole. Interestingly, this mutation did not affect the *in vitro* formation of ThiS-COSH, which was produced at the same rate by both wild type ThiF and ThiF(C184S). These results led Begley and co-workers to suggest that the ThiFS crosslinked complex might be the ultimate sulphur donor in the thiazole biosynthesis (**Scheme 1.10**) in *E. coli*. Despite the identification of these intermediates, the sulphur transfer to any potential thiazole precursor, which could then undergo cyclisation, has not been as yet successfully reconstituted *in vitro*. Therefore in *E. coli*, the biological functions and origin of ThiS-COSH and the ThiFS complex remain to be elucidated, as well as the role played, *in vivo*, by ThiI.

ThiG and ThiH, the last two enzymes required for the formation of the thiazole ring, are likely to be involved in the last steps of the biosynthesis, a complex cyclisation reaction that would conceivably require sulphur transfer from the ThiFS conjugate (or ThiS-COSH) to Dxp, condensation with Tyr and cyclisation to the thiazole product. Relatively little is known about these enzymes, especially about ThiG. Searches for conserved domains in the ThiG sequence have revealed significant alignment with two proteins involved in histidine biosynthesis: N'-[(5'-phosphoribosyl)formimino]-5-aminoimidazole-4-carboxamide ribonucleotide isomerase (HisA) and the synthase (or cyclase) subunit of the imidazole glycerol phosphate synthase (HisF) (12). In particular, HisF catalyses the formation of the imidazole ring of histidine from an acyclic precursor which contains a Dxp-like moiety; thus future studies and further characterisation of ThiG may elucidate functional analogies between these enzymes (79,80).

A very recent study by Begley and co-workers, who successfully reconstituted *in vitro* thiazole biosynthesis in *Bacillus subtilis* (81), might support the role of cyclase for ThiG. *B. subtilis* shares some metabolic components with *E. coli*, including some of the biosynthetic proteins, ThiFSG, ThiI and NifS (an IscS ortholog), and two precursors, Dxp and Cys. ThiF and ThiS have been shown to have virtually identical functions to those of the *E. coli* enzymes, and the same might be for ThiG, which catalyses the condensation and cyclisation of the identified precursors to Thz-P (81) (**Scheme 1.11**). However, whilst *B. subtilis* depends upon ThiO, an oxygen dependent flavoenzyme, to utilize glycine to provide the C2-N3 fragment of the thiazole (13,36,82), *E. coli* and other enteric organisms use tyrosine to provide the C2-N3 unit and substitutes ThiO with an oxygen *sensitive* protein, ThiH (48,83). This suggests analogies, but also significant differences, in the biosynthetic strategies adopted by the two organisms to assemble the thiazole.



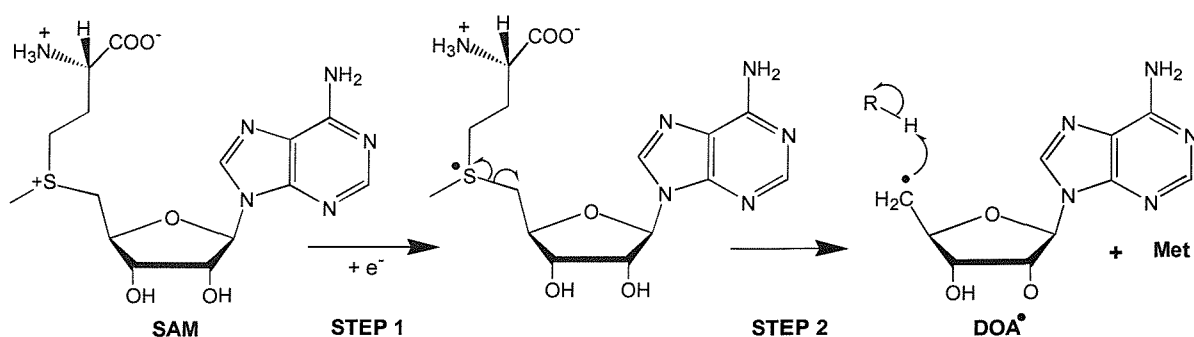
Scheme 1.11. Thiazole biosynthesis in *B. subtilis*. All four cysteine desulphurases (X), NifS, YrvO, NifZ and CSD, identified in the organism were able to transfer the sulphur atom from Cys to ThiS-COAMP *in vitro*. Adapted from (81).

On the basis of sequence similarities, ThiH has been classified as a member of the ‘radical SAM’ superfamily (84). All the members of this family have been shown or predicted to be Fe-S cluster enzymes requiring *S*-adenosyl methionine (SAM) for activity. A highly conserved cysteine triad, CxxxCxxC (**Figure 1.3**), has been identified amongst the over 600 potential SAM-dependent radical enzymes.

ThiH	83-94	N L C A N D C T Y C G F
BioB	51-62	G A C P E D C K Y C P Q
LipA	82-93	A I C T R R C P F C D V
ArrAE	24-31	S G C V H E C P G C Y N
PflAE	27-38	Q G C L M R C L Y C H N
Kam	131-142	N Q C S M Y C R Y C T R

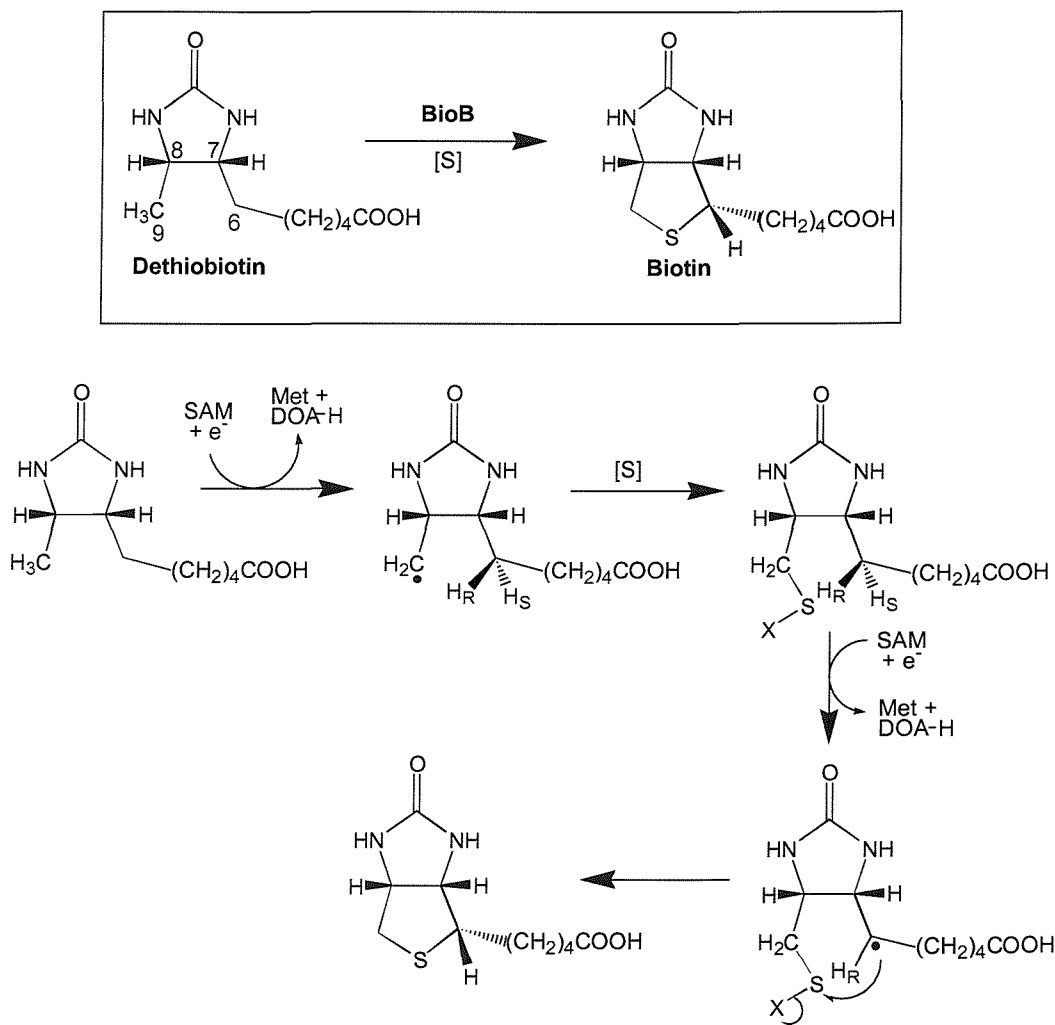
Figure 1.3. Alignment of *E. coli* ThiH with sequences from BioB, LipA, ArrAE and PflAE from *E. coli* and Kam from *Bacillus halodurans*.

This cysteine motif has been shown or supposed to provide the actual ligands for the Fe-S clusters within a number of well characterised family members such as lysine 2,3-amino mutase (Kam) (85,86), lipoyl synthase (LipA) (87,88), biotin synthase (BioB) (89,90), pyruvate formate-lyase activating enzyme (PflAE) (91) and anaerobic ribonucleotide reductase activating enzyme (ArrAE) (92). Kam, LipA, BioB, PflAE, ArrAE and others, depend on SAM for activity and catalyse Fe-S cluster-mediated radical reactions initiated by the formation of a transient 5'-deoxyadenosyl radical (DOA) (**Scheme 1.12**) (73,85,93,94).



Scheme 1.12. Reductive cleavage of SAM to the DOA radical and methionine. The DOA radical can then abstract a H atom from a suitable donor (R-H). Steps 1, 2 and/or the H atom abstraction may be concerted.

This radical, in turn, can abstract a hydrogen atom from either the protein backbone [as in PflAE (95-97) and ArrAE (98,99)] or from the substrate [as in Kam (86), BioB (100) and probably LipA (87,88)], generating another catalytically essential radical which leads to the formation of the respective products. **Scheme 1.13** outlines the reaction catalysed by BioB and the proposed mechanism for the sulphur insertion into dethiobiotin (100,101).



Scheme 1.13. Proposed mechanism for the BioB catalysed formation of biotin. Reductive cleavage of SAM by the $[4\text{Fe}-4\text{S}]^+$ cluster of the enzyme produces the DOA radical which abstracts a hydrogen from the methyl group of dethiobiotin. After the formation of the first C-S bond, a second DOA radical activates position 6 by abstracting the *proS* H, and cyclisation occurs. The source of sulphur, [S], has been proposed to be the cubane $[4\text{Fe}-4\text{S}]$ cluster of BioB (102,103). Adapted from (100).

Spectroscopic and biochemical evidence (85,94) obtained from studies on the characterised SAM-dependent radical enzymes, indicates that the DOA radical might derive directly from the reductive cleavage of SAM by the Fe-S centre, and several studies have now suggested that a $[4\text{Fe}-4\text{S}]^+$ cluster is essential for activity (88,97,99,104). Because of the oxidative degradation of the clusters during the purification (83,87,105-107), most of these Fe-S cluster proteins are isolated containing a mixture of $[2\text{Fe}-2\text{S}]$, $[3\text{Fe}-4\text{S}]$ and $[4\text{Fe}-4\text{S}]$ clusters; incubation with exogenous iron and sulphide increases the fraction of $[4\text{Fe}-4\text{S}]^{2+}$ clusters, but the reduced form can only be obtained by an enzymatic source of electrons, the NADPH/flavodoxin reductase/flavodoxin system (108-110), or by strong chemical reductants such as sodium dithionite or photoreduced deazaflavin (88,99,102,111). The so obtained $[4\text{Fe}-4\text{S}]^+$ clusters of Kam and PflAE have been recently shown to interact directly with SAM (112,113), and in the case of PflAE, the interaction occurs through the binding of this cofactor at the non-cysteinyl-ligated unique Fe site (112,114) (in these enzymes the cluster is chelated to three cysteines of the CxxxCxxC triad, whilst the fourth ligand has not been identified) (**Figure 1.4**). This direct interaction might provide an easier route to the reduction and homolytic scission of SAM (**Scheme 1.12**), which is predicted to be a common mechanistic feature to all the members of the radical SAM family.

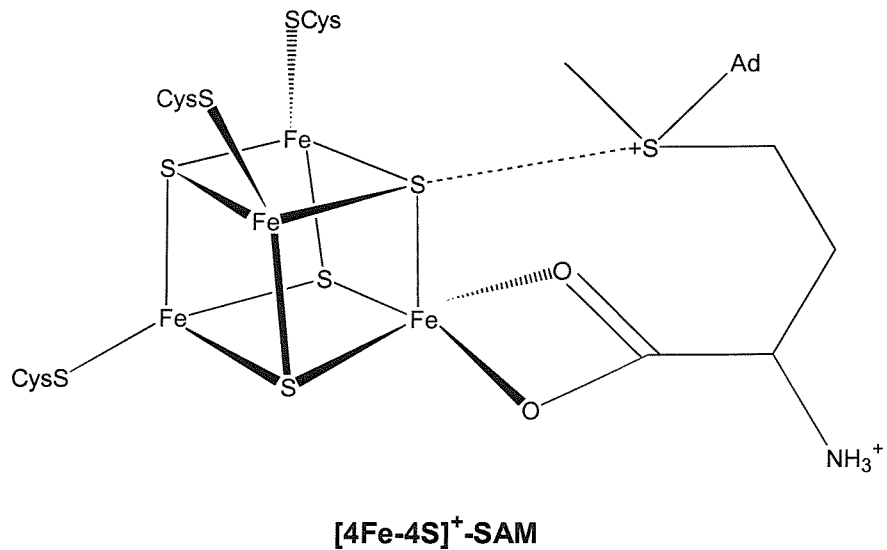


Figure 1.4. Model of the interaction of SAM with the $[4\text{Fe}-4\text{S}]^{2+/+}$ cluster of PflAE. Adapted from (112).

Besides including enzymes of known function, this family also includes several potential and as yet uncharacterised candidates such as ThiH. Interestingly, amongst the numerous members, the ThiH sequence most closely resembles that of BioB which catalyses a sulphur insertion reaction (**Scheme 1.13**). The intriguing possibility that ThiH could be mechanistically related to biotin synthase or to other SAM-dependent radical enzymes, thus suggesting a plausible role for this protein in the thiazole biosynthesis, stimulated our interest in this enzyme. This thesis describes the work which has led to the isolation and initial characterisation of a ThiGH complex, to the demonstration that it contains an oxygen sensitive Fe-S cluster associated with ThiH (83), and to the successful measurement, *in vitro*, of thiazole forming activity in an *E. coli* cell-free extract containing such a complex.

Chapter 2.

Expression Studies on ThiH

2.1. Introduction

The investigation of the mechanism through which the thiazole moiety of thiamine is assembled in *E. coli*, and possibly in other enteric bacteria (**Scheme 1.10**), required the expression and characterisation of ThiH, a potential Fe-S cluster protein (section 1.3.3). Initial attempts to express this protein confirmed its poor solubility and its marked tendency to form inclusion bodies, a finding that has already reported by others (40). This prompted us to consider possible solutions to the problem. The current chapter describes the different strategies employed with the objective of improving soluble ThiH expression.

The formation of inclusion bodies (insoluble aggregates) is a typical cellular response when large amounts of insoluble protein are produced, and it is particularly common when the expression is under the control of the strong T7 promoter (115). Misfolding is one of the main causes of protein aggregation and it can occur either during the assembly of the nascent polypeptide chain or as a consequence of protein unfolding induced by stress conditions, such as high temperatures (116). Relatively soluble proteins can be easily over-produced at 37 °C, yielding large amounts of enzyme after just 3 hours from the induction; conversely, the expression of insoluble proteins can be sometimes improved by lowering the expression temperature and the rate of protein synthesis, so that the cellular machinery can better cope with the unusual high expression of a certain polypeptide (117).

With the purpose of optimising the expression level of ThiH, different expression temperatures and different expression systems were investigated. In particular, plasmids were constructed to allow the co-expression of ThiH with other thiamine biosynthetic enzymes and with proteins shown, in several cases, to increase the solubility of eukaryotic and bacterial target polypeptides: GroESL (115,118-120), thioredoxin 1 (115,118) and the proteins encoded by the *isc* (iron-sulphur cluster) operon, IscSUA, HscAB and Fdx (121-123).

GroEL (57 kDa) is a ATP-dependent chaperonin which catalyses protein folding, both *in vivo* and *in vitro*, by providing a physically defined compartment where proteins can complete their folding process (Figure 2.1). This cylindrical compartment is formed by two GroEL homo-heptameric rings, stacked back to back (116,124). Within this cavity the protein folding is assisted by another homo-heptameric ring constituted by GroES subunits (10 kDa), which binds to the GroEL complex. The over-expression of a recombinant protein can easily overwhelm the machinery of molecular chaperons in the bacterial host, that is why the co-expression of a target protein with the GroEL/GroES complex could potentially increase its solubility.

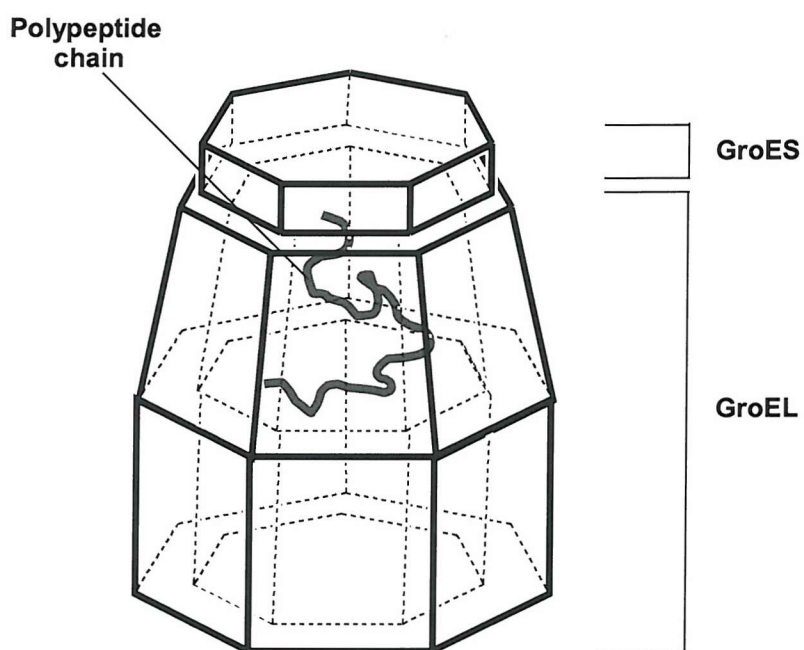
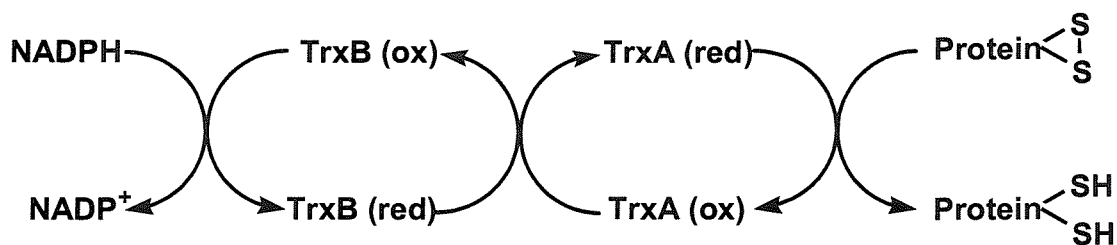


Figure 2.1. Schematic representation of the cylindrical cavity created by the GroEL/GroES complex, and inside which newly synthesised polypeptide chains can complete their folding.

E. coli TrxA or thioredoxin 1 (125) is a small protein (12 kDa) with a low redox potential of -270 mM (126), whose function is to reduce the disulphide bridges in cytoplasmic proteins, such as ribonucleotide reductase (127), which become oxidised as part of their catalytic cycle, and must therefore be reduced to continue functioning

(Scheme 2.1). In a bacterial cell, the formation of S-S bridges is normally confined to the periplasmic space, since the cytoplasmic environment is kept highly reducing by the large amounts of reduced glutathione present (126,128). But occasionally, when *E. coli* cells are grown aerobically, undesired formation of disulphide bonds may occur in cytoplasmic proteins, thus inactivating them or causing misfolding and aggregation. Co-expression of recombinant proteins with TrxA is often employed to improve the solubility of eukaryotic proteins expressed in *E. coli* as TrxA provides a more reducing cellular environment similar to that found in eukaryotic cells (118).



Scheme 2.1. Redox cycle through which TrxB (thioredoxin reductase) and TrxA catalyse the reduction of disulphide bridges formed in cytoplasmic proteins.

The proteins encoded by the *iscRSUA-hscBA-fdx* (Figure 2.2) operon assist Fe-S cluster assembly *in vivo*, a key step in the post-translational maturation of Fe-S cluster proteins (53,129). More specifically, IscSUA, HscBA and Fdx directly participate in the assembly reaction, whilst IscR acts as a transcriptional repressor of the operon (130). IscS (45 kDa), already introduced in section 1.3.3, catalyses the removal of sulphur from cysteine. The so formed persulphide, in the active site of IscS, transfers the sulphur atom to IscU (14 kDa) which, in turn provides a scaffold for the assembly of an unstable [2Fe-2S] or [4Fe-4S] cluster (131,132). In addition to IscU, IscA (13 kDa) can also assemble an unstable [2Fe-2S] cluster (133,134); these transient clusters are then probably transferred to apo acceptor proteins. The insertion of a cluster into a specific target may require HscA (66 kDa) and HscB (20 kDa), molecular chaperones which exhibit sequence similarity to DnaK and the co-chaperone DnaJ, respectively (135). HscA and HscB have been shown to interact with IscU (136,137),

although the biological relevance and function of this and other interactions observed *in vitro* amongst the Isc proteins, remain to be elucidated (138). Finally, Fdx is an adrenodoxin-type ferredoxin containing a stable [2Fe-2S] cluster, which might act as electron donor in a still unknown step of the cluster assembly (139).



Figure 2.2. Genes constituting the *isc* operon: *iscR* (486 bp), *iscS* (1233 bp), *iscU* (384 bp), *iscA* (321 bp), *hscB* (515 bp), *hscA* (1848 bp), *fdx* (333 bp).

Fe-S cluster biosynthetic machinery may be required for the assembly and maintenance of the potential Fe-S centre in ThiH (48), and an insufficiency of this machinery could be the reason for ThiH's instability and tendency to aggregate. Therefore, the co-expression of this enzyme with the Isc proteins, as well as with GroESL and TrxA, was investigated.

2.2. Results and Discussion

All plasmids described in this chapter are listed in **Table 2.1**.

Name	Insert	Parental Plasmid
pRL200	<i>Nde</i> 1/ <i>Bam</i> H1 <i>thiH</i>	pET-24a(+)
pRL220, pRL220*	<i>Nco</i> 1/ <i>Xho</i> 1 <i>thiH</i>	pBAD/HisA
pRL221	<i>Nco</i> 1/ <i>Xho</i> 1 <i>thiH</i> , <i>Xho</i> 1/ <i>Eco</i> R1 <i>groELS</i>	pBAD/HisA
pRL222	<i>Nco</i> 1/ <i>Xho</i> 1 <i>thiH</i> , <i>Xho</i> 1/ <i>Eco</i> R1 <i>trxA</i>	pBAD/HisA
pRL400	<i>Nco</i> 1/ <i>Bam</i> H1 <i>thiGH</i>	pET-24d(+)
pRL800	<i>Nco</i> 1/ <i>Bam</i> H1 <i>thiGH-His</i>	pET-24d(+)
pRL820	<i>Nco</i> 1/ <i>Xho</i> 1 <i>thiGH-His</i>	pBAD/HisA
pRL821	<i>Nco</i> 1/ <i>Xho</i> 1 <i>thiGH-His</i> , <i>Xho</i> 1/ <i>Eco</i> R1 <i>iscSUA-hscBA-fdx</i>	pBAD/HisA
pRL1000	<i>Nco</i> 1/ <i>Bam</i> H1 <i>thiFSGH-His</i>	pET-24d(+)
pRL1020	<i>Nco</i> 1/ <i>Xho</i> 1 <i>thiFSGH-His</i>	pBAD/HisA
pRL1021	<i>Nco</i> 1/ <i>Xho</i> 1 <i>thiFSGH-His</i> , <i>Xho</i> 1/ <i>Eco</i> R1 <i>iscSUA-hscBA-fdx</i>	pBAD/HisA
pRL1300	<i>Nco</i> 1/ <i>Xho</i> 1 <i>thiCEFSGH-His</i>	pBAD/HisA
pRL1500	<i>Nco</i> 1/ <i>Xho</i> 1 <i>thiEFSGH-His</i>	pBAD/HisA

Table 2.1. List of plasmids whose construction is herein described. A complete list of all the assembled plasmids can be found in Appendix A.

2.2.1. *pRL200 and pRL220: T7 Compared with araBAD Promoter*

It had already been reported that ThiH expressed from a pET-derived plasmid was highly insoluble (40), therefore a different expression system was considered. pRL200 and pRL220 were the first plasmids assembled to investigate the expression

level of ThiH (Figure 2.3). Both plasmids carry *thiH* (1.1 kbp), but the gene expression is controlled by the T7 promoter in pRL200 (pET-24a(+) derivative) and by the *araBAD* promoter in pRL220 (pBAD/HisA derivative, Table 2.1).

pRL200 was transformed into *E. coli* BL21(DE3) which encodes the T7 RNA polymerase, and pRL220 was initially transformed into *E. coli* LMG194. With the purpose of comparing promoters of different strength and different induction conditions, these cells were grown in 2YT medium and induced at 28 °C with increasing concentrations of inducer, IPTG and L-arabinose, respectively.

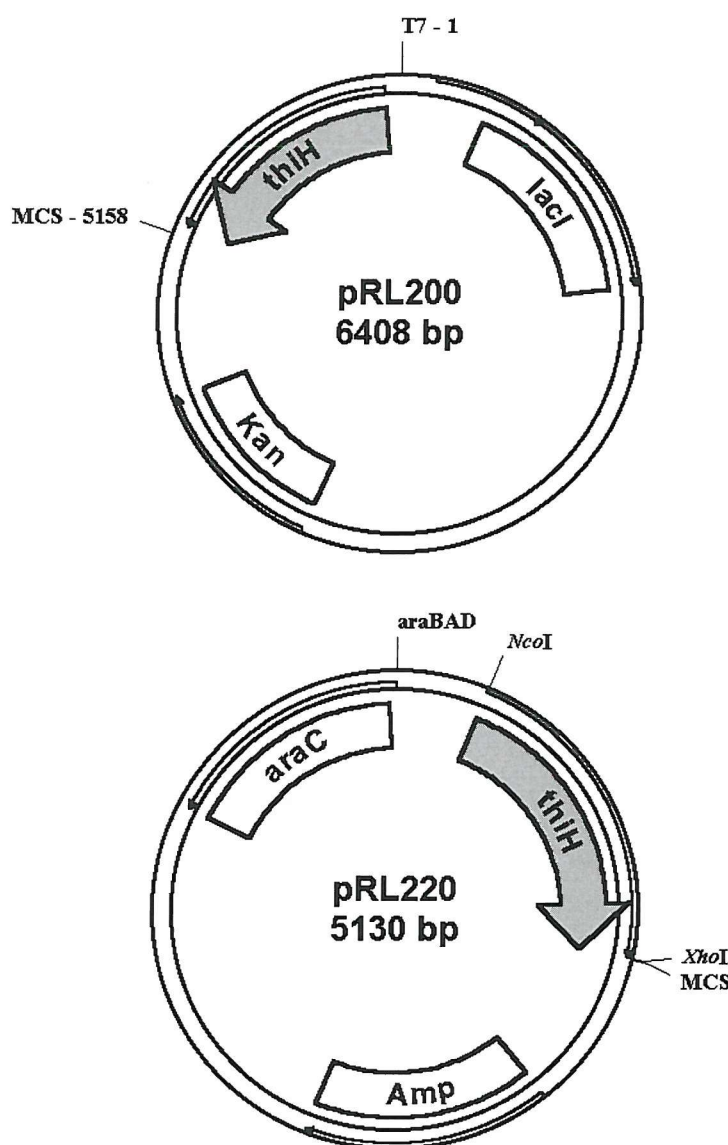


Figure 2.3. Maps of pRL200 and pRL220, not to scale. MCS = Multiple Cloning Site.

SDS-PAGE analysis of soluble and insoluble fractions from both strains revealed that a comparable amount of soluble ThiH was produced, regardless of either promoter or inducer concentration (**Figure 2.4**); conversely, the amount of insoluble protein was shown to be clearly dependant upon the strength of the promoter and slightly less sensitive to the inducer concentration (**Figure 2.5**). This was particularly true for the leaky pET system, from which expression was obtained even in the absence of inducer (lane 5, **Figure 2.5**).

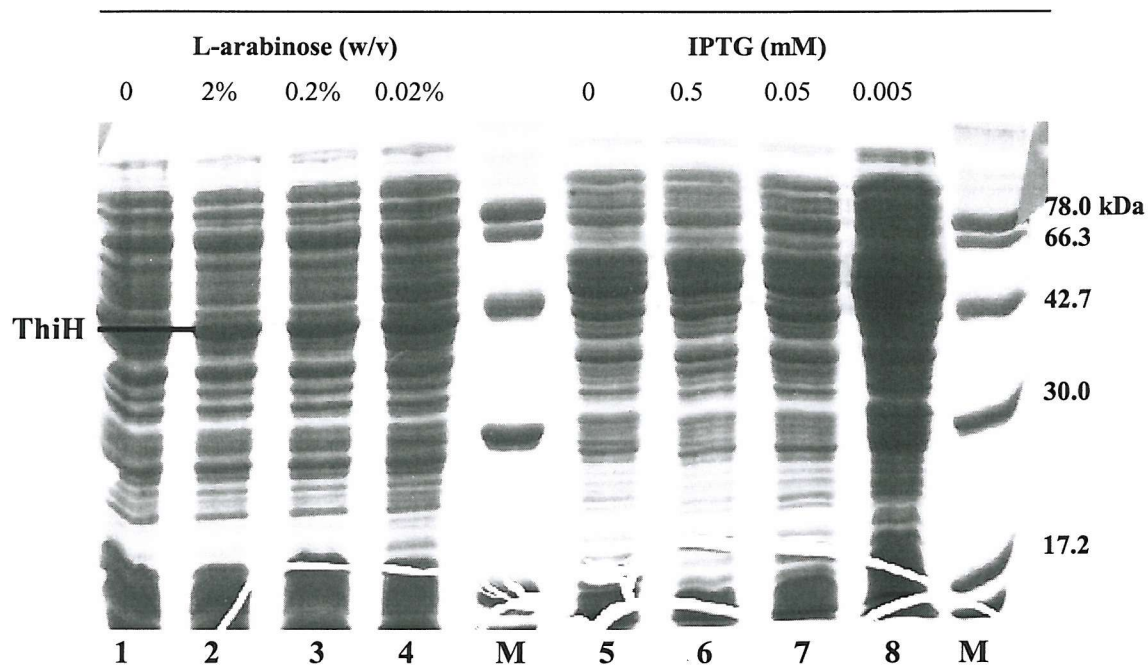


Figure 2.4. Coomassie Blue stained 15 % SDS-PAGE gel of soluble proteins produced by pRL220/LMG194 (lanes 1-4) and pRL200/BL21(DE3) (lanes 5-8) after induction with increasing concentrations of L-arabinose or IPTG, as indicated. M = molecular weight marker.

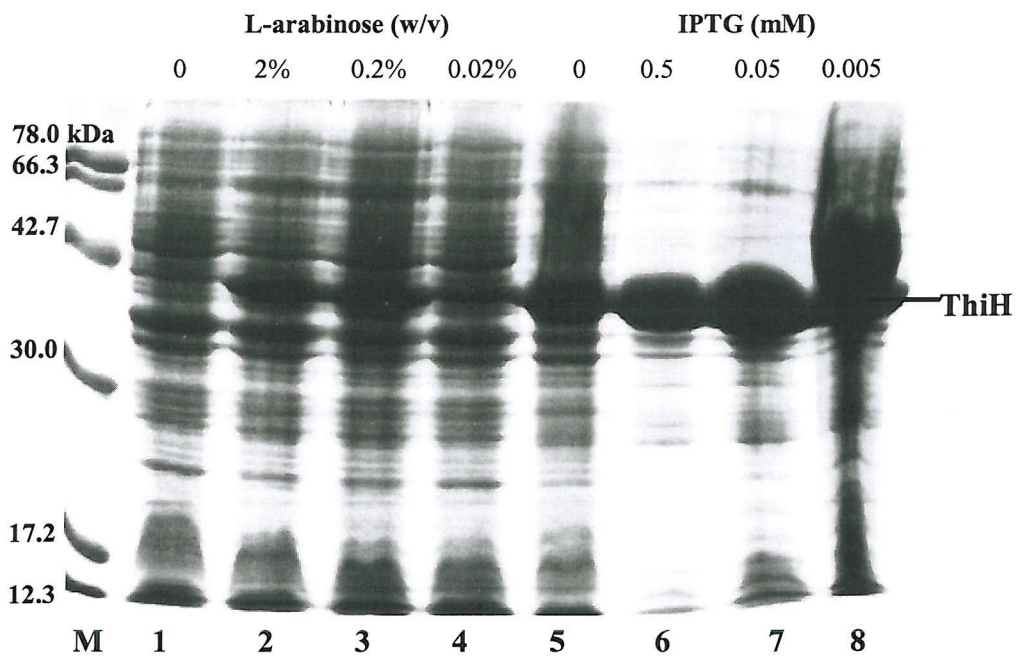


Figure 2.5. Coomassie Blue stained 15 % SDS-PAGE gel of insoluble proteins produced by pRL220/LMG194 (lanes 1-4) and pRL200/BL21(DE3) (lanes 5-8) after induction with increasing concentrations of L-arabinose or IPTG, as indicated. M = molecular weight marker.

2.2.2. *pRL221 and pRL222: Co-expression of ThiH with GroEL/GroES and TrxA*

As the strength of the promoter did not seem to affect the solubility of ThiH, two more plasmids were assembled carrying *thiH* in combination with *groESL* and *trxA*. Plasmids harbouring *groESL* (2.0 kbp) and *trxA* (360 bp) between the 5' *Xho*1 and 3' *Eco*R1 restriction sites were assembled by L. Peters (123). These fragments were excised and subcloned into *Xho*1/*Eco*R1 restricted pRL220, resulting in pRL221 and pRL222, respectively (Figure 2.6). To ensure high expression level of these downstream genes, an additional ribosome binding site was introduced by PCR between the 5' *Xho*1 site and the start codon.

pRL221 and pRL222 were transformed into both BL21(DE3) and LMG194. These cells, pRL220/BL21(DE3) and pRL220/LMG194 were grown in parallel, and the ThiH expression level compared at 15, 22 and 37 °C.

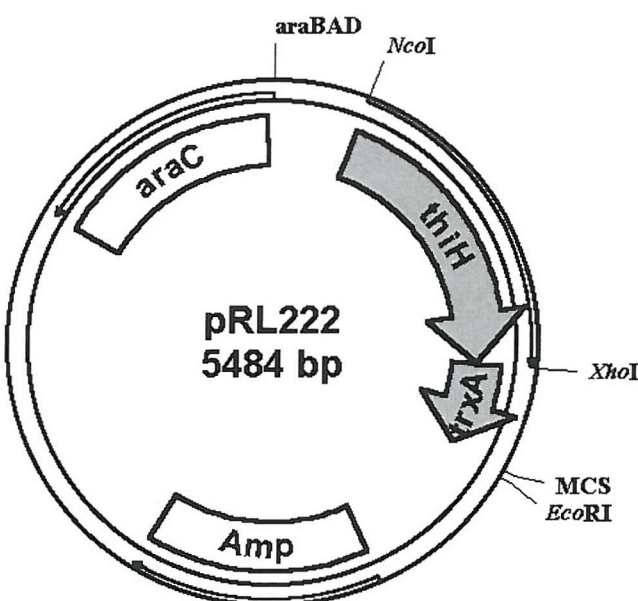
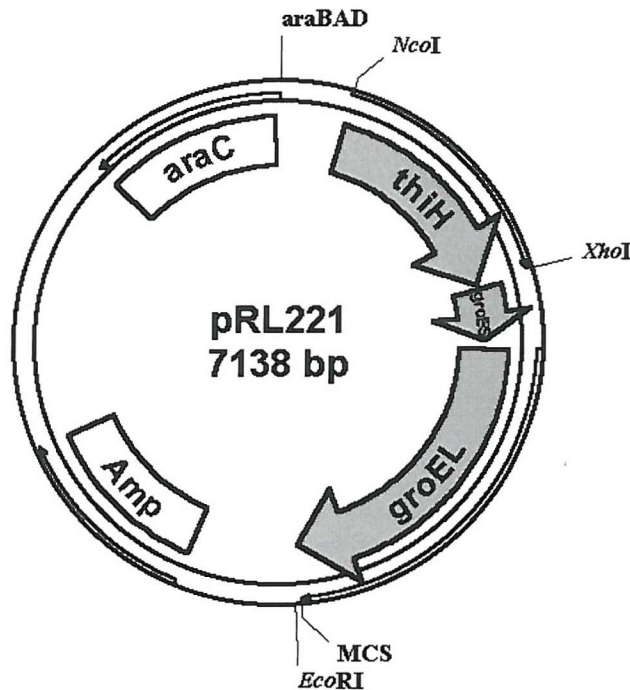


Figure 2.6. Maps of pRL221 and pRL222, not to scale. MCS = Multiple Cloning Site.

Analysis of cleared lysates and cell pellets by SDS-PAGE led to the following conclusions: i) at a certain temperature, and provided the cells contained the same plasmid, the *E. coli* strain made little or no difference to the expression level; ii) there was no increase in the amount of soluble ThiH when co-expressed with GroEL/ES or TrxA, at any of the tested temperatures; iii) variations of temperature between 15°C (Figure 2.7) and 37 °C (Figure 2.8) did not affect the level of soluble protein expression. However higher temperatures did result in increasing amounts of insoluble ThiH and GroEL. GroEL (57 kDa) is clearly visible on a 15 % SDS-PAGE gel, whilst GroES (14 kDa) and Trx (12 kDa) migrated too quickly and were not observed.

These results indicated that neither the formation of unusual disulphide bonds nor a GroEL/ES correctable misfolding, were the principle cause of ThiH poor solubility, unaffected by factors such as promoter strength, bacterial strain, temperature and co-expression with accessory proteins.

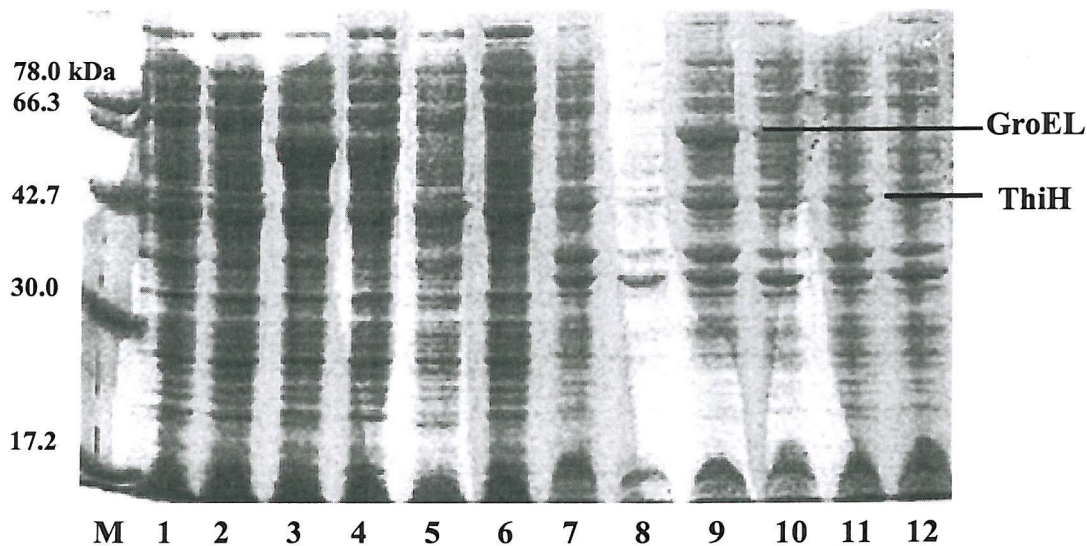


Figure 2.7. Coomassie Blue stained 15 % SDS-PAGE gel of soluble (lanes 1-6) and insoluble (lanes 7-12) proteins produced at 15 °C by pRL220/LMG194 (lanes 1, 7), pRL220/BL21(DE3) (lanes 2, 8), pRL221/LMG194 (lanes 3, 9), pRL221/BL21(DE3) (lanes, 4, 10), pRL222/LMG194 (lanes 5, 11) and pRL222/BL21(DE3) lanes (6, 12). M = molecular weight marker.

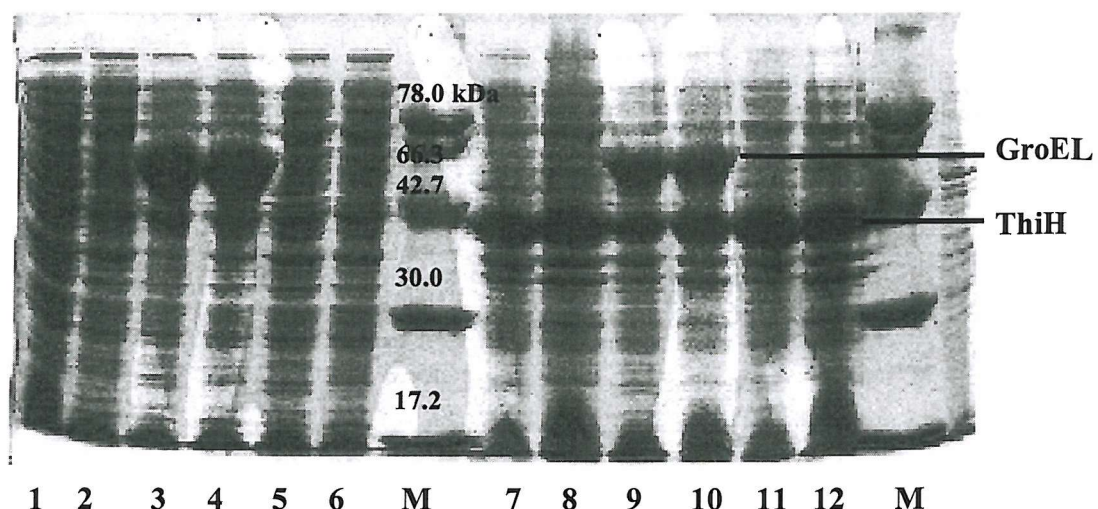


Figure 2.8. Coomassie Blue stained 15 % SDS-PAGE gel of soluble (lanes 1-6) and insoluble (lanes 7-12) proteins produced at 37 °C by pRL220/LMG194 (lanes 1, 7), pRL220/BL21(DE3) (lanes 2, 8), pRL221/LMG194 (lanes 3, 9), pRL221/BL21(DE3) (lanes, 4, 10), pRL222/LMG194 (lanes 5, 11) and pRL222/BL21(DE3) lanes (6, 12). M = molecular weight marker.

2.2.3. *Mutations in thiH: Assembling of pRL220**

DNA sequencing of pRL220 revealed the presence of four mutations in *thiH*. As these DNA mutations were not conservative, *thiH* was amplified again using Pfu Turbo, a DNA polymerase which possesses a 3'-5' exonuclease activity (proofreading activity), and therefore, a reduced rate of base misincorporation with respect to the previously used Taq polymerase.

A new pBAD-derived plasmid, otherwise identical to pRL220 (Figure 2.3), was assembled and it was named pRL220*. As the insolubility of ThiH could have been caused by a structural instability due to these mutations, the expression experiment described in section 2.2.1 was repeated at 22 °C, and the ThiH expression from pRL220*/LMG194 and pRL200/BL21(DE3) compared (Figures 2.10 and 2.11, lanes 1-2). The results confirmed previous observations, i.e. different strains and different

promoters made very little difference to the expression level of soluble ThiH, indicating that the presence of the mutations was not the main cause of ThiH poor solubility.

All the subsequent amplifications were carried out by using Pfu Turbo.

2.2.4. *pRL400: Co-expression of ThiH with ThiG*

Begley and co-workers reported that ThiF and ThiS, co-expressed from a pET-derived plasmid, co-eluted through several purification steps, suggesting the formation of a ThiFS complex (71). This finding led us to investigate the co-expression of ThiH with other thiamine biosynthetic enzymes, and pRL400, a pET-derived plasmid harbouring the *thiGH* (1.9 kbp) subsection of the *thiCEFSGH* operon was assembled (Figure 2.9).

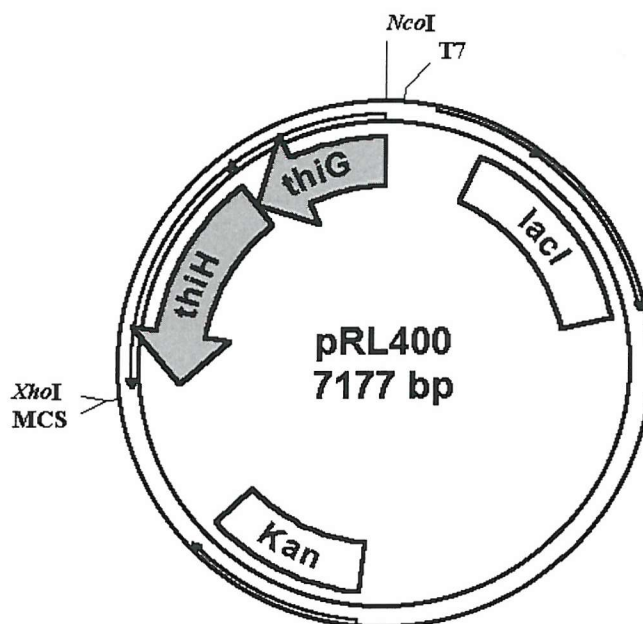


Figure 2.9. Map of pRL400. MCS = Multiple Cloning Site.

This plasmid was transformed into BL21(DE3) and the expression level of soluble ThiH from these cells and from pRL200/BL21(DE3) (section 2.2.1) was compared at 22 and 37 °C (Figure 2.10). SDS-PAGE analysis revealed that more ThiH was accumulated in pRL400/BL21(DE3) cleared lysate, and confirmed that temperature variations had little effect on the amount of soluble protein. Proteins produced as insoluble aggregates are shown in Figure 2.11.

These results indicated that the co-expression with ThiG produced an increase in the solubility of ThiH, consistent with the existence of some sort of stabilising effect exerted by ThiG. It is likely that this stabilization effect was acting at a protein level, rather than at a mRNA level, since *thiH* could be translated in large amounts, as indicated by the presence of inclusion bodies. The gels also showed that ThiG (27 kDa) and ThiH were present in comparable amounts in both the soluble and insoluble cell fractions.

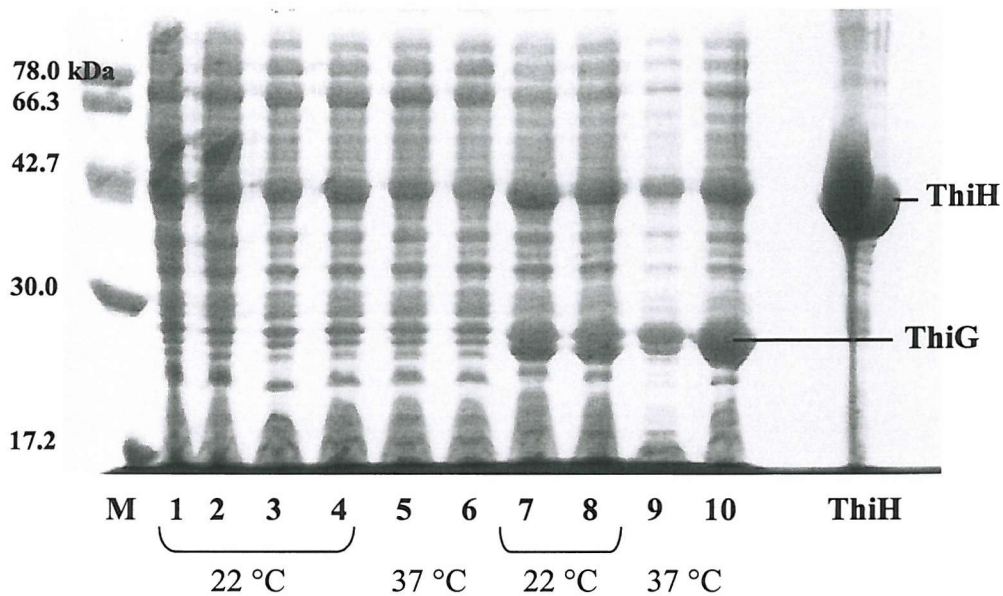


Figure 2.10. Coomassie Blue stained 15 % SDS-PAGE gel of soluble proteins expressed at 22 °C (lanes 1-4, 7-8) and 37 °C (lanes 5-6, 9-10) from pRL220*/LMG194 (lanes 1, 2) pRL200/BL21(DE3) (lanes 3-6) and pRL400/BL21(DE3) (lanes 7-10). Experiments were carried out in duplicate. M = molecular weight marker.

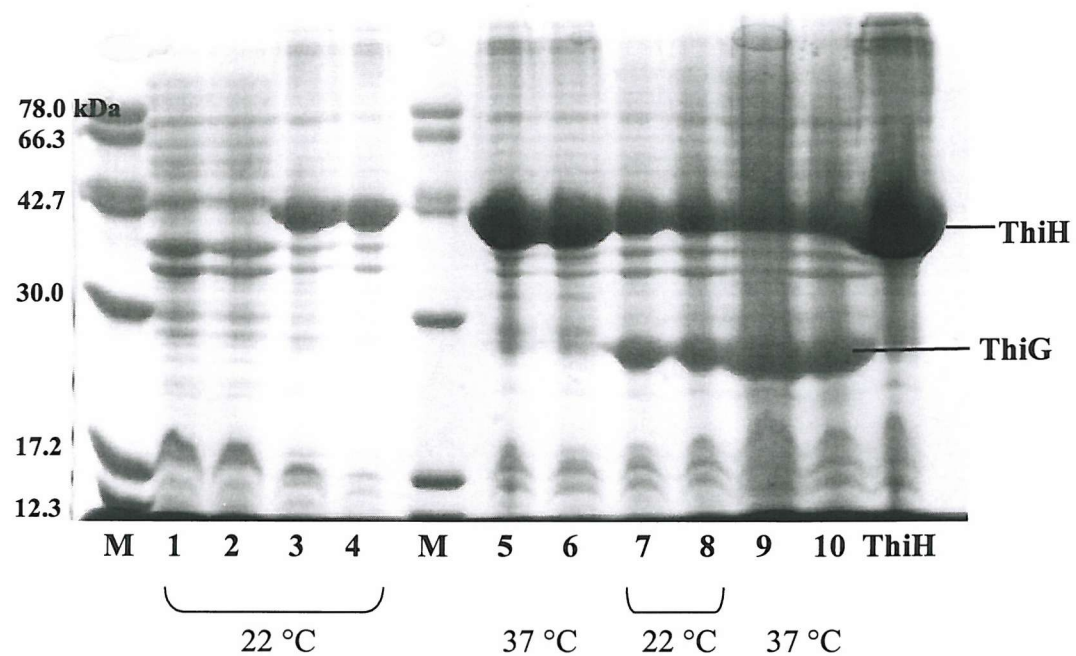
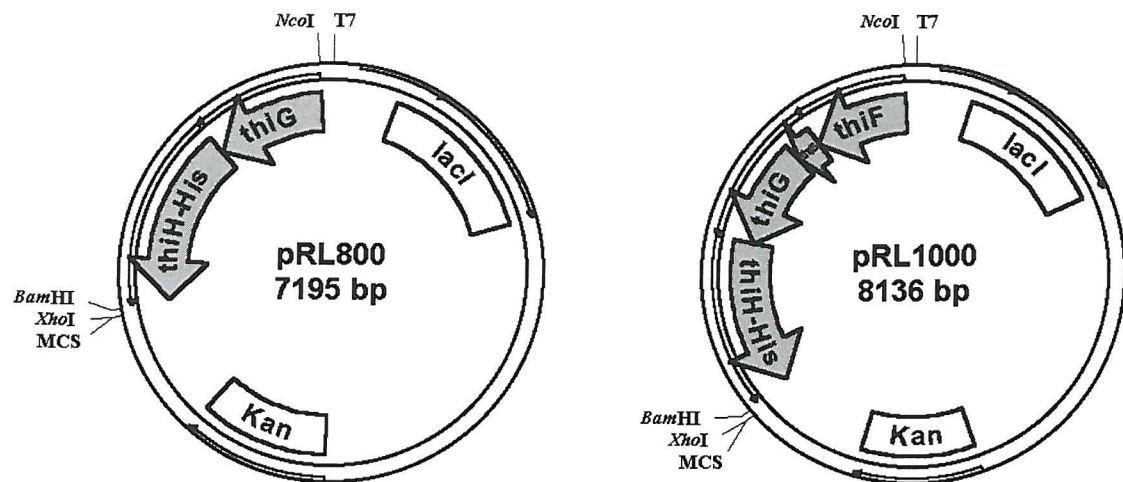


Figure 2.11. Coomassie Blue stained 15 % SDS-PAGE gel of insoluble proteins expressed at 22 °C (lanes 1-4, 7-8) and 37 °C (lanes 5-6, 9-10) from pRL220*/LMG194 (lanes 1, 2) pRL200/BL21(DE3) (lanes 3-6) and pRL400/BL21(DE3) (lanes 7-10). Experiments were carried out in duplicate. M = molecular weight marker.

2.2.5. *pRL800/820 and pRL1000/1020: Co-expression of Hexahistidine-tagged ThiH with ThiG and ThiFSG*

Despite the success of the ThiGH co-expression strategy, the absolute amount of ThiH produced by pRL400/BL21(DE3) was accounting for just 4-6 % of the total soluble proteins, as estimated by gel densitometry. In order to simplify the isolation of such a small amount of protein, pRL800 (Figure 2.12) was assembled, encoding ThiG and a C-terminal hexahistidine-tagged ThiH (ThiH-His). The expression of hexahistidine-tagged proteins and their subsequent isolation by metal-affinity chromatography, has been a successfully employed strategy for the purification of a number of well characterised Fe-S cluster enzymes (88,89,140,141).



NcoI/XbaI restriction
and subcloning into
pBAD/HisA

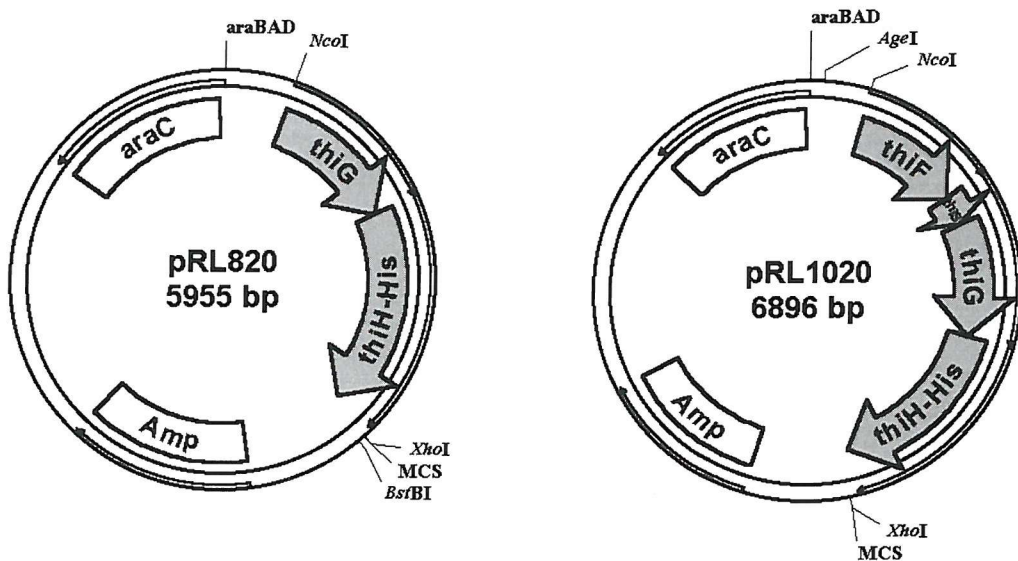


Figure 2.12. Maps of pRL800, pRL1000 and the respective derivatives pRL820 and pRL1020, not to scale. MCS = Multiple Cloning Site.

To further explore the potentiality of the co-expression strategy, besides *thiGH-His*, a larger subsection of the *thiCEFSGH* operon, *thiFSGH-His* (2.9 kbp), was amplified and cloned into pET-24d(+). The resulting plasmid was named pRL1000. pRL800 and pRL1000 were transformed into BL21(DE3), and the ThiH expression level from these cells and from pRL400/BL21(DE3) (section 2.2.4) was compared at 28 °C (Figure 2.13).

The analysis of cleared lysates and pellets by SDS-PAGE showed that all the samples produced comparable amounts of both ThiG and ThiH, regardless of the co-expression with ThiFS or the presence of the hexahistidine tag in ThiH. ThiG and ThiF have very close molecular weights (27 kDa), and ThiF was more clearly visible in the insoluble fraction from pRL1000/BL21(DE3) (lane 9, Figure 2.13), just above ThiG. ThiS (7 kDa) was not detected, as it either migrated too quickly or ran as a diffuse band on the 15 % gel. However the expression of ThiS from pRL1000/BL21(DE3) was indirectly confirmed by subsequent experiments described in section 4.2.4.

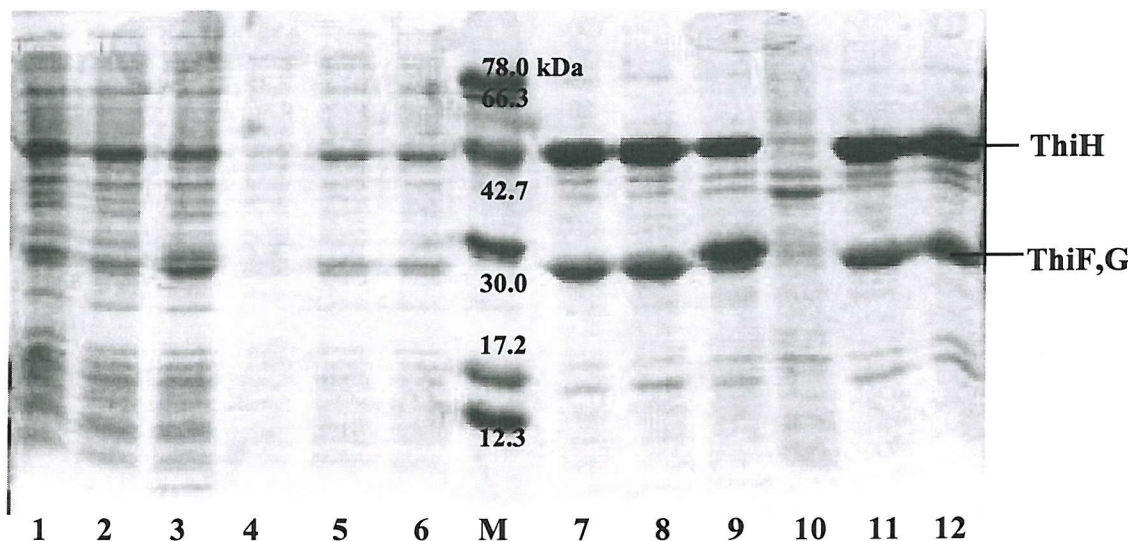


Figure 2.13. Coomassie Blue stained 15 % SDS-PAGE gel of soluble (lanes 1-6) and insoluble (lanes 7-12) proteins expressed from pRL400/BL21(DE3) (lanes 1-2, 7-8), pRL800/BL21(DE3) (lanes 3-4, 9-10) and pRL1000/BL21(DE3) (lanes 5-6, 11-12) at 28 °C. The experiment was carried out in duplicate. M = molecular weight marker.

These initial results seemed to indicate that ThiF and ThiS were not enhancing the soluble expression level of ThiH. However, when the expression experiments were scaled up, from 10 ml to 5 l cultures, a dramatic difference between pRL800 and pRL1000 became evident: whilst pRL800/BL21(DE3) cells grew poorly after the induction, consistently yielding 5-15 g of cell paste, an improved yield of pRL1000/BL21(DE3) biomass (25-30 g) could routinely be obtained.

In addition to the yield, samples of ThiGH-His complex isolated from pRL800/BL21(DE3) showed different characteristics from samples isolated from pRL1000/BL21(DE3) (sections 3.2.2-3.2.5), suggesting that the presence of ThiFS was, in some way, affecting the assembly of the ThiGH-His complex.

Two other plasmids, pRL820 and pRL1020 were subsequently obtained by excising *thiGH-His* and *thiFSGH-His* from pRL800 and pRL1000, respectively, and subcloning the fragments into *Nco1/Xho1* restricted pBAD/HisA (**Figure 2.12**). These two plasmids were originally assembled solely to complete the series of pET- and pBAD-derived plasmids. However, due to the comparable ThiGH-His expression level and to a slightly improved yield in cell paste with respect to pRL1000/BL21(DE3), pRL1020/BL21(DE3) became the expression system of choice for the large scale production and subsequent purification of the ThiGH-His complex. pRL820 was not routinely used for expression experiments, but it was found useful as intermediate in the construction of pRL821 (section 2.2.6) (**Figure 2.15**), and a ThiGH-His sample isolated from pRL820/BL21(DE3) was also characterised (sections 3.2.2 and 3.2.4).

Figure 2.14 summarises the main findings on ThiH (or ThiH-His) solubility as influenced by the co-expression with other thiamine biosynthetic enzymes.

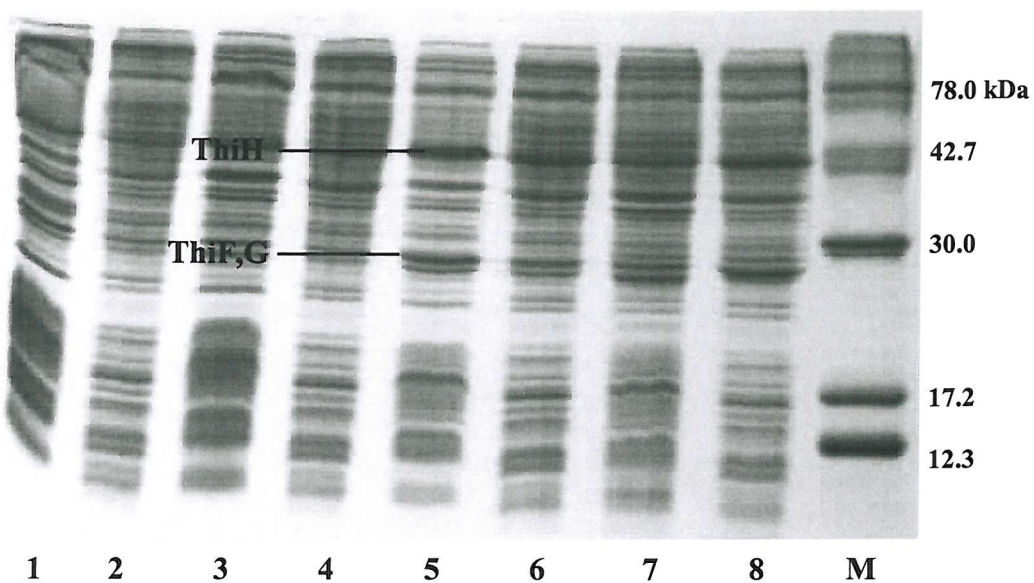


Figure 2.14. Coomassie Blue stained 15 % SDS-PAGE gel of soluble proteins expressed from pET-24d(+)/BL21(DE3) (lane 1), pBAD/HisA/BL21(DE3) (lane 2), pRL200/BL21(DE3) (lane 3), pRL220*/BL21(DE3) (lane 4), pRL800/BL21(DE3) (lane 5), pRL820/BL21(DE3) (lane 6), pRL1000/BL21(DE3) (lane 7) and pRL1020/BL21(DE3) (lane 8) at 28 °C. M = molecular weight marker.

2.2.6. *pRL821: Co-expression of ThiGH-His with the Isc Proteins*

pRL821 was assembled to investigate the effect of the Isc proteins, IscSUA-HscBA-Fdx (section 2.1), on the soluble expression level of ThiGH-His (Figure 2.15). The plasmid harbouring *iscSUA-hscBA-fdx*, pMK400 (123), was constructed by Dr. M. Kriek in our laboratory. Suitable restriction sites for subcloning this insert into a *thiGH-His*-carrying plasmid were found in pRL820. The resultant *pRL821* was transformed into BL21(DE3). Figure 2.16 shows the proteins accumulated in pRL800/BL21(DE3) and pRL821/BL21(DE3) cleared lysates and pellets, compared after two independent large scale expression experiments. Due to the closeness of ThiH-His and IscS (45 kDa) molecular weights, it was not possible to estimate any potential difference in the expression level of ThiH-His; ThiG expression level did not seem to have been affected, but this protein is not expected to bear an Fe-S cluster.

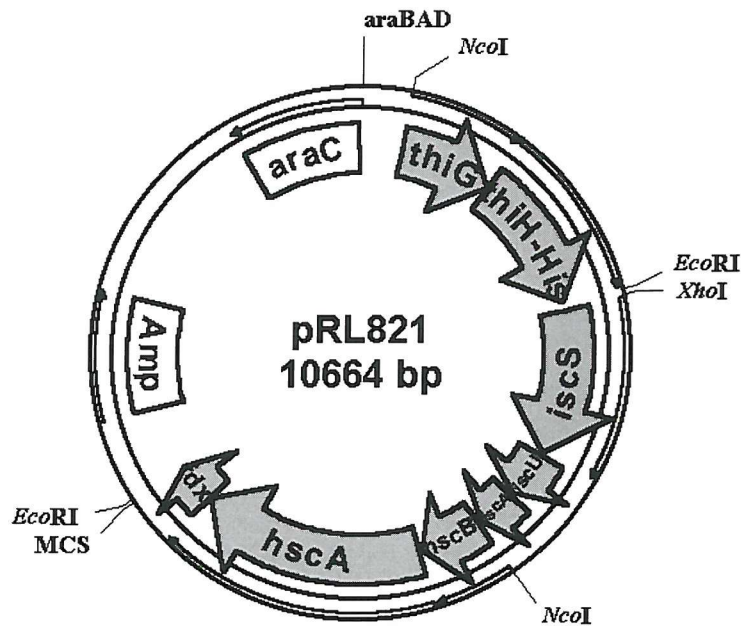


Figure 2.15. Map of pRL821. MCS = Multiple Cloning Site.

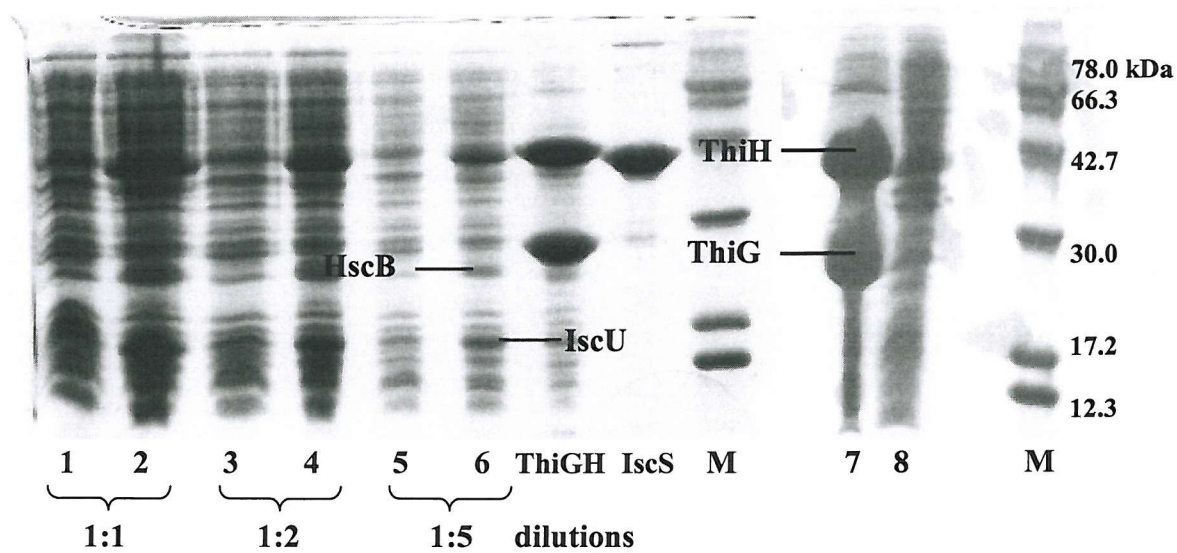


Figure 2.16. Coomassie Blue stained 15 % SDS-PAGE gel of soluble (lanes 1-6) and insoluble proteins (7-8) expressed from pRL800/BL21(DE3) (odd lanes) and pRL821/BL21(DE3) (even lanes) at 28 °C. Samples in lanes 3-4 and 5-6 were 1:2 and 1:5 dilutions, respectively, of samples loaded on lanes 1-2. M = molecular weight marker.

As very little information could be obtained from the comparison of the expression levels, ThiGH-His, expressed from pRL821/BL21(DE3) was purified and characterised (sections 3.2.2-3.2.3). The difference in the amount of insoluble proteins produced from pRL800/BL21(DE3) and pRL821/BL21(DE3) (lanes 7-8 **Figure 2.16**) is highly likely to be due to the different promoter's strength, and it was observed in other experiments (section 2.2.1). With regard to the other enzymes encoded by pRL821, the overall expression of these proteins is very similar to that reported by Kriek and co-workers (123).

2.2.7 pRL1021: Co-expression of *ThiFSGH-His* with the *Isc* Proteins

pRL1021 was one of the last plasmids to be assembled (**Figure 2.17**). It was obtained by restricting pRL1020 with *AgeI* and *XhoI* to excise *thiFSGH-His*, subsequently subcloned into similarly digested pMK400H (123).

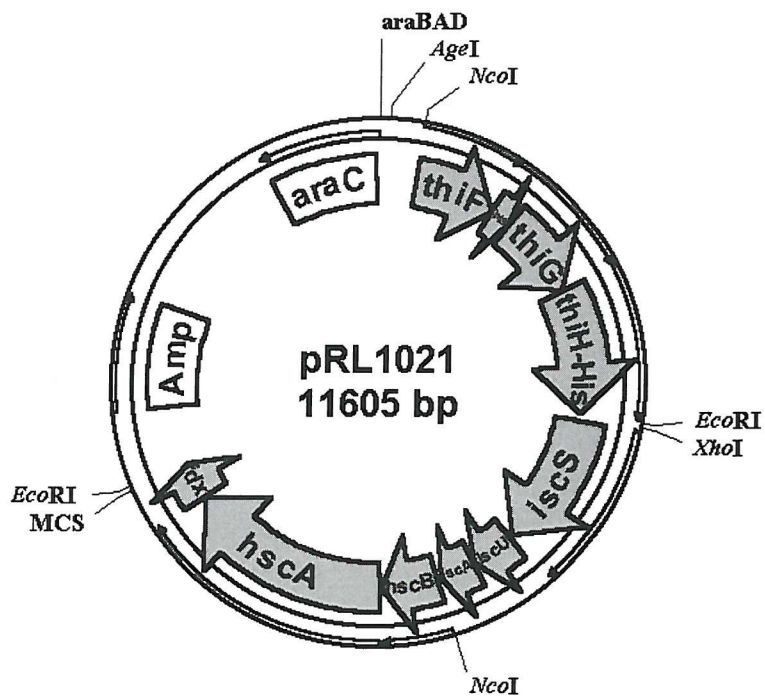


Figure 2.17. Map of pRL1021. MCS = Multiple Cloning Site.

Metabolic studies on thiamine biosynthesis in *S. typhimurium* have provided supporting evidence for the potential existence of an oxygen sensitive Fe-S cluster in ThiH and for the role played by the Isc proteins in maintaining active ThiH for thiazole biosynthesis (48,76). Therefore, the potential effect of reduced oxygenation on the soluble expression level of ThiH-His from pRL1021/BL21(DE3) was investigated. Cultures of pRL1021/BL21(DE3) (10 ml in 50 ml tubes) were induced when the OD₆₀₀ reached 0.2 or 0.6 and immediately transferred to 15 ml capped tubes or left in 50 ml capped tubes, to obtain partial anaerobic conditions during the following 5 h incubation. The cells were then harvested and lysed to analyse the ThiGH-His expression level. Taking ThiG as reference point (IscS and ThiH-His are not resolved on the gel), SDS-PAGE analysis showed little influence on the expression level by either aeration or induction point (Figure 2.18).

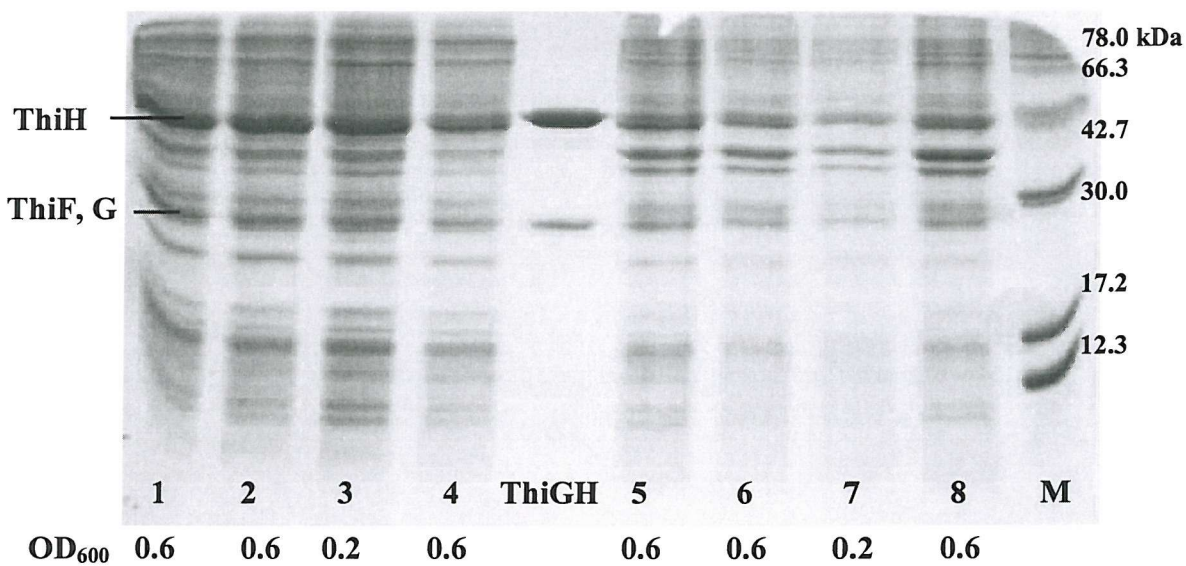


Figure 2.18. Coomassie Blue stained 15 % SDS-PAGE gel of soluble (lanes 1-4) and insoluble (lanes 5-8) proteins expressed from pRL1021/BL21(DE3) at 28 °C. Cell cultures were induced when OD₆₀₀ = 0.6 or OD₆₀₀ = 0.2 as indicated, then moved to 50 ml tubes (lanes 1-3, 5-7) or to 15 ml tubes (lanes 4, 8). M = molecular weight marker. The pellets were diluted several times before being loaded onto the gel and that it is why the expression level of soluble and insoluble proteins seems comparable.

pRL1021/BL21(DE3) was subsequently grown on a large scale to isolate and analyse the ThiGH-His complex produced by this expression system (sections 3.2.2-3.2.5).

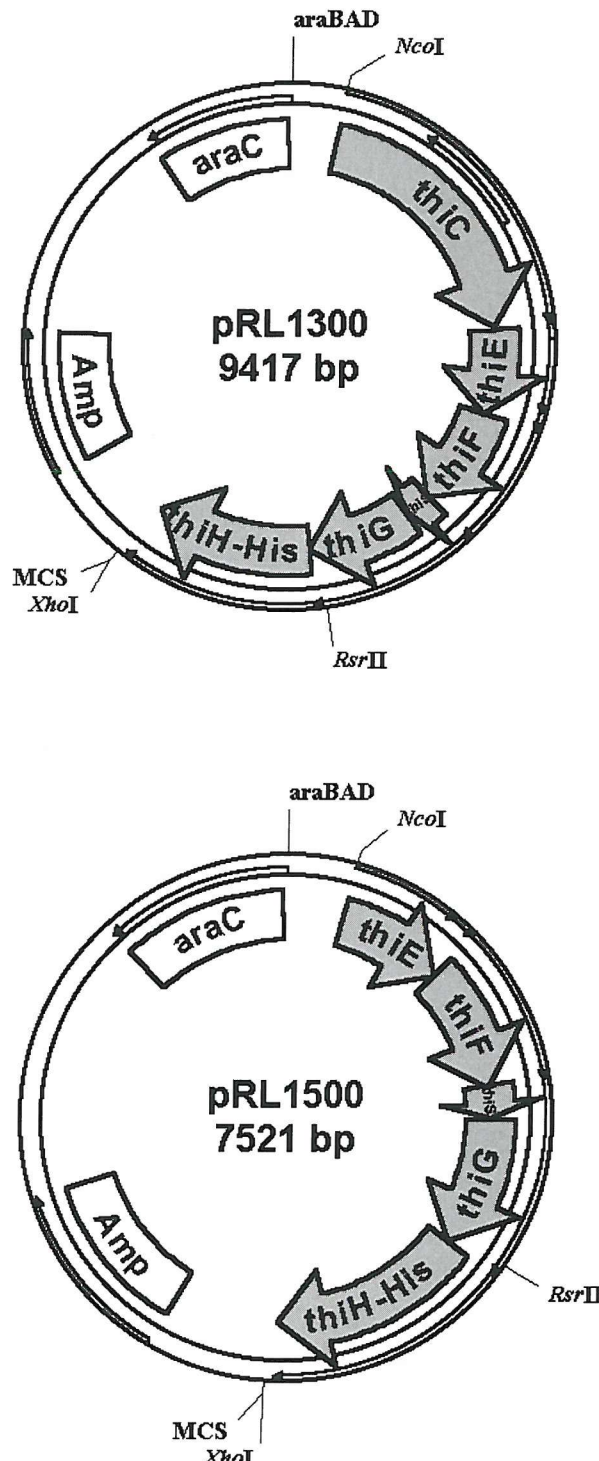


Figure 2.19. Maps of pRL1300 and pRL1500, not to scale. MCS = Multiple Cloning Site.

2.2.8. *pRL1300* and *pRL1500*: Expression of *ThiCEFSGH-His* and *ThiEFSGH-His*.

The assembly of pRL1300 and pRL1500 (Figure 2.19) finally allowed the co-expression of ThiH-His with all the proteins encoded by the *thiCEFSGH* (5.0 kbp) operon. Proteins expressed from pRL1020/BL21(DE3), pRL1300/BL21(DE3) and pRL1500/BL21(DE3), independently grown on a large scale, were analysed by SDS-PAGE (Figure 2.20). Given that the protein concentration in the cleared lysates was the same (4 mg/ml), the overall over-expression from pRL1500 appeared to be poor (Figure 2.20, lane 3), and surprisingly, whilst ThiE (23 kDa) was produced as insoluble protein from pRL1300, it was not produced at a detectable level from pRL1500. Several subsequent attempts to assemble a plasmid over-expressing solely ThiE, revealed that the over-production of this protein was undetectable from pBAD-derived plasmids, whereas it was mainly produced as insoluble inclusion bodies from a pET-derived plasmid (section 4.2.2). It is still unclear why ThiE was over-produced from a pBAD-derived plasmid exclusively when co-expressed with ThiC.

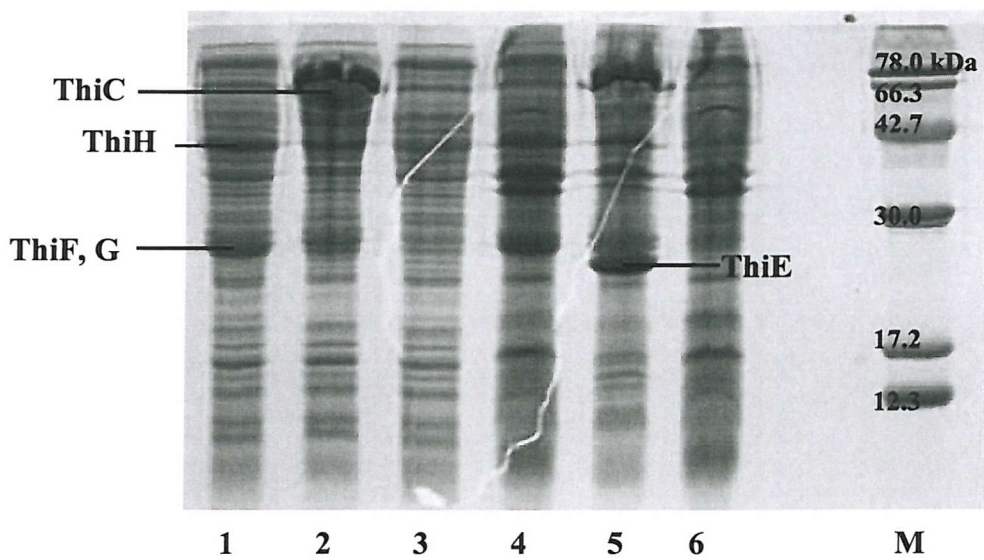


Figure 2.20. Coomassie Blue stained 15 % SDS-PAGE gel of soluble (lanes 1-3) and insoluble (lanes 4-6) proteins expressed from pRL1020/BL21(DE3) (lanes 1, 4), pRL1300/BL21(DE3) (lanes 2, 5) and pRL1500/ BL21(DE3) (lanes 3, 6) at 28 °C. M = molecular weight marker.

On the other hand, ThiC (**Figure 2.20**, lane 2) appeared to be relatively soluble, whilst ThiG and ThiH-His solubility did not seem to have been improved by the co-expression with ThiCEFS. The ThiGH-His complex was not isolated from pRL1300/BL21(DE3) and pRL1500/BL21(DE3).

2.3. Summary and Conclusions

Several plasmids carrying *thiH* alone or in combination with other genes have been assembled in the attempt of increasing the soluble expression level of ThiH. Finding a suitable expression system for ThiH proved to be more difficult than expected, since the variation of those parameters which normally affect the solubility of a protein, i.e. strength of the promoter, temperature and bacterial strain, appeared to be rather ineffective in the case of this protein. It was therefore necessary to consider other strategies.

There is considerable literature precedent for the expression of poorly soluble eukaryotic or bacterial proteins being improved by co-expressing them with the GroEL/ES chaperon system or with TrxA. Therefore, this co-expression strategy seemed to be a reasonable starting point and pRL221 and pRL222 were assembled. Unfortunately the solubility of ThiH did not benefit from the presence of these accessory proteins, indicating that neither a simple folding problem nor the formation of undesirable disulphide bridges were the main cause of its insolubility.

The reported existence of a complex between two thiazole biosynthetic enzymes, ThiF and ThiS, stimulated the assembly of pRL400, a plasmid encoding the last two ORFs of the *thiCEFSGH* operon. The co-expression of ThiG and ThiH did succeed in improving the solubility of ThiH, and represented the first step towards an optimised expression system. After pRL400, all the plasmids subsequently assembled encoded a hexahistidine-tagged ThiH, ThiH-His, starting from pRL800 which carried *thiGH-His*. The evidence that the co-expression with ThiG was positively affecting ThiH stability, led to the assembly of two other plasmids, pRL821 and pRL1000. From pRL821, ThiG and ThiH-His could be expressed together with the Isc proteins, which had been shown to increase the solubility of some Fe-S cluster enzymes; from pRL1000, ThiGH-His could be expressed together ThiF and ThiS. In both cases, the

soluble expression level of ThiH-His did not seem to have been further improved, although this was more difficult to estimate in the case of pRL821, due to the inability of resolving IscS from ThiH-His by SDS-PAGE. Therefore ThiGH-His was isolated from different expression systems and characterised, as described in Chapter 3. Large scale expression experiments and analysis of purified ThiGH-His samples highlighted differences, amongst the expression systems, which could have never been revealed by a simple SDS-PAGE analysis of proteins derived from small scale expression experiments. From these experiments, pRL1000/BL21(DE3) and pRL1020/BL21(DE3), both over-expressing ThiFSGH-His, emerged as the best expression systems.

ThiH-His soluble expression level was not further increased even when this protein was over-expressed from pRL1021, pRL1300 and pRL1500, harbouring *thiFSGH-His-iscSUA-hscBA-fdx*, *thiCEFSGH-His* and *thiEFSGH-His*, respectively. Amongst these systems, the ThiGH-His complex was isolated and characterised only from pRL1021/BL21(DE3). In conclusion, pRL1020/BL21(DE3) remains the best source of soluble ThiGH-His.

Chapter 3.

Isolation and Initial Characterisation of the ThiGH-His Complex

3.1. Introduction

The expression studies described in Chapter 2 led to the finding that the solubility of ThiH (or ThiH-His) could be increased by co-expressing this protein with ThiG. Several plasmids were also assembled to allow the co-expression of ThiGH-His with other thiamine biosynthetic enzymes (section 2.2.5) or with the Isc proteins (sections 2.2.6 and 2.2.7). With the purpose of characterising ThiH-His and to investigate whether the presence of these proteins affected the properties of the enzyme, ThiGH-His were over-expressed from different expression systems and isolated under anaerobic conditions. During the purification procedure ThiG was consistently found to co-elute with ThiH-His, suggesting the formation of a potential ThiGH-His complex. Furthermore, the availability of purified samples of ThiH-His allowed, for the first time, investigation of the potential Fe-S cluster by metal and sulphide analyses and by UV-visible and EPR spectroscopies.

In this chapter data are presented to demonstrate that ThiH-His is a novel Fe-S protein able to form a large hetero-multimeric complex with ThiG. Some of these data have already been published in (83).

3.2. Results and Discussion

3.2.1. Aerobic Purification of ThiH from pRL400

The first attempts to isolate ThiH from the cleared lysate of pRL400/BL21(DE3), over-expressing ThiG and ThiH (section 2.2.4), were carried out under aerobic conditions. ThiH was partially purified by ion exchange chromatography

(Figure 3.1), followed by desalting through gel filtration (Figure 3.2), and further purification through hydrophobic interaction chromatography (Figure 3.3) (section 7.5.1). After the third chromatographic step, ThiH eluted from the Source Phe column was still impure and mainly contaminated by a protein with a molecular weight very close to that of ThiG (27 kDa). During the screening of a range of dye affinity media, to which a protein can bind either because of substrate/cofactor similarities or through hydrophobic or ion exchange interactions, ThiH was found to bind to Blue Sepharose CL-6B resin (Sigma), which was therefore used to further purify the protein eluted from the previous steps (section 7.5.1). SDS-PAGE analysis of the eluate (Figure 3.4) revealed that, even though most of the 26 kDa protein was removed during the washing, the residual amount was distributed through fractions containing ThiH.

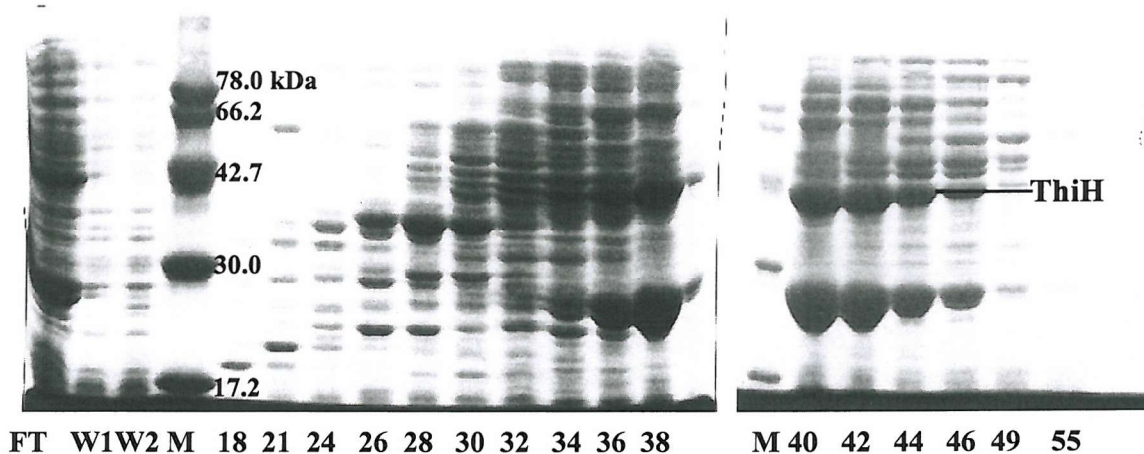


Figure 3.1. Ion exchange chromatography. Coomassie Blue stained 15 % SDS-PAGE gels of proteins eluted from the Q-Sepharose column. FT = flow through, W1, W2 = washings; M = molecular weight marker. The numbers correspond to fraction numbers. Fractions 37-43 were pooled, concentrated and applied to a gel filtration column (Superdex 200, Figure 3.2).

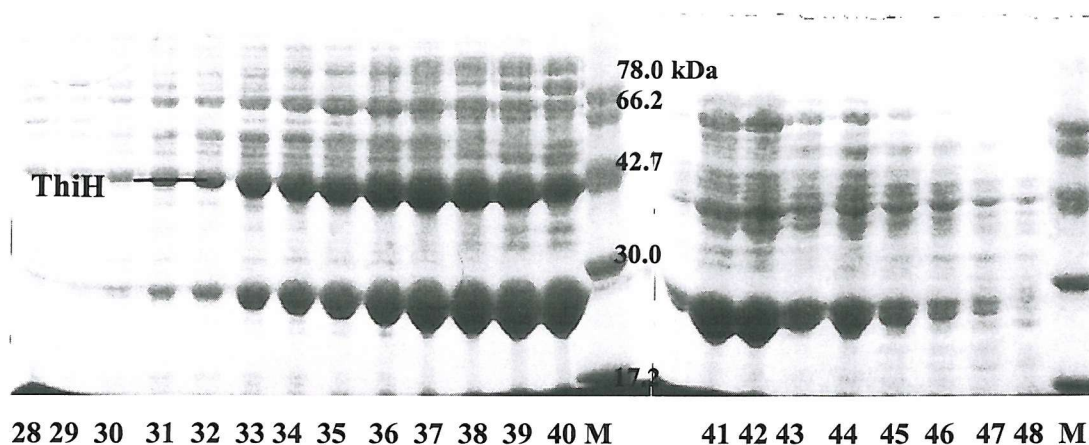


Figure 3.2. Gel filtration chromatography. Coomassie Blue stained 15 % SDS-PAGE gels of proteins eluted from the Superdex 200 (S-200) column. M = molecular weight marker. The numbers correspond to fraction numbers. Fractions 33-40 and 41-45 were separately pooled and applied to a Source Phe column (**Figure 3.3**).

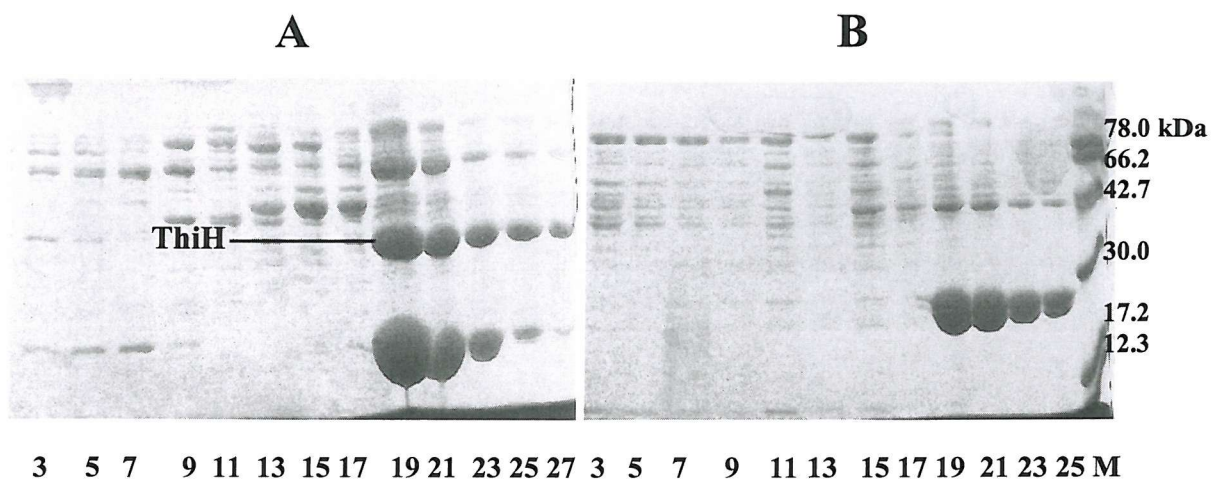


Figure 3.3. Hydrophobic interaction chromatography. Coomassie Blue stained 15 % SDS-PAGE gels of fractions eluted from the column Source Phe column. A: purification of fractions 33-40 from the S-200 column (**Figure 3.2**). B: purification of fractions 41-45 from the S-200 column. M = molecular weight marker. The numbers correspond to fraction numbers. Fractions 19-25 from both purifications were pooled and applied to the Blue Sepharose column (**Figure 3.4**).

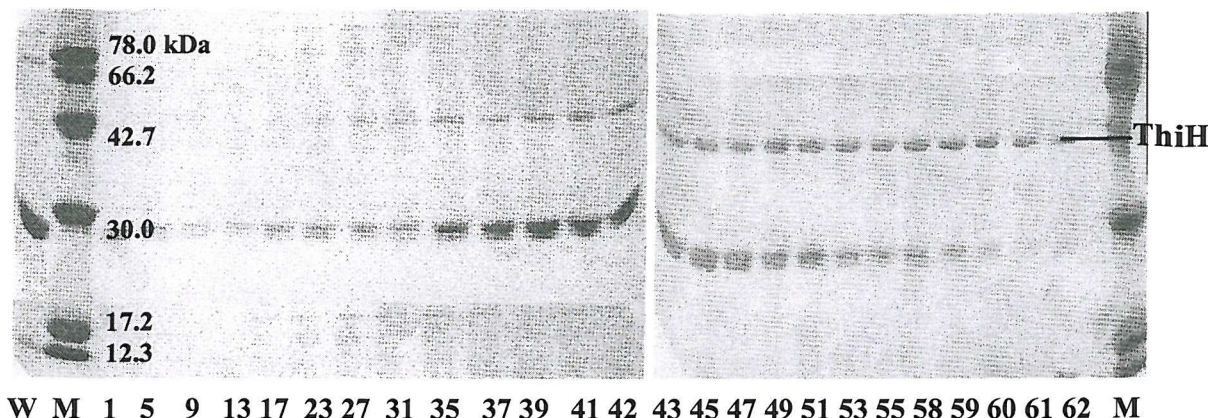


Figure 3.4. Affinity chromatography. Coomassie Blue stained 15 % SDS-PAGE gels of fractions eluted from the Blue Sepharose column. W = washing; M = molecular weight marker. The numbers correspond to fraction numbers.

Despite the fact that aerobically purified ThiH was never obtained in high yields or with a high purity, these experiments allowed two interesting observations. Firstly, fractions containing ThiH were characterised by a pale brown colour which tended to fade over time; secondly, the 26 kDa protein co-eluted with ThiH through several chromatographic steps.

Fe-S cluster proteins are normally coloured because of their characteristic absorbance between 400 and 500 nm; more specifically they tend to be dark reddish-brown if containing [4Fe-4S] or [3Fe-4S] clusters (142-144) or deep red if containing [2Fe-2S] clusters (87,107,145). Most of these proteins, then, undergo cluster degradation when treated with an oxidant such as $K_3[Fe(CN)_6]$ (107,146), or following exposure to air (105,145). Thus the short-lived brownish colour of the ThiH-containing fractions provided the first piece of evidence supporting the potential existence of an Fe-S cluster in the protein, and led to the development of an anaerobic purification protocol.

The persistent co-elution of the 26 kDa protein with ThiH was intriguing, and the potential formation of a ThiGH complex certainly deserved further investigation. Therefore, with the objective of facilitating the isolation and subsequent characterisation of ThiH alone or in a complex, it was decided to append a hexahistidine tag to the C-terminus of the protein and to express it as ThiH-His.

3.2.2. Anaerobic Purifications of ThiGH-His

ThiH-His was over-expressed from BL21(DE3) cells transformed with pRL800, 820, 821, 1000, 1020 and 1021 (Chapter 2). Depending on the expression system, variable yields in cell paste were obtained (**Table 3.1**).

Expression System [vector/BL21(DE3)]	Cell Paste Yield (g/5 l cultures)
pRL800	5-15
pRL820	27-28
pRL821	~ 30
pRL1000	25-30
pRL1020	28-32
pRL1021	27*

Table 3.1. Cell paste yields obtained from different ThiGH-His expression systems.

* Grown just once.

ThiH-His and any associated protein were isolated under anaerobic conditions (< 2 ppm O₂) by nickel affinity chromatography immediately followed by a gel filtration step (section 7.5.2). Purified ThiH-His proved to be a very unstable protein with a marked tendency to precipitate. The use of buffers containing glycerol and a relatively low NaCl concentration, as well as the prompt removal of the imidazole by gel filtration, helped to prevent precipitation. Due to this instability, safe long term storage of purified samples at -80 °C required the addition of extra glycerol to a final concentration of 25 % (w/v), and a ThiH-His concentration not exceeding 6-7 mg/ml. This optimised purification protocol typically yielded 30-50 mg of ThiH-His (with variable amounts of ThiG) from about 30 g of cell paste.

ThiH-His was anaerobically isolated for the first time from pRL800/BL21(DE3). Rather surprisingly, SDS-PAGE analysis of the proteins isolated from this system by the affinity chromatography, showed the presence of the 26 kDa protein (**Figure 3.5**) already observed during the aerobic purification of ThiH (section 3.2.1).

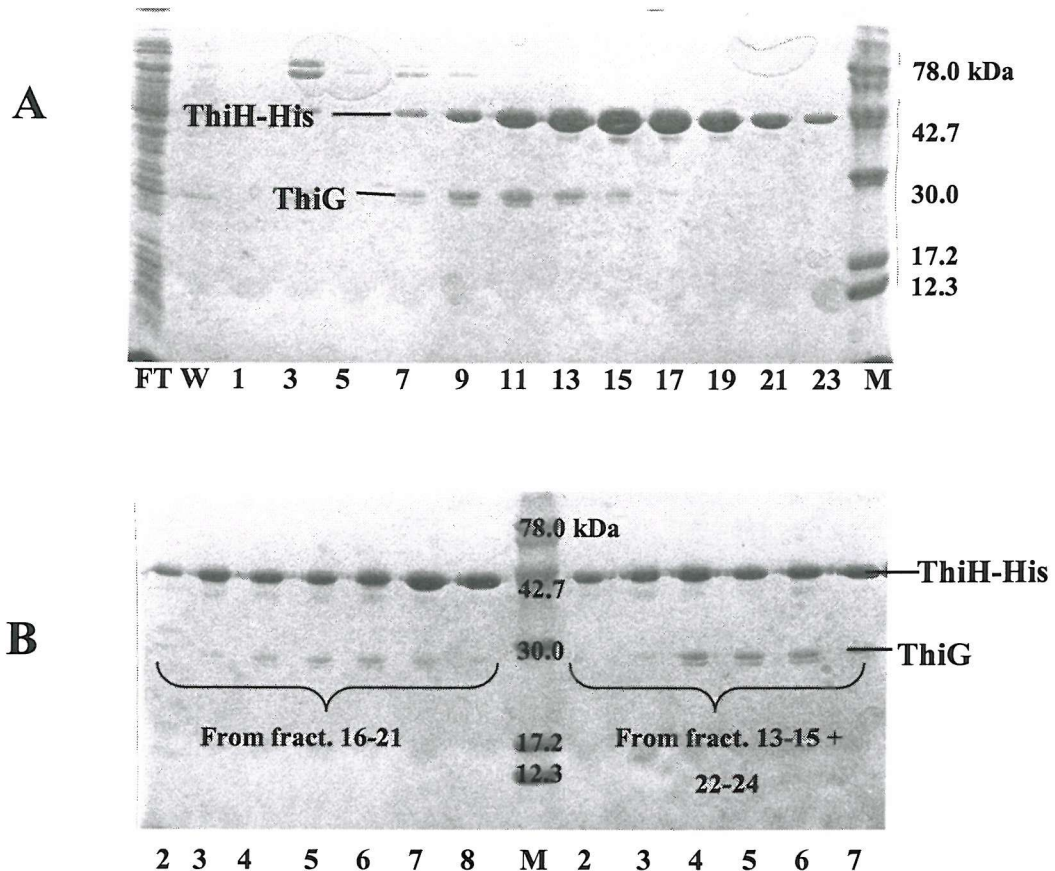


Figure 3.5. Purification of ThiGH-His from pRL800/BL21(DE3). Coomassie Blue stained 15 % SDS-PAGE gels of proteins eluted from A: nickel-chelating column and B: gel filtration column. FT = flow through; W = washing; M = molecular weight marker. The numbers correspond to fraction numbers. Fractions 16-21 and 13-15 + 22-24 from the nickel-chelating column were separately pooled and gel filtered.

N-terminal sequencing of that band revealed that the first seven amino acids corresponded to the ThiG sequence. The identity of the protein was later confirmed by ESI-MS analysis (**Figure 3.6**) of a ThiGH-His sample isolated from pRL1020 (**Figure**

3.11), which showed the presence of two species with masses consistent with those expected for ThiH-His (found 44140.9 Da, calculated 44143.0 Da) and ThiG (found 26889.4 Da, calculated 26896.1 Da). Despite being co-expressed with ThiGH-His, neither ThiF nor ThiS were detected in that sample, indicating the potential formation of a complex constituted solely by ThiG and ThiH-His.

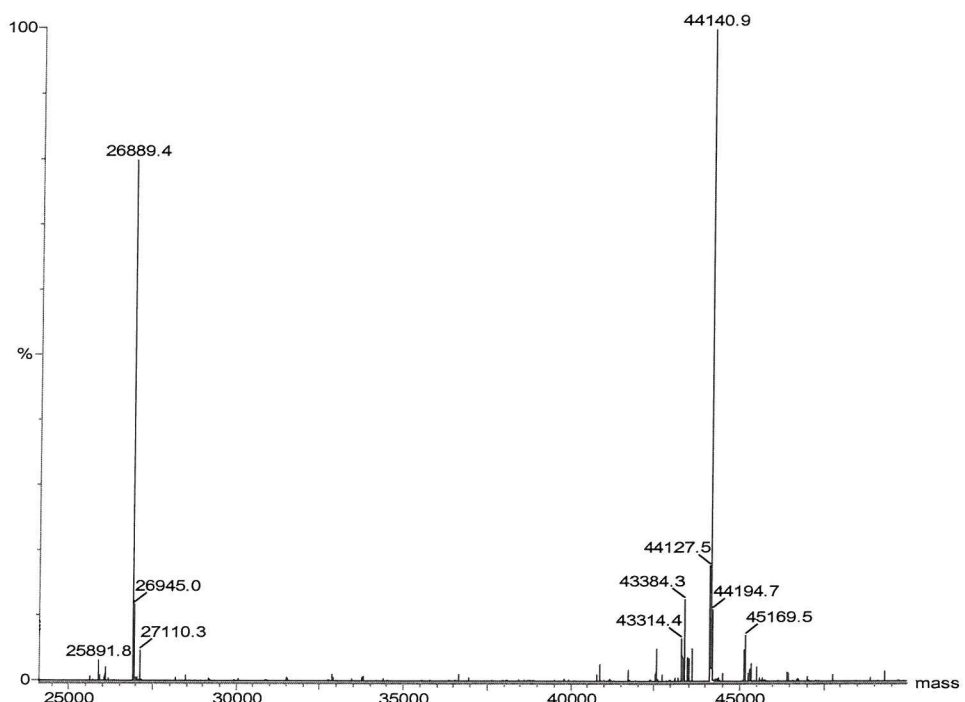


Figure 3.6. ESI-MS of ThiGH-His isolated from pRL1020/BL21(DE3).

ThiG and ThiH-His were then isolated from pRL821/BL21(DE3) cells grown in 2YT medium supplemented with FeSO_4 (0.4 mM) immediately after the induction (section 7.5.2). During the elution of ThiH-His from the nickel-chelating column, two sets of equally concentrated fractions, named A and B and different in colour, were observed; they were separately pooled and each pool desalting and concentrated (Figure 3.7). Batch A was blackish and darker than batch B. SDS-PAGE analysis revealed the presence of a 23 kDa protein in both batches, but slightly more abundant in batch A. Interestingly, the same protein was also detected in purified ThiGH-His samples isolated from pRL1021/BL21(DE3) grown without exogenously added iron (Figure

3.8), and occasionally, with a much weaker intensity, in samples isolated from other expression systems. Batches A and B were further analysed by analytical gel filtration chromatography (section 3.2.3).

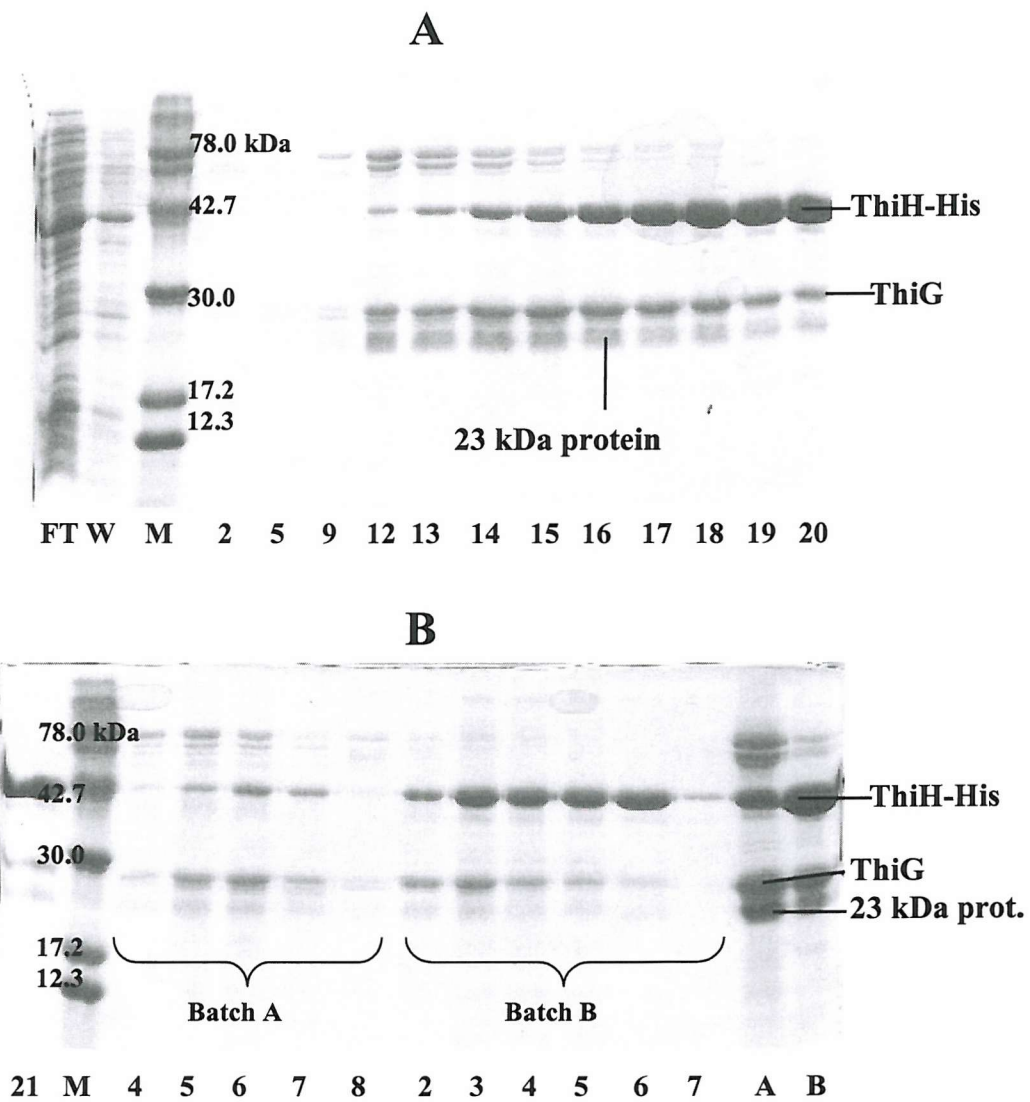


Figure 3.7. Purification of ThiGH-His from pRL821/BL21(DE3). Coomassie Blue stained 15 % SDS-PAGE gels of proteins eluted from A: nickel-chelating column and B: gel filtration column. FT = flow through; W = washing; M = molecular weight marker. A = concentrated and gel filtered batch A; B = concentrated and gel filtered batch B. The numbers correspond to fraction numbers. Fractions 11-15 (batch A) and 15-21 (batch B) from the nickel-chelating column were separately pooled and gel filtered.

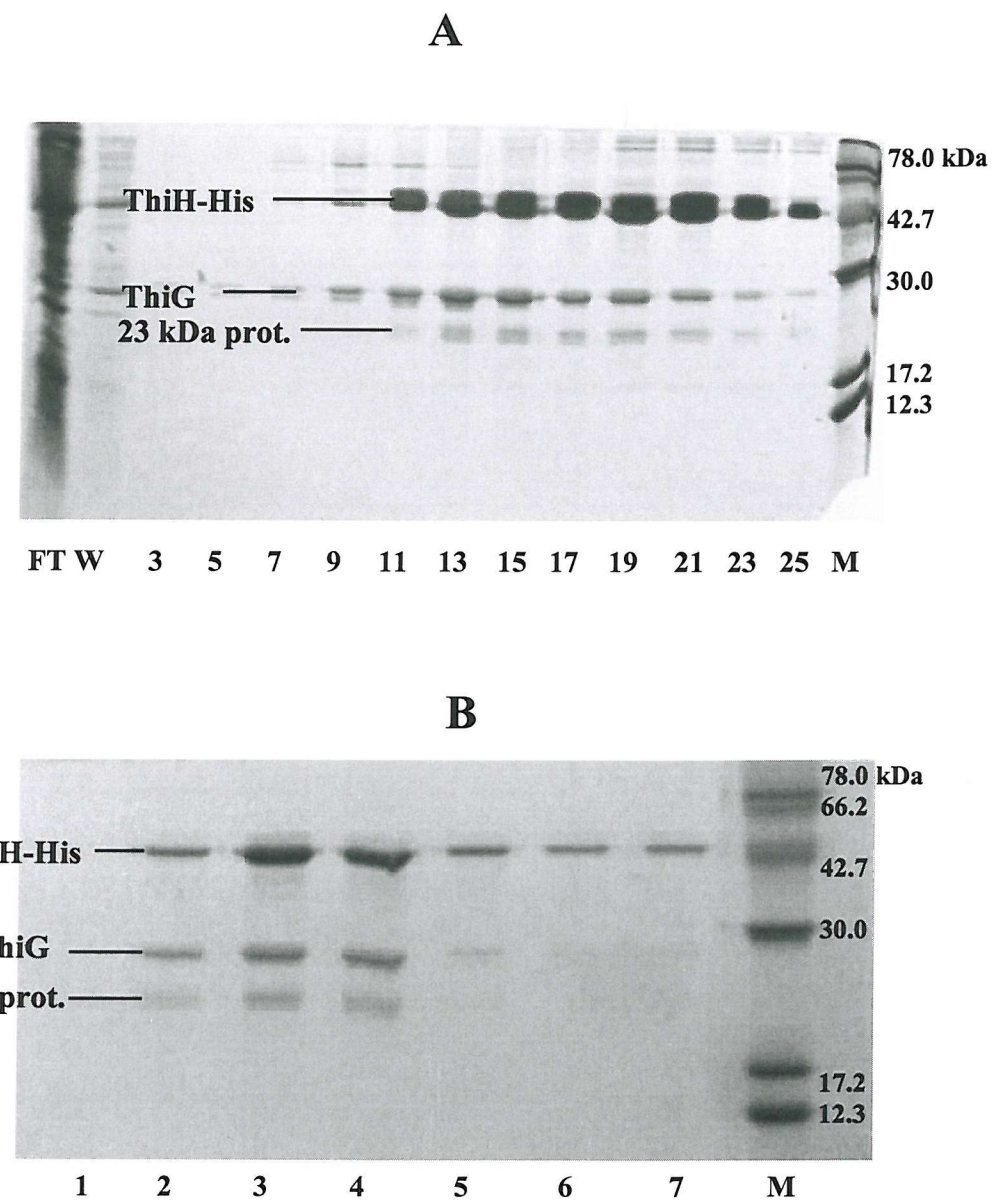


Figure 3.8. Purification of ThiGH-His from pRL1021/BL21(DE3). Coomassie Blue stained 15 % SDS-PAGE gels of proteins eluted from A: nickel-chelating column and B: gel filtration column. FT = flow through; W = washing; M = molecular weight marker. The numbers correspond to fraction numbers. Fractions 15-20 from the nickel-chelating column were pooled and gel filtered.

Figures 3.5, 3.9, 3.10 and 3.11 show the elution profile of ThiG and ThiH-His isolated from pRL800, 820, 1000 and 1020 in BL21(DE3), respectively.

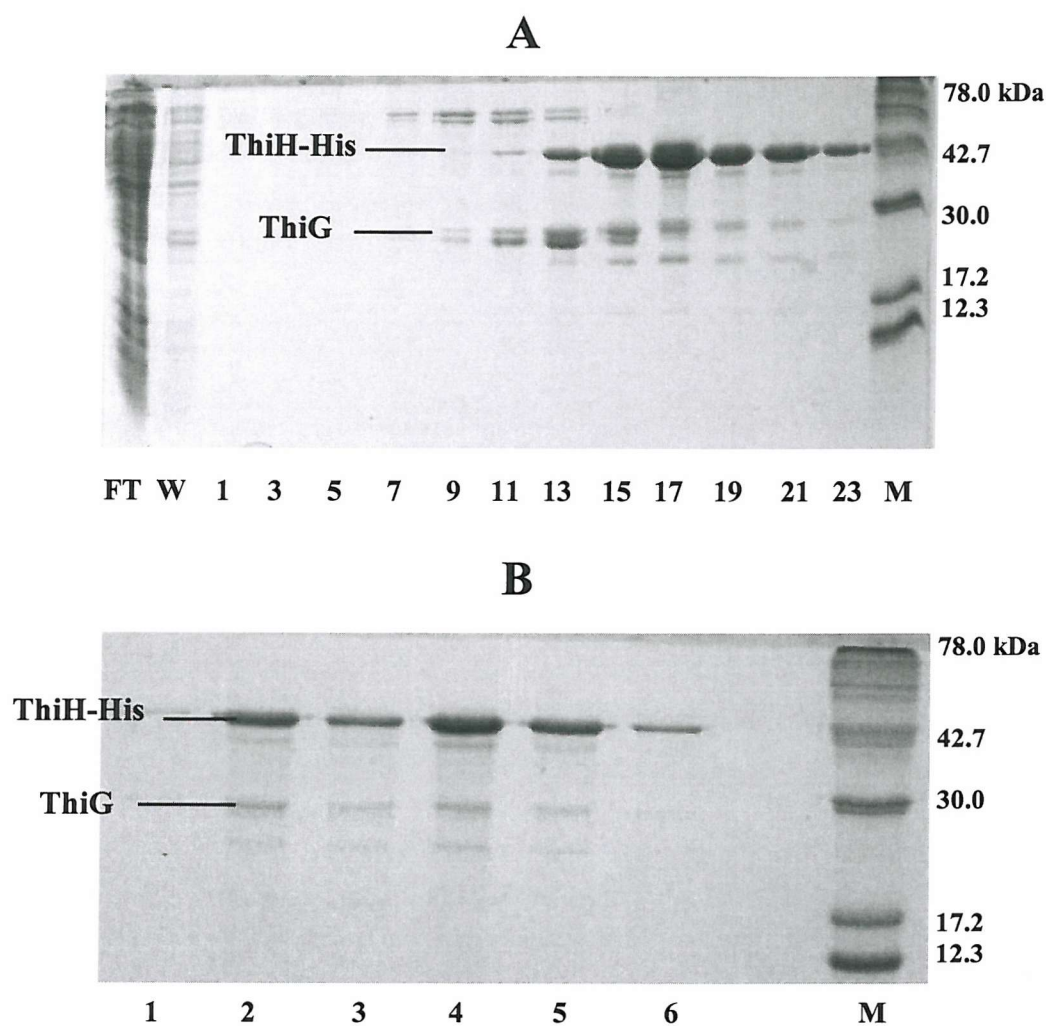


Figure 3.9. Purification of ThiGH-His from pRL820/BL21(DE3). Coomassie Blue stained 15 % SDS-PAGE gels of proteins eluted from A: nickel-chelating column and B: gel filtration column. FT = flow through; W = washing; M = molecular weight marker. The numbers correspond to fraction numbers. Fractions 15-21 from the nickel-chelating column were pooled and gel filtered.

The amount of ThiG associated with ThiH-His after the two chromatographic steps is clearly different between the ThiGH-His and ThiFSGH-His over-expressing systems (**Figure 3.12**). This amount was estimated by gel densitometry and found to be approximately 0.2 and 1.0 mol equivalents of the ThiH-His, respectively. Since these results were highly consistent amongst vectors carrying identical inserts, one possible explanation is that the presence of *thiFS* in the plasmid favoured the association of

ThiG and ThiH-His, although it is still unclear whether *thiFS* is affecting the synthesis or stability of the mRNA, or whether there is a direct interaction amongst the expressed proteins. Both SDS-PAGE and ESI-MS analyses, however, seemed to rule out the presence of ThiF and ThiS proteins in purified ThiGH-His samples isolated from pRL1000/BL21(DE3) and pRL1020/BL21(DE3).

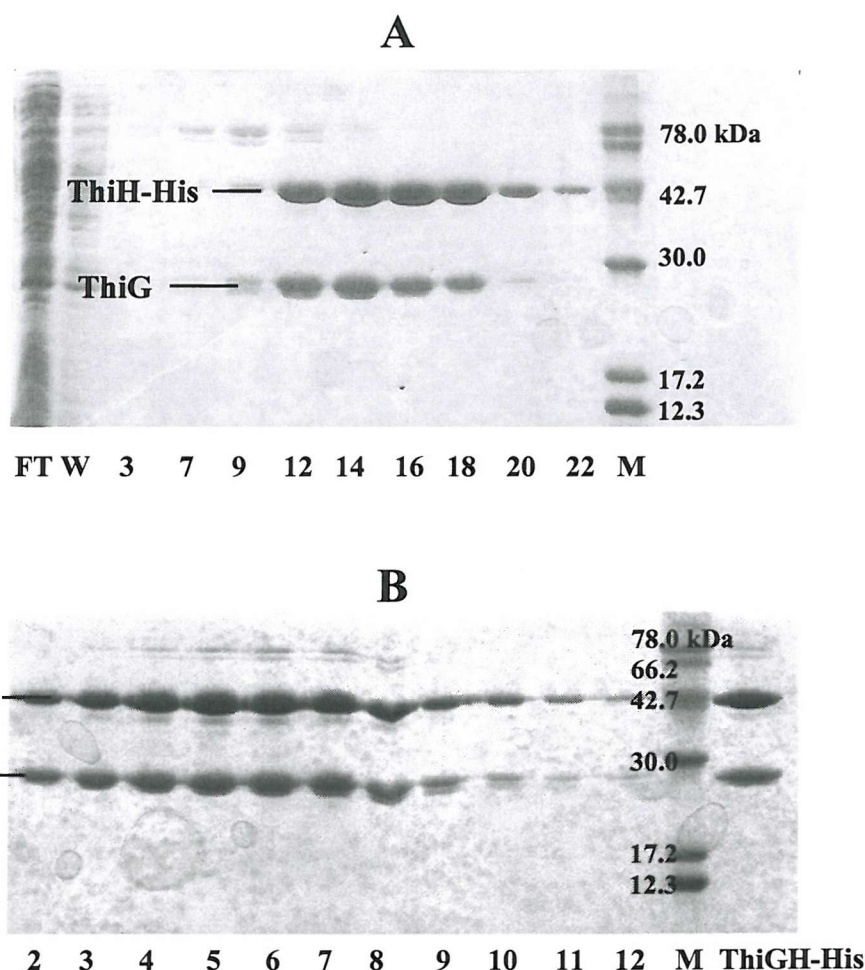
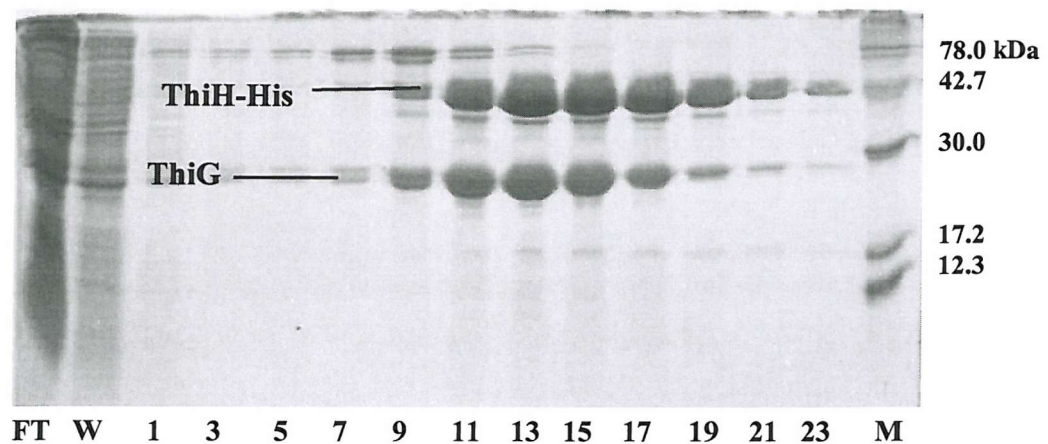


Figure 3.10. Purification of ThiGH-His from pRL1000/BL21(DE3). Coomassie Blue stained 15 % SDS-PAGE gels of proteins eluted from A: nickel-chelating column and B: gel filtration column. FT = flow through; W = washing; M = molecular weight marker. The numbers correspond to fraction numbers. Fractions 11-17 from the nickel-chelating column were pooled and gel filtered.

A



B

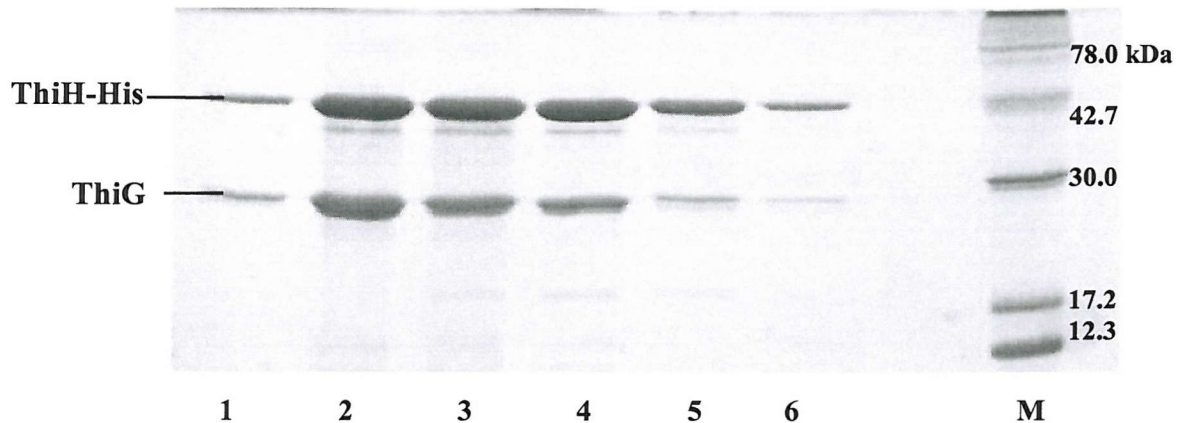


Figure 3.11. Purification of ThiGH-His from pRL1020/BL21(DE3). Coomassie Blue stained 15 % SDS-PAGE gels of proteins eluted from A: nickel-chelating column and B: gel filtration column. FT = flow through; W = washing; M = molecular weight marker. The numbers correspond to fraction numbers. Fractions 13-19 from the nickel-chelating column were pooled and gel filtered.

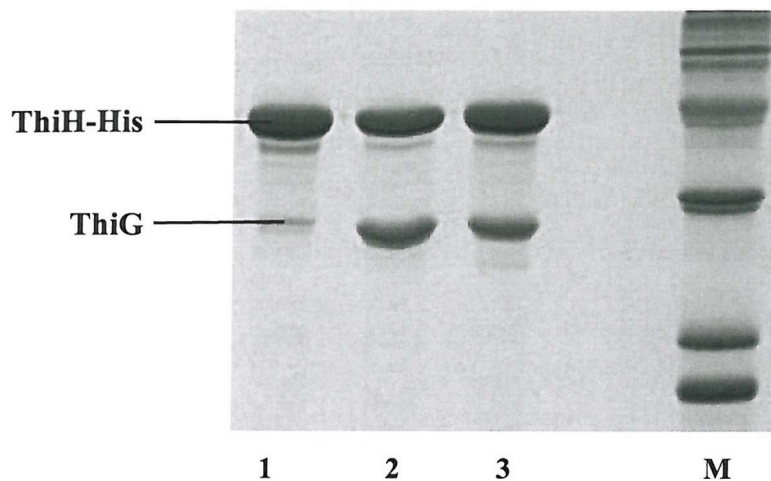


Figure 3.12. Coomassie Blue stained 15 % SDS-PAGE gel of purified ThiGH-His samples isolated from pRL800/BL21(DE3) (lane 1), pRL1000/BL21(DE3) (lane 2) and pRL1020/BL21(DE3) (lane 3). M = molecular weight marker.

3.2.3. Analytical Gel Filtration Chromatography

As mentioned in the previous section, the ratio of ThiG to ThiH-His in purified protein samples was observed to vary. As a result of this variation, and unless otherwise stated, the term 'ThiGH-His' is used to indicate the total amount of protein, without defining the proportion of ThiG and ThiH-His associated in the complex.

ThiGH-His samples were analysed by analytical gel filtration chromatography, under anaerobic conditions, to gain further information on the size of the potential complex. Samples were applied to an S-200 HR 10/30 pre-packed column (AP Biotech) (section 7.5.3) and protein elution monitored at 280 and 420 nm to simultaneously detect the absorption due to aromatic residues and to the presence of potential Fe-S clusters, respectively. Fractions were collected during the elution and subsequently analysed by SDS-PAGE. **Figures 3.13 and 3.14** show the chromatograms and the correspondent SDS-PAGE gels obtained from the gel filtration of ThiGH-His samples isolated from pRL800 and pRL1000 in BL21(DE3), respectively. In both cases ThiH-His was eluted at $t \sim 23$ min in a complex with ThiG and at $t \sim 30$ min as a monomer.

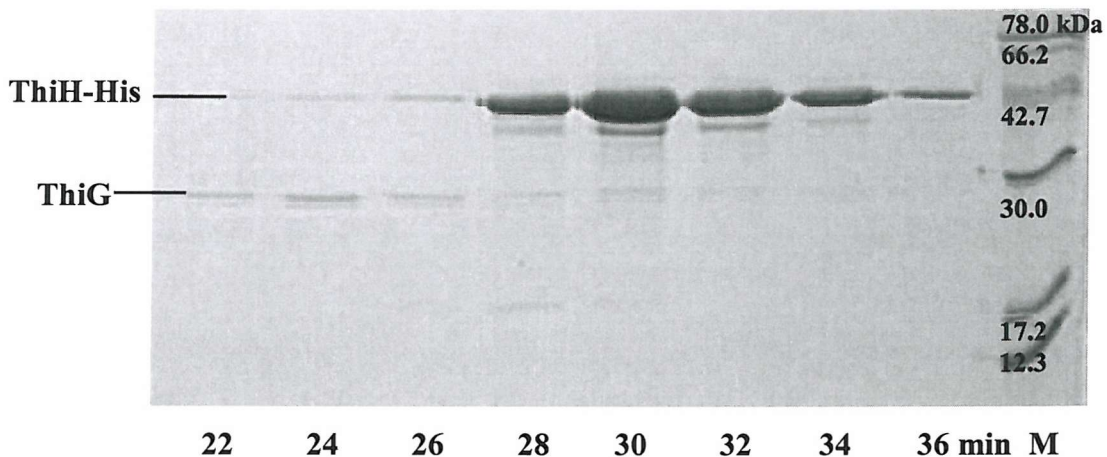
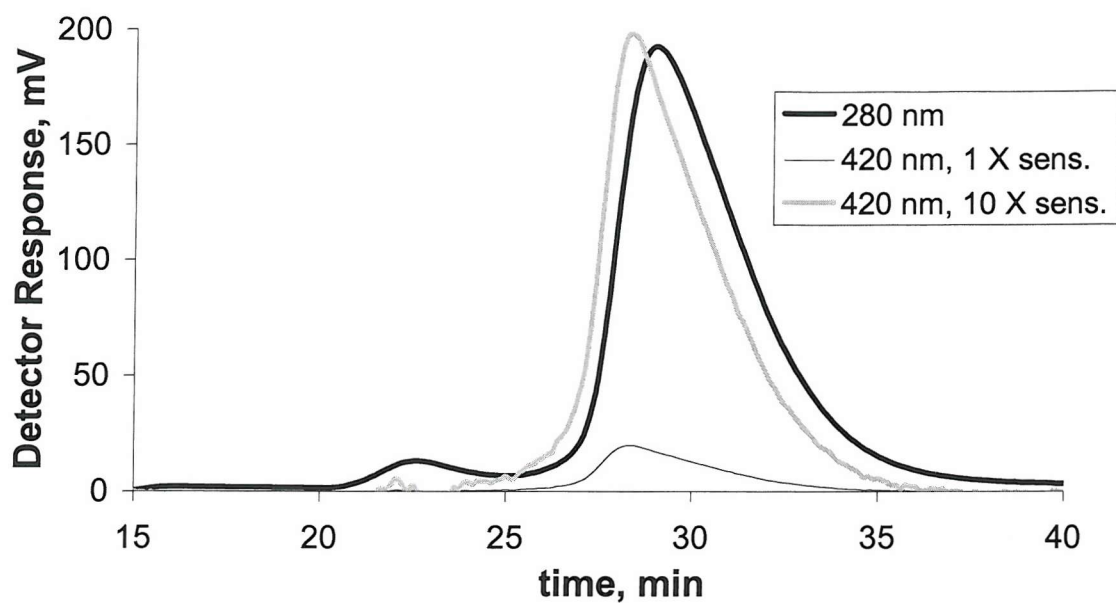


Figure 3.13. Analysis of ThiGH-His isolated from pRL800/BL21(DE3) by analytical gel filtration chromatography. Chromatogram and Coomassie Blue stained 15 % SDS-PAGE gel of fractions eluted from the S-200 HR column. The trace labelled '420 nm, 10 X sens.' was mathematically obtained from the trace '420 nm, 1 X sens.' by multiplying by 10 the corresponding values. M = molecular weight marker. The numbers correspond to the fraction numbers and to the retention time of the eluted proteins. Original data from HPLC file: HPLC\Methods\S200gf.061.

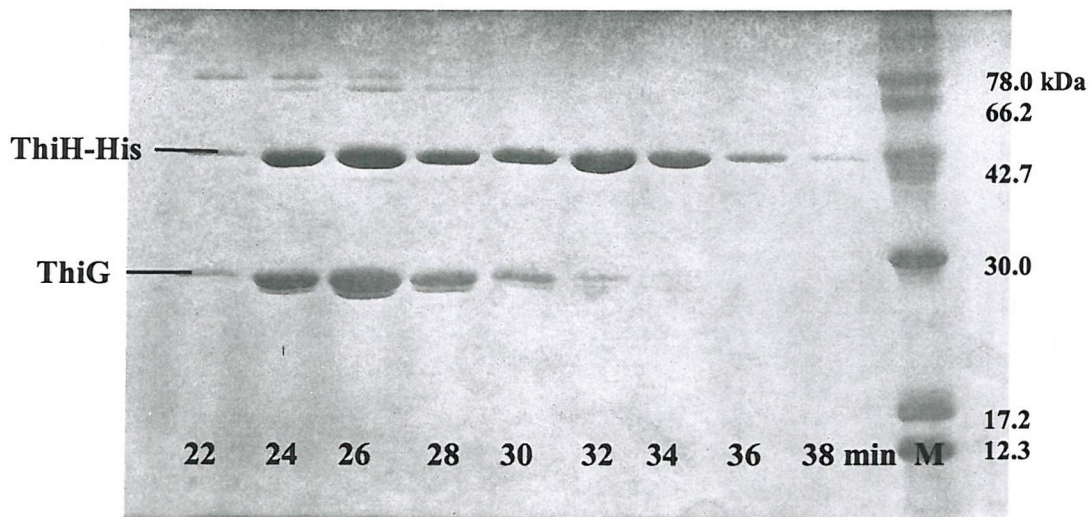
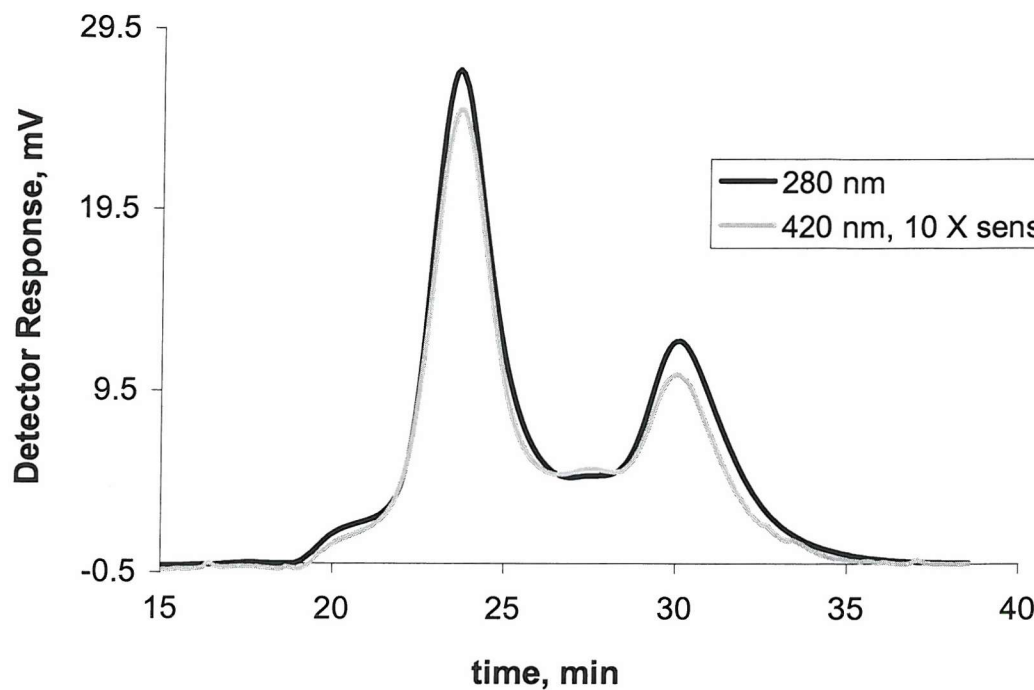


Figure 3.14. Analysis of ThiGH-His isolated from pRL1000/BL21(DE3) by analytical gel filtration chromatography. Chromatogram and Coomassie Blue stained 15 % SDS-PAGE gel of fractions eluted from the S-200 HR column. M = molecular weight marker. The numbers correspond to the fraction numbers and to the retention time of the eluted proteins. Original data from HPLC file: HPLC\Methods\S200gf.010.

By comparison with standard proteins of known size, the retention time of 23 min was found to correspond to an apparent molecular weight of >400 kDa, thus suggesting the formation of a large multimeric complex, seemingly constituted by equal amounts of ThiG and ThiH-His; the retention time of 30 min corresponded to an apparent molecular weight of 44 kDa, perfectly consistent with the actual size of ThiH-His. The proportion of ThiGH-His complex was variable and limited by the amount of ThiG, thus being very low ($\leq 10\%$) in samples isolated from pRL800 and pRL821/BL21(DE3), and much higher (50-80 %) in samples isolated from pRL1000 and pRL1020/BL21(DE3) (section 3.2.2). The chromatograms also showed that both the complex and monomeric ThiH-His absorbed at 420 nm, consistent with the presence of an Fe-S cluster in this protein. By gel filtering a ThiGH-His sample [from pRL1000/BL21(DE3)] on a preparative scale, the portion of ThiH-His present as a monomer was separated from that associated with ThiG and the iron content of both fractions assayed (section 3.2.4, **Table 3.2**).

As mentioned in section 3.2.2, during the anaerobic purification of the ThiGH-His expressed from pRL821/BL21(DE3), two differently coloured samples containing a 23 kDa impurity and named batch A and B, were isolated. Analysis by gel filtration chromatography and SDS-PAGE of batch B gave very similar results to those shown in **Figure 3.13**; analogous analysis of batch A provided clues on the nature of the 23 kDa protein. This protein was eluted from the S-200 HR column together with high molecular weight proteins in fractions showing a very strong absorption at 420 nm (fractions 22-26, **Figure 3.15**), thus explaining the dark colour of the batch. Although the high molecular weight proteins could have contributed to the absorption at 420 nm, these 60-70 kDa proteins were also eluted in colourless fractions from other purifications (**Figure 3.9 A**, fractions 7-11); therefore it seemed more likely that the chromophore absorbing at that wavelength was associated with the 23 kDa protein. N-terminal sequencing of the protein and a database search based on the knowledge of the first seven residues (SHHHEGL) identified a hypothetical protein, YqjI containing eleven histidines in a sequence of forty residues, and thus explaining the high affinity for the nickel-chelating column. At first it was hypothesised that the high expression level of this protein might have been promoted by the addition of FeSO_4 to the culture medium (section 3.2.2). However, the persistency of the band even after the elimination

of exogenously added iron, and above all, the fact that it was virtually absent in ThiGH-His samples isolated from other expression systems, led to the conclusion that this small protein might be related to the Isc proteins encoded by both pRL821 and pRL1021. The nature of this correlation is presently unclear as the function of the protein is thus far unknown.

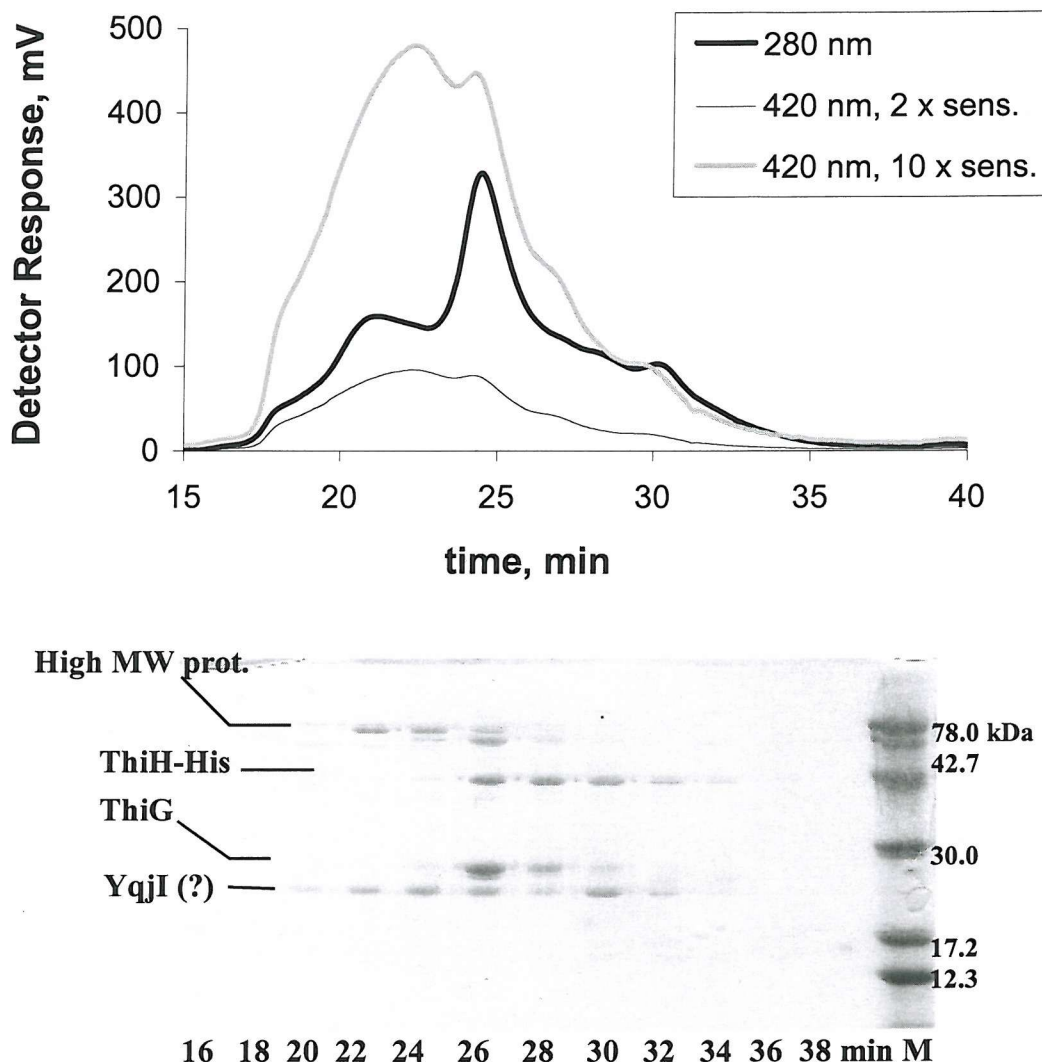


Figure 3.15. Analysis of ThiGH-His isolated from pRL821/BL21(DE3), batch A, by analytical gel filtration chromatography. Chromatogram and Coomassie Blue stained 15 % SDS-PAGE gel of fractions eluted from the S-200 HR column. The trace labelled '420 nm, 10 X sens.' was mathematically obtained from the trace '420 nm, 1 X sens.' by multiplying by 10 the corresponding values. M = molecular weight marker. The numbers correspond to the fraction numbers and to the retention time of the eluted proteins. Original data from HPLC file: HPLC\Methods\S200gf.004.

3.2.4 Metal and Sulphide Analyses

ThiGH-His samples isolated from different sources (section 3.2.2) were analysed for iron and sulphide content by the methods of Fish and Beinert (147,148), respectively (section 7.5.4) (**Table 3.2**). The presence of iron and other metals such as zinc and nickel was also investigated by ICP-AES (Inductively Coupled Plasma Atomic Emission Spectroscopy), which independently confirmed the estimation of the iron content by the method of Fish. We are very grateful to Dr. N. Shaw (Lonza, Switzerland) for the ICP-AES analysis.

ThiGH-His from [vector/BL21(DE3)]	S ²⁻	Fe	Fe (AES)	Ni (AES)	Zn (AES)
	mol/mol ThiH-His				
pRL800	0.69 ± 0.02	0.45 ± 0.05	0.45 ± 0.01	0.039 ± 0.001	0.33 ± 0.05
pRL820	2.31 ± 0.08	0.87 ± 0.02	0.95	≤ 0.1	≤ 0.1
pRL1000	2.32 ± 0.06	0.91 ± 0.03	0.95	≤ 0.1	≤ 0.1
pRL1020	1.87 ± 0.09	0.96 ± 0.03	0.90 ± 0.01	0.044 ± 0.005	0.22 ± 0.05
pRL1021	2.4 ± 0.1	1.36 ± 0.03	1.28	≤ 0.2	0.2 ± 0.1
pRL1000, M*	1.50 ± 0.04	0.57 ± 0.02	-	-	-
pRL1000, C *	2.8 ± 0.2	0.87 ± 0.02	-	-	-

Table 3.2. Sulphide and metal content of ThiGH-His samples isolated from different expression systems. The S²⁻ and Fe values represent the mean of three independent measurements ± SD. Where possible, the measurements of Fe, Ni and Zn by ICP-AES were obtained in duplicate and they are expressed as mean ± SD.

* M = ThiH-His monomer and C = ThiGH-His complex. M and C were obtained by gel filtration of a purified sample of ThiGH-His (section 7.5.3). The iron and sulphide content of that specific sample was 0.86 ± 0.03 and 2.18 ± 0.07 mol/mol ThiH-His, respectively.

Based on the data so far presented and also on the lack of an Fe-S cluster binding motif in ThiG (section 1.3.3), it is probably correct to assume that this protein did not contribute to the metal content of the samples.

Table 3.2 shows that all the samples contained iron and inorganic sulphide thus supporting, together with the brownish colour and the absorption at 420 nm, the existence of an Fe-S cluster in ThiH-His. In particular, the colour was consistent with the presence of a [3Fe-4S] or [4Fe-4S] cluster, or even a mixture of the two species (143,144). Despite the fact that the proteins were isolated under anaerobic conditions, all the ThiGH-His samples contained sub-stoichiometric amounts of iron and sulphide, typically 1 Fe and 2 S atoms per ThiH-His polypeptide chain. Therefore only about 25 % of ThiH-His could contain a potential [4Fe-4S] cluster. The isolation of proteins with just a fraction of their intact clusters is not uncommon and it is mainly due to oxidative degradation which might occur either during the expression or purification procedure (141,143,149).

The analysis of samples from different expression systems allowed some interesting observations. For example, ThiH-His isolated from pRL800/BL21(DE3) contained the lowest iron and sulphide content. This was initially interpreted as a result of the lower amount of ThiG present in the corresponding ThiGH-His sample (section 3.2.2), as ThiG could have shielded and protected, in some way, the cluster in ThiH-His from degradation. However, samples isolated from pRL820/BL21(DE3) with an equally low content in ThiG, and also pure ThiH-His monomer, contained more iron and definitely more sulphide than ThiGH-His from pRL800/BL21(DE3), thus indicating that there was no direct correlation between the ThiG content of the complex and the iron content in ThiH-His. The low content in iron and sulphide of ThiGH-His samples isolated from pRL800/BL21(DE3), and the poor yield in cell paste (**Table 3.1**), may be a consequence of the conspicuous production of inclusion bodies from this expression system (**Figure 2.16**, lane 7), which could not only overwhelm the Fe-S cluster biosynthetic machinery but ultimately become toxic for the cells themselves.

Conversely, ThiH-His isolated from pRL1021/BL21(DE3) contained the highest iron and sulphide content, hence suggesting that the expression with the Isc proteins might have assisted and promoted the cluster assembly in the protein. However, the ThiGH-His sample analysed contained a 23 kDa impurity (**Figures 3.7**

and 3.8) which probably bears a strong chromophore (section 3.2.3) and this might have contributed to the iron balance, therefore these data alone are not conclusive on the effect of the Isc proteins on the iron content in ThiH-His.

ICP-AES analysis of nickel and zinc in the samples indicated that the residual amount of nickel (from the nickel–chelating column) was negligible. Some zinc, which may have been bound adventitiously, was also detected but, presently, there is no evidence suggesting any structural or catalytic role for this metal in the thiazole biosynthesis¹.

3.2.5 Spectroscopic Properties of the Complex

Figure 3.16 shows the UV-visible spectra of as isolated and equally concentrated ThiGH-His samples and pure ThiGH-His complex. The spectrum of ThiH-His monomer is shown in **Figure 3.17**.

These spectra, recorded in air tight cuvettes, exhibit absorption maxima in the range 390-410 nm characteristic for sulphide-to-iron charge transfers within Fe-S centres ($\epsilon = 4000\text{-}7000 \text{ M}^{-1} \text{ cm}^{-1}$) (87,107), and a shoulder at 340 nm. Slight differences in the position of the maxima or in the relative intensity of the shoulder at 340 nm, amongst samples isolated from different sources, are not necessarily significant and might be due to subtle oxidative effects. Conversely, the intensities of the absorption maxima between 390 and 410 nm seem to be consistent with and to reflect the iron content of the samples (section 3.2.4). The spectra resemble those reported for LipA and PflAE, and are consistent with the presence of a mixture of [3Fe-4S] and [4Fe-4S] clusters (143,144).

¹ The effect of the addition of Zn^{2+} (50 μM) on the *in vitro* thiazole synthase activity (Chapter 6) of reaction mixtures containing de-repressed pRL1020/83-1 proteins, purified ThiGH-His, Tyr, ATP and Hmp, was investigated. The presence of the metal halved the activity (11 pmol/mg of protein/h), probably as a result of the ThiGH-His inactivation or inhibition.

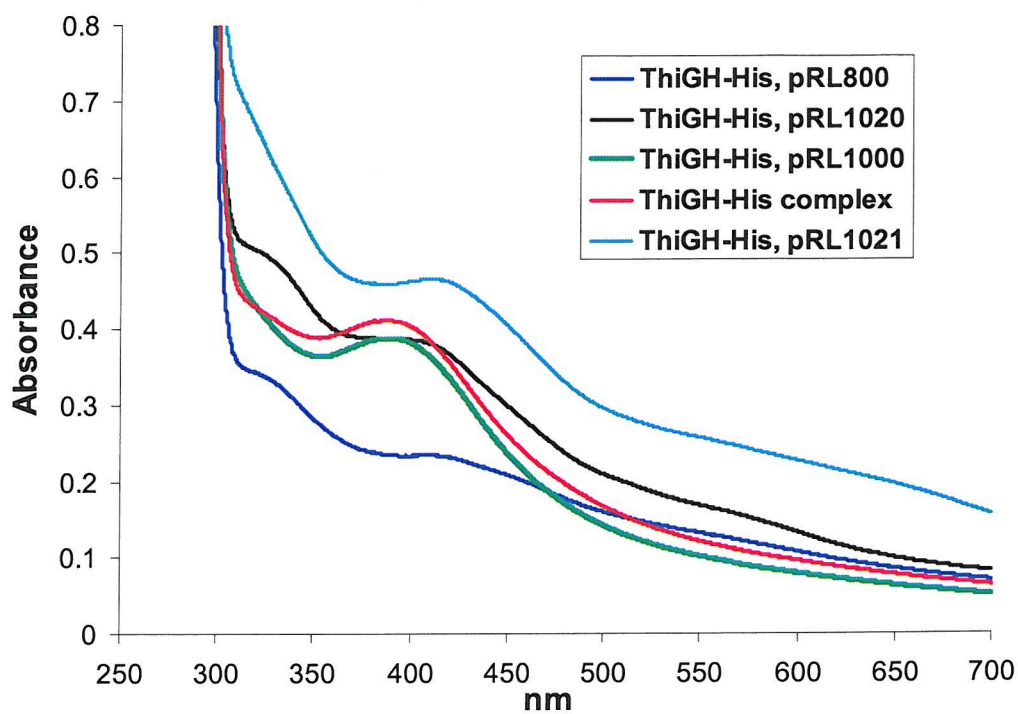


Figure 3.16. UV-visible spectra of ThiGH-His samples and ThiGH-His complex. The ThiH-His concentration in all the samples was 3 mg/ml. Spectra were recorded in 50 mM Tris-HCl, 5 mM DTT, 25 % (w/v) glycerol.

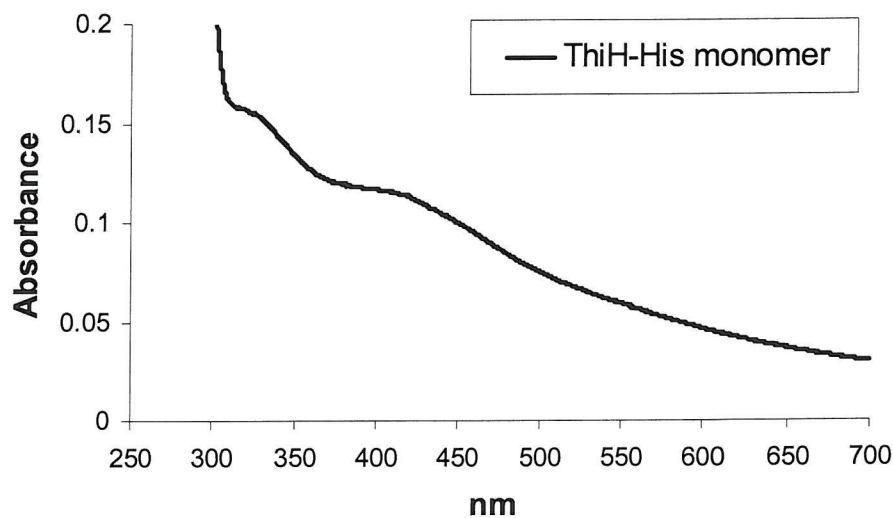


Figure 3.17. UV-visible spectrum of ThiH-His monomer, 1 mg/ml in 50 mM Tris-HCl, 5 mM DTT, 25 % (w/v) glycerol.

Fe-S clusters can easily interconvert, depending on the oxidising or reducing conditions (107,142,145,146,150), undergo conversion from the free to the protein-bound form (107) and also oxidative degradation (105) (**Figure 3.18**). Therefore, with the purpose of confirming the presence of an oxygen sensitive prosthetic group, the effect of exposing ThiGH-His to air was investigated.

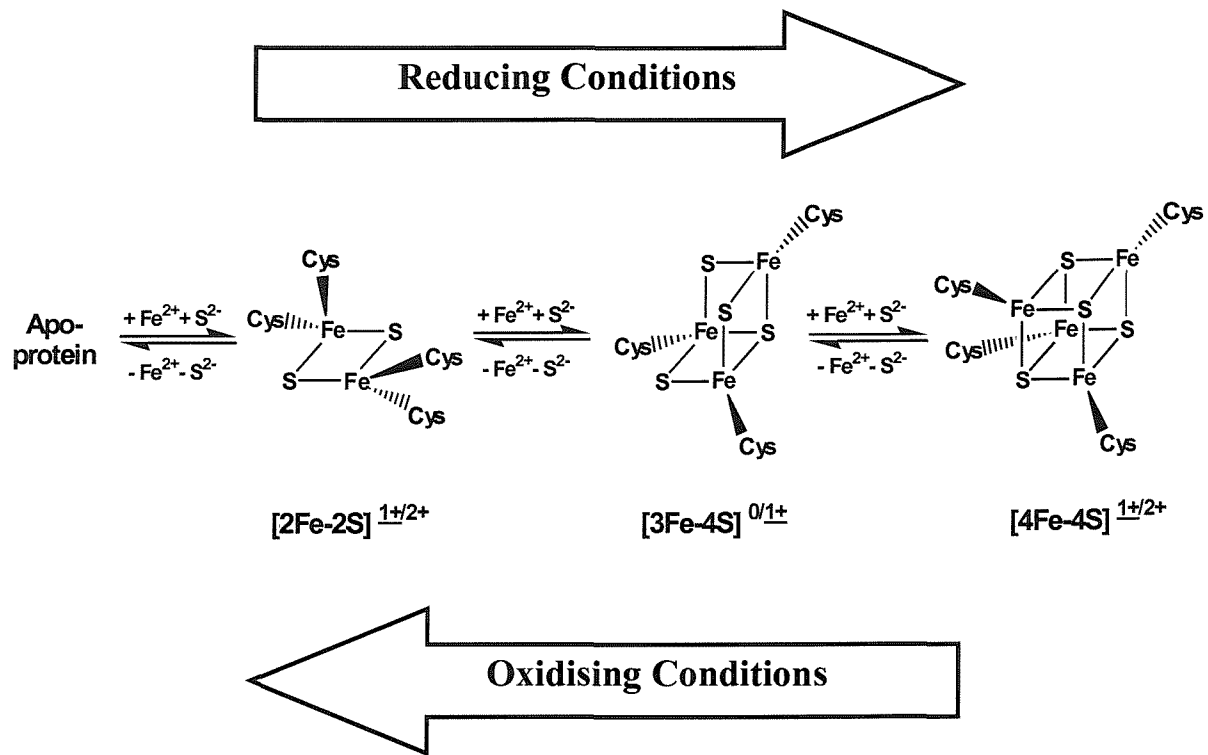


Figure 3.18. Interconversion between Fe-S clusters. Reducing conditions favour the conversion from a [2Fe-2S] to a [4Fe-4S] proceeding through the incorporation of endogenous or exogenous iron and sulphide; oxidising conditions, instead, promote the degradation of [4Fe-4S] to [2Fe-2S] clusters with loss of iron and sulphide. [3Fe-4S] clusters are probable formed as stable intermediates during of the interconversion between [2Fe-2S] and [4Fe-4S] clusters. Extreme oxidising conditions can also cause complete cluster destruction. The EPR active oxidation states of the clusters have been underlined.

A protein sample was transferred to an uncapped cuvette and UV-visible spectra recorded every hour for 7 hours. Within the first two hours of exposure, the absorption

at 410 nm decreased rapidly, indicating cluster oxidation and probably degradation (87) (**Figure 3.19**). After 2 hours, the UV-visible spectra remained virtually unchanged; however, samples exposed to air overnight, precipitated.

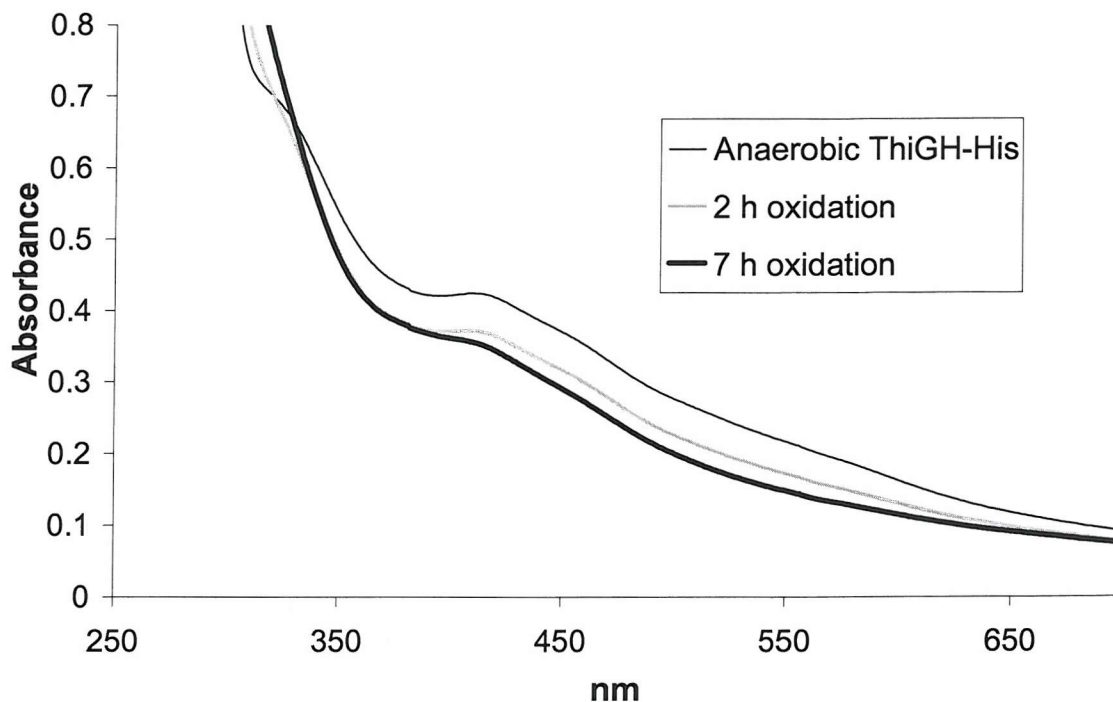


Figure 3.19. UV-visible spectra of ThiGH-His (4-5 mg/ml in ThiH-His) from pRL800/BL21(DE3) before and after exposure to air. The cuvette containing the sample was uncapped, mixed and spectra recorded every hour until the trace did not exhibit any further change (7 h). The spectra were recorded in 50 mM Tris-HCl, 5 mM DTT, 25 % (w/v) glycerol.

Besides undergoing oxidation, Fe-S clusters can also be reduced by dithionite or by 5-deazaflavin plus irradiation (87,88,107,143,151,152). The ultimate reduced state for a [4Fe-4S] cluster is the +1 which is EPR active and UV-visible featureless (143,153). **Figure 3.20** shows the changes in the absorption at 410 nm of a ThiGH-His sample incubated with 5-deazaflavin (DAF) and irradiated with a commercial light projector for 45 min: very similar spectra were obtained for photoreduced aconitase containing a $[4\text{Fe}-4\text{S}]^+$ (154).

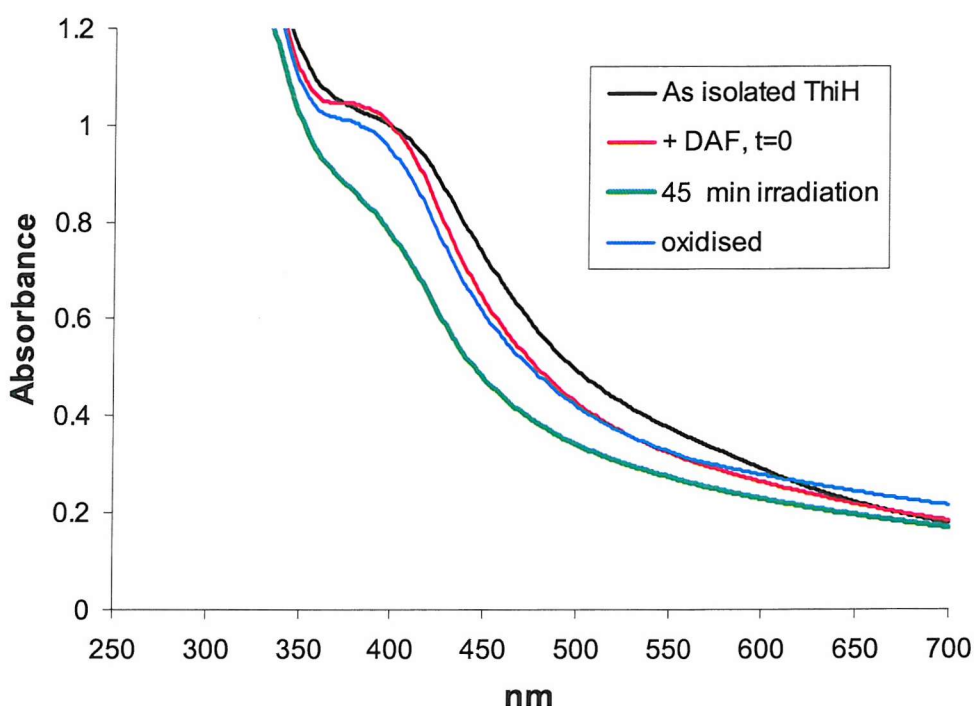
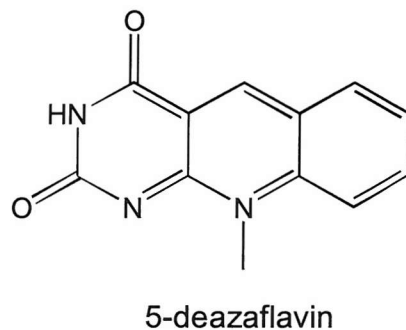


Figure 3.20. UV-visible spectra of ThiH-His from pRL1020/BL21(DE3) (6 mg/ml in ThiH-His) in 50 mM Tris-HCl, 5 mM DTT, 25 % (w/v) glycerol. The sample was anaerobically incubated with 5-deazaflavin (33 μ M) and irradiated for 45 min with a light projector. The cuvette was then uncapped, mixed, returned to the glove box and the spectrum recorded after 30 min.

At the end of the incubation time the ThiH-His sample was almost colourless. As for other Fe-S proteins, the process was reversible and exposure to air restored the initial UV-visible trace (146,152). Taken together, these results strongly suggested the presence of an Fe-S cluster in ThiH-His.

The presence of an Fe-S centre in ThiH-His was then independently confirmed by EPR. The EPR spectra of ThiGH-His isolated from pRL1020/BL21(DE3) were recorded and analysed by Prof. D. J. Lowe and Dr. S. A. Fairhurst (John Innes Centre, Norwich) (83) and are shown in **Figure 3.21**.

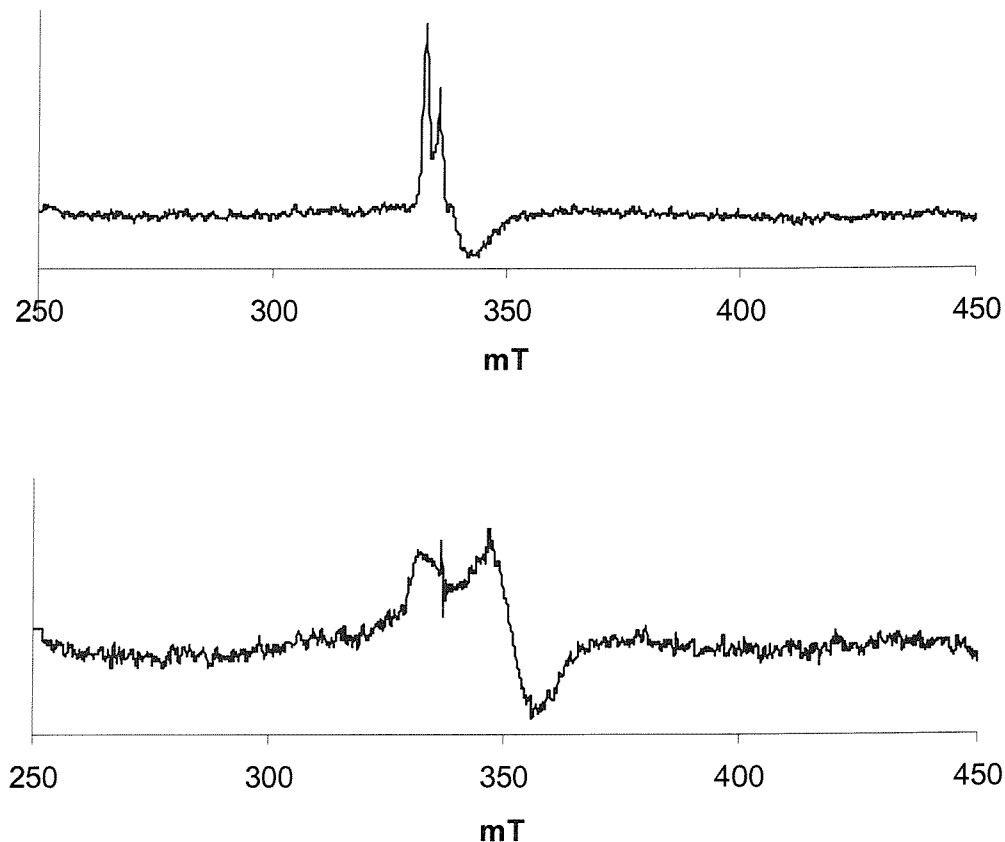


Figure 3.21. X-band EPR spectra of ThiGH-His (114 μM in ThiH-His) isolated from pRL1020/BL21(DE3). A: as isolated; B: after reduction with dithionite (1 mM, 30 min).

The spectrum of the as isolated protein showed a signal typical of a [3Fe-4S] cluster (**Figure 3.21, A**) which integrated to 0.7 μM ; upon reduction with dithionite a new signal, characteristic of $S = 1/2$ species and consistent with a $[4\text{Fe}-4\text{S}]^+$ cluster ($g_{\parallel} = 2.02$ and $g_{\perp} = 1.91$) appeared (**Figure 3.21, B**). This signal integrated to 1.1 μM . As

ThiH-His (5 mg/ml, 114 μ M) contained roughly 1 Fe/polypeptide chain, about 6 % of the clusters present in the protein were detectable by EPR.

The reductant-induced conversion of cluster states to $[4\text{Fe}-4\text{S}]^{2+/+}$ seems to be a quite common property to the radical SAM enzymes (84,94) (section 1.3.3), and the EPR spectra of as isolated and reduced ThiH-His are very similar to those of spore photoproduct lyase (151), LipA (88) and ArrAE (152), which are some of the characterised members of the radical SAM superfamily. Sequence homology searches by iterative profile methods (84) had identified ThiH as a potential family member, due to the presence of a conserved cysteine triad (CxxxCxxC) in its sequence. Interestingly, this classification of ThiH preceded the characterisation of the enzyme and the demonstration that it actually contains an Fe-S cluster (83). In fact, all the so classified radical SAM enzymes, have been shown or are predicted to be Fe-S proteins requiring *S*-adenosylmethionine to catalyse Fe-S cluster-mediated radical reactions initiated by the formation of a 5'-deoxyadenosyl radical. Despite the fact that the role of the cluster in ThiH remains to be elucidated, there is evidence supporting the SAM requirement for *in vitro* thiazole biosynthetic activity of *E. coli* cell-free extracts containing purified ThiGH-His (Chapter 6). Further spectroscopic characterisation of the cluster in ThiH is required to substantiate the hypothesis of the involvement of a radical mechanism in the biosynthesis of the thiazole moiety of vitamin B₁ in *E. coli*.

3.2.6 *In Vivo* Activity of the ThiH-His Expressed from pRL1020/BL21(DE3)

The expression of ThiH as a hexahistidine-tagged protein did certainly facilitate its isolation and characterisation. The presence of a (His)₆ tag does not normally interfere with the spectroscopic features or activity of the proteins to which it is appended (81,88,107,141). In the case of ThiH-His this was verified by investigating its ability to complement *thiH*⁻ mutants *in vivo*. *E. coli* KG33 cells are auxotrophic for the thiazole moiety of vitamin B₁ and are known to contain a lesion in ThiH (39). These cells, transformed with pRL1020 showed a vigorous growth on thiamine deficient medium, whilst the same cells transformed with pBAD/HisA (control plasmid) grew poorly (Figure 3.22). These complementation experiments indicated that ThiH-His

encoded by pRL1020 was active, thus allowing the KG33 cells to produce the thiazole and therefore thiamine.

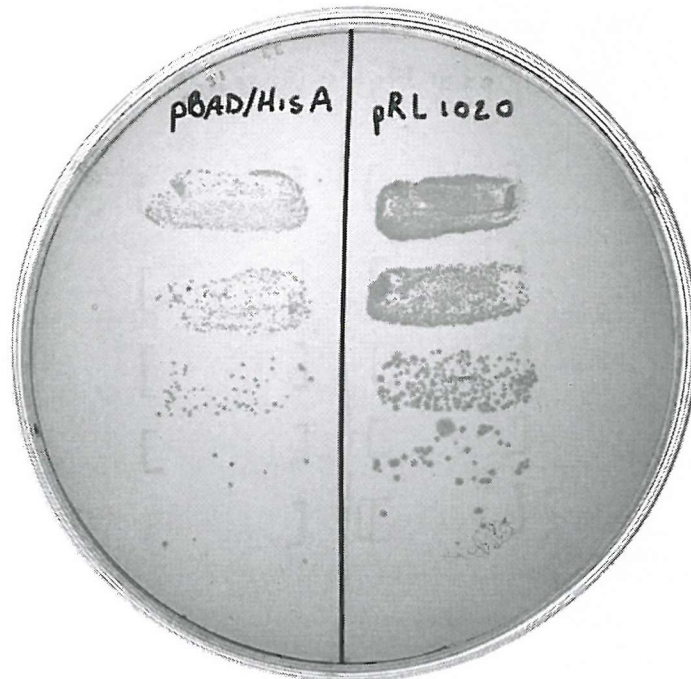


Figure 3.22. Complementation experiment. 5 tenfold serial dilutions of pBAD/HisA/KG33 and pRL1020/KG33 cultures ($OD_{600} \sim 1.3$) were plated onto TPP-free selective solid medium containing arabinose, Tyr, Cys and Hmp. The plate was incubated at $37^\circ C$ for 36 h.

3.2.7 Chemical and Enzymatic Reconstitution Experiments

The biogenesis of iron-sulphur clusters is a complex process which requires a consortium of conserved proteins, the Isc proteins (section 2.1), to assemble and insert these prosthetic groups into specific targets. However protein-bound [2Fe-2S] and [4Fe-4S] clusters can be formed *in vitro* by reconstitution reactions in which the apo-

protein is incubated with excess iron and sulphide (5-10 molar excess) under anaerobic conditions (91,102,155,156). The yield of this reaction varies from protein to protein; for example, [4Fe-4S] cluster proteins such as BioB and LipA can be fully reconstituted to contain about 4 Fe/polypeptide chain (87,107), whilst reconstituted ArrAE and MiaB contain only 2-3 Fe/polypeptide chain (99,141).

The Isc proteins were purified by Dr. T. Ziegert in our laboratory (157). Attempts to reconstitute ThiH-His were carried out either by the traditional chemical method (102,107,156) or enzymatically, by incubating ThiGH-His with just IscS or with IscSUA, HscBA and Fdx, in the presence of cysteine and iron. The chemical and enzymatic methods were more or less equally efficient, and apparently reconstituted ThiGH-His samples were found to contain 2-3 Fe/monomer. However, it must be pointed out that at the time these experiments were carried out, suitable analytical spectroscopic techniques were not available to confirm that all the iron and sulphide had been successfully included in a functional Fe-S cluster. In the case of ThiGH-His, this analysis would have been extremely useful, since the presence of glycerol in the reaction mixture caused the formation of colloidal FeS, which could have been adsorbed on the surface of the protein and not easily removed even after EDTA treatment and gel filtration. In fact, control experiments in which BSA (a protein that does not contain a natural Fe-S cluster) was incubated with iron and sulphide in the presence of glycerol, followed by EDTA treatment and gel filtration, showed that (presumably) colloidal FeS had become associated with the protein, which exhibited UV-visible features very similar to those of a real Fe-S cluster protein.

Since the glycerol, which could not be removed as it was essential for the stability of the protein (section 3.2.2), seemed to interfere with the procedure, no further attempt to reconstitute ThiH-His was made.

3.3 Summary and Conclusions

ThiH (or ThiH-His) was isolated from ThiGH over-expressing systems under both aerobic and anaerobic conditions. A 26 kDa protein, subsequently identified as ThiG by ESI-MS and N-terminal sequencing, was found to co-elute with ThiH under either conditions, suggesting the formation of a relatively stable complex. Due to the bleaching of aerobically purified ThiH samples, an anaerobic purification protocol was developed to avoid oxidative degradation of the potential Fe-S cluster in the protein. Anaerobically purified ThiH-His had a persistent, stable brownish colour but showed a marked tendency to precipitate, and could only be concentrated and frozen in the presence of high glycerol concentrations.

ThiH-His anaerobically isolated from different expression systems, was found to co-elute with different amounts of ThiG, and an almost 1:1 ThiGH-His mixture could be routinely obtained from ThiFSGH-His over-expressing systems such as pRL1000 and pRL1020/BL21(DE3). Neither ThiF nor ThiS were detected in purified ThiGH-His samples isolate from these sources, but the presence of these proteins or of the correspondent genes in pRL1000 or pRL1020, allowed the recovery of larger amounts of potential ThiGH-His complex. The properties of the ThiGH-His complex were confirmed by analytical gel filtration chromatography, and the size of the complex estimated to be approximately 400 kDa.

Elemental analysis was used to quantify the amount of iron and sulphide present in ThiGH-His samples from several sources. Despite the fact that these samples were isolated under anaerobic conditions, approximately 1Fe and 2S per ThiH-His polypeptide chain were retained, thus indicating partial oxidative cluster degradation. However, the remaining Fe-S clusters could be detected by UV-visible and EPR spectroscopies, which indicated that ThiH-His contained a mixture of [3Fe-4S] and [4Fe-4S] clusters. Unfortunately, the data currently available are not sufficient to determine which one of these species is important for the biological activity of the protein, although as a potential radical SAM enzyme, ThiH-His might be expected to require a reduced [4Fe-4S]⁺ cluster to participate in the biosynthesis of the thiazole.

Finally, a complementation experiment using cells containing a mutation in *thiH*, showed that ThiH-His encoded by pRL1020 is active *in vivo*.

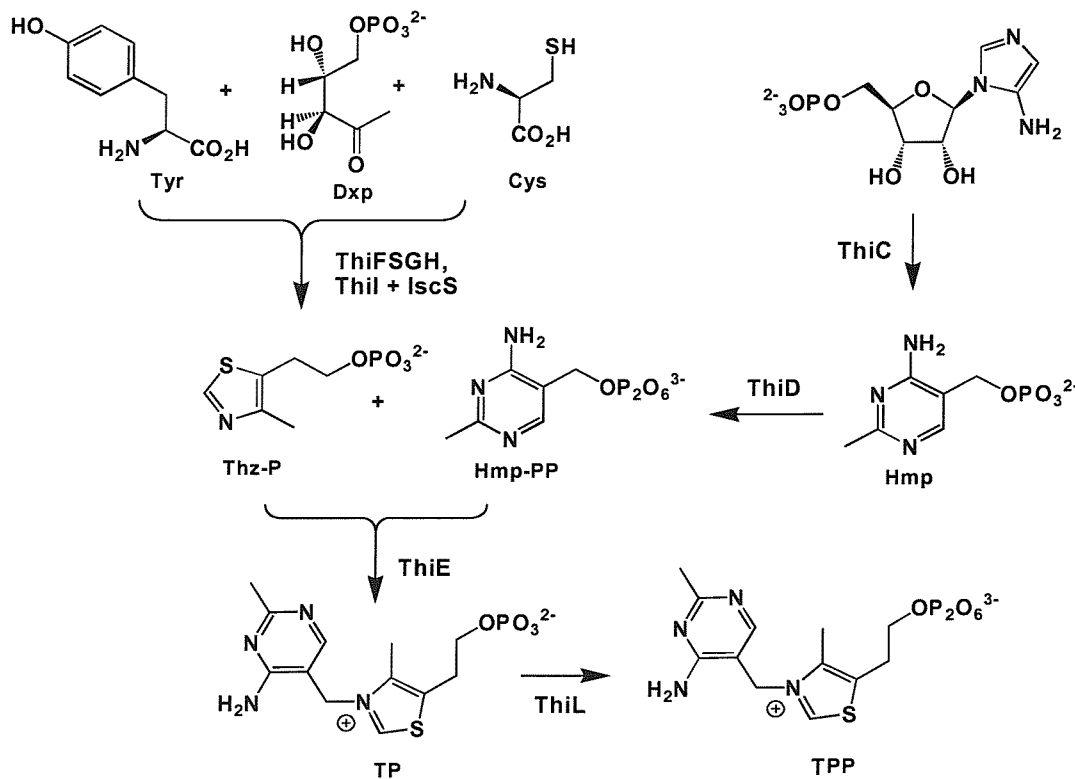
The data presented in this chapter demonstrated for the first time that ThiH is an Fe-S cluster protein which can be isolated in a large complex with ThiG. The initial hypothesis that ThiG might provide some protection of the Fe-S cluster in ThiH-His was discredited by the metal analysis of different ThiGH-His samples, which revealed similar iron contents in samples with different ThiG contents, and by the co-elution of ThiG and ThiH-His during the aerobic purification, which suggested that this complex could potentially exist even under conditions which do not favour the integrity of the cluster. The elucidation of the function of the cluster in ThiH and of the nature and purpose of the interaction between ThiG and ThiH in the thiazole formation, awaits further structural and biochemical analysis.

Chapter 4.

Expression of Thiamine Biosynthetic Enzymes and Synthesis of Thiamine Precursors

4.1. Introduction

As described in Chapter 1 (sections 1.3.2 and 1.3.3), the biosynthesis of the thiazole ring of vitamin B₁ from the precursors Tyr, Cys and Dxp requires at least six enzymes, ThiFSGH, ThiI and IscS. Once assembled, the Thz-P is coupled to Hmp-PP by ThiE to yield thiamine monophosphate (TP). The pyrimidine moiety of thiamine is biosynthesised through an independent pathway and is activated as the pyrophosphate, Hmp-PP, by ThiD (Scheme 4.1).



Scheme 4.1. Thiamine pyrophosphate (TPP) biosynthesis in *E. coli*.

In addition to the ThiGH-His expression systems described in Chapter 3, plasmids encoding other thiamine biosynthetic enzymes, ThiI, ThiE and ThiD, were assembled, and as a prerequisite to the investigation of the biosynthesis of the thiazole moiety of thiamine in *E. coli*, ThiF and ThiS were expressed and partially purified. Furthermore, the thiazole precursor Dxp was enzymatically synthesised using partially purified 1-deoxy-D-xylulose-5-phosphate synthase (Dxs), whilst the vitamin moieties Hmp and Thz-P were obtained through chemical synthesis.

4.2. Results and Discussion

4.2.1. Expression of *ThiI*

The *E. coli* *thiI* gene (1.5 kbp) was amplified by PCR using primers designed to introduce 5' *NcoI* and 3' *BamH1/Sac1* restriction sites. The resultant PCR product was first ligated into pBAD-TOPO and then subcloned into pET-24d(+). The pET-derived vector, pRL600 (Figure 4.1), was transformed into BL21(DE3), and ThiI (55 kDa) was expressed at 37 °C for 4 h.

Cleared lysate and pellet were analysed by SDS-PAGE, and soluble ThiI was clearly observable in the cleared cell lysate (Figure 4.2).

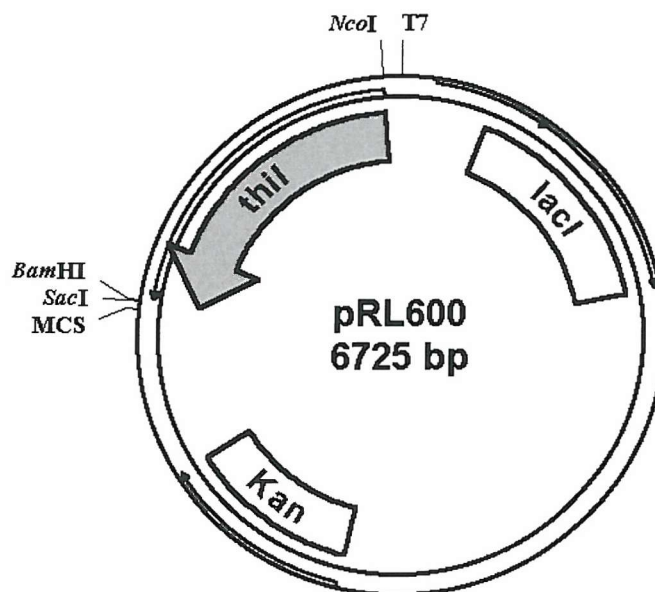


Figure 4.1. Map of pRL600. MCS = Multiple Cloning Site.

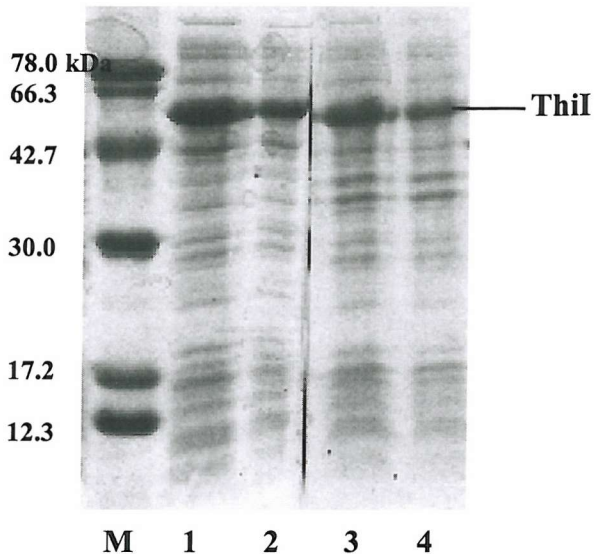


Figure 4.2. Coomassie Blue stained 15 % SDS-PAGE gel of soluble (lanes 1, 2) and insoluble (3, 4) proteins produced by two colonies of pRL600/BL21(DE3). M = molecular weight marker.

4.2.2. Expression of *ThiE*

E. coli thiE (660 bp) was amplified by PCR using primers designed to introduce 5' *Nco*1 and 3' *Xho*1 restriction sites. The reverse primer should have also introduced a C-terminal (His)₆ tag but, as the stop codon upstream the region encoding the tag was erroneously not removed, the expressed protein did not contain the six extra histidines.

The PCR product was ligated into pBAD-TOPO and then sequentially subcloned into pBAD/HisA, pBAD/His repair² and pET-24d(+). The resultant vectors were named pRL2000, 2020 and 2030, respectively, and transformed into BL21(DE3). Attempts to over-express *ThiE* (4 h at 37 °C) from pRL2000/BL21(DE3) and then from pRL2020/BL21(DE3), proved unsuccessful. In each experiment, both the cleared lysates and pellets were analysed by SDS-PAGE, but *ThiE* could not be detected in either of the two protein fractions. Then, as Backstrom *et al.* had previously succeeded in expressing this protein from a pET-derived vector (56), pRL2030 was assembled (Figure 4.3). The vector was transformed into BL21(DE3) and C43(DE3), and *ThiE* expressed at 37 °C for 4 h from both strains. SDS-PAGE analysis of cleared lysates and

² pBAD/His repair was assembled by Dr. M. Kriek in our laboratory and was obtained from pBAD/HisA by insertion of a sequence encoding a N-terminal (His)₆ tag in frame with any ligated gene product.

pellets from pRL2030/BL21(DE3) and pRL2030/C43(DE3) finally revealed the presence of ThiE (23 kDa) in the insoluble protein fractions (**Figure 4.4**).

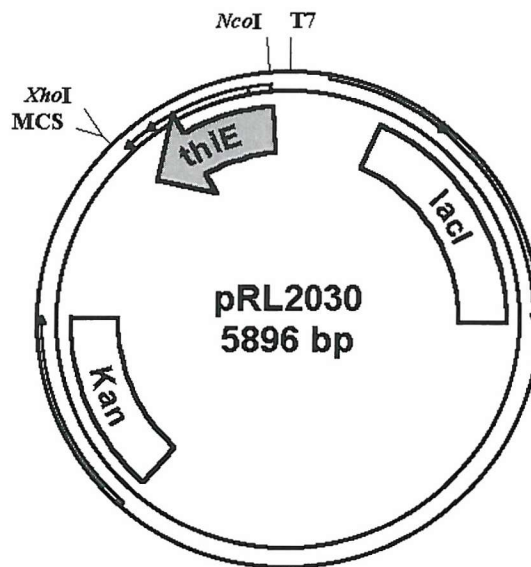


Figure 4.3. Map of pRL2030. MCS = Multiple Cloning Site.

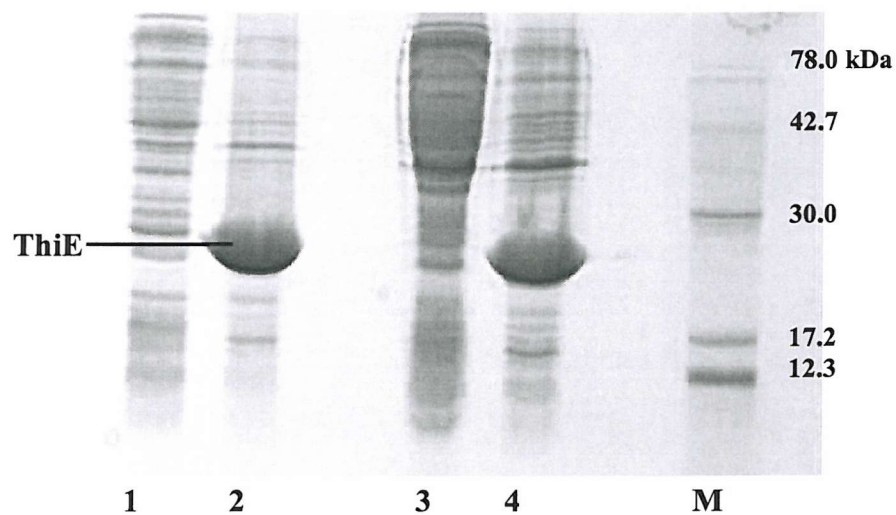


Figure 4.4. Coomassie Blue stained 15 % SDS-PAGE gel of soluble (lanes 1, 3) and insoluble (lanes 2, 4) proteins produced by pRL2030/BL21(DE3) (lanes 1, 2) and pRL2030/C43(DE3) (lanes 3, 4). M = molecular weight marker.

In these experiments the strength of the promoter proved to be crucial, as expression of ThiE could only be obtained from a pET-derived vector. This was rather surprising since ThiE had previously been tentatively identified by SDS-PAGE in the insoluble protein fraction of induced BL21(DE3) transformed with pRL1300, a pBAD-derived vector harbouring the whole *thiCEFSGH-His* (section 2.2.8) operon. However, neither soluble nor insoluble ThiE expression was obtained from BL21(DE3) transformed with pRL1500, another pBAD-derived vector encoding ThiEFSGH-His. In summary, these results seem to indicate that the expression of ThiE is extremely sensitive to the specific expression system, and that it can be dramatically affected by either the strength of the promoter or the presence of other co-expressed proteins.

4.2.3. Expression of *ThiD*

pRL2200 and pRL2220 (Figure 4.5), pBAD and pET-derived vectors, respectively, harbouring the same *thiD-His* (830 bp) gene between 5' *Nco*1 and 3' *Xho*1 restriction sites, were assembled to express ThiD as a hexahistidine-tagged protein. However, sequencing of pRL2200 revealed that the fourth histidine of the (His)₆ tag had been mutated, during the PCR amplification, to a proline. As the expressed ThiD-His did not efficiently bind to a nickel-chelating column, the protein will be referred to as ThiD.

pRL2200 and pRL2220 were transformed into BL21(DE3). ThiD (28.6 kDa) was expressed from pRL2200/BL21(DE3) at 37 °C for 6 h and from pRL2220/BL21(DE3) at 37 °C for 4 h, in two separate experiments. SDS-PAGE analysis of the soluble and insoluble protein fractions from both strains revealed that the protein was mainly present as inclusion bodies (Figure 4.6).

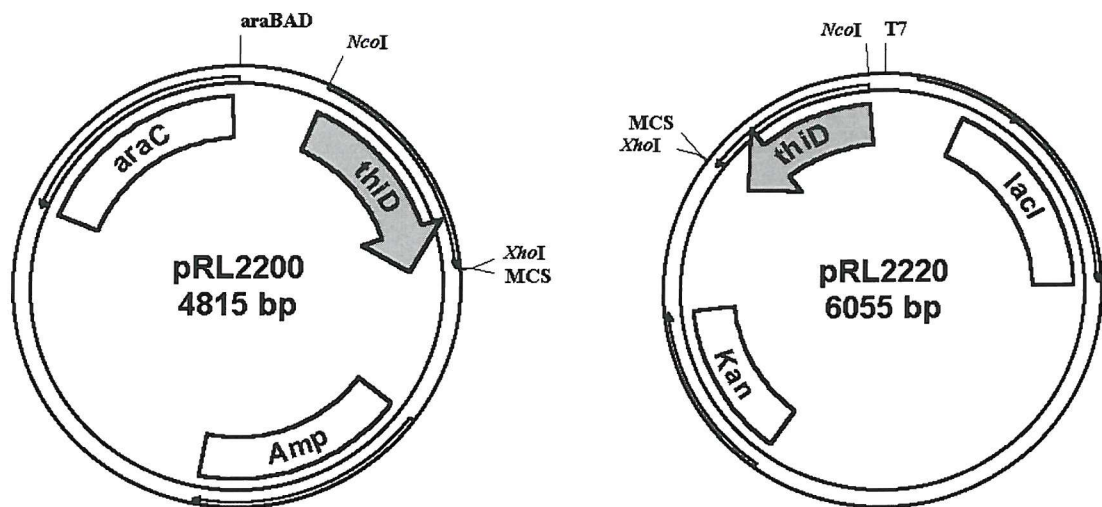


Figure 4.5. Maps of pRL2200 (left hand side) and of pRL2220 (right hand side). Maps not to scale. MCS = Multiple Cloning Site.

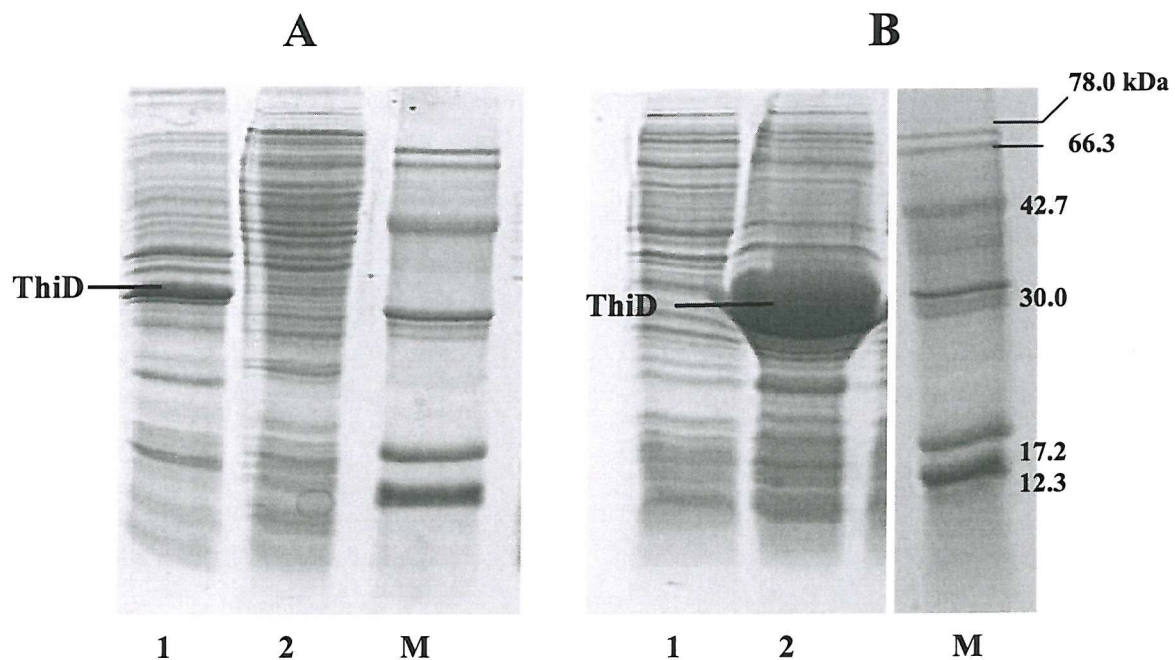
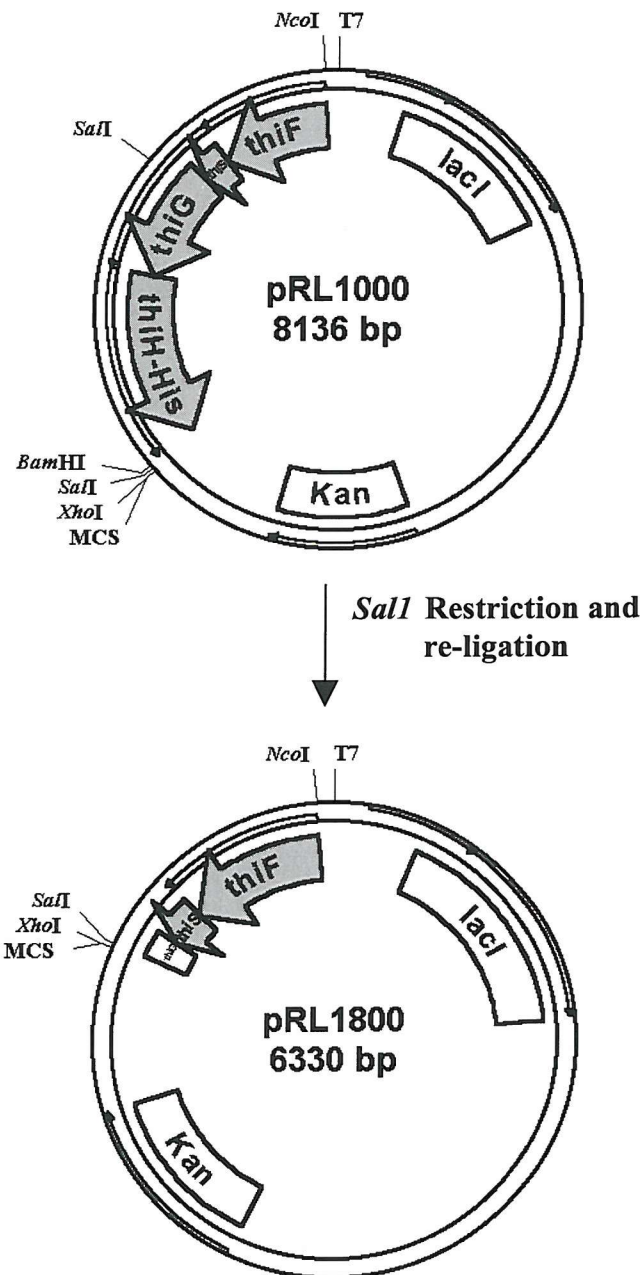


Figure 4.6. Coomassie Blue stained 15 % SDS-PAGE gels. A: proteins expressed from pRL2200/BL21(DE3), pellet (lane 1) and cleared lysate (lane 2). B: proteins expressed from pRL2220/BL21(DE3), cleared lysate (lane 1) and pellet (lane 2). M = molecular weight marker.

4.2.4 Expression and Purification of *ThiFS* from pRL1800/BL21(DE3)

pRL1800 was obtained from pRL1000 (section 2.2.5), a vector harbouring *thiFSGH-His*, by excising *thiH* and part of *thiG* with *SalI* (**Scheme 4.2**).



Scheme 4.2. Assembling of pRL1800 from pRL1000. Maps are not to scale. MCS = Multiple Cloning Site.

The resultant vector, encoding ThiFS, was then transformed into BL21(DE3) and the expression level of the two proteins compared at 27 and 37 °C after 12-14 h of induction. As the solubility of both ThiF and ThiS was visibly higher at 27 °C (Figure 4.7), the proteins were routinely expressed at this temperature.

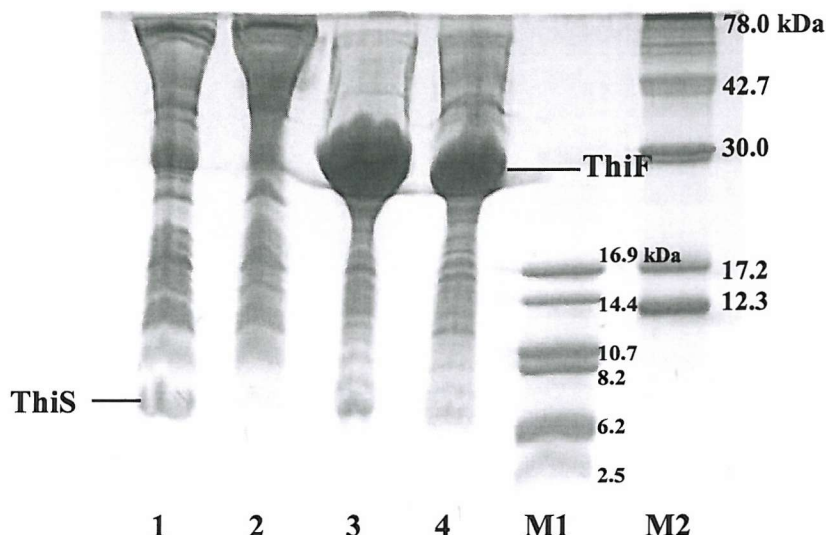


Figure 4.7. Coomassie Blue stained 18 % SDS-PAGE gel of proteins expressed from pRL1800/BL21(DE3) at 27 (lanes 1, 3) and 37 °C (lanes 2, 4): cleared lysates (lanes 1, 2) and pellets (lanes 3, 4). M1 = low molecular weight marker. M2 = high molecular weight marker. Despite the fact that ThiS had previously been reported to stain poorly with Coomassie Blue (71), the protein was clearly visible on 18 % gels (see also Figures 4.8 and 4.11).

ThiF and ThiS were purified as described by Taylor *et al.* (71), first by ammonium sulphate precipitation at 4°C, followed by dialysis, and then by ion exchange chromatography. In our hands ThiF and ThiS did not co-elute (Figure 4.8), and the respective fractions were separately pooled and further purified by gel filtration chromatography (Figures 4.9-4.10).

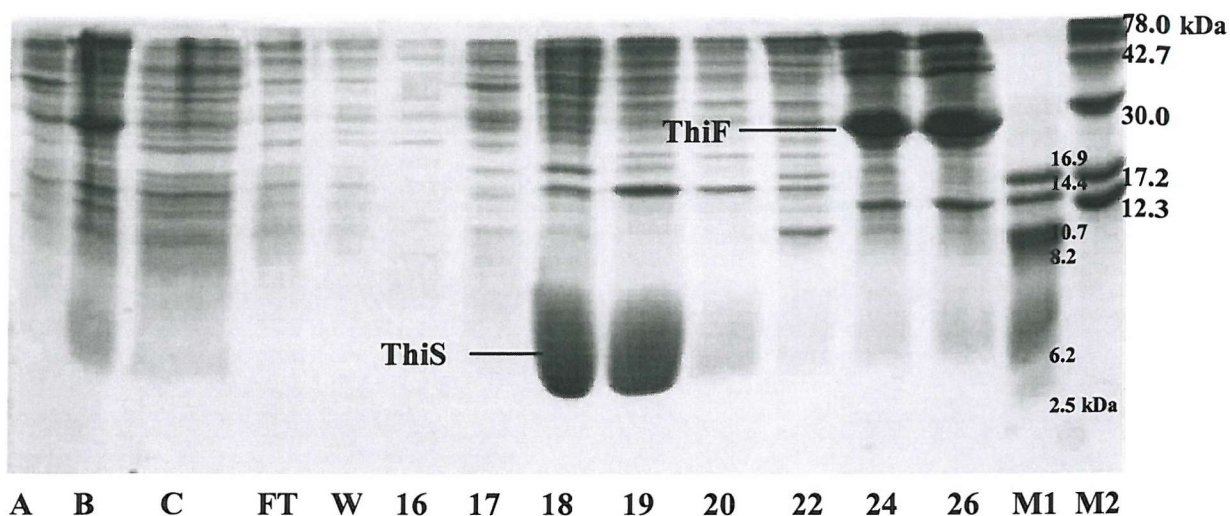


Figure 4.8. First step in the ThiFS purification. Coomassie Blue stained 18 % SDS-PAGE gel of pellets and supernatant from the $(\text{NH}_4)_2\text{SO}_4$ precipitation, and fractions eluted from the ion exchange column (Q-Sepharose). Lanes A and B: 0-20 % and 20-50 % pellets from the $(\text{NH}_4)_2\text{SO}_4$ precipitation, respectively; lane C: supernatant from the 50 % saturation with $(\text{NH}_4)_2\text{SO}_4$. The solubilised 20-50 % pellet was applied onto a Q-Sepharose column. FT = flow through; W = washing; M1 = low molecular weight marker; M2 = high molecular weight marker. Numbers correspond to the fraction numbers. Fractions 18-19, enriched in ThiS, and fractions 24-26, enriched in ThiF, were pooled, concentrated and applied to a S-75 gel filtration column.

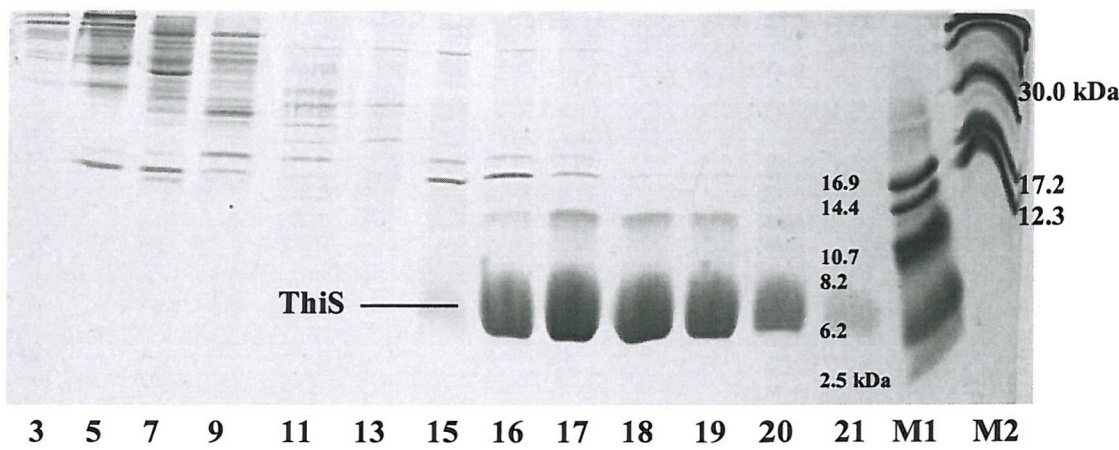


Figure 4.9. ThiS purification. Coomassie Blue stained 18 % SDS-PAGE of fractions eluted from the gel filtration column (S-75). M1 = low molecular weight marker; M2 = high molecular weight marker. Numbers correspond to the fraction numbers.

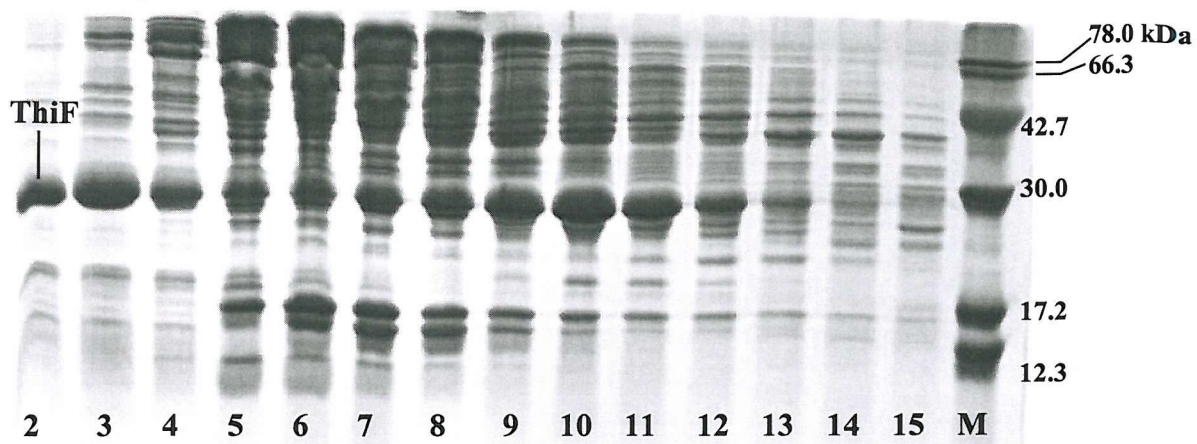


Figure 4.10. ThiF purification. Coomassie Blue stained 15 % SDS-PAGE gel of fractions eluted from the gel filtration column (S-75). M = molecular weight marker. Numbers correspond to the fraction numbers. Fractions 2-3 from 2 purifications were pooled and concentrated.

ThiS (7 kDa) was purified to a high purity (> 95 %) (Figure 4.11), as estimated by SDS-PAGE, and in relatively high yield (80 mg from 27 g of cell paste). However, ThiF (27 kDa) was obtained rather less pure (Figure 4.11), in a much lower yield (the purest fractions from two purifications were pooled to give 20 mg of protein from a total amount of 77 g of cell paste), and was not further purified.

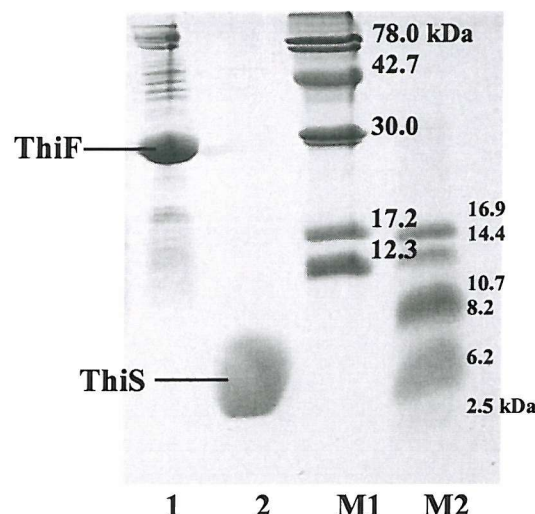


Figure 4.11. Coomassie Blue stained 18 % SDS-PAGE gel of purified ThiF (lane 1) and ThiS (lane 2). M1 = high molecular weight marker; M2 = low molecular weight marker.

Samples of ThiS and ThiF were analysed by ESI-MS. The molecular weights were determined to be 7309.1 and 27068.2 kDa, respectively. These results are in very good agreement with the calculated molecular weights based on the amino acid sequences of the two proteins: 7311.3 kDa for ThiS and 27068.9 kDa for ThiF which contains an extra N-terminal valine deriving from the introduction of the 5' *Nco*1 restriction site during the amplification of the *thiFSGH-His* fragment (section 2.2.5).

4.2.5 Expression and Purification of Dxs-His

BL21(DE3) cells transformed with a pET-23b-derived vector encoding a hexahistidine-tagged Dxs (67 kDa) were kindly donated by Prof. A. Boronat (10). Dxs-His was expressed from these cells at 22 °C for 5 h. **Figure 4.12** shows the expression level of the protein in either the soluble or insoluble fractions.

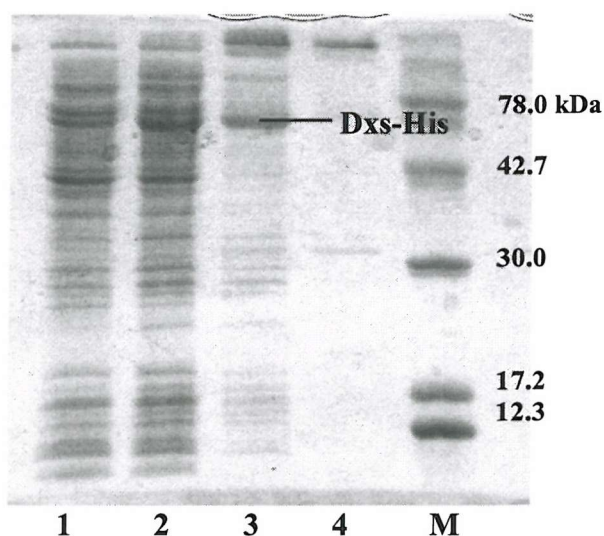


Figure 4.12. Coomassie Blue stained 15 % SDS-PAGE gel of soluble (lanes 1, 2) and insoluble (3, 4) proteins expressed from 2 colonies of BL21(DE3) transformed with a pET-23b-derived vector encoding Dxs-His. Colony 1 = lanes 1, 3; colony 2 = lanes 2, 4. M = molecular weight marker.

Dxs-His was purified by nickel affinity and gel filtration chromatographies to 50-60 % purity (**Figure 4.13**), as estimated by SDS-PAGE analysis. The purification

yielded 170 mg of partially purified Dxs-His from 19 g of cell paste, and this protein was used for the enzymatic synthesis of 1-deoxy-D-xylulose-5-phosphate without any further purification.

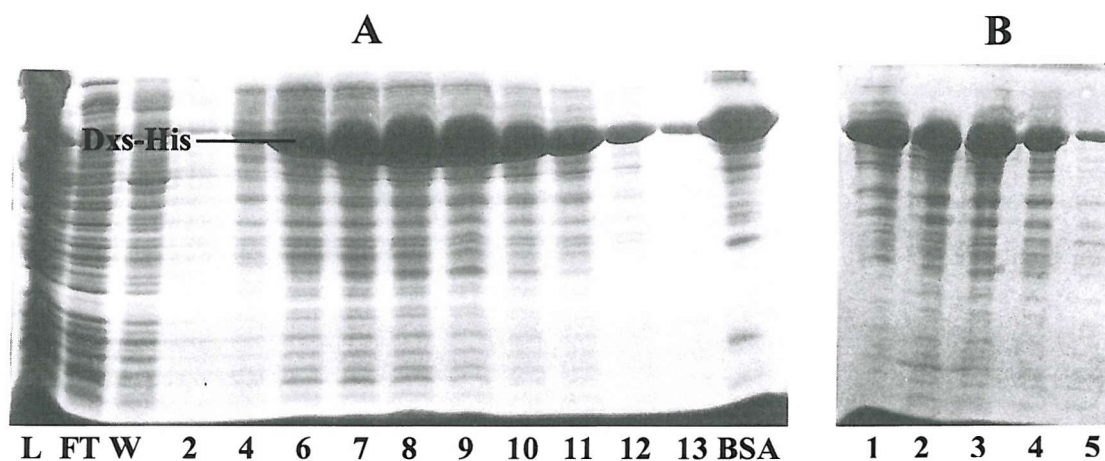
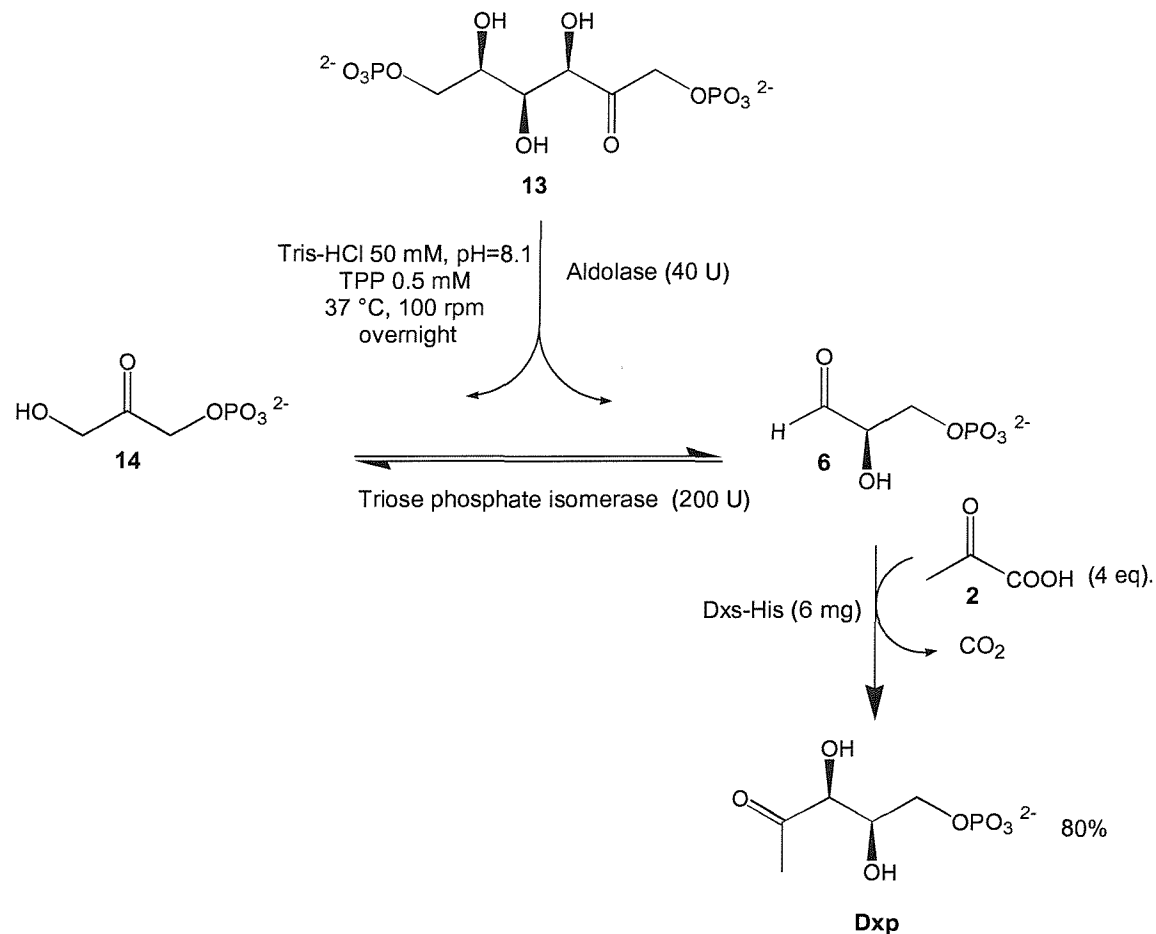


Figure 4.13. Dxs-His purification. Coomassie Blue stained 15 % SDS-PAGE gel of fractions eluted from the nickel-chelating (A) and gel filtration (B) columns. L = cleared lysate; FT = flow through; W = washing. Numbers correspond to the fraction numbers. Fractions 7-12 from the nickel-chelating column were applied to a gel filtration column (S-75). BSA was used as molecular weight marker.

4.2.6. Enzymatic Synthesis of 1-deoxy-D-xylulose-5-phosphate (Dxp)

Dxp was enzymatically synthesized as described by Taylor *et al.* (158) (**Scheme 4.3**), by using partially purified Dxs-His (section 4.2.5) and commercially available aldolase and triose phosphate isomerase (Sigma). The progress of the reaction was monitored by TLC analysis (159), and when it was judged to be complete (> 80 % conversion), the proteins were removed by ultrafiltration (10 kDa MWCO) and the mixture freeze-dried.

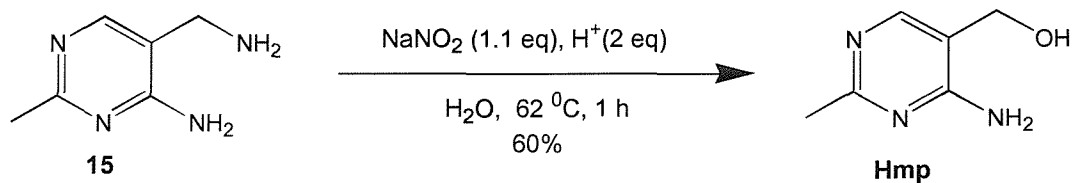
Dxp was purified by semi-preparative HPLC to remove any trace of residual thiamine pyrophosphate (added to the reaction mixture as Dxs-His cofactor, section 1.2).



Scheme 4.3. Enzymatic synthesis of 1-deoxy-D-xylulose-5-phosphate.

4.2.7. *Synthesis of 4-amino-5-hydroxymethyl-2-methylpyrimidine (Hmp)*

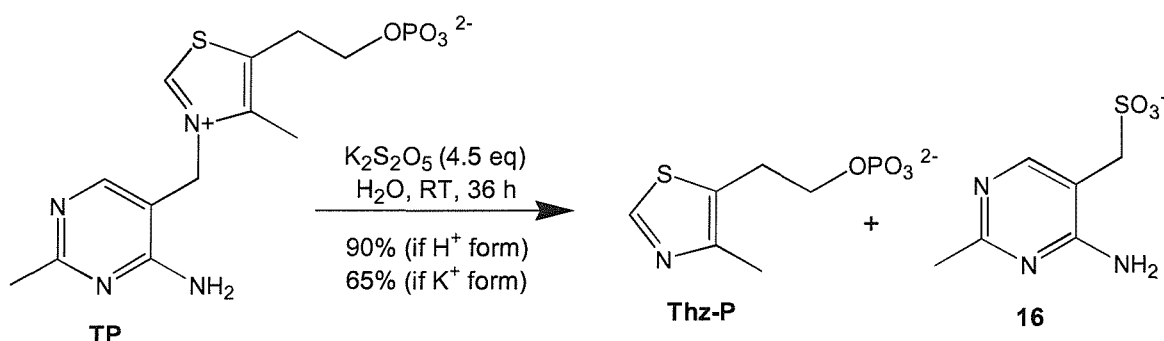
Hmp was synthesised from 4-amino-5-aminomethyl-2-methylpyrimidine (14) as described by Westphal and Andersag (160) (**Scheme 4.4**) and purified by silica chromatography. The product was obtained as a white to off-white powder in fair yield (60 %).



Scheme 4.4. Synthesis of 4-amino-5-hydroxymethyl-2-methylpyrimidine (Hmp).

4.2.8. Synthesis of 4-methyl-5-(β -hydroxyethyl)thiazole phosphate (Thz-P)

4-methyl-5-(β -hydroxyethyl)thiazole phosphate was obtained by bisulphite cleavage of thiamine monophosphate (161). The compound crystallised from the reaction mixture at 4 °C and was recovered in good yield and highly pure (> 90 %) without further purification (**Scheme 4.5**).



Scheme 4.5. Synthesis of 4-methyl-5-(β -hydroxyethyl)thiazole phosphate (Thz-P).

4.3. Summary and Conclusions

Plasmids encoding various proteins potentially required for assaying *in vitro* thiazole formation in *E. coli*, were assembled. The expression level of ThiI, ThiE and ThiD from the respective vectors transformed into BL21(DE3) was investigated, and ThiF and ThiS were expressed and purified.

The thiamine precursors, Hmp, Thz-P and Dxp were synthesised following published procedures, and in particular, the availability of a source of Dxs allowed the enzymatic synthesis of 1-deoxy-D-xylulose-5-phosphate.

Chapter 5.

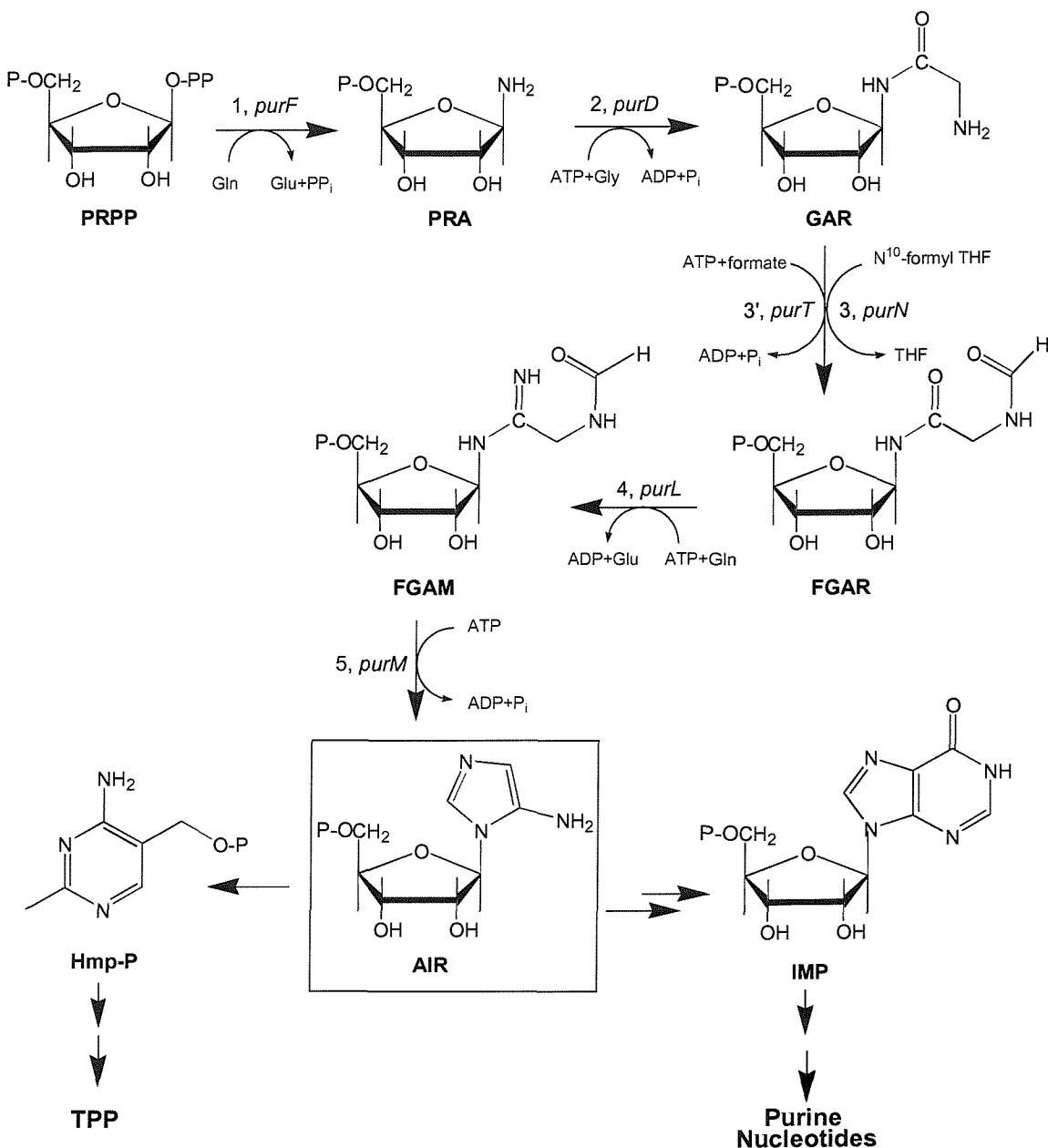
In Vivo Studies on Thiamine Biosynthesis

5.1. Introduction

Bacterial cultures grown in TPP-free minimal media normally produce very small quantities of thiamine pyrophosphate [15 µg per 1 of culture (5)]. However, if the growth medium is supplemented with the vitamin (0.1-0.2 µM), efficient uptake results in high intracellular concentrations [140 µg of TPP/mg of dry cells, as estimated in *S. typhimurium* (60)] (60,61). Increased levels of TPP have been correlated with the loss of thiamine biosynthetic activity in both *E. coli* and *S. typhimurium* cells (60,61,68). This effect has been rationalised in terms of repression, rather than inhibition, exerted from the vitamin on its own biosynthesis (41,43,44,61,162). More recent studies by Winkler and co-workers (64) have provided supporting evidence for the negative regulatory role of TPP, which has been shown to bind to untranslated regulatory regions in *thiM* and *thiC* mRNAs, thus resulting in attenuation of either transcription or translation of these key operons involved in thiamine biosynthesis (section 1.3.2).

The addition of adenosine or adenine during the growth phase of enteric bacteria, such as *A. aerogenes* (163), *S. typhimurium* (60,68) and *E. coli* (30,61,162), is known to cause a decrease in the intracellular concentration of thiamine pyrophosphate. The consequent release of the vitamin repression is then expected to lead to increased levels of TPP biosynthetic enzymes; in fact, Kawasaki and co-workers have demonstrated that *E. coli* cells pre-treated with adenine possessed increased ThiE and ThiMD activities (61).

Adenosine and adenine are negative regulators of the *de novo* purine biosynthesis (17,164,165), the main pathway by which 5-aminoimidazole ribotide (AIR) is assembled (**Scheme 5.1**).

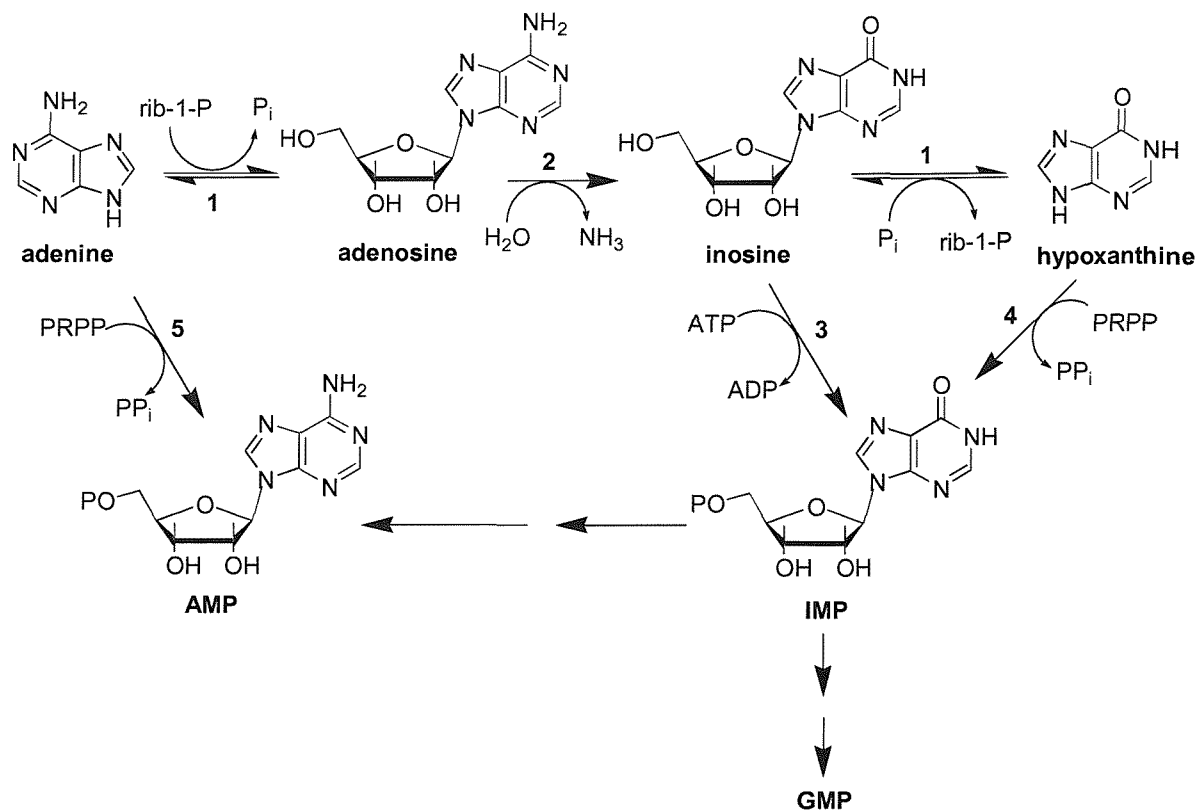


Scheme 5.1. Formation of AIR through the first five steps of the *de novo* purine biosynthesis. 1: glutamine PRPP amidotrasferase; 2: GAR synthetase; 3: GAR transformylase N; 3': GAR transformylase T; 4: FGAM synthetase; 5: AIR synthetase. The genes encoding the respective enzymes are indicated. Abbreviations are as follows: PRPP, 5-phosphoribosyl-1-pyrophosphate; PRA, 5-phosphoribosylamine; GAR, glycinamide ribonucleotide; FGAR, formylglycinamide ribonucleotide; FGAM, formylglycinamide ribonucleotide; AIR, 5-aminoimidazole ribonucleotide; IMP, inosine 5'-monophosphate. Adapted from (17).

As AIR is a branch point metabolite which is converted to purine nucleotides and to Hmp for thiamine biosynthesis (section 1.3.2), the addition of adenosine or adenine to growing bacterial cultures is thought to reduce thiamine biosynthesis by decreasing the pools of this intermediate.

An alternative minor biosynthetic route to AIR and Hmp has been recently discovered, in *S. typhimurium*, by D. Downs and co-workers (166-169). Under aerobic growth conditions, this alternative pyrimidine biosynthetic (APB) pathway can bypass only the first enzyme of the *de novo* purine biosynthesis, phosphoribosylpyrophosphate amidotransferase (PurF, **Scheme 5.1**), requiring the remaining purine biosynthetic enzymes to assemble AIR. It is therefore likely that the APB pathway is also subjected to the regulation by adenine or adenosine. Furthermore, the function of this pathway is dependent on the medium composition, and PurF-*independent* thiamine biosynthesis does not normally occur in minimal glucose or citrate media, such as those used in the experiments described here.

Once inside cells, adenosine and adenine can be interconverted. One of the proposed mechanisms through which these compounds might repress the *de novo* purine biosynthesis is their conversion to hypoxanthine (17,170-172) (**Scheme 5.2**). Hypoxanthine and guanine have been suggested to be PurR co-repressors (172), and PurR is the protein which controls the gene expression of almost all the enzymes required in the *de novo* purine biosynthetic pathway (172). Besides being a source of hypoxanthine, adenine has also been shown to increase the levels of *purR* mRNA (173), and as its addition to the growth medium results in increased pools of AMP/ATP (172), feedback inhibition of PurF is another possible way in which adenine might control the *de novo* purine biosynthesis (17).



Scheme 5.2. Pathways of purine interconversion. 1: purine nucleoside phosphorylase; 2: adenosine deaminase; 3: guanosine kinase; 4: hypoxanthine phosphoribosyltransferase; 5: adenine phosphoribosyltransferase. Abbreviations are as follows: rib-1-P, ribose 1-phosphate; PRPP, 5-phosphoribosyl-1-pyrophosphate; IMP, inosine 5'-monophosphate. The addition of adenine (40 mg/l) to the growth medium of wild type *E. coli* has been shown to increase the adenosine deaminase (2) and purine nucleoside phosphorylase (1) levels 14 and 1.4 times, respectively (17).

Whilst the TPP content in *E. coli* K12 has been more efficiently lowered by adenine under the conditions adopted by Kawasaki (61), *A. aerogenes* (163), *S. typhimurium* LT-2 (60,68) and *E. coli* 83-1 (30) have been de-repressed in the presence of adenosine.

Adenosine treated *E. coli* 83-1 has been successfully used for *in vivo* studies on thiamine biosynthesis, allowing the identification of tyrosine (30) and Dxp (29) as precursors of the thiazole ring of the vitamin. As the de-repression of thiamine biosynthesis observed upon treating bacterial cells with adenosine has been proposed to

result from the accumulation of thiamine biosynthetic enzymes (61), these de-repressed cells had potential to provide an optimised cell-free system to allow thiazole biosynthesis to be assayed *in vitro*.

As a prerequisite to the investigation of *in vitro* thiazole biosynthesis using extracts from adenosine treated *E. coli* 83-1, preliminary studies on the *in vivo* thiamine production by these cells were conducted.

Another *E. coli* strain, KG33, which is a Thz-P auxotroph and was used for *in vivo* complementation experiments (section 3.2.6), was considered as a potential system for *in vitro* studies. pBAD/HisA/KG33 was de-repressed by thiamine starvation and the correspondent cleared lysate assayed for *in vitro* thiazole biosynthesis in the presence of purified ThiGH-His.

5.2. Results and Discussion

Unless otherwise specified, the term 'thiamine' is used to indicate any vitamin form, without regard to the extent of phosphorylation.

*5.2.1. Effect of the Adenosine Treatment on the Production of TPP by *E. coli* 83-1*

E. coli 83-1 cells, Tyr/Trp/Phe auxotrophs were a generous gift from Prof. R. Azerad and Prof. M. Therisod. These cells were incubated with adenosine under experimental conditions analogous to those adopted by Newell and Tucker in their investigation of the de-repression of thiamine biosynthesis in *S. typhimurium* LT2 (mutant T) (60,68). However, modifications to the growth medium were required to provide the auxotrophic growth requirements for *E. coli* 83-1 (30), which include the aromatic amino acids Phe, Trp and Tyr. Besides being essential for growth, Tyr is also one of the thiazole precursors, therefore if this amino acid was not provided, *E. coli* 83-1 would have to rely on the Tyr scavenged from protein degradation for *de novo* thiamine biosynthesis.

The time course of the *in vivo* de-repression and subsequent burst in thiamine production in *E. coli* 83-1 was investigated in detail. Each experiment consisted of two parts. During the first part, cells were grown in the presence of adenosine (300 mg/l)

for exactly 2.5 h before being harvested. In the second part, the cell pellets were washed and re-suspended in medium lacking any growth component and containing no supplements, Tyr plus Hmp or Thz-P plus Hmp. During either phase of the experiment, cell samples were withdrawn every 30 min and the thiamine content estimated by the thiochrome assay (174) (section 7.7.1).

Figure 5.1 shows the difference in the TPP content between adenosine treated and untreated cells (negative control) during the first part of the experiment. As expected, the addition of adenosine during the growth phase, caused a drop in the initial TPP content (3-4 ng/mg wet cells), with the vitamin level remaining low for about 2 h, before starting to increase towards the end of this first phase.

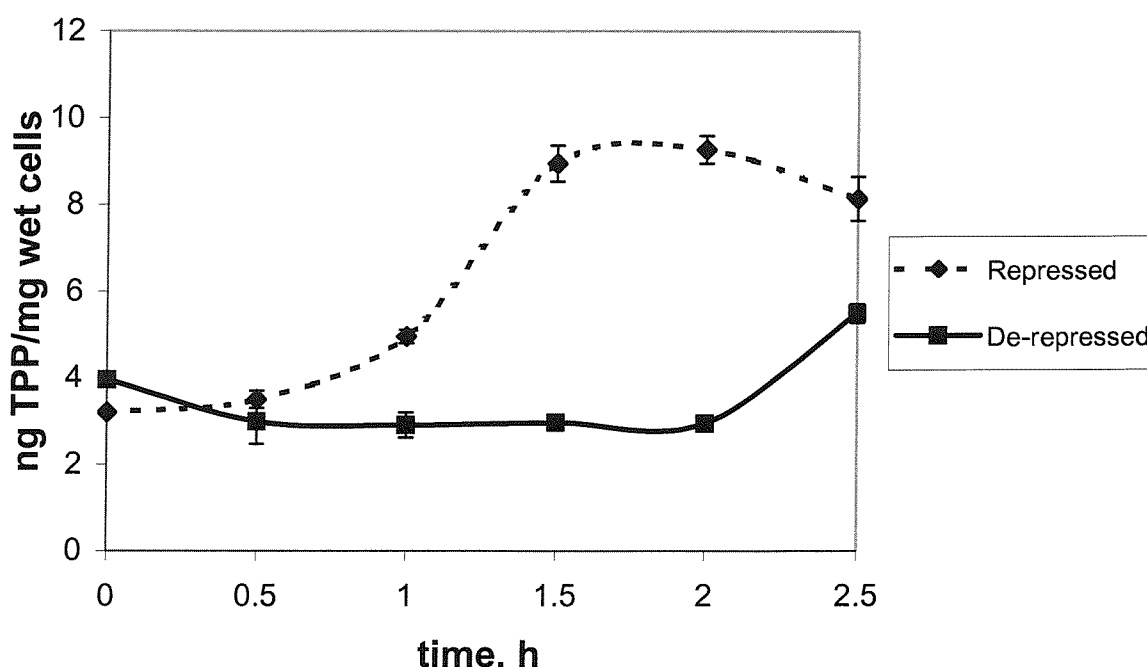


Figure 5.1. TPP content of *E. coli* 83-1 incubated with (solid line) or without (dashed line) adenosine. The experiments were carried out in duplicate. Original data from HPLC files: HPLC\Methods\FLUC18_2.061, 67

During the period of low thiamine concentration, *E. coli* 83-1 was freed from the vitamin repression and could accumulate higher (de-repressed) levels of

biosynthetic enzymes, thus being able to produce approximately 1.5-3 times more TPP than the negative control using the Tyr and Hmp provided in the medium (second part of the experiment, **Figure 5.2**). Under these conditions, the burst in the vitamin production may be ascribed to *de novo* synthesis of thiazole (30,175), since this moiety does not accumulate in TPP depleted cells, such as adenosine-treated cells or in mutants unable to assemble Hmp-PP (60,163).

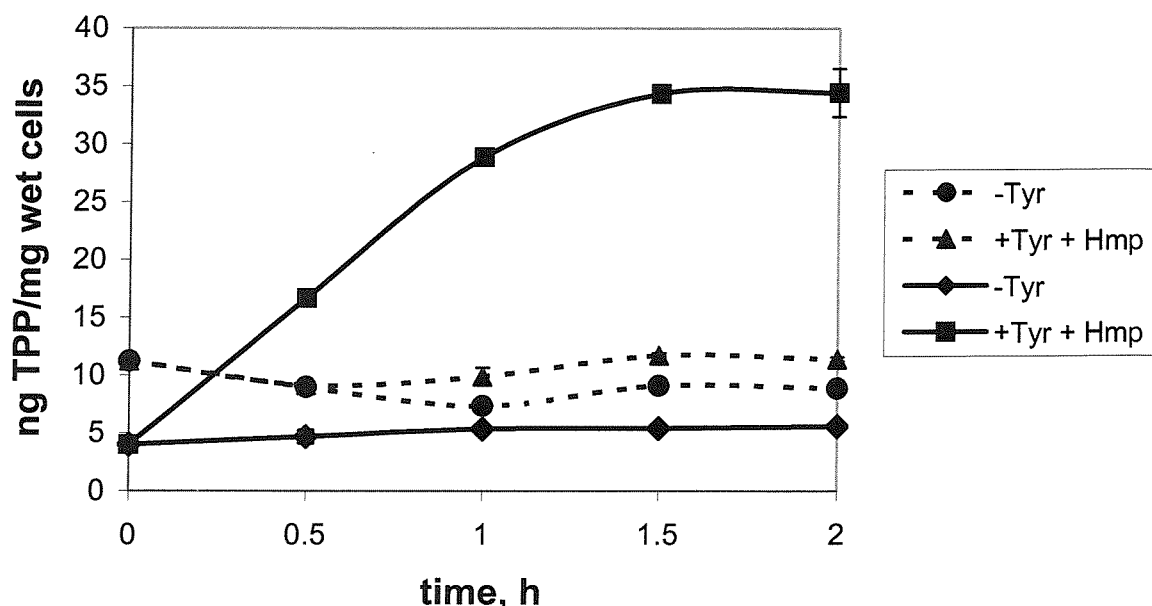


Figure 5.2. TPP production by washed cell suspensions of *E. coli* 83-1 previously incubated with (solid lines) or without (dashed lines) adenosine. The experiments were carried out in duplicate and the error was estimated to be $\leq 8\%$. Original data from HPLC files: HPLC\Methods\FLUC18_2.061, 62, 66.

In a positive control experiment, using media supplemented by the addition of not only Hmp, but also Thz-P, both adenosine treated and untreated cells were able to produce 60-70 ng of TPP/mg wet cells (**Table 5.1**, column 4). This suggests that in experiments where the medium was supplemented with Hmp and thiazole precursors, any Thz-P produced would be rapidly converted to TPP, and that neither ThiD nor

ThiE were limiting the TPP formation. Indeed, these results strongly suggest that, under the conditions investigated, thiazole biosynthesis is likely to be the rate-limiting step.

Initial Culture Conditions	- Tyr	+ Tyr+ Hmp	+ Thz-P+ Hmp
+ adenosine	5.6 ± 0.1	34 ± 2	64 ± 4
- adenosine	8.9 ± 0.2	11.4 ± 0.2	67 ± 1

Table 5.1. Effect of adenosine treatment on the TPP content (ng/mg wet cells) of washed cell suspensions of *E. coli* 83-1. Cells were initially cultured for 2.5 h in DM1 medium with or without adenosine, as indicated, then transferred to fresh DM medium supplemented as indicated, and incubated for 2 h. The data are the mean of 2 independent measurements ± SD.

The observation that the pre-incubation with adenosine had lowered the intracellular TPP concentration and, as a result, may have increased the expression level of the rate determining thiazole biosynthetic enzymes, contrasted with the activities of ThiD and ThiE which were not equally affected. This is an unexpected result since the genes encoding these two proteins belong to the *thiMD* and *thiCEFSGH* operons and ought therefore to be subjected to coordinated repression by thiamine (41,43,61,64,162). Despite the lack of a simple explanation for these results, Newell and Tucker observed a precisely analogous effect with the *Salmonella* mutant used for their studies (60). An alternative regulatory mechanism, operating at the translational or metabolic level can be invoked to explain these observations, but it is clear that more than one factor is controlling the balance of the different thiamine biosynthetic enzymes.

In summary, the results obtained from the de-repression of *E. coli* 83-1 are in very good agreement with those obtained from analogous experiments on *S. typhimurium* (60,68). In fact, if a correction factor of 0.1 or 0.2 [the dry mass content is

normally 10-20 % of the wet mass (176)] is used for the conversion of the dry weight (used to express the results obtained from the studies on *S. typhimurium*) to the wet weight of cells, the TPP content in the two organisms is numerically very close and varies in a similar way during both phases of the de-repression experiment.

Thus, the U-shaped variation in the vitamin content during the 2.5 h of the adenosine treatment was observed to be a quite typical common feature. A possible explanation for this shape is provided by studies on the metabolism of adenosine in *E. coli* (171). These studies demonstrated that 10 min after the addition of this nucleoside (93 mg/l) to growing bacterial cultures, hypoxanthine and inosine (**Scheme 5.2**) began to be excreted into the medium, with adenosine being completely metabolised after 70 min. The total amount of inosine and hypoxanthine excreted after 100 min corresponded to 98.5 % of the adenosine initially added, with the remaining 1.5 % being taken up by the cells in the form of hypoxanthine for nucleic acid biosynthesis, as no *de novo* purine biosynthesis occurs in the presence of adenosine or its metabolites (section 5.1). This rapid extracellular production and accumulation of hypoxanthine, which also results in an increased intracellular concentration of the co-repressor, could actually be related to the decrease in the intracellular TPP level after just 30 min from the addition of adenosine.

It is more difficult to explain the abrupt increase in the vitamin content 2 h after the addition of the purine nucleoside. Both *S. typhimurium* LT2 and *E. coli* 83-1 seem to be able to overcome the repression of the known pathways to AIR (section 5.1), under conditions in which at least the extracellular concentration of hypoxanthine is expected to be high. Again, an alternative regulatory mechanism can be invoked, but our current understanding of the factors controlling the cross-talk amongst different biosynthetic pathways is still fragmentary.

5.2.2. Comparison between Adenosine Treated 83-1 and pRL1020/83-1 Cells in the Presence of β -L-arabinose

As the assembly of Thz-P was observed to be rate limiting for TPP production in de-repressed *E. coli* 83-1 cultures, the effect of expression plasmids encoding structural genes known to be required for Thz-P biosynthesis under these conditions,

was investigated. The de-repression experiments described above were repeated using the *E. coli* pRL1020/83-1 strain, obtained from the transformation of the 83-1 cells with pRL1020, a plasmid encoding ThiFSGH-His (83).

E. coli 83-1 and pRL1020/83-1 were cultured in the presence of adenosine (to de-repress thiamine biosynthesis) and β -L-arabinose (to induce the expression of ThiFSGH) for 2.5 h (Figure 5.3). However, washed cell suspensions of pRL1020/83-1 produced only marginally more TPP than 83-1 (Figure 5.4), and comparative analysis of the proteins in the cleared cell lysates by SDS-PAGE, did not show an appreciable difference in the protein expression levels (Figure 5.5). This maybe due to the short induction time or it may be a function of the high glucose content of the growth medium acting to repress expression from pRL1020 (177).

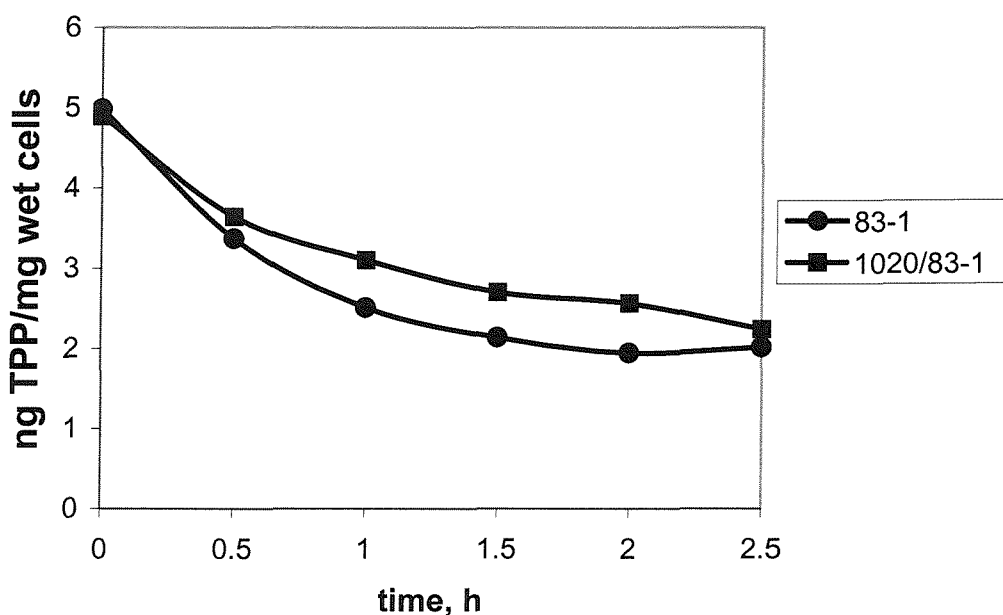


Figure 5.3. TPP content of *E. coli* 83-1 and pRL1020/83-1 incubated with adenosine in the presence of β -L-arabinose. Original data from HPLC files: HPLC\Methods\FLUC18_2.076-77.

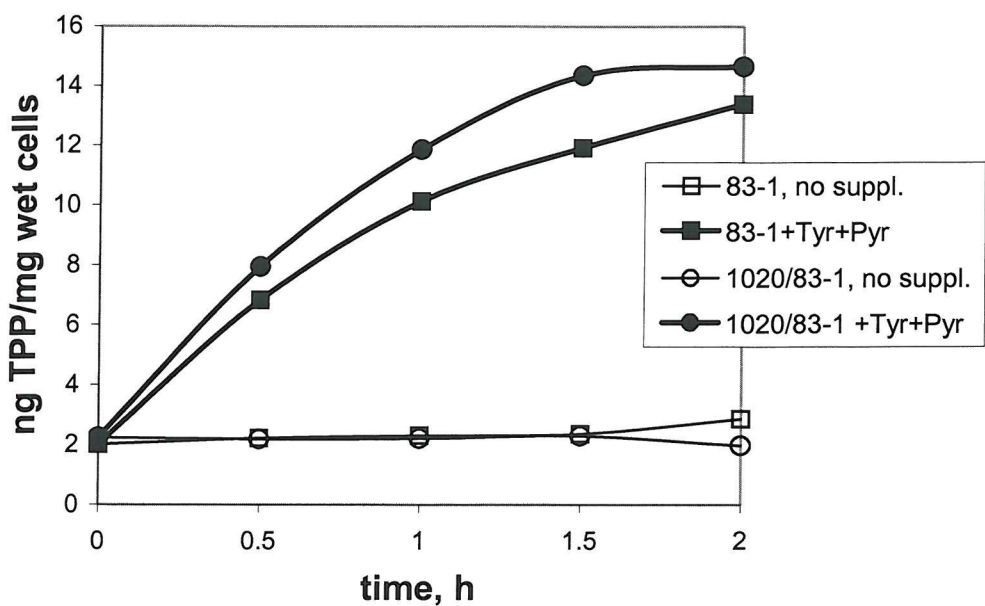


Figure 5.4. TPP production by washed cell suspensions of *E. coli* 83-1 and pRL1020/83-1, previously incubated with adenosine and β -L-arabinose. Original data from HPLC files: HPLC\Methods\FLUC18_2.076-77.

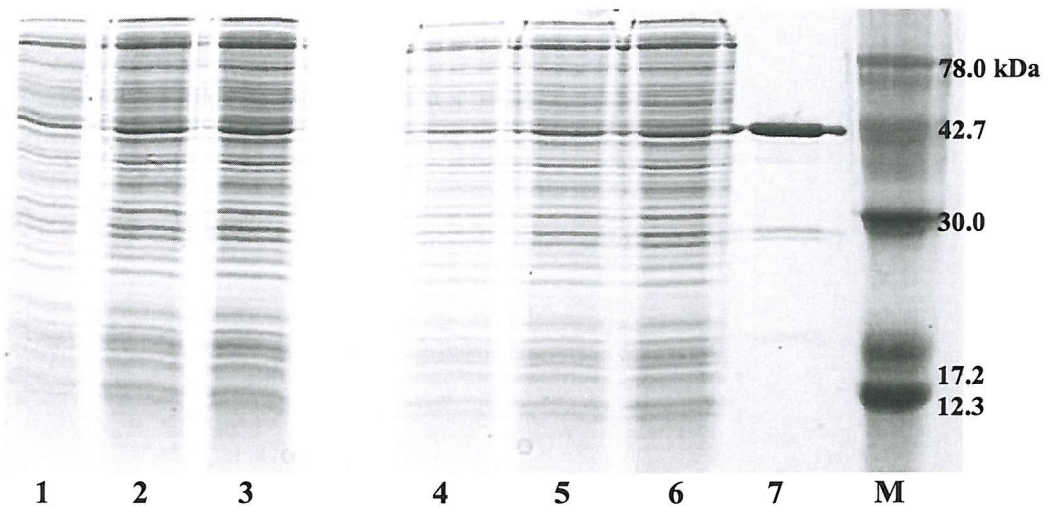


Figure 5.5. Coomassie Blue stained 15 % SDS-PAGE gel of soluble proteins expressed during the adenosine treatment of *E. coli* pRL1020/83-1 (lanes 1-3) and 83-1 (lanes 4-6) in the presence of β -L-arabinose. 50 (lanes 1, 4), 100 (lanes 2, 5) and 150 (3, 6) μ g of protein were loaded. Lane 7: purified ThiGH-His from pRL800. M = molecular weight marker.

Interestingly, at the end of the adenosine treatment (i.e. 2.5 h into the de-repression phase) the TPP level in both *E. coli* 83-1 and pRL1020/83-1 was still low, probably as a result of the persistence of repressing conditions for the *de novo* purine biosynthesis (Figure 5.3). This might be in some way related to the presence of the arabinose, as the omission of the sugar in all the subsequent large scale de-repression experiments (Chapter 6), resulted in the typical U-shaped variation in the thiamine content of adenosine treated pRL1020/83-1. As the presence of pRL1020 did not alter the response to the adenosine treatment, but conveniently conferred ampicillin resistance, extracts from de-repressed *E. coli* pRL1020/83-1 were used to assay thiazole biosynthesis *in vitro*.

5.2.3. De-repression Experiments on *E. coli* KG33 Cells

The addition of adenosine or adenine during the growth phase of enteric bacteria de-represses thiamine biosynthesis by lowering the pools of AIR and therefore the intracellular vitamin content. A similar effect could in principle be obtained by pre-culturing mutants blocked in one or more steps of thiamine biosynthesis in rich media (containing enough vitamin to support the growth), and then allowing them to grow in a TPP-free medium until they consume most of the vitamin they have sequestered. At that point, all the biosynthetic steps prior to the blockage should become de-repressed, allowing the accumulation of specific intermediates. For example, mutants unable to assemble the thiazole have been shown to accumulate the pyrimidine portion of the vitamin (45,60,67). However, as previously mentioned, accumulation of Thz-P in mutants unable to synthesise Hmp-PP has not been observed, and it has been proposed that this compound might exert a feedback inhibition on its own biosynthesis (60,163).

E. coli KG33 contains a mutation in ThiH responsible for the Thz-P auxotrophy of this strain (section 3.2.6) (39). As the other genes encoded by the *thiCEFSGH* operon of these cells are intact, starvation of thiamine should allow the de-repression of all the biosynthetic steps prior to that catalysed by ThiH, thus potentially leading to increased expression levels of ThiCEFSG and possibly, to the accumulation of the direct ThiH substrate. Cell-free extracts from such de-repressed *E. coli* KG33 could

then provide an optimised system to test the *in vitro* thiazole synthase activity of purified ThiGH-His.

To provide evidence supporting this hypothesis, *E. coli* KG33, transformed with pBAD/HisA to confer ampicillin resistance, was de-repressed by thiamine starvation. 2YT medium, which contains the equivalent of 1.3 mg/l of TPP (the vitamin is present as unphosphorylated thiamine) and TPP-supplemented (3 mg/l, section 7.7.3) Davis-Mingioli medium (178) were chosen as rich growth media. pBAD/HisA/KG33 cells were cultured in these media overnight, then harvested, washed and transferred to TPP-free Davis-Mingioli medium. Samples were withdrawn every 90 min for 10-12 h to monitor the cellular growth and to estimate the thiamine content. **Figures 5.6 and 5.7** show the time course of bacterial growth and consequent decrease in the intracellular TPP content.

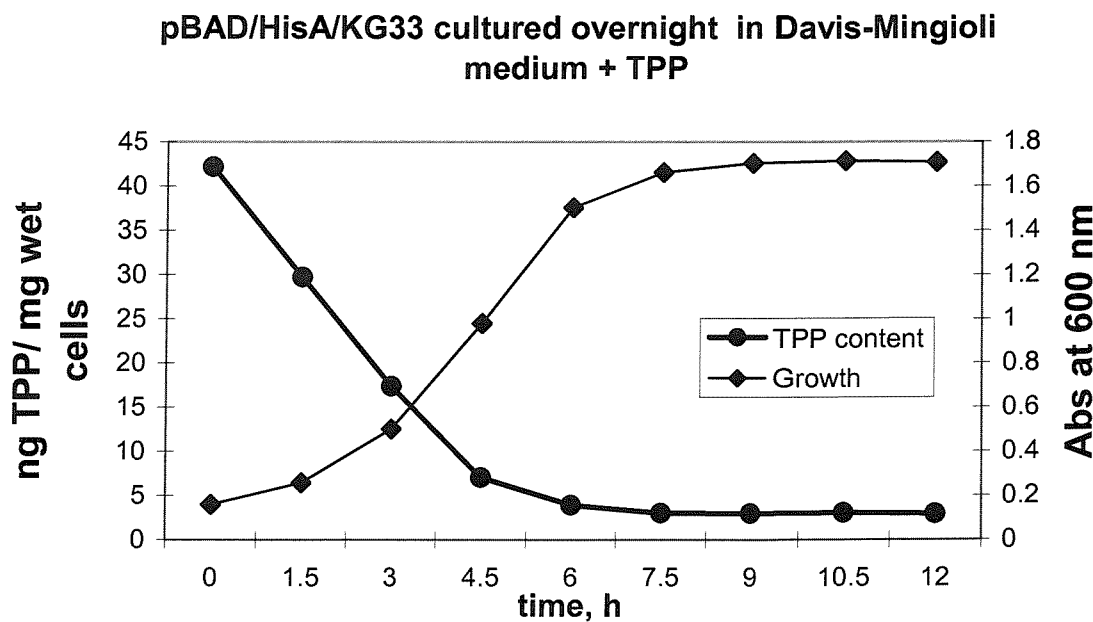


Figure 5.6. Time course of pBAD/HisA/KG33 growth in minimal Davis-Mingioli medium, and consequent depletion in TPP. Cells were previously cultured overnight in Davis-Mingioli medium supplemented with 3 mg/l TPP. The experiment was carried out in duplicate. The error associated with the estimation of the TPP content was $\leq 5\%$ and the error associated with measurement of the optical density of two independent cultures was $\leq 1\%$. Original data from HPLC file: HPLC\Methods\FLUC18.041.

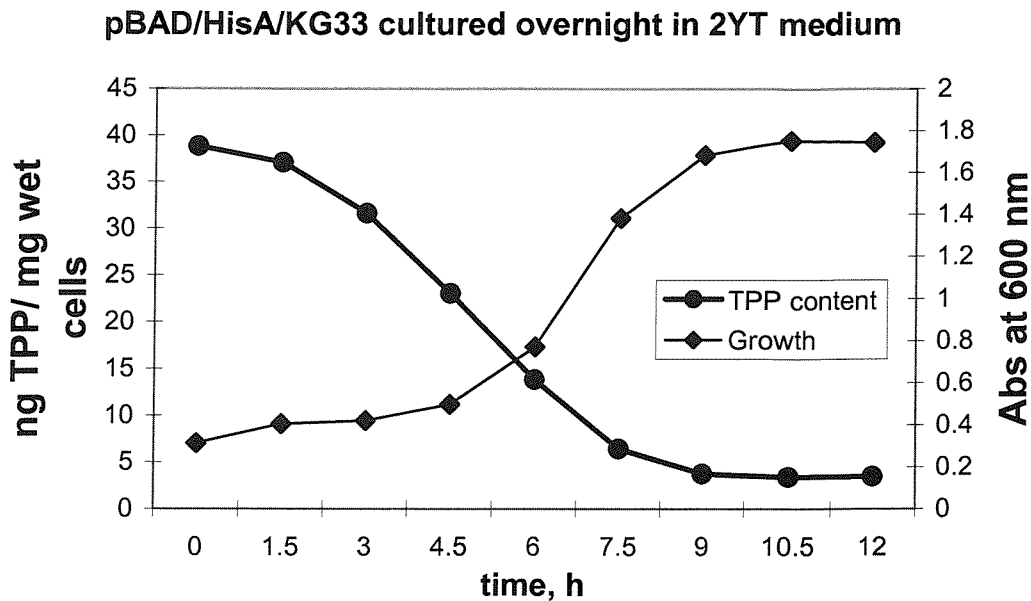


Figure 5.7. Time course of pBAD/HisA/KG33 growth in minimal Davis-Mingioli medium, and consequent depletion in TPP. Cells were previously cultured overnight in 2YT medium. The experiment was carried out in duplicate. The error associated with the estimation of the TPP content was $\leq 7\%$ and the error associated with measurement of the optical density of two independent cultures was $\leq 1.5\%$. Original data from HPLC files: HPLC\Methods\ FLUC18.042, 43.

Cells cultured overnight in either 2YT or the TPP-supplemented Davis-Mingioli media contained approximately 40 ng of TPP/mg of wet cells and grew until the intracellular vitamin concentration dropped to 4-5 ng/mg of wet cells, which appears to be the amount below which growth stops and thiamine biosynthesis might be expected to become de-repressed (60). A similar TPP content was found in *E. coli* 83-1 cells cultured overnight in DM1 medium which contains limiting amounts of growth requirements (section 5.2.1).

As pBAD/HisA/KG33 grown in TPP-enriched Davis-Mingioli medium was able to consume the vitamin accumulated overnight more quickly than cells cultured in 2YT (Figures 5.6 and 5.7), the first medium was chosen to prepare large scale cultures of de-repressed cells able to provide the required components for an *in vitro* thiazole synthase assay. It would not have been possible to investigate thiamine biosynthesis *in*

vivo as with *E. coli* 83-1, since pBAD/HisA/KG33 is unable to express active ThiH (section 3.2.6). Cleared lysates from thiamine depleted cells were incubated with purified ThiGH-His, Hmp and the thiazole precursors Dxp, Cys and Tyr for 4 h at 37 °C, under anaerobic conditions. Analysis of the reaction mixtures (**Figure 5.8**) revealed that the minimal amount of thiamine produced by the pBAD/HisA/KG33 lysate was not increased by the addition of purified ThiGH-His. The lysate, however, was able to form thiamine from exogenously added Hmp and Thz-P, thus indicating that ThiD and ThiE were not limiting the formation of the vitamin. Therefore, an almost totally inactive thiazole biosynthetic pathway appears to be responsible for the extremely low thiamine-forming activity of the pBAD/HisA/KG33 lysate supplemented with the thiazole precursors and purified ThiGH-His. The reason why the addition of purified ThiGH-His did not produce any effect is presently unclear.

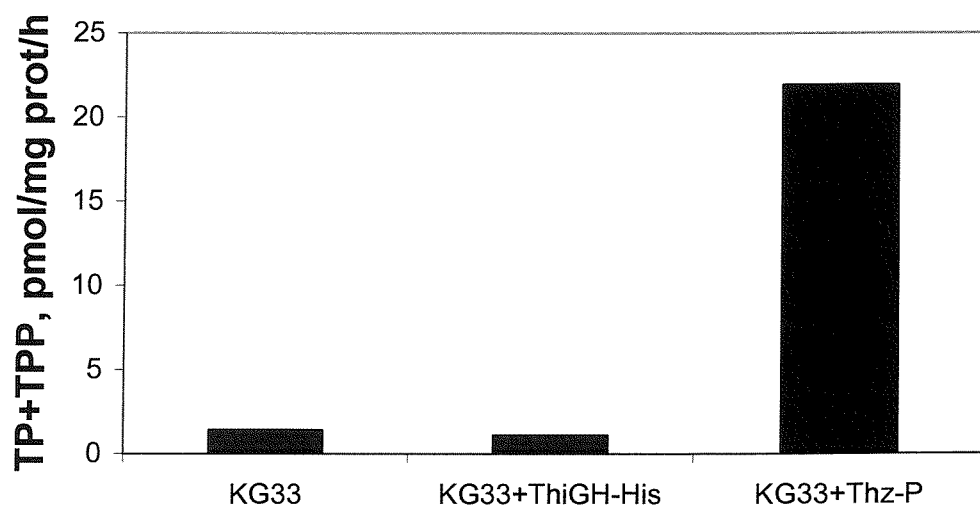


Figure 5.8. Overall TP and TPP production. *In vitro* complementation of a cleared lysate from thiamine depleted pBAD/His/KG33 with purified ThiGH-His. Original data from HPLC file: HPLC\Methods\ FLUC18_2.008.

5.3. Summary and Conclusions

Thiamine pyrophosphate regulates its own biosynthesis by repressing translation and transcription of key biosynthetic enzymes. This repression can be partially removed by decreasing the intracellular vitamin content.

The addition of adenine or adenosine to growing cultures of enteric bacteria has been shown to result in thiamine depletion by decreasing the pools of one of the precursors of the vitamin, AIR, produced through the *de novo* purine biosynthesis. As a consequence, adenosine treated *E. coli* 83-1 cells were able to produce up to 3 times more vitamin B₁ than untreated cells, under conditions in which *de novo* thiamine biosynthesis can be ascribed to *de novo* thiazole biosynthesis. As the incubation with adenosine is likely to increase the expression level of thiamine biosynthetic enzymes, *E. coli* 83-1 treated in this way proved to be a suitable system for studies on *in vitro* thiazole biosynthesis.

Under the conditions investigated, the biosynthesis of the thiazole appeared to be rate limiting. However, transformation of *E. coli* 83-1 with pRL1020, and induction of ThiFSGH-His expression during the de-repression of the resultant strain, did not result in any appreciable increase in thiazole/thiamine production.

Finally, the attempt to de-repress *E. coli* pBAD/HisA/KG33, derived from a Thz-P auxotroph strain, by thiamine starvation, proved to be unsuccessful. In fact, *in vitro* complementation of a cleared lysate derived from these de-repressed cells with purified ThiGH-His did not result in increased thiazole biosynthetic activity. This cellular system was not further used for *in vitro* studies.

Chapter 6.

*In Vitro Reconstitution of the Thiazole Synthase Activity Using *E. coli* Cell-free Extracts*

6.1. Introduction

In vivo feeding studies and isolation and characterisation of relevant auxotrophic mutants, have led to the identification of proteins and precursors involved in the biosynthesis of the thiazole ring of thiamine in different organisms (Chapter 1). The combined effort of several groups has also succeeded in elucidating most of the mechanistic details of the sulphur transfer from cysteine to the C-terminal carboxylate of ThiS (49,71,77,179), and two potential direct sulphur donors for Thz-P assembly, ThiS-COSH (71) and a ThiFS crosslinked complex (38), have been identified in *E. coli*. However, none of the subsequent steps in thiazole biosynthesis has been so far elucidated, due to difficulties encountered in the development of a functional *in vitro* thiazole synthase assay. These final steps would conceivably involve ThiG and ThiH and require sulphur transfer from the ThiFS conjugate (or ThiS-COSH) to Dxp, condensation with Tyr and cyclisation to the thiazole product.

Very recently, Begley and co-workers have successfully reconstituted *in vitro* thiazole biosynthesis using a fully defined biosynthetic system containing *B. subtilis* purified proteins and the thiazole precursors Cys, Gly and Dxp (81). Although *B. subtilis* shares some metabolic components with *E. coli*, including some of the biosynthetic proteins (ThiFSG, ThiI and IscS) and two precursors, Dxp and Cys, the thiazole biosynthetic pathways also differ significantly (section 1.3.3). In fact, whilst *B. subtilis* depends upon ThiO, an oxygen dependent flavoenzyme and utilise glycine (13,82), *E. coli* uses tyrosine and substitutes ThiO with an oxygen *sensitive* protein, ThiH (48,83). Thus, the potential inactivation of ThiH by dioxygen might explain why previous attempts to obtain *in vitro* thiazole biosynthesis by aerobically incubating



over-expressed *E. coli* ThiFSGH and ThiI with Dxp and radiolabelled ThiS-COSH or Tyr, failed to produce any detectable amount of thiazole product (13,180).

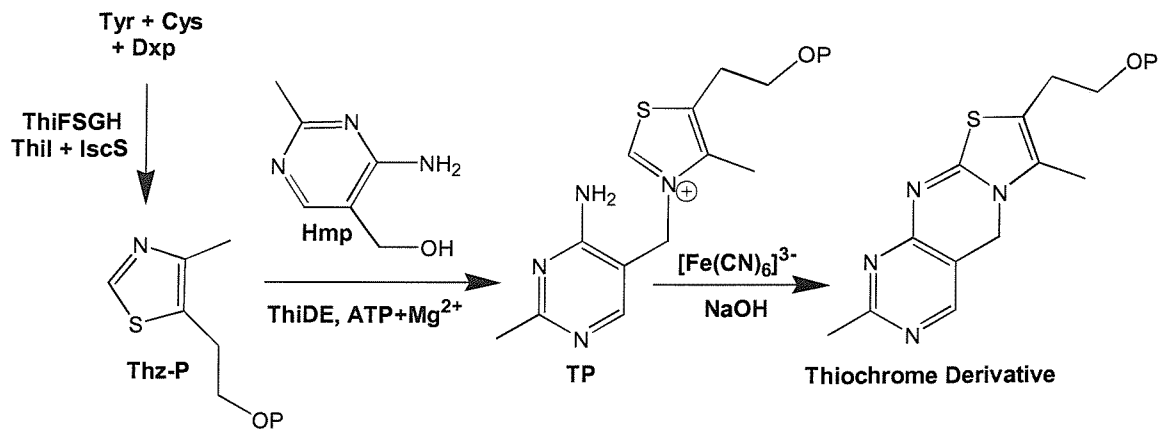
This chapter describes the successful reconstitution of *in vitro* thiazole biosynthetic activity using a cell-free system containing extracts from adenosine treated *E. coli* pRL1020/83-1 (Chapter 5) and purified ThiGH-His [from pRL1020/BL21(DE3)], under anaerobic conditions. The dependency of the thiazole synthase activity on the concentration of Tyr, Cys and Dxp, and on the addition of ThiFS and SAM/NADPH, was also investigated.

6.2. Results and Discussion

6.2.1. *In Vitro Assay Strategy and Conditions*

Several problems were overcome during the development of a functional thiazole synthase assay:

1) *Direct detection of Thz-P is difficult.* As previously mentioned, the thiazole has been proposed to exert a feedback inhibition on its own biosynthesis (60,163). This might explain why this compound is normally present at low levels (32,35) and does not accumulate in cells (section 5.2.3), and consequently, why the direct detection of Thz-P is difficult (35,60). In fact, most of the previous *in vivo* studies on thiazole biosynthesis using labelled precursors, relied on the isolation of the final product, i.e. labelled thiamine, from which the thiazole could then be obtained by bisulphite cleavage (section 4.2.8) and thus characterised (29-33). Employing a similar strategy, the assay described here relies on the efficient coupling any thiazole produced to Hmp-PP and on the measurement of the thiamine content (TP and TPP) by quantitative oxidation to the fluorescent thiochrome derivatives and HPLC analysis (35,81,174,181,182). Under these assay conditions, the amount of *de novo* thiamine produced corresponds directly to the amount of *de novo* Thz-P produced (**Scheme 6.1**).



Scheme 6.1. Coupled assay strategy. Hmp is pyrophosphorylated to Hmp-PP by ThiD. ThiE then efficiently couples any Thz-P assembled from Tyr, Cys and Dxp to Hmp-PP. The resultant TP and TPP are oxidised to fluorescent derivatives [thiochrome method (174), section 7.3, method 16 B], and analysed by HPLC.

2) *Thiamine biosynthesis is repressed.* The tight regulation of thiamine biosynthesis can be overcome by the addition of adenosine (or adenine) to the growth medium (60,61,68,163). Adenosine-treated, de-repressed cells therefore have the potential to provide an optimised cell-free system suitable for a thiazole synthase assay. This suitability was confirmed by the detailed *in vivo* studies on the de-repression of *E. coli* 83-1 described in Chapter 5. *E. coli* 83-1 was transformed with pRL1020, as it conveniently conferred ampicillin resistance, and then used throughout the investigation of *in vitro* thiazole biosynthesis.

3) *E. coli* accumulates intracellular TPP when cultured on rich media. When cultured on rich media (such as 2YT or LB), *E. coli* sequesters thiamine, resulting in very high intracellular levels of background TPP (> 1 nmol/mg of protein). As this was found to compromise the accurate estimation of *de novo* thiamine biosynthesis, cleared lysates from pRL1020/BL21(DE3), grown and induced in 2YT medium (section 7.3), were routinely gel filtered, whilst cleared lysates from adenosine-treated pRL1020/83-1 (grown in minimal medium) were gel filtered when required. Gel filtration of the cell lysates efficiently reduced the TPP and TP backgrounds (**Table 6.1**).

For sake of clarity, the gel filtered pRL1020/BL21(DE3) and pRL1020/83-1 lysates will be referred to as ‘ThiGH-enriched protein fraction’ and ‘de-repressed 83-1 proteins’, respectively.

Cleared Lysate	Before Gel Filtration		After Gel Filtration	
	TPP	TP	TPP	TP
(pmol/mg of protein)				
pRL1020/BL21	> 1000	70	220-250	0.5-5
pRL1020/83-1	150-170	15-20	60-100	2-5

Table 6.1. TPP and TP content of cleared lysates from pRL1020/BL21(DE3) and de-repressed pRL1020/83-1 cells before and after gel filtration through a NAP-10 column.

4) *Thiazole biosynthesis must be the rate limiting step in a coupled assay.* Control experiments demonstrated that the de-repressed pRL1020/83-1 cleared lysates were able to produce thiamine at more than 50 pmol/mg of protein/h when supplied with Hmp and Thz-P in the presence of ATP and Mg²⁺ (Figure 6.3, sample 6). This was far greater than the rate of *de novo* thiazole biosynthesis observed in assays containing solely Hmp and the thiazole precursors, and indicated that the ThiD dependent pyrophosphorylation of Hmp and the ThiE dependent coupling of Thz-P and Hmp-PP to yield TP or TPP were not rate limiting under the assay conditions.

5) *ThiH contains an oxygen sensitive Fe-S cluster.* Elegant metabolic studies with *Salmonella enterica* mutants (48,76,183) and the characterisation of purified *E. coli* ThiGH-His (83) (Chapter 3) demonstrated that ThiH contains an oxygen sensitive Fe-S cluster required for Thz-P biosynthesis; therefore the thiazole synthase activity was assayed under anaerobic conditions.

Reaction mixtures typically contained the components listed in Table 6.2.

Component	Volume or Final Conc.
De-repressed pRL1020/83-1 lysate (40-45 mg/ml) or proteins (15-25 mg/ml)	100 μ l
ThiGH-enrich. protein fract. (15-25 mg/ml) or purified ThiGH-His (8-9 mg/ml)	100 μ l
Tyr	1.6 mM
Cys	1.6 mM
Dxp	1.0 mM
Hmp	0.6 mM
ATP	20 mM
Mg ²⁺ *	20 mM
DTT *	5 mM

Table 6.2. Components present in a typical assay. Reaction volumes ranged between 250 and 350 μ l, as required.

*: MgCl₂ and freshly prepared DTT were added to the anaerobic reaction buffer [Tris-HCl 50 mM, pH 8.0, glycerol 20 % (w/v)] used to re-suspend the cell paste; the presence of these components in the reaction mixtures will be henceforth implied.

To determine the background levels of TP and TPP present in the assays, control reactions were prepared and immediately stopped for analysis, whilst the remaining reactions were incubated for 4 h at 37 °C. At the end of the incubation, proteins were removed by acid precipitation followed by centrifugation, and the supernatants oxidised by the addition of a strongly alkaline K₃[Fe(CN)₆] solution and analysed by RP-HPLC (174) (section 7.3, method 16 B). A typical HPLC trace is shown in **Figure 6.1**. For each set of conditions, the amounts of TP and TPP were estimated separately, the respective background levels subtracted, and the results, corresponding to *de novo* thiamine biosynthesis, expressed as pmol/mg of protein/h.

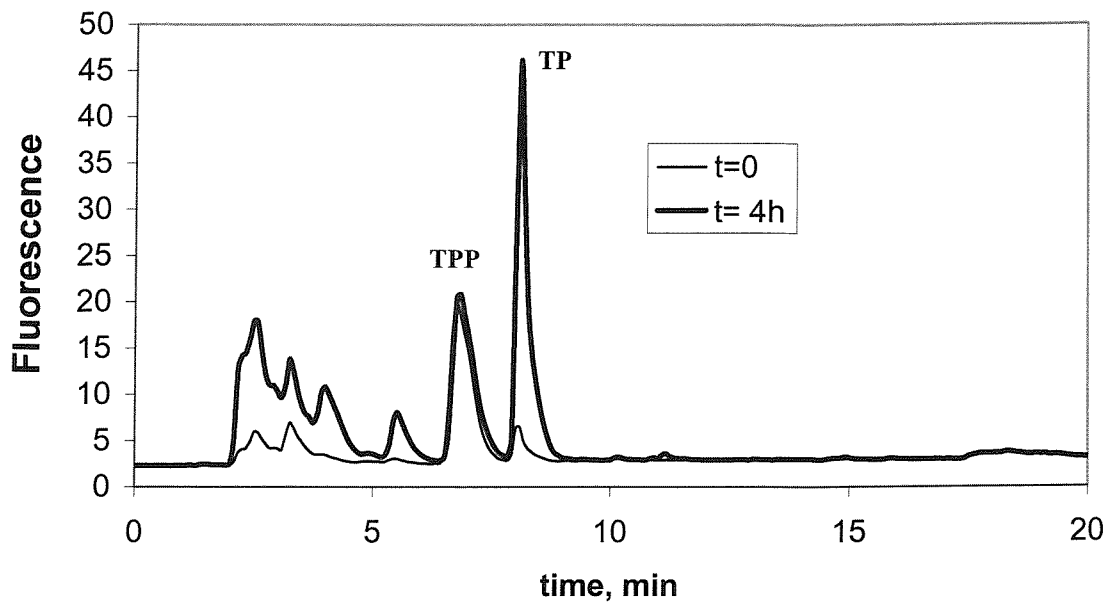


Figure 6.1. HPLC traces of oxidised reaction mixtures containing the de-repressed pRL1020/83-1 proteins, purified ThiGH-His, ATP, Hmp and Tyr. One of the reactions was immediately stopped ($t = 0$), whilst the other was stopped after 4 h incubation at 37 °C ($t = 4\text{h}$). Retention times for TPP and TP are 6.7 and 8.1 min, respectively (chromatographic system 1, section 7.3, method 16 B). Original data from HPLC file: HPLC\Methods\FLUC18_2.070.

6.2.2. Thiazole Synthase Activity in *E. coli* Cleared Cell Lysates

Using the assay strategy described above, *de novo* production of both TP and TPP was measured in the de-repressed pRL1020/83-1 lysate, anaerobically incubated with ATP, Hmp and the thiazole precursors, Tyr, Cys and Dxp. This basal activity was estimated at approximately 7 pmol/mg of protein/h (Figure 6.2, column 1 and Figure 6.3, sample 2) and was confirmed to be higher than the activity measured in lysates derived from repressed cells (4-5 pmol/mg of protein/h, Figure 6.3, sample 1). However, the difference in thiamine biosynthetic activity between de-repressed and repressed cells was more pronounced *in vivo* (1.5-3 times) than *in vitro* (about 1.5 times).

The gel filtered pRL1020/BL21(DE3) cleared lysate, containing over-expressed ThiFSGH-His, was also assayed under identical conditions and shown to be active, producing almost exclusively TPP (8-11 pmol/mg of protein/h, **Figure 6.2**, column 7). This was a surprising result as earlier attempts to measure *in vitro* thiazole biosynthesis from a ThiFSGH over-expressing extract had been unsuccessful (13,180). However, the thiazole synthase activity described herein was assayed in an expression system optimised for the soluble expression of the ThiGH-His complex (Chapter 2), and maintained under anaerobic conditions.

As *in vivo* studies (Chapter 5) and control experiments (section 6.2.1) had demonstrated that thiazole biosynthesis was likely to be the rate limiting step for *de novo* thiamine biosynthesis, the effect of mixing the pRL1020/BL21(DE3)-derived fraction and the de-repressed 83-1 lysate was investigated. Mixtures containing different ratios of these two extracts were assayed (**Figure 6.2**) and showed activities higher than either individual extract (to a maximum of 16.5 pmol/mg of protein/h), which may indicate that the two extracts could be providing complementary components.

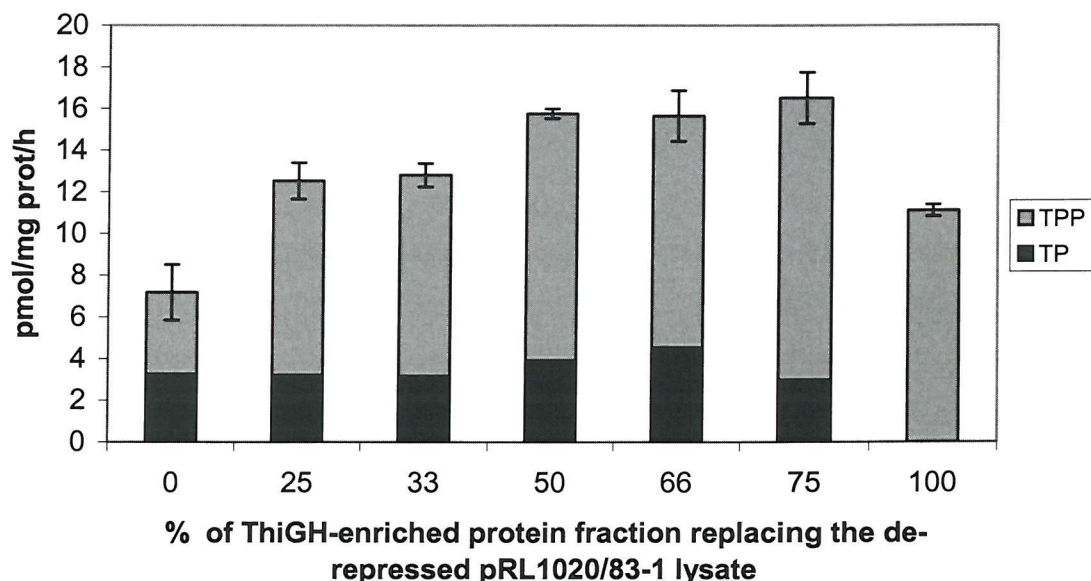


Figure 6.2. *De novo* TP and TPP production from mixtures of ThiGH-enriched protein fraction and de-repressed pRL1020/83-1 lysate containing increasing amounts (0 to 100 %) of ThiGH-enriched protein fraction. All samples contained ATP, Hmp, Tyr, Cys and Dxp. Original data from HPLC files: HPLC\Methods\FLUC18_2.071,72.

The addition of the ThiGH-enriched protein extract also increased the TPP:TP ratio when compared with the de-repressed 83-1 lysate, revealing a difference in the thiamine phosphate kinase (ThiL, 35 kDa) activities of the two extracts.

6.2.3. Comparing the Effect of the ThiGH-Enriched Protein Fraction and Purified ThiFS and ThiGH-His

The increased activity obtained by mixing the ThiGH-enriched protein fraction and the de-repressed pRL1020/83-1 cell lysate suggested the possibility that the rate enhancing component(s) provided by ThiGH-enriched protein fraction were the over-expressed proteins. As induced pRL1020/BL21(DE3) over-produces ThiFSGH-His, the effect of adding purified ThiFS (section 4.2.4) and ThiGH-His (section 3.2.2) to the pRL1020/83-1 lysate was investigated, and compared with the effect exerted by the addition of the ThiGH-enriched protein fraction. **Figure 6.3** shows that whilst the addition of both purified ThiGH-His and ThiGH-enriched protein fraction resulted in an approximate 3-fold increase in activity, the addition of ThiFS had a much less pronounced effect. More detailed studies on the effect exerted by ThiF and ThiS on the thiazole biosynthetic activity of reaction mixtures containing de-repressed pRL1020/83-1 proteins and purified ThiGH-His are described in section 6.2.5.

These results suggested the possibility that the amount of ThiGH present in the de-repressed 83-1 cell lysate was limiting the rate of thiamine biosynthesis, and provided for the first time evidence for *in vitro* thiazole synthase activity of the ThiGH-His complex, isolated under carefully controlled anaerobic conditions, as described in Chapter 3. Interestingly, the addition of ThiGH-His to the de-repressed 83-1 lysate or proteins led consistently and almost exclusively to *de novo* production of TP but to little or no TPP (see also **Figures 6.5** and **6.15**). The relationship between the ThiGH-His dependent TP biosynthesis and the efficiency of ThiL dependent phosphorylation to form TPP has yet to be fully elucidated.

As purified ThiGH-His could efficiently substitute for the ThiGH-enriched protein fraction, producing the largest increase in the basal activity of the de-repressed pRL1020/83-1 lysate, this simplified system was used for subsequent studies.

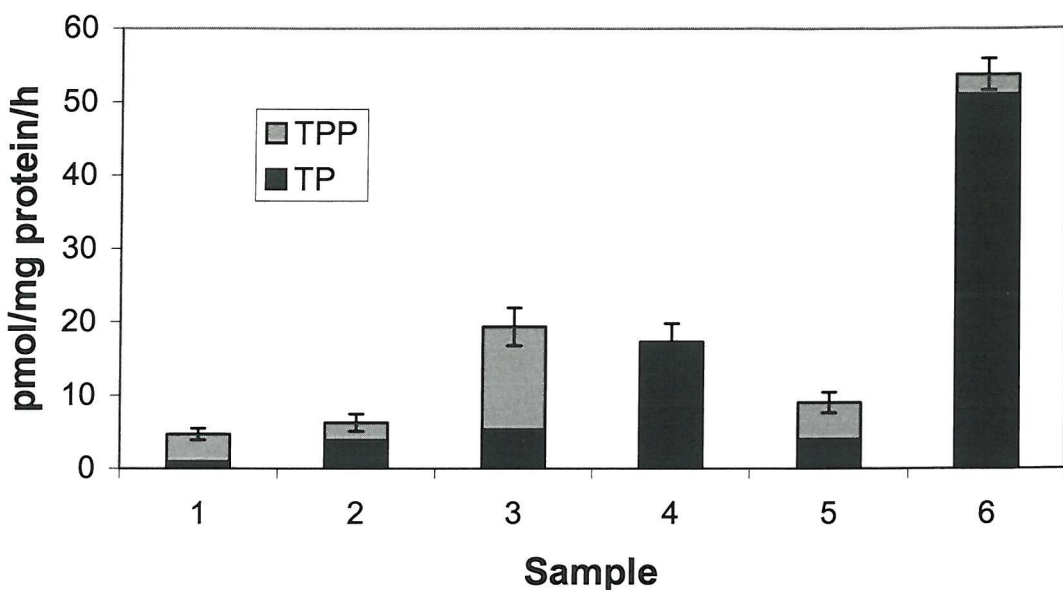


Figure 6.3. *De novo* TP and TPP production. All samples contained Tyr, Cys, Dxp, ATP and Hmp. Sample 1 (from a separate experiment; original data stored in the HPLC file: HPLC\Methods\FLUC18_2.084): repressed pRL1020/83-1 cleared lysate; sample 2: de-repressed pRL1020/83-1 cleared lysate; sample 3: sample 2 plus ThiGH-enriched protein fraction; sample 4: sample 2 plus purified ThiGH-His; sample 5: sample 2 plus purified ThiFS (1.1 mg/ml); sample 6: sample 2 plus Thz-P (0.6 mM). Original data from HPLC file: HPLC\Methods\FLUC18_2.041.

Experiments were conducted at a relatively high concentration of ThiGH-His (2.3-3.3 mg/ml, final concentration), which might intuitively be expected to maximise turnover. However, in subsequent investigations, a decrease in activity at these high ThiGH-His concentrations was observed, consistent with either the effect of a more pronounced protein precipitation or with other components becoming rate limiting (section 6.2.6).

The effect of pre-incubating the ThiGH-His complex with iron and sulphide (1 hour, under anaerobic conditions) prior to the addition to the reaction mixtures was also investigated (original data from HPLC file: HPLC\Methods\FLUC18_2.08). The reconstitution did not appear to increase the activity, and ‘as isolate’ ThiGH-His was almost exclusively used in all the subsequent experiments.

6.2.4. Thiazole Synthase Activity Dependency on the Concentration of the Precursors

The concentration dependence of the thiazole synthase activity was determined for the known thiazole precursors, Dxp, Tyr and Cys, in reaction mixtures containing de-repressed pRL1020/83-1 lysate and purified ThiGH-His. In particular, to remove any potential interference from endogenous amounts of these metabolites, the de-repressed cell lysate was desalted using a NAP-10 column and the protein-containing, high molecular weight fraction isolated. Initial experiments with this de-repressed pRL1020/83-1 protein fraction showed that it retained at least the same level of activity of the unfractionated lysate (15-20 pmol/mg of protein/h, compare sample 3 in **Figure 6.3** with **Figure 6.4 A, B, C**), providing a further simplification of the system for *in vitro* studies.

The precursor dependent activity was investigated by varying the concentrations of each of the known precursors, otherwise maintaining the standard assay conditions (**Table 6.2**). In these experiments, the Dxp concentration was increased from 0 to 3.7 mM³, and the Cys concentration from 0 to 2 mM, but rather surprisingly, in both cases the *de novo* thiamine production was almost completely unaffected by the presence of these two putative precursors (**Figure 6.4 A and B**). Conversely, the thiazole synthase activity appeared to be absolutely dependent on the presence and concentration of Tyr up to approximately 0.2 mM (**Figures 6.4 C** and **6.5**).

³ All the HPLC traces from the Dxp dosage showed the presence of an extra peak with a retention time almost identical to that of unphosphorylated thiamine (10.4 min, method 16 B, chromatographic system 1). The production of this substance, not detected in any other set of conditions, was not included in the calculations to estimate the amount of *de novo* TP and TPP biosynthesised. Due to the small amounts produced, no attempt to characterise this compound was made.

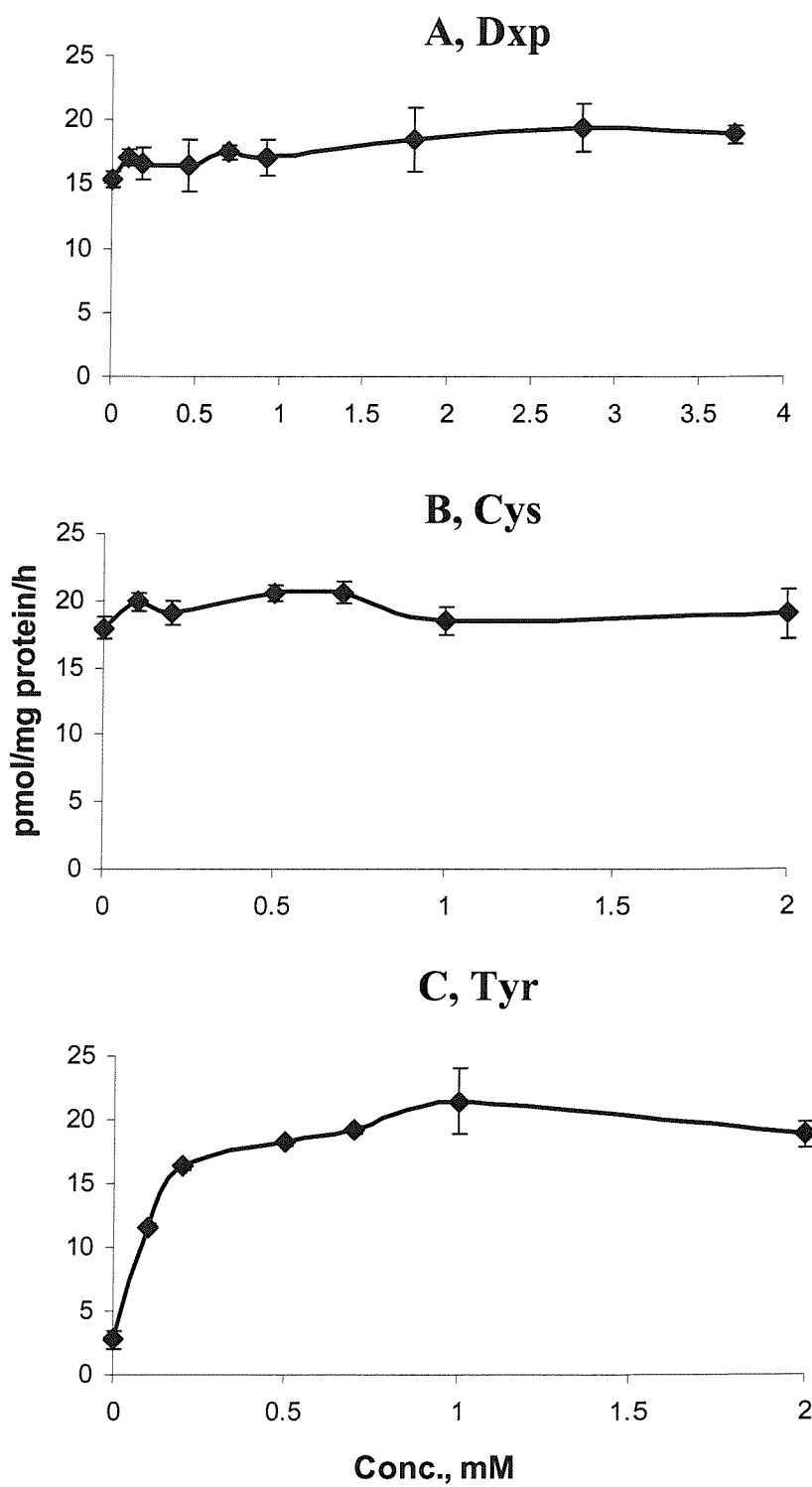


Figure 6.4. Effect of the concentration of Dxp (A), Cys (B) and Tyr (C) on the overall production of TP and TPP. In these experiments the amount of TPP produced varied from 0 to 20 % of the total thiamine production. Original data from HPLC files: HPLC\Methods\FLUC18_2.018, 19, 24, 28.

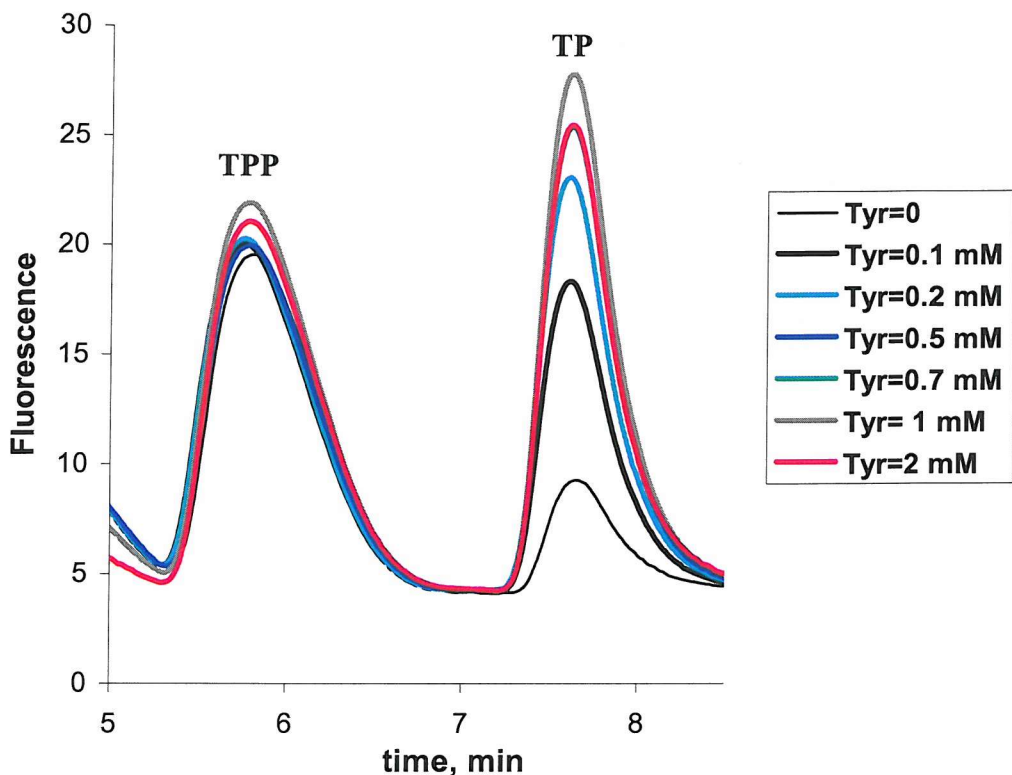
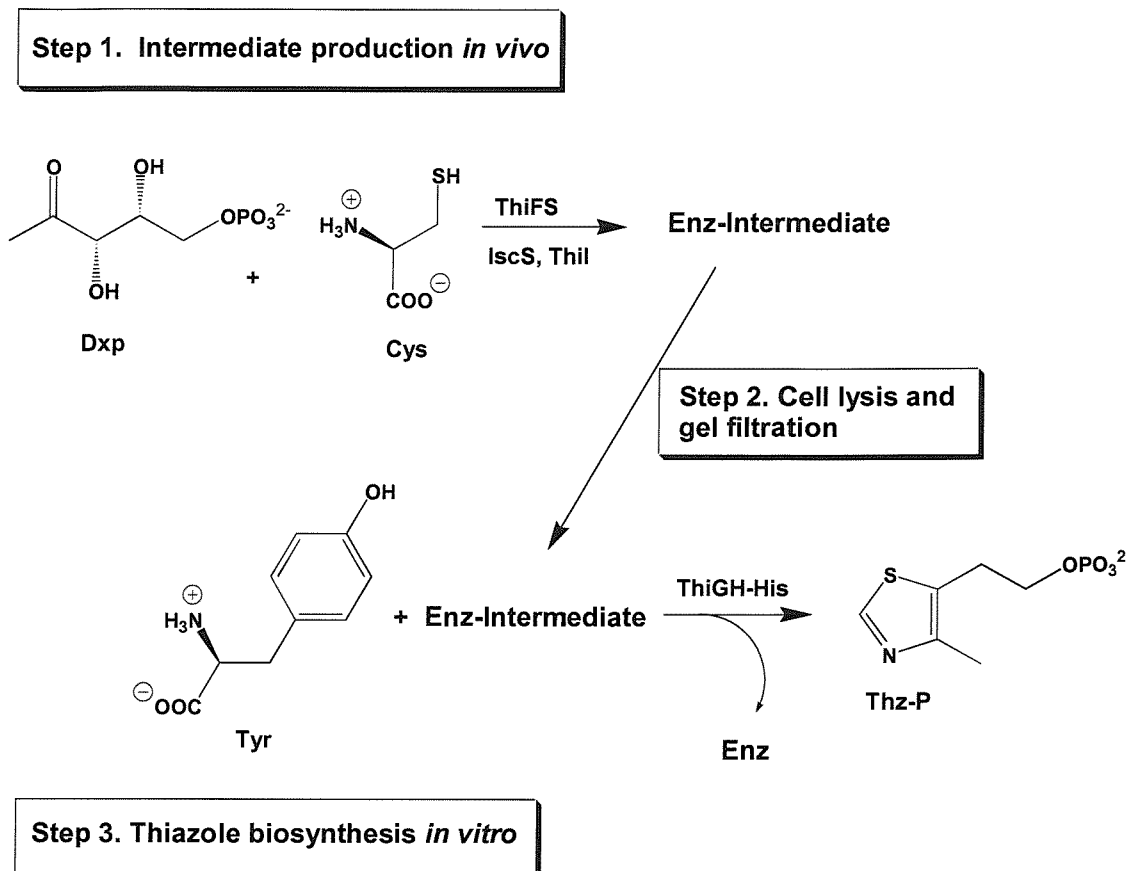


Figure 6.5. HPLC traces of oxidised reaction mixtures incubated with increasing concentrations of Tyr (0-2 mM) for 4 h at 37 °C. All samples also contained Cys, Dxp, ATP and Hmp. Original data from HPLC file: HPLC\Methods\FLUC18_2.024.

Subsequent studies on thiazole synthase activity were conducted using a further simplified system containing Tyr as the only exogenously added thiazole precursor. Therefore, and unless otherwise indicated, the term ‘standard assay’ refers to a mixture containing the following components: de-repressed pRL1020/83-1 proteins, purified ThiGH-His, ATP, Hmp and Tyr.

These results raised the intriguing question of the actual source of the C₅ unit and sulphur atom that are incorporated into Thz-P during these experiments. The component that provides these atoms appeared to co-elute with the proteins when the de-repressed pRL1020/83-1 lysate was applied onto a NAP-10 gel filtration column, consistent with the potential existence of a protein-bound intermediate formed *in vivo*.

A model of thiazole biosynthesis, as it could occur in our *in vitro* assay, is outlined in **Scheme 6.2**.



Scheme 6.2. Proposed model for Thz-P formation under the *in vitro* assay conditions described here. The enzyme-bound intermediate is formed *in vivo*, during the de-repression phase (step 1). Cells are then harvested, lysed and the lysate applied to a NAP-10 column (step 2). The intermediate is then eluted with the other de-repressed pRL1020/83-1 proteins and introduced in the assays where it is required for Thz-P biosynthesis (step 3).

With regard to the potential structure of this intermediate, it is interesting to note that the studies by Park *et al.* (81) on thiazole biosynthesis in *Bacillus subtilis* have provided evidence for a C-terminal derivative of ThiS (Figure 6.6) that contains the

atoms originating from Dxp and Cys. Such an enzyme bound intermediate may therefore be common to the thiazole forming pathways of tyrosine/ThiH dependent organisms (such as *E. coli*) and glycine/ThiO dependent organisms (such as *B. subtilis*).

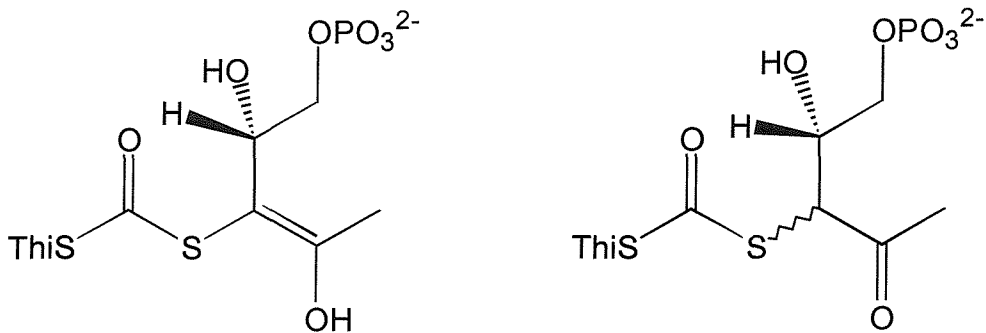


Figure 6.6. Proposed structure of an enzyme-bound intermediate and its tautomer for ThiGH-His dependent thiazole biosynthesis (81).

6.2.5. Thiazole Synthase Activity: Effect of ThiF and ThiS

The addition of both ThiF and ThiS to assays containing the de-repressed pRL1020/83-1 lysate and all the other components listed in **Table 6.2**, produced a slight increase in the basal thiazole biosynthetic activity (section 6.2.3, **Figure 6.3**). The effect of these two proteins was further investigated in reaction mixtures containing de-repressed pRL1020/83-1 proteins and Tyr, plus or minus Cys and Dxp. **Figure 6.7** shows the unexpected results obtained from this experiment. In fact, analysis of the reaction mixtures and estimation of the thiamine content revealed that, unlike the effect produced on the pRL1020/83-1 cleared lysate, the addition of either ThiFS (sample 3) or Dxp plus Cys (sample 1) slightly decreased the basal activity of the pRL1020/83-1 proteins, whilst the combination of ThiFS and Dxp plus Cys seemed to further enhance this inhibitory effect (samples 3 and 4). Furthermore, in the presence of ThiFS, the addition of ThiGH-His (sample 4) was not able to restore the activity measured in sample 2.

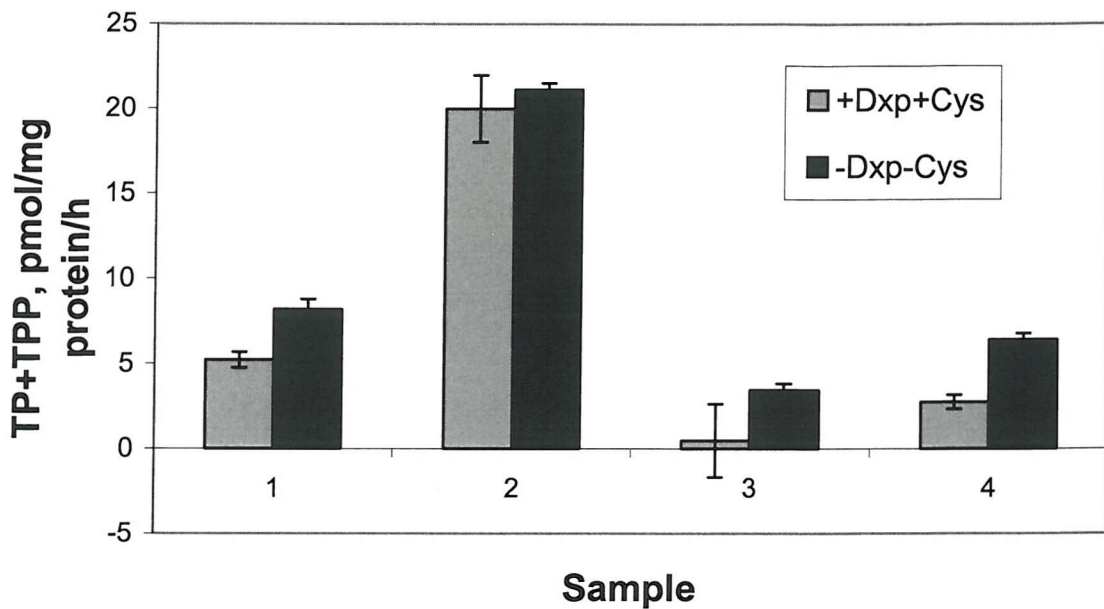


Figure 6.7. Effect of ThiFS on the production of TP and TPP by de-repressed pRL1020/83-1 proteins. Sample 1: de-repressed pRL1020/83-1 proteins; sample 2: sample 1 plus ThiGH-His (2.3 mg/ml); sample 3: sample 1 plus ThiFS (1.1 mg/ml); sample 4: sample 1 plus ThiGH-His plus ThiFS. All samples contained Tyr, ATP and Hmp. Original data from HPLC file: HPLC\Methods\FLUC18_2.056.

Because of the limited number of experiments, it is not possible to provide an exhaustive explanation for the results here obtained. In particular, it is difficult to justify the almost opposite effects exerted by ThiFS, Dxp and Cys on the activities of the de-repressed pRL1020/83-1 proteins and lysate. One possible explanation is that the lysate might contain a low molecular weight component, removed from the pRL1020/83-1 proteins, which allows the conversion of ThiFS and/or Dxp plus Cys into a suitable thiazole precursor.

Apart from the sulphur atom and the N3-C2 unit, the remaining atoms constituting the thiazole ring derive entirely from Dxp; it is therefore likely that the enzyme which catalyses the cyclisation reaction contains a binding site for a Dxp-derived intermediate. Thus, competitive binding of the sugar to this active site could explain the reduced thiazole synthase activity observed upon addition of a relatively high concentration (1 mM) of Dxp to reaction mixtures containing the de-repressed

pRL1020/83-1 proteins. The effect exerted by ThiFS, enhanced by Cys and Dxp, is more difficult to justify, since these two proteins are, in principle, required for thiazole biosynthesis. However, if an intermediate such as that shown in **Figure 6.6** was the substrate for ThiG or ThiH, again, competitive binding of ‘unmodified’ ThiS (i.e. without sulphur or Dxp derivative covalently bound) to the active site could explain the decrease in activity (**Figure 6.7**, sample 4).

In order to gain further insight into the nature of this inhibitory effect, ThiF and ThiS were individually added to a mixture containing de-repressed pRL1020/83-1 proteins and ThiGH-His, under similar conditions to those just described. The results are shown in **Figure 6.8**.

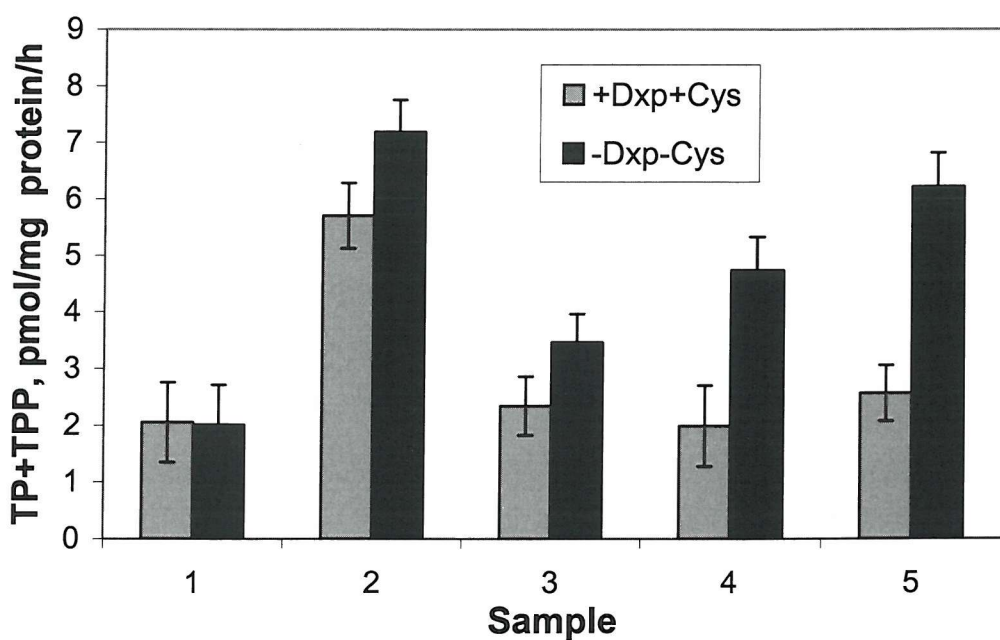


Figure 6.8. Effect of ThiFS on the overall TP and TPP production of de-repressed pRL1020/83-1 proteins. Sample 1: de-repressed pRL1020/83-1 proteins; sample 2: sample 1 plus ThiGH-His (2.3 mg/ml); sample 3: sample 2 plus ThiF (0.9 mg/ml); sample 4: sample 2 plus ThiS (0.3 mg/ml); sample 5: sample 2 plus ThiF plus ThiS. All samples contained Tyr, ATP and Hmp. Original data from HPLC file: HPLC\Methods\FLUC18_2.073.

Although the basal activity of the de-repressed pRL1020/83-1 proteins, in this experiment, was approximately 3 times lower than that normally measured (section 6.2.2), the general trend confirmed the previously observed inhibitory effect of Dxp plus Cys, particularly evident in the presence of either ThiF or ThiS or both (samples 3, 4 and 5). Furthermore, the data seem to indicate that both proteins, individually, were able to reduce the thiazole synthase activity measured in mixtures containing the de-repressed pRL1020/83-1 proteins and ThiGH-His. Further experiments are required to elucidate the mechanism through which ThiF and ThiS, in excess with respect to their naturally balanced concentration in the pRL1020/83-1 proteins, negatively affect the *de novo* thiazole biosynthesis. However, it is tempting to speculate that the assembly of the thiazole may require the interaction between ThiGH and suitably ‘modified’ or ‘activated’ ThiFS.

As already mentioned, the lysate used for this experiment showed a remarkably low basal activity (the highest activity measured was approximately 7 pmol/mg of protein/h, **Figure 6.8**) despite the fact that the assays were prepared by the usual protocol (section 7.8.2). This unexpected variation in activity has not been fully characterised, but repeated experiments have shown that the protein solution eluted from the gel filtration column occasionally has low activity.

6.2.6. Time Course and Effect of the Concentration of ThiGH-His

Reaction mixtures containing cleared lysates or protein fractions (sections 6.2.2 and 6.2.3) did not normally show any sign of precipitation at the end of the 4 h incubation at 37 °C. Conversely, assays containing purified ThiGH-His, even at very low concentrations, showed sign of precipitation after about 2 h. This was probably caused by the high instability and marked tendency of the ThiGH-His complex to precipitate (Chapter 3). Despite this clearly observable protein precipitation, a time course experiment demonstrated that thiamine biosynthesis occurred in an approximately linear manner (rate = 8 pmol/mg of protein/h) up to 2 hours and continued at a reduced rate (rate = 2 pmol/mg of protein/h) up to at least 6 hours (**Figure 6.9**), with the reaction products remaining stable for at least 24 h at 37 °C. An

attempt to minimise protein aggregation by adding BSA at a relatively high concentration (2 mg/ml) proved unsuccessful.

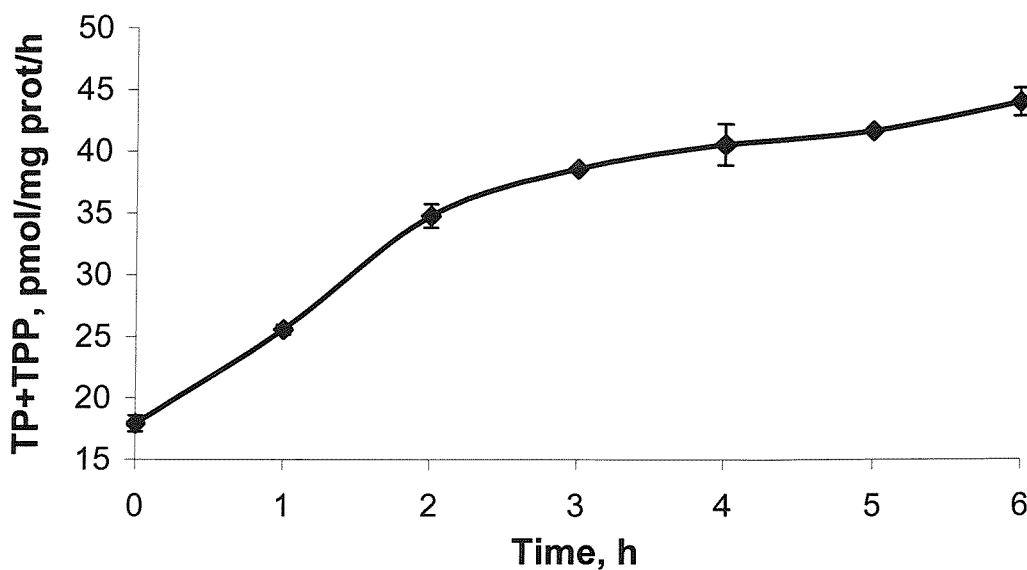


Figure 6.9. Time course of the production of TP and TPP. All Samples contained de-repressed pRL1020/83-1 proteins, ATP, Hmp and Tyr. Original data from HPLC file: HPLC\Methods\FLUC18_2.070.

As the experiment described in section 6.2.3 suggested that the amount of ThiGH in the de-repressed pRL1020/83-1 lysate (or proteins) could be limiting the *de novo* production of thiamine, the effect of varying the concentration of ThiGH-His in the assay was also investigated (Figure 6.10). The amount of thiamine produced was approximately proportional to the ThiGH-His added, up to a final concentration of 2 mg/ml, after which additional ThiGH-His gave no increase and in fact decreased the overall yield of thiamine. Careful observations of the assays revealed the presence of precipitate in all the reaction mixtures, although it appeared to be more pronounced in those samples containing more than 1 mg/ml of ThiGH-His. This aggregation may, at least in part, account for the decreased activity in assays containing a higher concentration of complex.

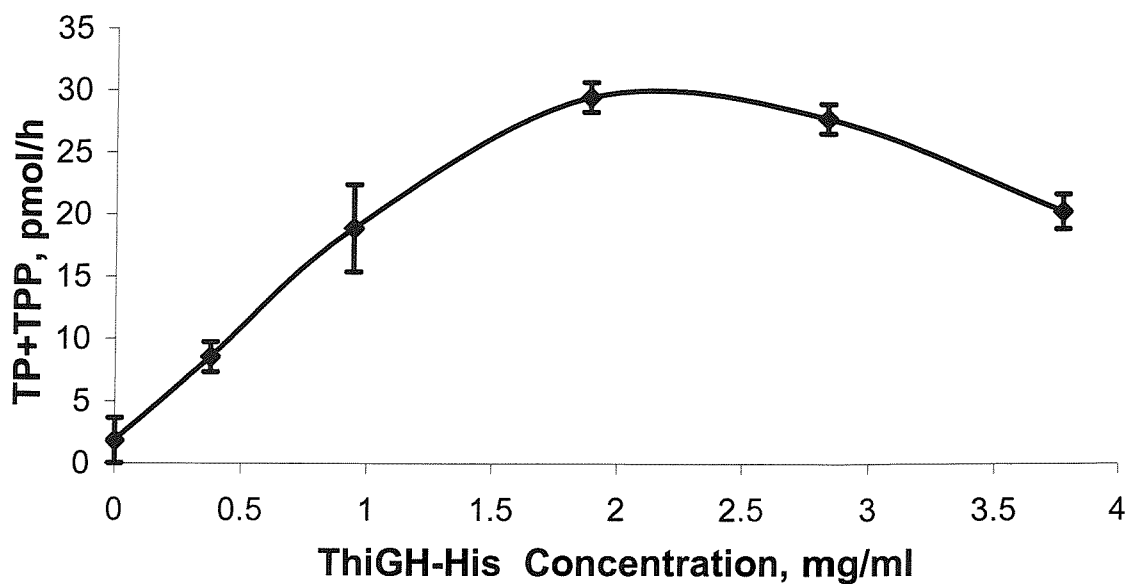


Figure 6.10. Effect of ThiGH-His on thiamine biosynthesis. Overall TP and TPP production in each assay. Samples contained de-repressed pRL1020/83-1 proteins, Hmp, ATP and Tyr. Original data from HPLC files: HPLC\Methods\FLUC18_2.053, 54.

Alternatively, it may be that when ThiGH-His is present at a concentration above 2 mg/ml, other essential components become rate limiting in the assay. In fact, the experiments described in section 6.2.2, suggested that the high activity obtained by mixing the de-repressed pRL1020/83-1 lysate and the ThiGH-enriched protein fraction, could result from the availability of different and complimentary components provided by each extract. The principle component provided by ThiGH-enriched protein fraction is likely to be ThiGH-His, but the active components provided by the de-repressed pRL1020/83-1 lysate (or proteins), and potentially accumulated as a result of the adenosine treatment, have yet to be fully characterised.

Despite the fact that the *in vitro* assay here reported has allowed, for the first time, detection of *de novo* thiazole biosynthesis, the specific substrates and reactions catalysed by ThiG and ThiH-His remain to be identified. The formation of the thiazole could require several steps and the interaction of ThiG and ThiH with other auxiliary

proteins present in the de-repressed pRL1020/83-1 lysate (or proteins). These proteins might participate in thiazole biosynthesis by assembling direct substrates for ThiG or ThiH, or by activating these enzymes. This would not be unexpected in the case of ThiH, since this Fe-S cluster protein might require repairing and/or reduction of the cluster to remain active (48,76,88,97,99,104). Although it is difficult, at this stage, to discriminate amongst different potential mechanisms of thiazole formation, the decrease in activity shown in **Figure 6.10** may be consistent with the hypothesis of a complex multistep process. In fact, if only one other component was limiting thiamine biosynthesis at high ThiGH-His concentrations, the activity would be expected to reach a plateau. The almost proportional decrease in activity, instead, may indicate the existence of more than one rate-limiting step. Elucidation of the detailed mechanism through which Thz-P is biosynthesised in *E. coli* awaits the reconstitution of *in vitro* thiazole synthase activity in a fully defined biosynthetic system.

6.2.7. Preliminary Fractionation Experiments on the De-repressed pRL1020/83-1 Cleared Lysate

In order to gain further evidence supporting the existence of other protein components limiting thiazole biosynthesis (section 6.2.6) at high ThiGH-His concentrations (> 2 mg/ml), the de-repressed pRL1020/83-1 lysate was fractionated by gel filtration chromatography, and the activity of the fractions tested in the presence of a reduced amount of unfractionated lysate (to provide ThiE and ThiD), ThiGH-His (2.3-3.2 mg/ml), Tyr, Hmp and ATP.

Aerobic fractionation of the lysate was at first carried out on an analytical scale (section 7.8.8). Proteins were eluted in fractions 3-5 (**Table 6.3** and **Figure 6.11**) and fractions 3-7 were tested for thiazole synthase activity. The results are shown in **Figure 6.12**.

Fraction Number	Retention Time (min)
1	0-10
2	10-20
3	20-30
4	30-40
5	40-50
6	50-60
7	60-70

Table 6.3. Fraction numbers and correspondent retention times of proteins eluted from the analytical gel filtration column (Superdex 200 HR 10/30, AP Biotech). Flow rate: 0.5 ml/min; fraction size: 5 ml.



Figure 6.11. Coomassie stained 15 % SDS-PAGE gel of proteins eluted from the analytical gel filtration column (Superdex 200 HR 10/30, AP Biotech). Numbers correspond to the fraction numbers. M = molecular weight marker. Proteins in fractions 3-5 were concentrated by using MWCO membrane filters (5 kDa). Fractions 6 and 7 were equally treated. Prior to the addition to the reaction mixtures, fraction aliquots (200 μ l) were degassed inside the glove box for 30 min.

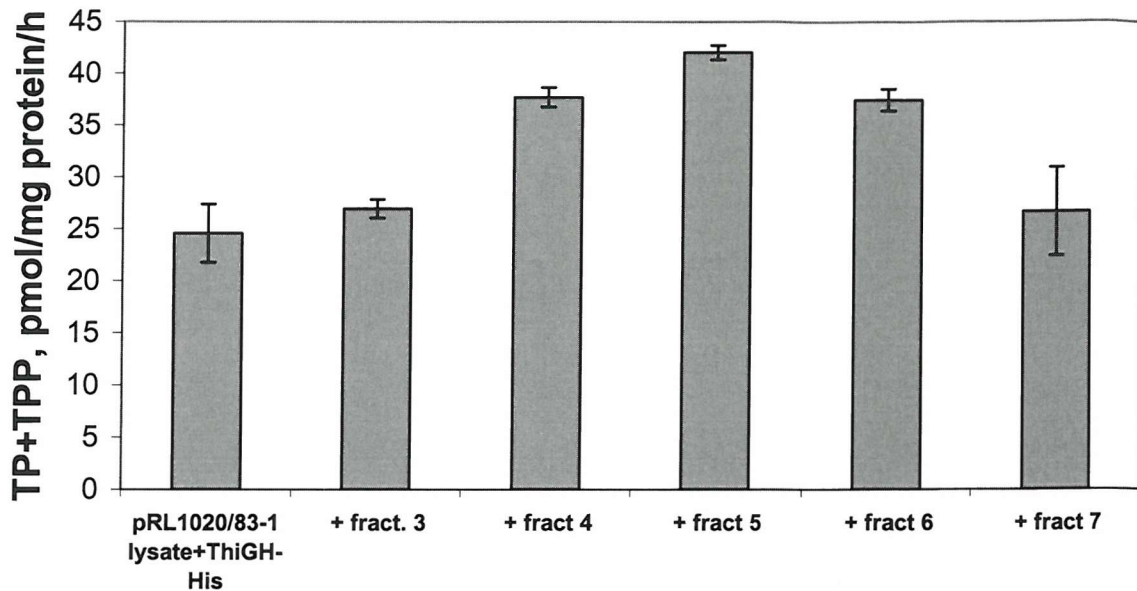


Figure 6.12. Activity test (overall TP and TPP production) on the fractions eluted from the analytical gel filtration column. Samples contained ATP, Hmp and Tyr. Original data from HPLC file: HPLC\Methods\FLUC18_2.046.

Estimation of the thiamine content revealed that one or more proteins eluted in fractions 4 and 5, and some low molecular weight component eluted in fraction 6, were able to appreciably increase (1.5 times) the thiazole synthase activity of reaction mixtures containing the de-repressed pRL1020/83-1 lysate (25 % of the amount typically used, **Table 6.2**) and purified ThiGH-His (**Figure 6.12**, sample 1). In particular, the addition of fraction 5 allowed *de novo* thiamine biosynthesis to occur at a rate higher than 40 pmol/mg of protein/h, one of the highest activities measured in the absence of *exogenously* added Thz-P. Therefore, these results strongly support the requirement for proteins, other than ThiGH-His, which could become rate limiting under the conditions investigated. As fractions 4 and 5 contained proteins of a wide range of sizes (**Figure 6.11**), the retention times could not be used to estimate the molecular weight of the potential active components. However, it is interesting to note that they were eluted in late fractions (retention times > 30 min, **Table 6.3**).

The fractionation experiment was repeated on a larger scale (18 ml of de-repressed pRL1020/83-1 lysate, section 7.8.8). Selected fractions were both analysed by SDS-PAGE (**Figure 6.13**) and tested for thiazole synthase activity (**Figure 6.14**).

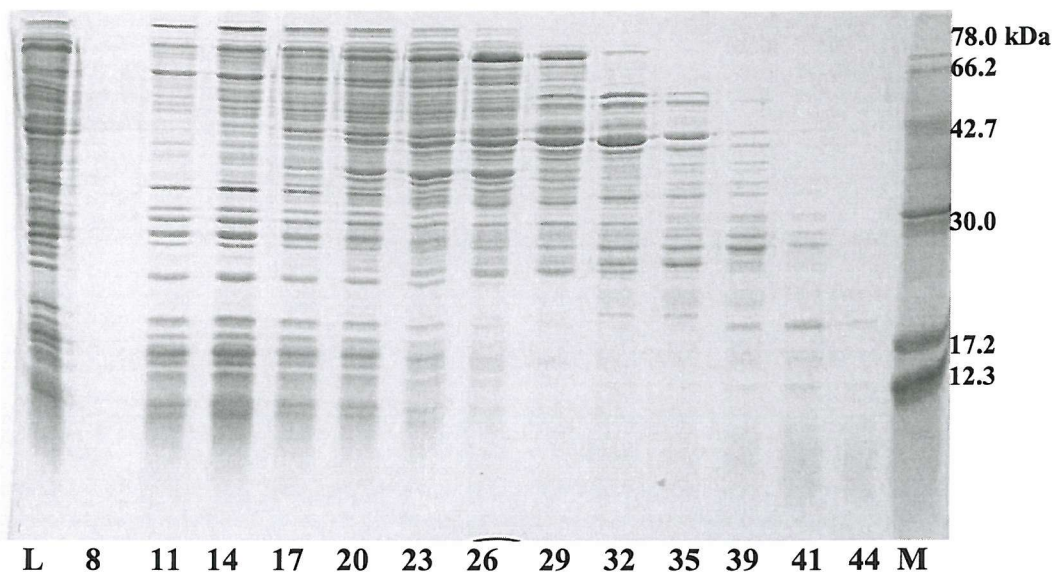


Figure 6.13. Coomassie stained 15 % SDS-PAGE gel of the de-repressed pRL1020/83-1 proteins eluted from the gel filtration column (S-200, 3.4 cm I.D. x 85 cm). Numbers correspond to the fraction numbers. M = molecular weight marker. Prior to the addition to the reaction mixtures, fraction aliquots (200 μ l) were degassed inside the glove box for 30 min.

Proteins eluted in fractions 26-32 enhanced the rate of thiamine biosynthesis up to 43 pmol/mg protein/h, in very good agreement with the results obtained from the small scale fractionation experiment; once again the active components were eluted in relatively late fractions, and a comparison between **Figure 6.11** (fractions 4 and 5) and **Figure 6.13** (fractions 29 and 32) reveals the consistent presence of at least one protein, around \sim 44 kDa. However, a substantial decrease in activity was also observed upon addition of fractions 35 and 41. Interestingly, this effect was very similar to that exerted

by purified ThiF and ThiS (section 6.2.5) added to standard assays plus or minus Dxp and Cys (**Figures 6.7 and 6.8**).

Identification of the proteins shown to either enhance or reduce the rate of thiazole biosynthesis is one of the immediate objective for future studies.

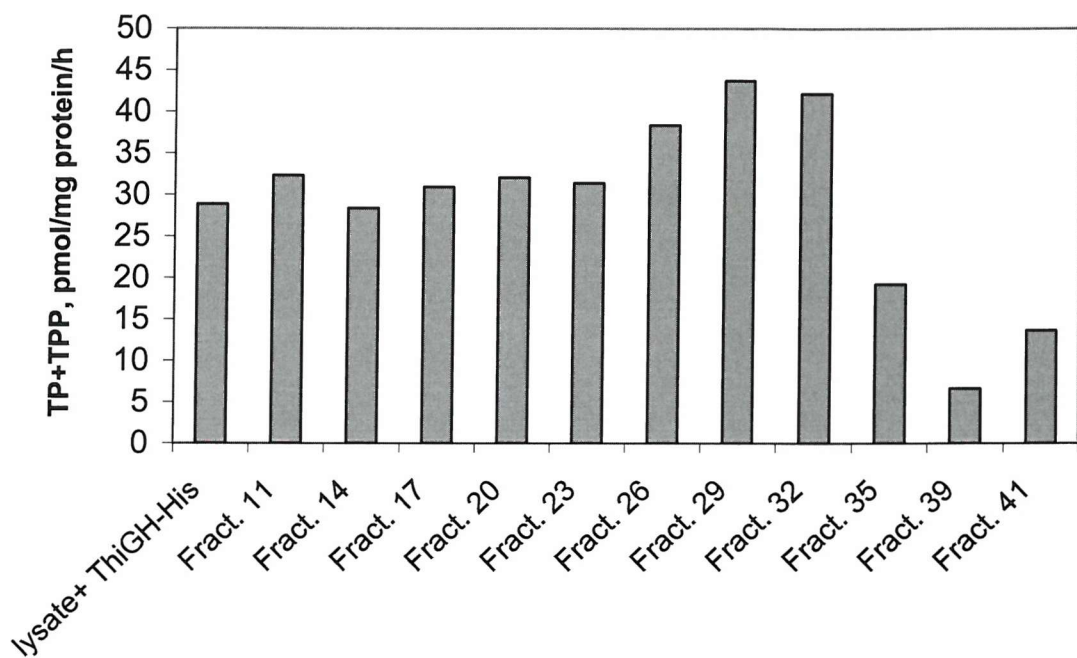


Figure 6.14. Activity test (overall TP and TPP production) on the fractions eluted from the gel filtration column (S-200, 3.4 cm I.D. x 85 cm). Experiments were not carried out in duplicate. Samples (200 μ l) were degassed for 30 min before being added to the reaction mixtures. Original data from HPLC file: HPLC\Methods\FLUC18_2.078.

6.2.8. Thiazole Synthase Activity: Preliminary Experiments on the Effect of SAM and Reducing Agents

As mentioned in Chapter 1 (section 1.3.3) ThiH shares the Fe-S cluster binding motif, CxxxCxxC, with members of the ‘radical SAM’ family (84), whose activity is dependent upon the presence of *S*-adenosyl methionine. Despite the fact that under the conditions initially investigated, ThiGH-His did not appear to require exogenously

added SAM to catalyse the thiazole formation, the effects of adding this co-factor and potential reducing agents, dithionite and NADPH, on the formation of thiamine were investigated (**Figure 6.15**). The addition of SAM and a reducing agent (samples 2 and 3) did indeed greatly increase the observed thiazole synthase activity, with NADPH being more effective than dithionite. Iron and sulphide have been used to reconstitute the Fe-S clusters of several ‘radical SAM’ enzymes (108,141,184) and were added to these thiazole synthase assays in an effort to maximize activity. In a separate experiment, the effect of the addition of SAM alone was examined and shown to result in a relatively modest increase in activity (**Figure 6.16**). The data shown in **Figures 6.15** and **6.16** have been converted to relative activities, expressed as percentage and plotted together in **Figure 6.17**.

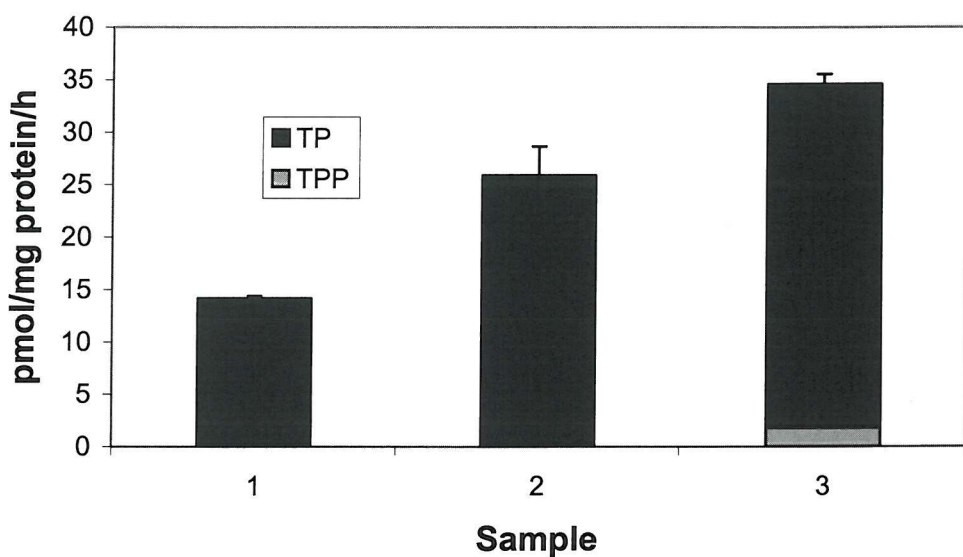


Figure 6.15. Effect of SAM and reducing agents on the production of TP and TPP. Sample 1: standard assay; sample 2: standard assay containing reconstituted ThiGH-His pre-incubated with dithionite (1 mM, 30 min), and SAM (1 mM); sample 3: standard assay containing reconstituted ThiGH-His, SAM (1 mM) and NADPH (1 mM). Original data from HPLC file: HPLC\Methods\FLUC18_2.084 (chromatographic system 2, section 7.3, method 16 B).

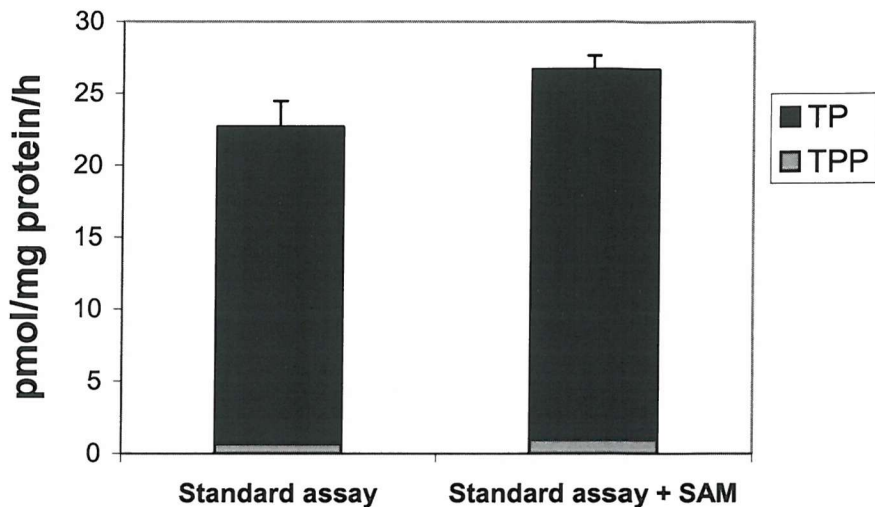


Figure 6.16. Effect of SAM (without addition of reductant) on the TP and TPP production of standard assays (de-repressed pRL1020/83-1 proteins, purified ThiGH-His, ATP, Hmp and Tyr). Original data from HPLC file: HPLC\Methods\FLUC18_2.070.

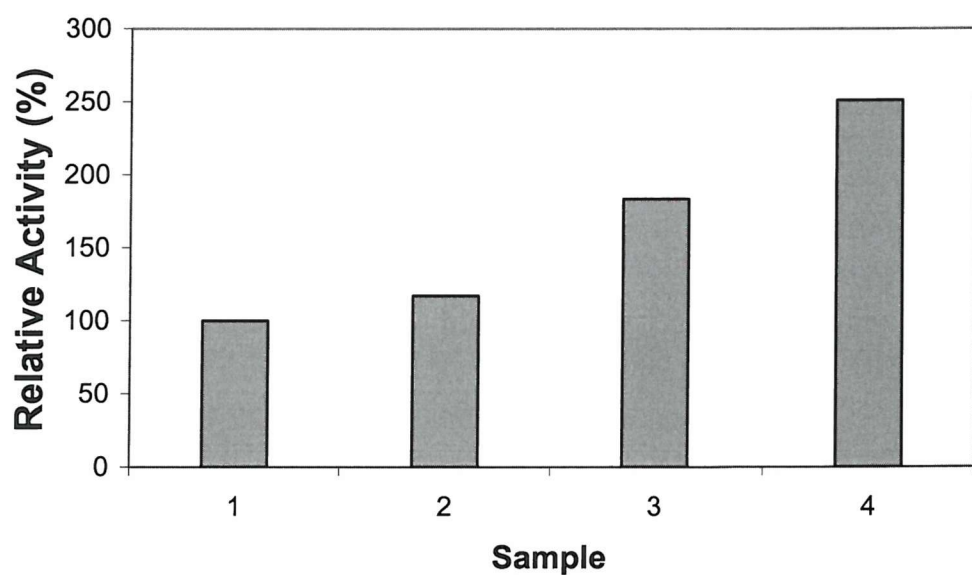


Figure 6.17. Effect of SAM and reducing agents on the TP and TPP production, expressed as relative activity (%). Sample 1: standard assay; sample 2: standard assay containing SAM (1 mM); sample 3: standard assay containing reconstituted ThiGH-His pre-incubated with dithionite (1 mM, 30 min) and SAM (1 mM); sample 4: standard assay containing reconstituted ThiGH-His, SAM (1 mM) and NADPH (1 mM).

One of the implications of these results is that the background thiazole synthase activity observed in our initial assays was dependent on endogenous SAM. The addition of high concentrations of ATP (20 mM), to permit the pyrophosphorylation of Hmp to Hmp-PP, may have had the additional beneficial effect of allowing sufficient SAM to be synthesized *in situ* by SAM synthetase (185), using methionine presumably scavenged from protein degradation.

The remarkable increase of activity (from 14 up to 34 pmol/mg protein/h, **Figure 6.15**) produced by the addition of both dithionite and NADPH also suggests that, under the conditions investigated, the rate of thiamine biosynthesis was limited by the concentration of a reducing agent. The physiological enzymatic source of electrons for many radical SAM enzymes is the NADPH/flavodoxin reductase/flavodoxin system (108-110), which can be substituted by strong chemical reductants such as sodium dithionite or photoreduced deazaflavin (88,99,102,111). Thus, the enhanced activity observed upon reduction of the ThiGH-His complex with dithionite, supports a mechanism in which NADPH is used by flavodoxin reductase and flavodoxin to reduce the cluster in ThiH-His (section 1.3.3).

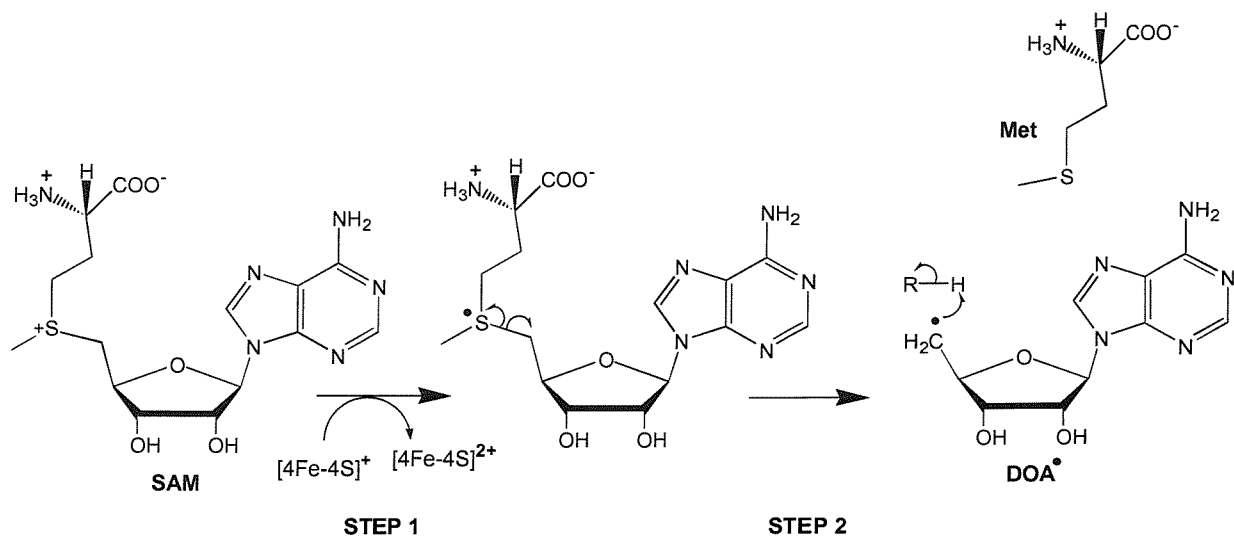
The fractionation experiments described in section 6.2.7, revealed that the addition of fractions enriched in yet unidentified proteins deriving from the de-repressed pRL1020/83-1 lysate, could result in a 1.5-fold increase of the thiazole synthase activity. In an attempt to rationalise these results, one could speculate that in assays containing either the de-repressed pRL1020/83-1 lysate or proteins, the activity depends on ThiGH-His and on the amount of endogenously reduced flavodoxin, which cannot be efficiently regenerated due to the low concentration or removal (by the gel filtration step) of NADPH; whilst, in the presence of an excess of physiological reductant, the flavodoxin/flavodoxin reductase system could work catalytically, with ThiGH-His remaining, potentially, the only limiting component. A very low endogenous concentration of NADPH could also explain why the gel filtration of the pRL1020/83-1 lysate did not decrease the activity (section 6.2.4).

The addition of SAM and NADPH has provided optimised conditions for thiazole biosynthesis, however, as this high activity is approaching the point (50 pmol/mg of protein/h, section 6.2.1) at which ThiD and ThiE may become limiting,

supplementation of the reaction mixtures with these two proteins may be required for future studies.

6.2.9. Proposed Mechanisms for Thz-P Biosynthesis

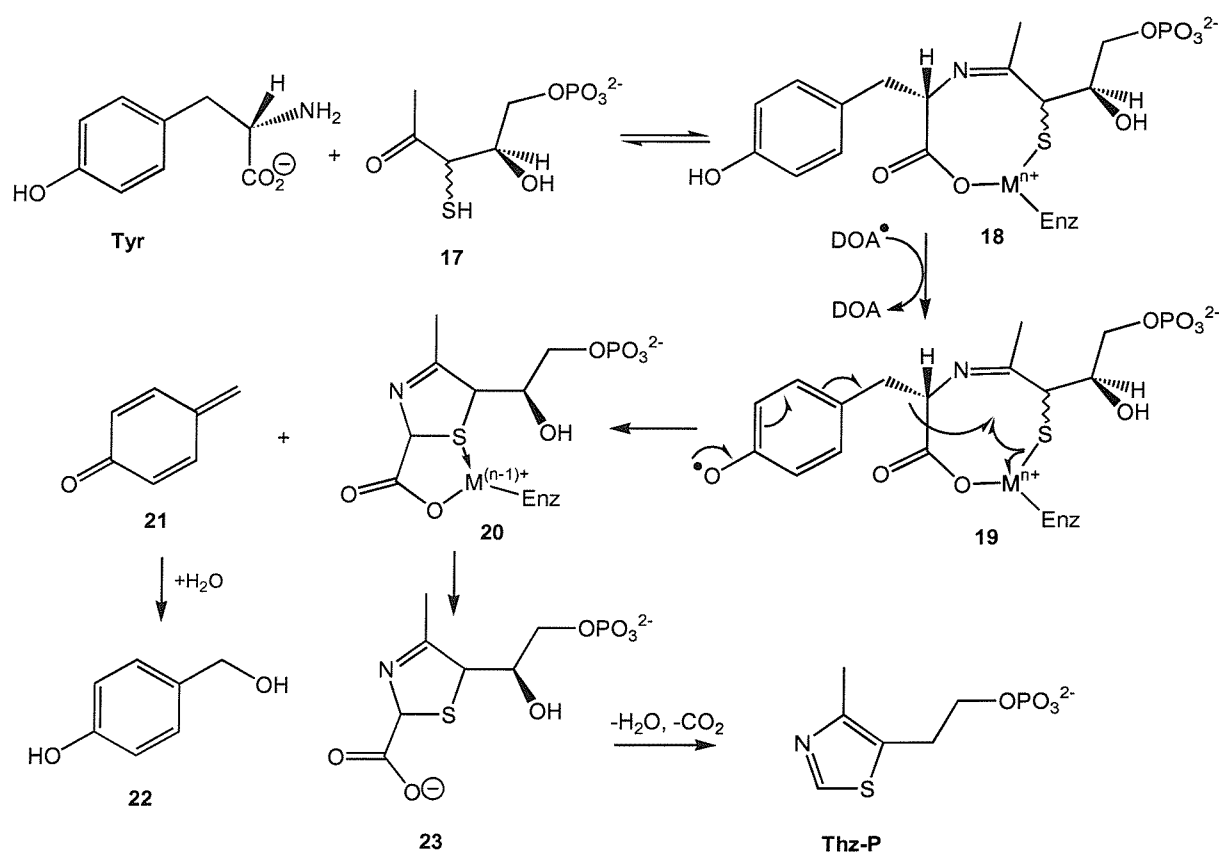
The stimulation of the thiazole synthase reaction by SAM and NADPH, together with the observed low stoichiometry of turnover (0.01-0.03 mol thiamine/mol ThiGH-His) are similar to the properties of other proteins that belong to the ‘radical SAM’ family of enzymes (88,108), although rigorous proof of this relationship will require a fully defined biosynthetic system. Radical SAM enzymes bind [4Fe-4S]^{2+/1+} clusters and SAM in close proximity (112,113,186,187) and are proposed, under suitable conditions, to generate a highly reactive DOA radical by reductive cleavage of SAM (**Scheme 6.3**). This radical, in turn, rapidly abstracts a hydrogen atom from a suitably placed donor (protein or substrate) to generate a second radical required for product formation (section 1.3.3).



Scheme 6.3. Reductive cleavage of SAM by a $[4\text{Fe}-4\text{S}]^+$ cluster to the DOA radical and methionine, and abstraction of an H atom from the substrate RH. Steps 1, 2 and/or the H atom abstraction may occur in a concerted fashion.

Several possible radical mechanisms involving SAM and the Fe-S cluster of ThiH can be envisaged leading to thiazole formation. One possibility is to use the SAM derived deoxyadenosyl radical to initiate the formation of a tyrosyl radical that leads to $\text{C}\alpha\text{-C}\beta$ bond cleavage. This side chain cleavage may be directly coupled to the cyclisation (**Scheme 6.4**) or lead to the formation of the glycine derived imine that has been identified as an intermediate in *B. subtilis* by Park *et al.* (81) (**Scheme 6.5**).

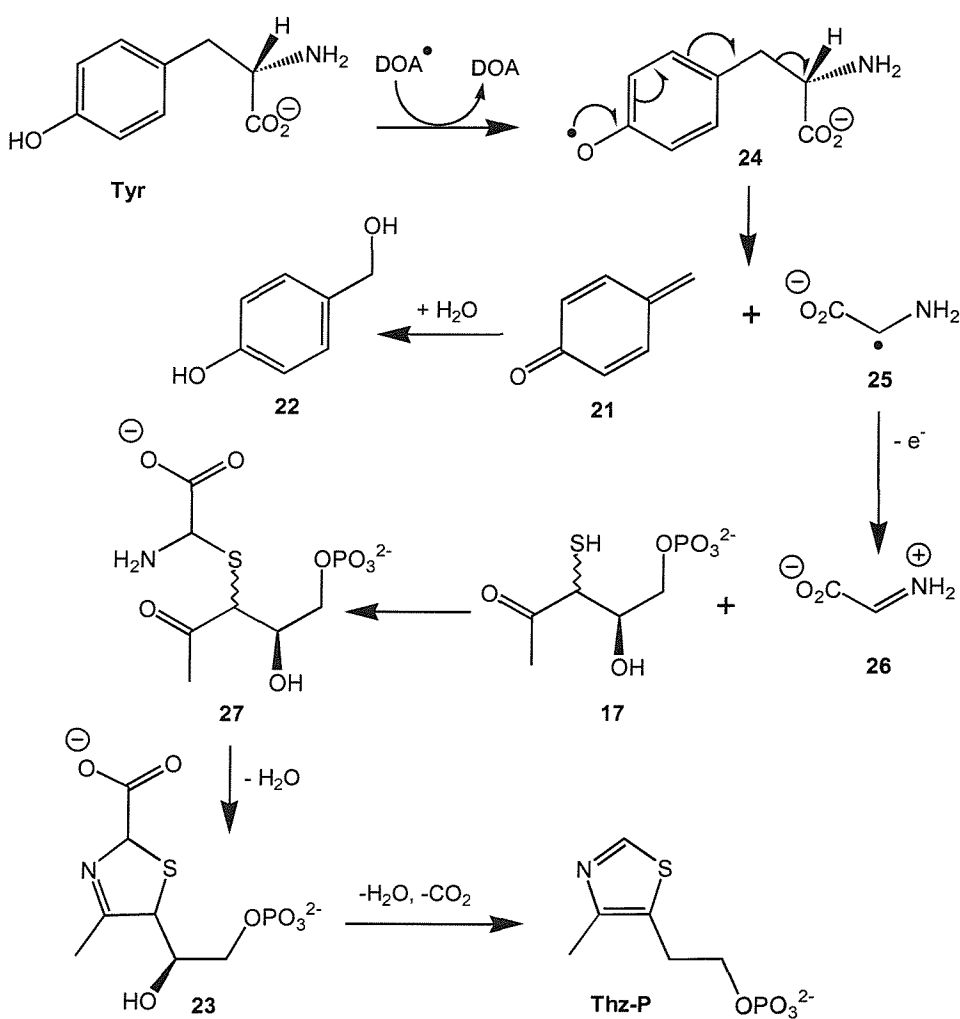
The first proposed mechanism (**Scheme 6.4**) would require Tyr and the thiodeoxy sugar **17** to form a Schiff base and chelate to an enzyme active site metal centre (**18**). A SAM-derived deoxyadenosyl (DOA) radical (or equivalent) could form the phenolic radical **19**, which may lead to $\text{C}\alpha\text{-C}\beta$ bond cleavage and release the quinone methide **21**.



Scheme 6.4. First proposed mechanism for Thz-P biosynthesis. The SAM derived deoxyadenosyl radical initiates the formation of a tyrosyl radical that leads to $\text{C}\alpha\text{-C}\beta$ bond cleavage. This side chain cleavage is then directly coupled to the cyclisation to Thz-P.

Hydration of **21** would lead to *p*-hydroxybenzyl alcohol **22**, a known thiamine biosynthetic by-product, whilst decarboxylation and dehydration of **23** would lead to Thz-P. In the formation of the C α -S bond by this mechanism, the metal ion is proposed to act as electron acceptor (for example, M = Fe $^{3+}/2^+$).

Alternatively (**Scheme 6.5**), the C α -C β bond cleavage which follows the formation of the tyrosyl radical **24**, could release the radical intermediate **25**, in addition to the quinone methide **21**.



Scheme 6.5. Second proposed mechanism for Thz-P biosynthesis. The SAM derived deoxyadenosyl radical initiates the formation of a tyrosyl radical that leads to C α -C β bond cleavage and then to the formation of the glycine derived imine **26** (81). Nucleophilic attack by **17** on **26**, intramolecular imine formation, dehydration and decarboxylation eventually lead to Thz-P.

As in the reaction catalysed by HemN (187), another radical SAM enzyme, a suitable and as yet unidentified electron acceptor is required to receive an unpaired electron from the radical intermediate **25**, leading, in this case, to the formation of the glycine derived iminium ion **26**. This iminium ion could undergo nucleophilic attack by the thiodeoxy sugar **17** to form **27**. Intramolecular imine formation would lead to the cyclic intermediate **23**, which will dehydrate and decarboxylate to Thz-P.

In both proposed mechanisms, Tyr acts as a substrate for ThiH, consistent with the observation that the Thz-P requirement of *S. typhimurium* strains containing mutations in the *isc* operon or in *gshA*, could be satisfied by the addition of this amino acid (48,76). In fact, the Thz-P auxotrophy of these mutants was suggested to arise from the damage of the Fe-S cluster in ThiH caused by the mutations, and the effect of Tyr was rationalised in terms of binding to the protein to stabilise it or to maximise the turnover of the residual active ThiH molecules. Involvement of precursor **17** in thiazole formation is supported by the data reported in section 6.2.4, and our current hypothesis is that this thiodeoxy sugar is released by the hydrolysis of an enzyme bound intermediate, possibly derived from ThiS (Figure 6.6) (81). The mechanisms proposed herein also suggest a role for ThiG, which could interact with the ThiS-bound intermediate and catalyse its hydrolysis. Then ThiG could either transfer **17** to ThiH (Scheme 6.4) or receive the glycine derived imine **26** from ThiH, and catalyse the cyclisation to Thz-P in its active site (Scheme 6.5). In the first case ThiH would conceivably be the active cyclase, whilst in the second case it would be ThiG to perform this role.

Data supporting such a role for ThiG are the sequence homology to HisF which catalyses the formation of the imidazole ring of histidine from an acyclic precursor which contains a Dxp-like moiety (79,80), and the 48 % sequence identity to *B. subtilis* ThiG, recently shown to catalyse the cyclisation of Dxp and the glycine imine **26** to Thz-P, in the presence of a source of sulphur (81).

Further experiments will be required to substantiate and also discriminate between these two potential mechanisms, both of which imply a close interaction between ThiG and ThiH, in agreement with the observed formation of a ThiGH complex (Chapter 3).

6.3. Summary and Conclusions

For the first time, using lysates or partially purified protein samples and an enzyme coupled assay, the thiazole synthase activity of *E. coli* has been measured.

De novo thiamine biosynthesis was initially detected in lysates obtained from de-repressed pRL1020/83-1 cells, and subsequently found to be increased (2.5-3 times) by the addition of the proteins derived from a ThiFSGH-His over-expressing BL21(DE3) lysate. Purified ThiGH-His and ThiFS were then tested for their ability to substitute for this fraction. The addition of purified ThiGH-His allowed complete recovery of the activity and demonstrated that this complex was involved in the rate limiting step. Purified ThiF and ThiS, instead, substituted less efficiently for the gel filtered pRL1020/BL21(DE3) lysate and were also shown to reduce the rate of thiamine biosynthesis in assays containing de-repressed pRL1020/83-1 proteins and purified ThiGH-His. This effect was exacerbated in the presence of Dxp and Cys.

Studies on the dependence of the thiazole synthase activity on the concentration of the known precursors, Tyr, Cys and Dxp, revealed that the activity was unaffected by either the addition or omission of Cys and Dxp in the assays, being instead completely dependant on the addition of Tyr. A further component that co-purified with the proteins derived from the de-repressed pRL1020/83-1 lysate, was also required and is presumed to provide the C₅ unit and sulphur for which Dxp and cysteine are known to be the original metabolic precursors. Besides providing this potential enzyme-bound intermediate, the de-repressed pRL1020/83-1 proteins were also found to supply other yet unidentified rate-enhancing protein components. The activity is also strongly stimulated by the addition of SAM and a reducing agent, with NADPH proving more effective than dithionite.

These results are consistent with our working model in which the thiazole is formed from tyrosine and an as yet uncharacterised intermediate by the ThiGH complex in a SAM/NADPH dependent reaction. Two potential radical mechanisms, based on the production of a DOA radical and, subsequently, of a tyrosyl radical, have been proposed.

The development of a functional *in vitro* assay to investigate thiazole biosynthesis in *E. coli* cell-free extracts, constitutes a major step forward in the elucidation of the detailed and complex mechanism through which this thiamine moiety

is assembled. Many of the problems inherent to the formation and detection of this compound were overcome by carefully optimising the biosynthetic system (extracts from de-repressed cells incubated under anaerobic conditions) and by exploiting a coupled assay and the highly sensitive thiochrome method. This strategy has allowed the investigation of several conditions leading to remarkable findings as well as to a progressive simplification of the assay itself. The experiments described here have brought to light the existence of potential new accessory proteins, and not previously reported precursors and cofactors involved in Thz-P assembly, and will help design experiments to elucidate the details of this highly challenging problem of thiazole biosynthesis in *E. coli*. Particularly exciting future experiments might include: (i) characterisation of the potential enzyme-bound intermediate formed *in vivo* and which might have the structure shown in **Figure 6.6** (the structure of this intermediate could also hold the key to understand why ThiF and ThiS exert an inhibitory effect on thiamine biosynthesis, under the conditions investigated); (ii) identification of the enzymes shown to increase the thiazole synthase activity in assays containing a relatively high ThiGH-His concentration (potential candidates are flavodoxin and flavodoxin reductase); (iii) elucidation of the role of SAM and the specific reactions catalysed by ThiG and ThiH by designing, for example, experiments to trap or detect hypothetical radical and non radical intermediates.

Chapter 7.

Experimental Methods

7.1 Materials

Primers were synthesised by Eurogentec Ltd (Southampton). Materials were purchased from the following suppliers: molecular biology reagents from either Promega or Qiagen; restriction enzymes from either Promega or New England Biolabs; Taq DNA polymerase, T4 DNA ligase and molecular weight markers for DNA electrophoresis from Promega; Pfu Turbo DNA polymerase and *E. coli* XL1-Blue cells from Stratagene; dNTPs from MBI Fermentas; electrophoresis grade agarose from either Bio-Rad or Gibco BRL; pBAD-TOPO and pBAD/HisA cloning systems, *E. coli* One Shot and LMG194 cells from Invitrogen; pET-24d(+), pET-24a(+) cloning systems and *E. coli* BL21(DE3) cells from Novagen; yeast-extract, bacto-tryptone and bacteriological agar from Oxoid; IPTG and kanamycin from Melford Laboratories; β -(+)-L-arabinose, $K_3[Fe(CN)_6]$ and glycerol from Avocado; polyacrylamide-bis polyacrylamide [30 % (w/v), 37.5:1] from Amresco; adenosine, 4-hydroxybenzoic acid, 2,3-dihydroxybenzoic acid and 4-aminobenzoic acid from Across; D-glucose and molecular weight markers for SDS-PAGE from BDH; HPLC grade solvents, K_2HPO_4 and KH_2PO_4 from Fisher Scientific; $HClO_4$ [20 % (w/v) solution] from Fluka; aldolase, triose phosphate isomerase (TPI) (both from rabbit muscle) and all other reagent grade chemicals from Sigma-Aldrich, unless otherwise stated. *S*-adenosylmethionine (SAM, tosylate salt) was a generous gift from Dr. H. Schroeder (BASF, Ludwigshafen, Germany).

Aluminum backed TLC plates (silica gel 60, F-254, 250 μ m) were obtained from Merck. PD-10 and NAP-10 columns, Superdex 200 HR 10/30 pre-packed column, Source Phe, Q-Sepharose High Performance, Superdex 75 (S-75), Superdex 200 (S-200) and Chelating Sepharose Fast Flow resins were from AP Biotech. Pressure cells (10, 50 and 250 ml) were purchased from Amicon and PM30, PM10 membranes,

Biomax Ultrafree 0.5 filter membranes (5k NMWL) and sterile 0.22 µm filters from Millipore. Analytical and semi-preparative HPLC columns were either generous gifts from Roche and Prof. T. Brown or were purchased from Fisher Scientific together with Costar Spin-X filters (0.22 µm). *E. coli* 83-1 cells were a generous gift from Prof. R. Azerad (René Descartes University, Paris) and Prof. M. Therisod (University of Paris South, Orsay) *E. coli* KG33 cells were kindly provided by the *E. coli* Genetic Stock Center (Yale University) and *E. coli* C43(DE3) from Prof. J. E. Walker (MRC laboratory, Cambridge). *E. coli* BL21(DE3) cells transformed with a pET-23b-derived plasmid encoding Dxs-His were a kind gift from Prof. A. Boronat (Barcelona University, Barcelona).

7.2. Equipment

Centrifugation: Samples (2-250 ml) were centrifuged at 4 °C in an Avanti J-25 centrifuge (Beckman). For samples of a volume less than 2 ml a microCentrifuge 4221 (ALC) at room temperature or a Biofuge Fresco (Heraeus) at 4 °C were used.

Determination of pH: Mettler Delta 340 pH meter connected to a Mettler Toledo Inlab 413 Combination Electrode was used for pH determination and adjustment. The pH meter was calibrated at pH 7.0 to 10.0 before use and stored in a saturated solution of KCl.

PCR, Sterilisation and Incubation: A Progene Thermal Cycler (Techne) was used for PCR amplifications. Media and heat stable solutions required for microbiological experiments were sterilised in a PriorClave autoclave (Priorclave Ltd) at 121 °C for 25 min. Bacterial cultures (solid and liquid) were incubated in an Innova 4400 Incubator Shaker (New Brunswick Scientific) or in an Innova 4230 Refrigerated Incubator Shaker (New Brunswick Scientific).

Cell Lysis by Sonication: Cells suspensions (from 0.1 to 30 g of cell paste) were lysed by sonication in ice baths using a Soniprep 150 sonicator (Sanyo).

Anaerobic Purifications: all the experiments and purifications requiring anaerobic conditions were carried out in a glove box (Belle Technology) kept in a N₂ atmosphere and containing less than 2 ppm O₂. The glove box was maintained at 19 °C in a temperature controlled laboratory.

UV-visible Spectroscopy, NMR and ESI-MS: absorbance readings and UV spectra were recorded on a Lambda 2 spectrophotometer (Perkin-Elmer). ^1H and ^{13}C NMR spectra were recorded using a AC300 (300 MHz, Bruker) spectrometer, and ESI-MS spectra were recorded on either a VG Platform single quadrupole or on a Waters ZMD quadrupole mass spectrometer.

FPLC and HPLC: A Pharmacia-LKB fast performance liquid chromatography (FPLC) unit was used for aerobic purifications at 4 °C; a Gilson System Workcenter including 321 pumps and 234 Gilson Autoinjector equipped with Tray 36 was connected to a Shimadzu RF-10Ax1 fluorimeter and/or to a Gilson UV/Vis-155 detector, and used for high performance liquid chromatography (HPLC) analysis at room temperature and anaerobic purifications at 19 °C.

Gel Densitometry Analysis: a Syngene Gene Genius imaging system and related software were used to estimate the relative amounts of proteins analysed by SDS-PAGE and revealed by Coomassie staining.

7.3. General Experimental Methods

Standard sterile techniques were applied throughout microbiological experiments. Growth media and heat stable solutions were autoclaved, whilst heat labile solutions (IPTG and antibiotics) were filter sterilised through 0.22 μm filters.

Growth media were supplemented with the appropriate antibiotic at the following concentrations: ampicillin, 100 $\mu\text{g}/\text{ml}$ and kanamycin, 30 $\mu\text{g}/\text{ml}$. Protein expression was induced by the addition of arabinose [0.2 % (w/v)] from pBAD-derived plasmids, and by the addition of IPTG (0.5 mM) from pET-derived plasmids.

Assembled plasmids and their resistance markers are listed in Appendix A.

The composition of media and other relevant solutions is given in Appendix B.

Method 1: PCR Amplification of Genes of Interest

Genomic DNA was isolated by the author using Magyx® Bacterial Genomic Midi Kit (Nuclyx) and following the manufacturer's recommended protocol. The primers used to amplify all the genes mentioned in this thesis are listed in **Table 7.9**.

PCR reactions (50 µl) were set up in sterilised tubes (200 µl) using the conditions reported in **Table 7.1**, however, in order to minimise the extension of partially annealed primers to non-specific sites on the genomic DNA, the DNA polymerase was added only after 3 min incubation at 95 °C (**Table 7.2**). This technique is called ‘hot start’ PCR.

Component	Stock Concentration	Volume	Total quantity
Pfu Turbo Buffer	10 X	5 µl	1 X
dNTPs	10 mM	2 µl	20 nmol
DNA template*	10 or 100 ng/µl	1 µl	10 or 100 ng
Primers	10 µM	2.5 µl/each	0.025 nmol
Pfu Turbo DNA polymerase	0.25 U/µl	5 µl	1.25 U
Sterile H ₂ O		to 50 µl	

Table 7.1. Conditions for PCR reactions. * Two reaction mixtures containing different amounts of DNA template (100 and 10 ng) were normally prepared for the amplification of target genes.

PCR reactions were processed in a thermocycler as reported in **Table 7.2**, then analysed on 1 % agarose gels by gel electrophoresis.

Nº of Cycles	T (°C)	time (min)
1	95	3
	80 (addition of the polymerase)	3
30	95 (denaturation)	1
	50 (annealing)	1
	72 (elongation)	1-1.5/kbp
1	72	10
	4	as required

Table 7.2. PCR amplification reaction cycle conditions. At the end of the last cycle, reaction mixtures were stored at 4°C until removed.

PCR products were purified using Wizard® PCR Preps DNA Purification System (Promega), as per manufacturer's instructions.

Method 2: A-tailing

Pfu DNA polymerase does not add an extra deoxyadenosine at the 3' ends of the amplified fragments. Therefore, in order to allow cloning into the pBAD-TOPO vector (method 3) which contains an extra deoxythymidine at the 3' ends, the purified PCR products (method 1) were A-tailed using Taq DNA polymerase and the conditions described in **Table 7.3**.

	Stock Concentration	Volume	Total Quantity
PCR product	20-100 ng/μl	7 μl	140-700 ng
Taq polymerase buffer	10 X	1 μl	0.9 X
MgCl ₂	25 mM	0.8 μl	20 nmol
ATP	2 mM	1 μl	2 nmol
Taq DNA polymerase	5 U/μl	1 μl	5 U

Table 7.3. A-tailing conditions.

The tubes (200 μl) were placed into the thermocycler and kept at 72°C for 30 min, then stored at -20 °C until used or immediately ligated into pBAD-TOPO vector.

Method 3: Cloning into pBAD-TOPO Vector

A-tailed PCR products (method 2) were ligated into pBAD-TOPO vector, as per manufacturer's instructions. Reaction mixtures (6 μl) were incubated at room temperature for 30 min and used to transform XL1-Blue or One Shot competent cells (method 4).

Method 4: Preparation of Competent Cells and Transformation

Competent cells were either purchased (One Shot and XL1-Blue) or prepared by the rubidium chloride method (188). Purchased competent cells were transformed as

per manufacturer's instructions; in the case of competent cells prepared by the rubidium chloride method, the general transformation method which follows has been successfully employed.

Aliquots of competent cells (50-200 μ l) contained in 1.5 ml tubes were thawed on ice for 10 min before adding, stirring gently, the total volume (6-10 μ l) of a ligation reaction (methods 3 or 9) or 1 μ l of purified plasmid DNA. The tubes were incubated on ice for 30 min and then heat-shocked for exactly 45 sec in a 42°C water bath. Cells were returned to ice for 2 min, mixed with room temperature SOC medium (950-800 μ l) and then transferred to 15 ml Falcon tubes. Cell suspensions were incubated in an orbital shaker at 37°C (230 rpm) for 1 h before being plated onto selective 2YT or supplemented DM agar plates (Appendix B). Positive colonies (those containing the correct construct), identified by PCR screening (method 5) or by Minipreps and analytical restriction digestion (methods 6 and 7), were stored as glycerol freezes (method 10).

Method 5: PCR Screening of Colonies

Colonies were screened for plasmids containing the correct inserts by direct colony PCR, using either suitable primers annealing to the vector (pBAD-TOPO or pBAD/His) or using one primer annealing to the vector and one annealing to the insert (**Table 7.9**). Colonies from plates were picked with sterile 10 μ l tips and dipped into 50 μ l PCR reactions set up as follows:

	Stock Concentration	Volume	Total quantity
Taq Polymerase buffer	10 X	5 μ l	1 X
MgCl ₂	25 mM	4 μ l	0.1 μ mol
dNTPs	10 mM	2 μ l	20 nmol
Primers	10 μ M	2.5 μ l	0.025 nmol
Taq DNA polymerase	0.5 U/ μ l	5 μ l	2.5 U
Sterile H ₂ O		33.5 μ l	

Table 7.4. Compositions of reaction mixtures prepared for PCR screening of positive colonies.

Each tip was then ejected into a 50 ml Falcon tube containing 2YT medium (5 ml) and cells were grown overnight at 37 °C for further investigation or storage.

PCR reaction mixtures were transferred to the thermocycler and heated at 95 °C for 10 min to lyse the cells and allow the release of both genomic and plasmid DNA. The remaining cycle conditions were identical to those reported in **Table 7.2**, including the ‘hot start’ technique (method 1).

Method 6: Plasmid DNA Isolation

Plasmid DNA was isolated using Wizard *Plus* Minipreps DNA Purification System (Promega) or a QIAprep Spin Miniprep Kit (Qiagen), as per manufacturer’s instructions. Sterile water (25-45 µl) was used to elute the purified plasmid DNA.

Method 7: Restriction Digestion (Analytical and Preparative)

Analytical restriction digestion of plasmid DNA (45 µl, 50-75 ng/µl) isolated from 5 ml bacterial culture (method 6) used the following conditions:

	Concentration	Volume	Total quantity
Plasmid	50-75 ng/µl	5 µl	250-375 ng
Appropriate Buffer	10 X	1 µl	1 X
BSA	1 mg/ml	1 µl	1 µg
Enzyme1	10 U/µl	0.5 µl	5 U
Enzyme 2	10 U/µl	0.5 µl	5 U
H ₂ O		2 µl	

Table 7.5. Conditions for analytical plasmid DNA restriction digestion. Total volume: 10 µl.

Preparative restriction digestion of plasmid DNA (25 µl, 100-300 ng/µl) isolated from 10 ml bacterial culture (method 6) used the following conditions:

	Volume	Concentration	Total quantity
Plasmid	20 μ l	100-300 ng/ μ l	2-6 μ g
Appropriate Buffer	3 μ l	10 X	0.9 X
BSA	3 μ l	1 mg/ml	3 μ g
Enzyme1	2 μ l	10 U/ μ l	20 U
Enzyme 2	2 μ l	10 U/ μ l	20 U

Table 7.6. Conditions for preparative plasmid DNA restriction digestion. Total volume: 30 μ l.

Reaction mixtures were incubated at 37 °C for 1-2.5 h and then analysed on a 1 % agarose gel by gel electrophoresis.

Method 8: Purification of Digested Fragments

Completed preparative digestion reactions (30 μ l) were loaded onto a 1 % low melting point agarose gel to separate the fragments of interest. The required bands were excised and the DNA recovered from the agarose using the Geneclean III Kit, as per manufacturer's instructions. Agarose gel electrophoresis analysis was used to estimate the concentration of the purified fragments by comparison with DNA markers of known concentration.

Method 9: Ligation into an Expression Vector

Samples of suitably restricted and purified plasmid and insert DNA were ligated under the following conditions:

	Concentration	Volume	Total quantity
Rapid Ligation Buffer	2 X	5 μ l	1 X
Plasmid	50 ng/ μ l	1 μ l	50 ng
Insert	25-100 ng/ μ l	x μ l*	
T4 DNA Ligase	3 U/ μ l	1 μ l	3 U
H ₂ O		To a final volume of 10 μ l	

Table 7.7. Conditions for the ligation of a DNA fragment into an expression vector. *x varied according to the size of both the vector and the insert, and was calculated to give 3:1 and 1:3 insert:vector molar ratios.

Ligation reactions were incubated overnight at 4 °C and then used to transform XL1-Blue or One Shot competent cells (method 4). Positive colonies were then identified either by PCR screening (method 5) or by plasmid DNA isolation followed by analytical restriction digestion (methods 6 and 7). Plasmid DNA from positive colonies was isolated and used (1 μ l) to transform BL21(DE3), LMG194, 83-1 or KG33 competent cells (method 4), as required.

Method 10: Glycerol Freeze Preparation

Permanent stocks of plasmid-bearing strains were prepared, for long term storage, adding glycerol (125 μ l) to an appropriate bacterial culture (500 μ l), mixing vigorously and storing at -80 °C.

Method 11: SDS-PAGE Analysis (189)

Protein purity and relative amounts of over-expressed proteins in soluble and insoluble cellular fractions (method 13) were determined by analysis of 15 % or 18 % SDS-PAGE gels (Bio-Rad Mini Protean II System, 200 V) revealed by Coomassie blue staining (Appendix B). For each sample, small amounts (20 μ l) of cleared lysate and re-suspended cell pellets, were mixed with 2 X SDS-PAGE loading buffer (20 μ l, Appendix B), heated at 90 °C for 5 min to denature the proteins and then loaded onto a SDS-PAGE gel.

Method 12: Estimation of Protein Concentration

Protein concentration was routinely determined by the method of Bradford (190). Briefly, Bradford reagent (1 ml) was added to a protein sample (20 μ l) and incubated at room temperature for 5 min, then A_{595} was measured using pure Bradford reagent as a control. The sample was diluted if A_{595} exceeded 1.0. Appropriate correction factors for proteins of unknown concentration were obtained from calibration curves constructed with BSA standards.

The individual concentrations of ThiH-His and ThiG in purified ThiGH-His samples were estimated by SDS-PAGE analysis (method 11) and gel densitometry against BSA standards. In particular, BSA samples (10 μ l, 0.5, 1.0 and 1.5 mg/ml) and the ThiGH-His sample being analysed (10 μ l, 1 mg/ml, as estimated by the Bradford assay) were diluted with water (10 μ l) and mixed with 2 X SDS-PAGE loading buffer (20 μ l), then loaded and resolved on a 15 % SDS-PAGE gel. The gel was allowed to de-stain for at least 18 h in SDS-PAGE de-stain solution (Appendix B), before analysing the bands by gel densitometry.

Method 13: Small Scale Expression Experiments

Cells from glycerol freezes were used to inoculate small scale cultures in 2YT medium (5 ml), incubated overnight at 37 °C. These cultures (100 μ l) were then used to inoculate fresh 2YT medium (10 ml in 50 ml Falcon tubes), and cells grown at 37 °C, 220 rpm, until the OD_{600} reached 0.4-0.6. At this point, the appropriate inducer (Appendix A) was added and cells were transferred to an incubator set at 15, 22, 28 or 37°C (depending on the strain and the experiment). The growth of the culture continued to be monitored by measuring the OD_{600} , and at the stationary phase ($OD_{600} = 1.8-2.3$) the culture was transferred to 15 ml Falcon tubes and cells harvested by centrifugation (JA-14 rotor with inserts to fit 15 ml Falcon tubes, 7500 rpm, 10 min, 4°C). Cell pellets were stored at -80 °C or immediately re-suspended in lysis buffer [$\sim 500 \mu$ l, Tris-HCl 50 mM, pH 8.0, glycerol 12 % (w/v)], transferred to 1.5 ml tubes, placed in an ice bath and lysed by sonication with 2 bursts of 10 sec with a 30 second rest. Cell debris was precipitated by centrifugation and the protein content of the supernatant estimated by the Bradford Assay (method 12). Supernatants and cell pellets re-suspended in lysis buffer ($\sim 500 \mu$ l) were then analysed by SDS-PAGE (method 11).

Method 14: Large Scale Expression Experiments

Cells from the glycerol freeze of interest were used to inoculate a starter culture in 2YT medium (100 ml), incubated overnight at 37 °C. This culture (50 ml) was then used as 1 % inoculum into fresh 2YT medium (5 l) aliquoted in 4 l flasks (~ 1.250 l of medium/flask), and cells grown at 37 °C. When the OD₆₀₀ reached 0.4-0.6, protein expression was induced by the addition of the appropriate inducer (Appendix A) and, depending on the experiment, cells were returned to the shaker at 37 °C or transferred to another shaker set at 22 or 28 °C. Cell growth continued to be monitored by measuring the OD₆₀₀ and, at the stationary phase (OD₆₀₀ = 1.8-2.3), cells were harvested by centrifugation (JA-14 rotor, 12000 rpm for 8 min at 4 °C). The resultant cell pellet was weighed and stored at –80 °C until used.

Method 15: Small Scale Nickel Spin Column Purification

Nickel spin columns were prepared by transferring 150 µl of Chelating Sepharose Fast Flow resin to a Quiagen Qiaquick spin column (Quiagen); excess storage liquid was removed by centrifugation (3000 rpm, 1 min, as were subsequent centrifugation steps for this method) and the resin was charged by re-suspending in NiSO₄ (300 µl, 0.2 M), followed by centrifugation. Each column was then washed with 50 mM Tris-HCl, pH 8.0 (2 x 700 µl), and 500-700 µl of cleared lysate (8-10 mg/ml) applied to permit the binding of the hexahistidine-tagged protein of interest. The lysate was left to stand for 1 min followed by centrifugation. The flow through was collected and re-applied, repeating the previous step. The column was then washed with solutions of increasing concentrations of imidazole (700 µl, 10, 20, 50 mM) in Tris-HCl, pH 8.0 buffer containing 0.5 M NaCl. The eluate was collected at each stage. The His-tagged protein was eluted by the addition of 50 µl of high imidazole buffer (50 mM Tris-HCl, pH 8.0, 0.5 M NaCl, 0.5 M imidazole), mixing well to re-suspend the resin, and left to stand for 5 min before centrifugation. Flow through and each of the eluate fractions were analysed by SDS-PAGE (method 11).

Method 16: Thiochrome Assay. Measurement of the Thiamine Content in Cell Pellets and in In Vitro Assays.

The amount of thiamine monophosphate and pyrophosphate produced both *in vivo* and *in vitro* was estimated by the thiochrome method, with only minor changes to the protocol described by Gerrits (174).

The following solutions were prepared: PCA1, 7.2 % (w/v) HClO_4 in H_2O [obtained by appropriate dilution of the 20 % (w/v) solution commercially available]; $\text{K}_3[\text{Fe}(\text{CN})_6]$, 12 mM in 3.35 M NaOH, freshly prepared and stored in the dark until used; H_3PO_4 , 1.4 M.

TP and TPP standards were prepared from 100 mM stock solutions of the respective hydrochloride salts in 100 mM HCl (21 and 23 mg, respectively, in 0.5 ml). These solutions were first diluted 10-fold in 100 mM HCl and then 100-fold in H_2O to a final concentration of 100 μM . Standards (1 ml) were then prepared as indicated in **Table 7.8**. 25 μl of these standard solutions were added to 1:1 mixture of H_2O :PCA1 (500 μl total volume) or to a 1:1:2 mixture of reaction buffer: H_2O :PCA1 (500 μl total volume), and the final mixtures oxidised under the conditions described in A or B (see below), respectively. As standards, samples and the oxidising agent are light sensitive, suitable precautions such as working in a dark room or protecting samples from light by wrapping them in foil, were taken. Oxidised mixtures are stable for at least 24 h, but cannot be frozen due to the formation of a precipitate.

A: Thiochrome method for the analysis of cell pellets. Frozen cell pellets from de-repression experiments (in 15 ml Falcon tubes) were thawed on ice for 10 min and then re-suspended in a 1:1 mixture of H_2O :PCA1 (2 ml for cell pellets of up to 80 mg of wet cells, 4 ml for heavier cell pellets); the white suspensions were sonicated on ice (3 bursts of 10 sec with 30 second rest) and the precipitated proteins removed by centrifugation (JA-14 rotor with inserts to fit 15 ml Falcon tubes, 7500 rpm, 10 min, 4°C). Supernatants (0.5 ml) were transferred to 1.5 ml tubes, and the following reagents were added in the dark, in the indicated order: H_2O (25 μl), MeOH (50 μl) and $\text{K}_3[\text{Fe}(\text{CN})_6]$ (100 μl). Tubes were capped, mixed and after 30-60 sec reactions mixtures were neutralised by the addition of H_3PO_4 (100 μl). Oxidised samples were filtered through 0.2 μm filters (Costar), then analysed (50 μl injections) by reverse phase HPLC using a Hypersil BDS C18 column (150 X 4.6 mm, 5 μ particle size) or a

Phenomenex ODS column (150 X 4.6 mm, 5 μ particle size), buffer A (140 mM K₂HPO₄, 12 % MeOH, 1.5 % DMF, 0.3 mM TBAH, pH 7.0) and buffer B (90 % CH₃CN, 10 % H₂O). The compounds were eluted at 0.8 ml/min with linear gradients between the following time points: t = 0 min, 0 % buffer B; t = 2 min, 0 % buffer B; t = 12 min, 30 % buffer B; t = 16 min, 65 % buffer B; t = 19 min, 65 % buffer B; t = 23 min, 0 % buffer B; t = 30 min, 0 % buffer B, and detected by fluorescence (excitation at 360 nm and emission at 454 nm). TPP and TP were eluted from the Hypersil column in 5.5 and 7.4 min, respectively, and from the Phenomenex column in 6.7 and 8.1 min, respectively.

B: Thiochrome method for the analysis of *in vitro* reaction mixtures. Due to the presence of DTT (sections 7.7.3 and 7.8.2) in the reaction mixtures to be oxidised, the thiochrome method had to be optimised by doubling the concentration of the K₃[Fe(CN)₆] solution (24 mM in 3.35 M NaOH).

To estimate the *de novo* thiamine production in *in vitro* assays, reactions were stopped at t = 0 and at t = 4 h by the addition of 500 μ l of PCA1, the volume adjusted to 1 ml with H₂O, and proteins precipitated by centrifugation (14000 rpm, room temperature). The supernatants (500 μ l) were oxidised, in the dark, by the addition of the following reagents in the indicated order: H₂O (50 μ l), MeOH (50 μ l) and K₃[Fe(CN)₆] (100 μ l). Tubes were capped, mixed and after 30-60 sec reactions mixtures were neutralised by the addition of H₃PO₄ (75 μ l). Oxidised samples were filtered through 0.2 μ m filters (Costar), then analysed (50 μ l injections) by reverse phase HPLC using a Phenomenex ODS column (150 X 4.6 mm, 5 μ particle size). Two slightly different chromatographic systems were used. System 1: identical to that described in A; system 2: the composition of buffer B was changed to 70 % MeOH, 30 % H₂O (as in the original method described by Gerrits) and a different elution program was adopted: t = 0 min, 0 % buffer B; t = 2 min, 0 % buffer B; t = 5 min, 20 % buffer B; t = 10 min, 20 % buffer B; t = 12 min, 40 % buffer B; t = 15 min, 40 % buffer B; t = 18 min, 0 % buffer B; t = 28 min, 0 % buffer B. Flow rate: 0.8 ml/min. The thiochrome derivatives of TPP and TP were eluted in 7.5 and 9.0 min, respectively.

100 μ M TP or TPP Stock Solution (μ l)	H ₂ O (μ l)	Final Conc. (μ M)
20	980	2
50	950	5
100	900	10
200	800	20
300	700	30

Table 7.8. Dilution series for TP or TPP standards.

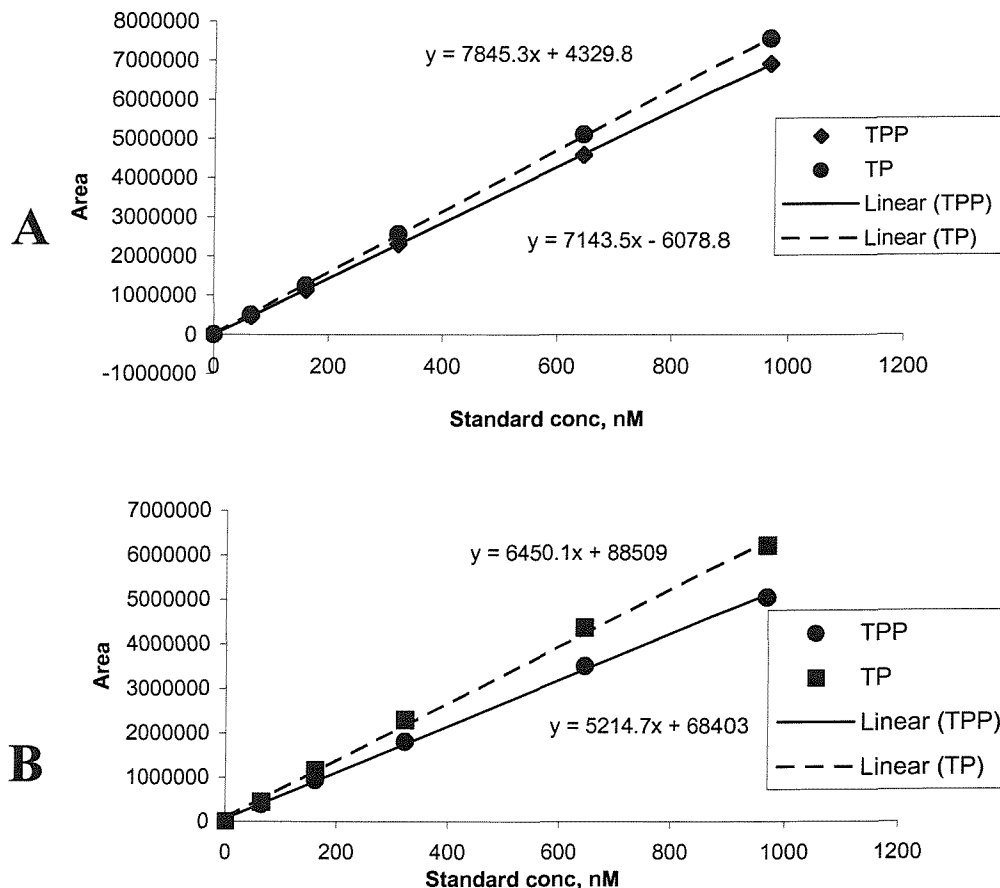


Figure 7.1. Typical TP and TPP calibration curves; (A) chromatographic systems 1 and (B) chromatographic system 2. The TP and TPP responses from both systems were quite similar. Area values were plotted against the final concentration of the standards in the oxidised mixtures.

7.4. Experimental for Chapter 2

Unless otherwise specified all genes were amplified using Pfu DNA polymerase (method 1) and the primers listed in **Table 7.9**.

Primer ID	Sequence 5' → 3'
THRHA	<i>CAT ATG AAA ACC TTC AGC GAT CGC</i>
THRHB	<i>GGA TCC TCA TAG TCT TTG CGA GGC GCG TCC</i>
THIHBAD1	<i>CCA TGG <u>TCA</u> AAA CCT TCA GCG ATC GCT</i>
THIHBAD2	<i>CTC GAG TCA TAG TCT TTG CGA GGC GCG TCC</i>
THIG1	<i>CCA TGG <u>TCT</u> TAC GTA TTG CGG ACA AA</i>
ThiHRevHis Tag	<i>GGA TCC TCA GTG GTG GTG GTG GTG GTG TAG TCT</i> <i>TTG CGA GGC GCG TCC CAG</i>
THIFS1	<i>CCA TGG <u>TCA</u> ATG ACC GTG ACT TTA TG</i>
thiC FORWARD	<i>CCA TGG <u>TCT</u> CTG CAA CAA AAC TGA CCC GCC G</i>
thiE FORWARD	<i>CCA TGG <u>TCT</u> ATC AGC CTG ATT TTC CTC C</i>
ThiE-His Rev	<i>CTC GAG TCA GTG GTG GTG GTG GTG CGG TCA</i> <i>TTCA TCG CCA ACT</i>
ThiI1	<i>CCA TGG <u>TCA</u> AGT TTA TCA TTA AAT TG</i>
ThiI2	<i>GAG CTC GGA TCC TTA CGG GCG ATA TAC CTT</i>
thiD-F	<i>CCA TGG <u>TCA</u> AAC GAA TTA ACG CTC TGA CGA</i>
thiD-His-R	<i>CTC GAG TCA GTG GTG GTG GTG GTG GTG CCA CCA</i> <i>GGC GTG GAA GTG GTG AAC CG</i>
PBAD FORWARD	<i>ATG CCA TAG CAT TTT TAT CC</i>
PBAD REVERSE	<i>GAT TTA ATC TGT ATC AGG</i>
PBAD HIS REV	<i>GGC TGA AAA TCT TCT CTC ATC CGC</i>
pET1	<i>CTA TAG GGA GAC CAC AAC</i>
SOT15	<i>CGC GAA ATT AAT ACG ACT CAC</i>

Table 7.9. List of primers used during this project. Italicised bases correspond to the restriction sites introduced. Underlined bases were added to allow the start codon introduced with the *Nco*1 restriction site to be in frame with the gene sequence. The

resultant *GTC* codon encoded for an additional N-terminal valine. PBAD FORWARD and PBAD REVERSE align to pBAD-TOPO; PBAD FORWARD and PBAD HIS REV align to pBAD/HisA; pET1 and SOT15 align to pET vectors. These primers have been used to identify positive clones by PCR screening (method 5).

The following general strategy has been employed to assemble the expression plasmids mentioned in Chapters 2 and 4. The genes of interest were amplified by PCR (method 1), A-tailed (if required, method 2) and ligated into pBAD-TOPO (method 3). Reaction mixtures were then transformed into either XL1-Blue or One Shot competent cells (method 4), plated onto selective 2YT solid medium. Positive clones were identified by either DNA isolation followed by analytical restriction digestion (method 7) or by PCR screening (method 5), and stored as glycerol freezes (method 10). Plasmids thus obtained were then isolated on a large scale (10 ml cultures, method 6), restricted (method 7) and the required fragments subcloned into expression vectors restricted to give complementary sticky ends (method 9). Reaction mixture were again transformed into XL1-Blue or One Shot competent cells and colonies screened for positive clones. Once isolated, positive clones were stored as glycerol freezes, and their plasmid DNA isolated and transformed into *E. coli* BL21(DE3) or LMG194 expression strains.

7.4.1. *pRL200 and pRL220: T7 Compared with araBAD Promoter*

thiH (1.1 kbp) was amplified by PCR (method 1) using two different sets of primers: THRHA and THRHB to introduce 5' *Nde*1 and 3' *Bam*H1 restriction sites (*thiH1*), and ThiHBAD1 and ThiHBAD2 to introduce 5' *Nco*1 and 3' *Xho*1 restriction sites (*thiH2*) (Figure 7.2 A). In both cases, the gene was amplified using Taq DNA polymerase. *thiH1* and *thiH2* were first ligated into pBAD-TOPO, resulting in pRL100 and pRL120, respectively, and then subcloned into pET-24a(+) on a *Nde*1/*Bam*H1 restriction fragment, and into pBAD/HisA on a *Nco*1/*Xho*1 fragment, respectively. The pET-derived plasmid was named pRL200 and the pBAD-derived plasmid pRL220.

pRL200 was transformed into BL21(DE3) and pRL220 into LMG194, and the resultant strains grown on a small scale (4 x 10 ml per strain, method 13) in 2YT medium. When the OD₆₀₀ reached approximately 0.5, pRL200/BL21(DE3) samples

were induced with 10-fold serial dilutions of IPTG (0.5 to 0.005 mM) and pRL220/LMG194 samples with 10-fold serial dilutions of arabinose [2 to 0.02 % (w/v)]. One sample per strain was not induced and used as negative control. Cultures were incubated for a further 5 h at 28 °C before being harvested.

The total amount of soluble proteins was determined by Bradford assay (method 12) and the expression level of ThiH, in either the cleared lysates or pellets, analysed by SDS-PAGE (method 11). pRL220 was subsequently transformed also into BL21(DE3).

7.4.2. *pRL221 and pRL222: Co-expression of ThiH with GroEL/GroES and TrxA*

pLP200 and pLP300, plasmids encoding GroEL/ES and TrxA, respectively, were assembled by L. Peters in our laboratory (123).

pRL220 (section 7.4.1) was restricted (method 7) with *NcoI* and *XhoI* and the thus excised *thiH2* gene subcloned into pLP200 and pLP300 restricted to give complementary sticky ends (method 9). The resultant plasmids were named pRL221 and pRL222 (Figure 7.3), respectively, and transformed into both LMG194 and BL21(DE3). pRL220/LMG194, pRL220/BL21(DE3), pRL221/LMG194, pRL221/BL21(DE3), pRL222/LMG194 and pRL222/BL21(DE3) were cultured on a small scale (method 13) and induced with arabinose. Cells were incubated for a further 4 h at 37 °C before being harvested. The same experiment was repeated at 15 °C and, in duplicate, at 22 °C. Cells were lysed and cleared lysates and pellets analysed by SDS-PAGE.

7.4.3. *Mutations in thiH: Assembling of pRL220**

thiH2 (section 7.4.1) was amplified by PCR using Pfu DNA polymerase, and pRL220* assembled by the same procedure followed to construct pRL220 (section 7.4.1). pRL220* was transformed into LMG194 (method 4). pRL220*/LMG194 and pRL200/BL21(DE3) were cultured on a small scale and ThiH expression induced by the addition of the appropriate inducer (method 13). Cultures were transferred to a different incubator set at 22 °C and cultured for a further 5 h, then harvested, lysed and analysed by SDS-PAGE.

7.4.4. *pRL400: Co-expression of ThiH with ThiG*

thiGH (1.9 kbp) was amplified using THIG1 as forward and THRHB as reverse primers (method 1) (**Figure 7.2 B**). The PCR product was first ligated into pBAD-TOPO and then subcloned into pET-24d(+) on a *Nco*1/*Bam*H1 fragment. The derived plasmids were named pRL300 and pRL400 respectively, and pRL400 was transformed into BL21(DE3). ThiH expression level from these cells, pRL200/BL21(DE3) and pRL220*/LMG194 was compared in a small scale expression experiment (method 13) carried out in duplicate. Cells were grown at 37 °C until the OD₆₀₀ reached approximately 0.5, then the appropriate inducer was added. After the induction, samples of pRL200/BL21(DE3) and pRL400/BL21(DE3) cells were returned to the incubator at 37 °C, while their duplicates and LMG194/pRL220* cells were transferred to a 22°C shaker. After 4-6 h (depending on the temperature) the cells were harvested and lysed. The total amount of soluble proteins was estimated by the Bradford assay (method 12) and the expression level of ThiH and ThiG, in either the cleared lysates and pellets, analysed by SDS-PAGE (method 11).

7.4.5. *pRL800/820 and pRL1000/1020: Co-expression of Hexahistidine-tagged ThiH with ThiG and ThiFSG*

thiGH-His (1.9 kbp) was amplified by PCR using THIG1 as forward and ThiHRevHis Tag as reverse primers (method 1). The PCR product was first ligated into pBAD-TOPO and then subcloned into pET-24d(+) on an *Nco*1/*Bam*H1 fragment, and into pBAD/HisA by restricting the pET-derived plasmid with *Nco*1/*Xho*1. The resultant plasmids were named pRL700, 800 and 820, respectively (Appendix A and **Figure 2.12**).

thiFSGH-His (2.9 kbp) was amplified by Dr. M. Kriek (method 1, modified with an elongation time of 7.5 min and 2.5 U/reaction of polymerase) using THIFS1 and ThiHRevHis Tag as forward and reverse primers, respectively (**Figure 7.2 C**). A cloning strategy identical to that just described yielded pRL900, 1000 and 1020, respectively (Appendix A and **Figure 2.12**).

Cultures of pRL400/BL21(DE3) (section 7.4.4), pRL800/BL21(DE3) and pRL1000/BL21(DE3) cells were cultured overnight to provide a 1 % inoculum for a

small scale expression experiment (method 13) carried out in duplicate. Cells were induced and grown at 28 °C for 5 h, then harvested and lysed. Protein expression in both the cleared lysates and pellets was analysed by SDS-PAGE (method 11).

7.4.6. *pRL821: Co-expression of ThiGH-His with the Isc Proteins*

pMK400, a plasmid bearing the *lipA* gene and the *iscSUA-hscBA-fdx* operon (4.9 kbp), was constructed by Dr. M. Kriek, in our laboratory (123). This operon was excised from pMK400 on a *BstB1/Xho1* fragment and subcloned into equally restricted pRL820, resulting in pRL821. As *BstB1* is most active at 65 °C whilst *Xho1* (and BSA) would be inactivated at that temperature, plasmids were first linearised with *BstB1* at 65 °C, and reaction mixtures allowed to cool down before adding BSA and *Xho1* (the optimal buffer for *BstB1* was compatible with *Xho1*, method 7).

pRL821 was transformed into BL21(DE3), and pRL821/BL21(DE3) and pRL800/BL21(DE3) (section 7.4.5) were cultured on a large scale (method 14) in two separate expression experiments carried out under the same conditions: induction with IPTG and growth at 28°C for 5 h. Growth of pRL800/BL21(DE3) yielded 16 g of cell paste whilst growth of pRL821/BL21(DE3) yielded 30 g of biomass. To compare the expression level from the two strains, small quantities of pRL800/BL21(DE3) (215 mg) and pRL821/BL21(DE3) (157 mg) were transferred to 1.5 ml eppendorf tubes, re-suspended in lysis buffer [645 and 470 µl respectively, 50 mM Tris-HCl, 12.5 % (w/v) glycerol] and lysed by sonication (method 13). The total amount of soluble proteins was determined by Bradford assay (method 12) and the protein expression level in both the cleared lysates and pellets analysed by SDS-PAGE (method 11).

7.4.7. *pRL1021: Co-expression of ThiFSGH-His with the Isc Proteins*

To assemble pRL1021, the *lipA* gene carried by pMK400 was excised with *Age1* and *Xho1* and replaced by the *Age1/Xho1 thiFSGH-His* fragment obtained from pRL1020 restricted with the same restriction enzymes. pRL1021 (Figure 7.4) was transformed into BL21(DE3).

2YT medium (4 x 10 ml in 50 ml tubes) was inoculated with an overnight starter culture of pRL1021/BL21(DE3), and cellular growth monitored by measuring

the OD at 600 nm. When the OD₆₀₀ reached 0.2, one of the samples was induced with arabinose and allowed to grow for a further 5 h at 28 °C. The remaining three samples were induced when the OD₆₀₀ reached 0.6. At this point, one of the cultures was transferred to a 15 ml capped tube and aerated together with the others (left in 50 ml capped tubes) at 28 °C for 5 h. At the end of the expression experiment, cells were harvested and cleared lysates and pellets analysed by SDS-PAGE (method 11).

7.4.8. *pRL1300 and pRL1500: Expression of ThiCEFSGH-His and ThiEFSGH-His*

thiCEFSGH-His (5.4 kbp) and *thiEFSGH-His* (3.5 kbp) were amplified by PCR using Expand Long Template PCR System (Roche), as per manufacturer's instructions (**Figure 7.2 D**). In particular, an annealing temperature of 60 °C and an elongation temperature of 68 °C with an elongation time of 6 min (method 1) were chosen to optimise the amplification. The primers used were thiC FORWARD and ThiHRevHis Tag to amplify *thiCEFSGH-His*, and thiE FORWARD and ThiHRevHis Tag to amplify *thiEFSGH-His*. The PCR products were ligated into pBAD-TOPO, and the resultant plasmids named pRL1200 and pRL1400, respectively. The *thiCEFSGH* operon contains a RsrII restriction site at the 3' end of the *thiG* sequence, therefore *thiCEFSG* (4.3 kbp) and *thiEFSG* (2.4 kbp) were excised with *NcoI* and *RsrII* from pRL1200 and pRL1400, respectively, and subcloned into appropriately restricted pRL1020 (**Figure 2.19**). The resultant plasmids were named pRL1300 and pRL1500 and transformed into BL21(DE3).

Protein expression from pRL1300/BL21(DE3) and pRL1500/BL21(DE3) was investigated on a small scale (method 13). Cell were induced with arabinose and grown for 5 h at 28 °C before being harvested. Cleared lysates and pellets were analysed by SDS-PAGE (method 11).

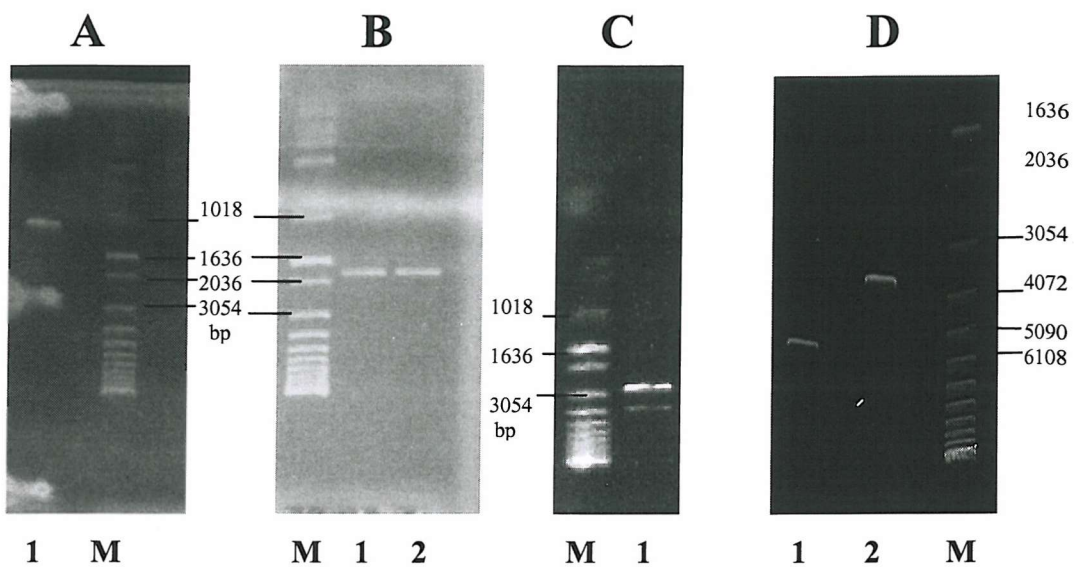


Figure 7.2. Purified PCR products. A: *thiH* (1.1 kbp), lane 1; B: *thiGH-His* (1.9 kbp), lanes 1-2; C: *thiFSGH-His* (2.9 kbp), lane 1; D: *thiCEFSGH-His* (5.4 kbp), lane 1 and *thiEFSGH-His* (3.5 kbp), lane 2. M = molecular weight marker.

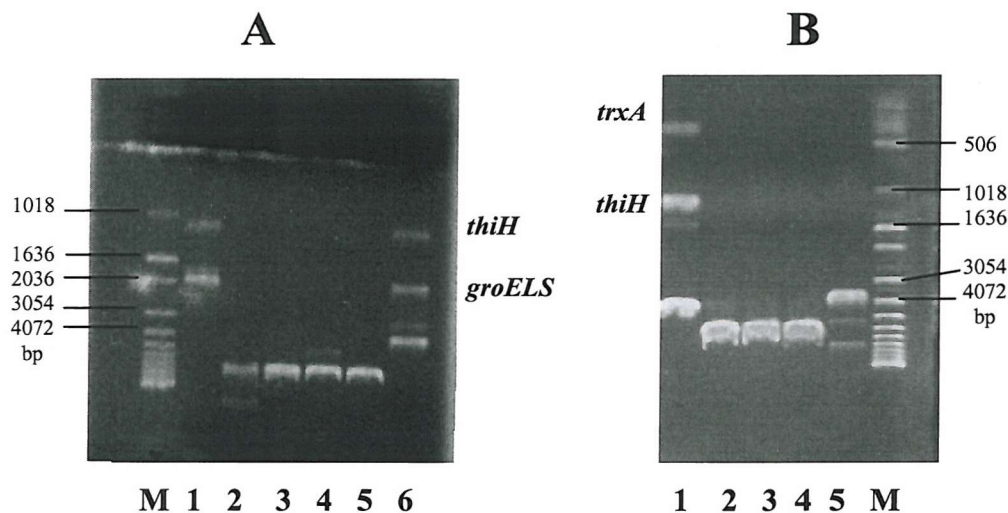


Figure 7.3. Identification of positive colonies containing pRL221 (A) and pRL222 (B) by plasmid DNA isolation and restriction. Gel A: amplified *thiH* and *groELS* genes used as reference (lane 1); isolated plasmid DNA (lane 2); restriction of plasmid DNA with: *EcoR1* (lane 3), *Xho1* (lane 4), *Nco1* (lane 5), *EcoR1* plus *Xho1* plus *Nco1* (lane 6, expected fragment sizes: 1.1, 2.0 and 4.0 kbp). Gel B: restriction of plasmid DNA with: *Nco1* plus *Xho1* plus *EcoR1* (lane 1, expected fragment sizes: 1.1, 0.4 and 4.0 kbp), *Nco1* (lane 2), *Xho1* (lane 3), *EcoR1* (lane 4); isolated plasmid DNA (lane 5). M = molecular weight marker.

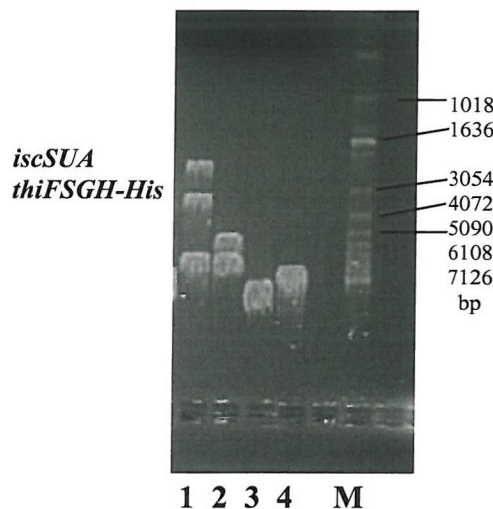


Figure 7.4. Identification of positive clones containing pRL1021 by plasmid DNA isolation and restriction with: *Nco*1 plus *Xho*1 (lane 1, expected fragment sizes: 2.0, 2.9 and 6.7 kbp), *Nco*1 (lane 2, expected fragment sizes: 4.9 and 6.7 kbp), *Xho*1 (lane 3). Isolated plasmid DNA (lane 4). M = molecular weight marker

7.5. Experimental for Chapter 3

7.5.1. *Aerobic Purification of ThiH from pRL400*

pRL400/BL21(DE3) was cultured on a large scale (method 14), induced with IPTG and grown at 28 °C for 5 h before being harvested. The cell paste was weighed and stored at –80 °C until used.

ThiH was isolated at 4 °C using the following buffers: lysis buffer, 50 mM Tris-HCl, pH 8.0, 12.5 % (w/v) glycerol; buffer A, 50 mM Tris-HCl, pH 8.0; buffer B, 50 mM Tris-HCl, pH 8.0, 0.5 M NaCl; buffer C, 50 mM Tris-HCl, pH 8.0, 0.7 M (NH₄)₂SO₄.

Cell paste (~30 g) was re-suspended in lysis buffer (90 ml) containing lysozyme (0.1 mg/ml) and benzonase (10 U/ml), and stirred for ~30 min. Cells were then lysed by sonication (15-20 times 30 sec bursts with 30 sec rest between each burst), in a glass beaker cooled with crushed ice, PEI [5 % (v/v) solution, pH 8.0] added [0.1-0.2 % (v/v) final concentration] and the cell debris was precipitated by centrifugation (JA-14 rotor,

12000 rpm for 30-40 min at 4°C). The cleared lysate was immediately applied to a Q-Sepharose column (300 ml) previously equilibrated with buffer A. The column was washed with the same buffer (2 column volumes), and proteins were eluted at 10 ml/min with an increasing gradient of buffer B from 0 to 100 % over 2 column volumes, followed by 2 column volumes of isocratic elution with 100 % buffer B. The purest fractions, as judged by SDS-PAGE analysis (method 11), were pooled, concentrated by ultrafiltration (30 kDa MWCO) to 7-10 ml and applied to a S-200 (2.6 cm I.D. x 60 cm) column. Proteins were isocratically eluted at 3 ml/min with buffer A. The most concentrated and purest fractions, as judged by Bradford assay (method 12) and SDS-PAGE analysis, were pooled and solid (NH₄)₂SO₄ was slowly added to a final concentration of 0.7 M. This solution was applied to a Source Phe column (30 ml) equilibrated with buffer C, and the column washed with the same buffer (2 column volumes) before eluting the proteins at 5 ml/min with an increasing gradient of buffer A from 0 to 100 % over 2 column volumes, followed by 2 column volumes of isocratic elution with 100 % buffer A. The purity of the fractions was analysed by SDS-PAGE and the purest fractions were pooled and stored at -80 °C. To further purify ThiH, the binding of this protein to various affinity columns (2.5 ml) was assessed using the Reactive Dye-Ligand Test Kit (Sigma), as per manufacturer's instructions. ThiH did most efficiently bind only to the Cibacron Blue 3GA-agarose column and a very similar dye supported on sepharose resin was used for the subsequent purification step. Proteins eluted from the Source Phe column were defrosted, concentrated to 10 ml and applied to a Blue Sepharose CL-6B (Sigma) column (50 ml) previously equilibrated with buffer A. The column was washed with buffer A (2 column volumes) and proteins eluted at 3 ml/min with an increasing gradient of buffer B from 0 to 100 % over 3 column volumes, followed by isocratic elution with 100 % buffer B (2 column volumes). Protein concentration and purity were estimated by Bradford assay and SDS-PAGE analysis; ThiGH eluted in a broad dilute peak, and in the most concentrated fractions protein concentration did not exceed 0.1 mg/ml, yielding 10 mg of highly purified ThiGH (> 90 %).

7.5.2. Anaerobic Purifications of ThiGH-His

The general protocol which follows has been used to isolate ThiGH-His from any of the expression systems described in section 3.2.2.

Cells were grown on a large scale as described in method 14. In particular, after the addition of the appropriate inducer, bacterial cultures were transferred to an incubator set at 28 °C and cultured for a further 5 h before being harvested. In some of the large scale expression experiments with pRL821/BL21(DE3), FeSO₄ (0.4 mM, 22 mg Fe/l) was added to the growth medium at the induction point.

ThiH was anaerobically purified in a glove box at 19°C using the following buffers: buffer A, 50 mM Tris-HCl, pH 8.0, 200 mM NaCl, 50 mM imidazole, 12.5 % (w/v) glycerol; buffer B, 50 mM Tris-HCl, pH 8.0, 500 mM NaCl, 50 mM imidazole, 12.5 % (w/v) glycerol; buffer C, 50 mM Tris-HCl, pH 8.0, 200 mM NaCl, 500 mM imidazole, 12.5 % (w/v) glycerol; buffer D, 50 mM Tris-HCl, pH 8.0, 5 mM DTT, 12.5 % (w/v) glycerol. Buffers, solutions, containers (bottles, jars, tubes, beakers etc.) and equipment required during the purification were degassed overnight inside the glove box. Columns and the HPLC system were placed outside the box but the buffer lines were introduced in a sealed gastight fashion into the box so that the anaerobic buffers could be pumped through the system and used to elute the proteins; the column eluate was fed back into the box to permit anaerobic fraction collection. Protein elution was monitored at 280 and 420 nm.

To the still frozen cell paste (27-30 g), lysozyme (0.1 mg/ml), benzonase (10 U/ml) and PMSF (100 mM stock solution in *i*-PrOH, 1 mM final concentration) were added under aerobic conditions; the cells were then introduced inside the glove box and re-suspended in anaerobic buffer A (90 ml) stirring continuously for ~30 min. The suspension was then withdrawn from the anaerobic box and rapidly lysed, on ice, by sonication (15-20 times 30 second bursts, 30 second rest between each burst). The lysate was returned to the box, allowed to degas (10 min), and after the addition of PEI [0.2 % (v/v)] cleared by centrifugation in gastight centrifuge tubes (JA-14 rotor, 12000 rpm, 30-40 min). The brown supernatant was applied to a Chelating Sepharose column (25 ml) previously charged with NiSO₄ (25 ml, 0.2 M) and equilibrated with anaerobic buffer A (10 column volumes). The column was washed with buffer B (4 column volumes), then buffer A (2 column volumes) and proteins were eluted at 5 ml/min with

an increasing gradient of buffer C from 0 to 50 % over 4 column volumes, collecting 5 ml fractions. High molecular weight impurities were normally eluted within the first 60-65 ml of the gradient, whilst the ThiGH-His complex was eluted in a broad peak between 45 and 200 ml (towards the end of the gradient). To avoid protein precipitation, the most concentrated and brown fractions (typically fractions 15-20), were immediately pooled and applied (up to 30-35 ml) to a S-75 gel filtration column (3 cm I.D. x 15 cm), previously equilibrated with anaerobic buffer D. Proteins were eluted isocratically at 2 ml/min and collected in 10 ml fractions. The most concentrated fractions were pooled, glycerol added to a final concentration of 25 % (w/v) and proteins concentrated by ultrafiltration (30 kDa MWCO) to 5-6 mg/ml, as the ThiGH-His complex precipitates above 7 mg/ml. Proteins were stored at -80 °C in this buffer (buffer E).

Protein samples (50 µl) were removed from the fractions collected during the elution from the nickel-chelating and the gel filtration columns, and subsequently analysed by SDS-PAGE (method 11). Due to the excellent reproducibility of this purification procedure, highly pure ThiGH-His was routinely obtained, in spite of the fact that the purity was not checked prior to pooling and concentrating the fractions. This was judged to be necessary to allow the highly unstable complex to be rapidly exchanged into a buffer in which it was more stable.

For the ESI-MS analysis, protein samples were prepared as follows: purified ThiGH-His (1 mg/ml) was applied to a NAP-10 column equilibrated in 20 mM ammonium formate. Proteins were eluted with 1.5 ml of the same buffer, with protein precipitation occurring almost immediately. The suspension was diluted 2-3 times with H₂O and the precipitate re-dissolved by the addition of formic acid to a final concentration of 10 % (v/v).

7.5.3. Analytical and Preparative Gel Filtration Chromatography Under Anaerobic Conditions

On an analytical scale, purified ThiGH-His samples (250-300 µl, 5-6 mg/ml) were applied to a Superdex 200 HR 10/30 pre-packed column equilibrated with anaerobic buffer D (section 7.5.2) and eluted with the same buffer at 0.5 ml/min.

Protein elution was monitored at 280 and 420 nm, and 1 ml fractions were collected. Fractions were then analysed by SDS-PAGE (method 11). Apparent molecular weights were derived by comparison with a standard chromatogram provided by the manufacturer of the pre-packed column.

To recover sufficient amounts of pure ThiGH-His complex and ThiH monomer for iron and sulphide analyses, a purified sample of ThiGH-His isolated from pRL1000/BL21(DE3) (4 ml), was applied to a S-200 column (I.D. 2.6 x 60 cm), previously equilibrated with buffer D, and eluted with the same buffer at 2 ml/min, collecting 10 ml fractions. Protein elution was monitored at 280 and 420 nm. Eluted proteins were analysed by SDS-PAGE (method 11) and fractions containing ThiGH-His complex and monomeric ThiH-His were separately pooled and concentrated to 3 mg/ml and 1 mg/ml, respectively, in buffer E (**Figure 7.5**).

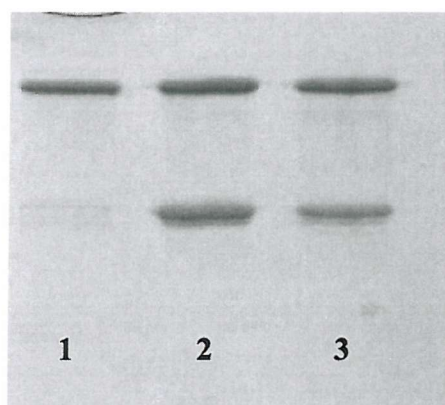


Figure 7.5. Coomassie Blue stained 15 % SDS-PAGE gel of ThiH-His monomer (lane 1) and ThiGH-His complex (lane 2) isolated from a purified sample of ThiGH-His (lane 3) by gel filtration chromatography.

7.5.4. Iron and Sulphide Analyses

Iron and sulphide were analysed by the methods of Fish (147) and Beinert (148), respectively, and were determined in triplicate. The ThiH-His content in the samples was estimated as described in method 12, and the data were expressed as mol of Fe or S /mol of ThiH-His.

For the iron analysis, the following solutions were prepared: reagent A, 0.142 M KMnO₄ in 0.6 N HCl, obtained by mixing equal volumes of 1.2 M HCl and 0.284 M KMnO₄ in H₂O (445 mg in 10 ml), and reagent B, 6.5 mM ferrozine, 13.1 mM neocuproine, 2 M ascorbic acid, 5 M ammonium acetate in H₂O, prepared by first dissolving the ammonium acetate (4.85 g) and ascorbate (4.4 g) in H₂O (12.5 ml) followed by ferrozine and neocuproine (40 mg each). Reagent A was freshly prepared every time, whilst reagent B was stored in the dark for no longer than 3 weeks. Standards were prepared from a stock solution of FeSO₄·7 H₂O (50 mg in 10 ml, 18.0 mM), after a 100 fold dilution (180 µM) with H₂O as indicated in **Table 7.10**.

ThiGH-His samples (300 µl, 5-6 mg/ml in ThiH-His) in buffer E (section 7.5.2) were first digested with trypsin (0.3 mg/ml, 37 °C, overnight) to facilitate the quantitative release of iron, then diluted to 1 ml with water and incubated, together with the standards, for 2 h at 60 °C after the addition of reagent A (500 µl). At the end of the 2 hour incubation, samples were allowed to cool down to room temperature before adding reagent B (100 µl). When the purple colour was completely developed (15-20 min) the A₅₆₂ of the samples was measured. If necessary, protein precipitate was removed by centrifugation before reading the absorbance. The amount of iron present in the ThiGH-His samples was estimated from standard calibration curves constructed in parallel (**Figure 7.6**).

Prior to the sulphide analysis, ThiGH-His samples were anaerobically desalted using a NAP-10 column, equilibrated in DTT-free buffer E, to remove the interference from the DTT present in the storage buffer. The following solutions were freshly prepared every time: 1 % (w/v) zinc acetate dihydrate in H₂O; 3 M NaOH; 0.1 % (w/v) DMPD (*N,N*-dimethyl-*p*-phenylenediamine monochloride) in 5 M HCl; 23 mM FeCl₃ in 1.2 M HCl. Standards were prepared from a stock solution of Na₂S·9 H₂O (10 mg/ml in 0.1 M NaOH, 41.6 mM), after a 2000-fold dilution in 0.1 M NaOH (20 µl in 10 ml, 8.3 µM), as indicated in **Table 7.11**.

A simplified version of the original Beinert method, which did not require the use of a magnetic stirrer and stirring bars in each tube, was adopted. Samples were individually treated. Briefly, zinc acetate (300 µl), immediately followed by the addition of NaOH (15 µl), was added to each protein sample (100 µl, 1.2-2.5 mg/ml in ThiH-His) and standard (100 µl), quickly capped and mixed. Samples were incubated

for 5 h at room temperature, during which a precipitate formed. DMPD (75 μ l) was then carefully pipetted to the bottom of each suspension, which resulted in the dissolution of the precipitate beginning at the bottom of the tube and proceeding upwards. Gentle mixing was stopped when only the top 2 mm of suspended precipitate remained. At this point FeCl_3 (5 μ l) was added, immediately capping the tube and mixing. Samples were incubated overnight at room temperature. Before reading the absorbance at 670, 710 and 750 nm, samples were diluted with H_2O (200 μ l) and protein precipitate removed by centrifugation. The readings at 670 nm, used for the calculation of the sulphide content, should not exceed 0.25. The amount of acid labile sulphide present in the ThiGH-His samples was estimated from the standard calibration curve constructed in parallel (Figure 7.7).

180 μM Fe^{2+} Stock Solution (μl)	H_2O (μl)	nmol of Fe^{2+}
400	600	72
350	650	63
300	700	54
250	750	45
200	800	36
150	850	27
100	900	18
50	950	9
30	970	5
10	990	2
0	1000	0

Table 7.10. Dilution series for iron standards.

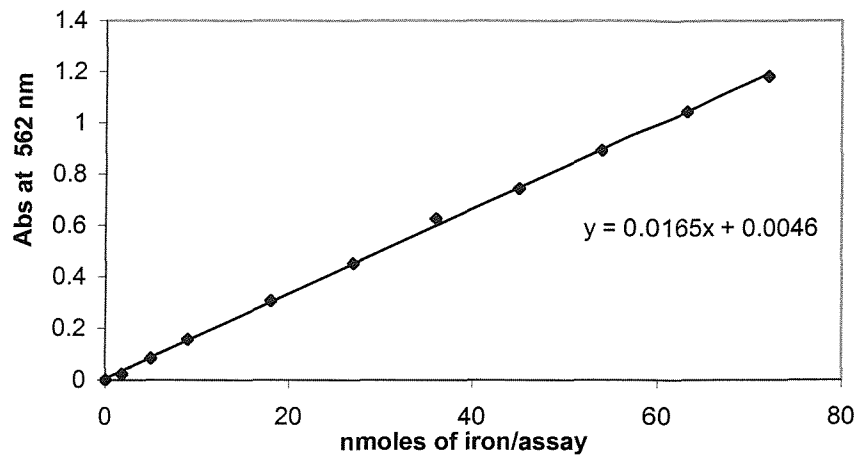


Figure 7.6. Typical iron standard curve. The volume of each assay was 1.6 ml.

8.3 μ M S ²⁻ Stock Solution (μ l)	Buffer (μ l)	nmol of S ²⁻
0	100	0
5	95	0.42
10	90	0.83
15	85	1.2
20	80	1.7
25	75	2.1
30	70	2.5
35	65	2.9
40	60	3.3
45	55	3.7
50	50	4.2

Table 7.11. Dilution series for sulphide standards.

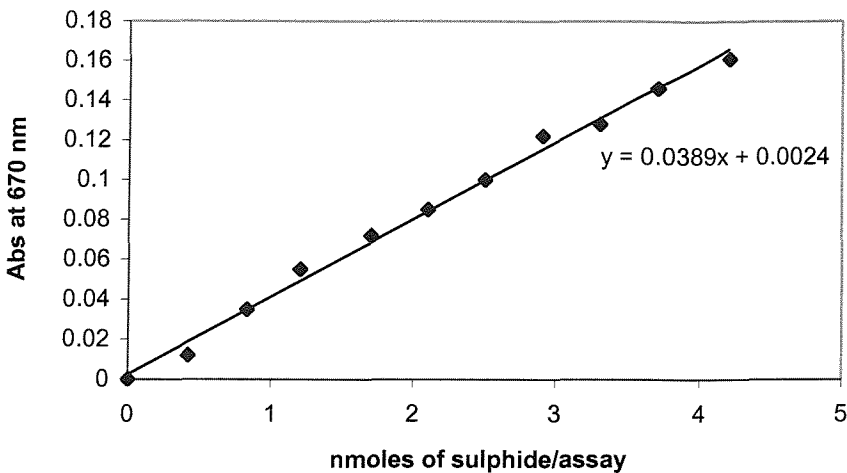


Figure 7.7. Typical sulphide standard curve. The final volume of each assay was 695 μ l.

7.5.5. UV-visible and EPR spectra

To record UV-visible spectra under anaerobic conditions, purified ThiGH-His samples (section 7.5.2) were defrosted inside the glove box, diluted to 3 mg/ml with anaerobic buffer E, and transferred to air-tight cuvettes. UV-visible spectra were recorded outside the glove box, in the range 250-700 nm, against buffer E.

5-deazaflavin was synthesised in our laboratory by M. Guirguis. UV-visible spectra of a ThiGH-His sample (600 μ l, 6 mg/ml) isolated from pRL1020/BL21(DE3) were recorded before and immediately after the addition of DAF (10 μ l of a 2 mM solution in 1:1 EtOH:H₂O mixture, 33 μ M final concentration). The capped cuvette was then placed 28 cm apart from a light projector (Plus U2-1080, P-VIP 120 W lamp) and irradiated outside the box. After 45 min irradiation, the brown colour of the ThiGH-His sample was observed to have faded and another UV-visible spectrum was recorded; then the cuvette was uncapped, exposed to air for about 10 min, mixed and returned to the anaerobic box where it was allowed to stand 30 min before recording a UV-visible spectrum.

EPR spectra were recorded at X-band on a Bruker ELEXYS 500 spectrometer with an ER094X microwave bridge using an ER4122SHQ cavity. To record EPR spectra of as isolated ThiGH-His, a protein sample (1 ml, 5-6 mg/ml in buffer E) was

defrosted inside the glove box, transferred to an EPR tube and frozen in liquid nitrogen; EPR spectra of reduced ThiGH-His were obtained after incubation with dithionite (1 mM, 30 min).

7.5.6. In Vivo Activity of the ThiH-His Expressed from pRL1020/BL21(DE3)

pBAD/HisA and pRL1020 were transformed into *E. coli* KG33 (method 4). Both transformants were grown in parallel in 2YT medium (10 ml) containing ampicillin (100 µg/ml). When the OD₆₀₀ reached ~ 1.3, cells were harvested (JA-14 rotor with inserts to fit 15 ml Falcon tubes, 7500 rpm, 10 min, 4°C) and washed with DM medium (2 x 5 ml, Appendix B) containing arabinose (0.2 %) and ampicillin. Pellets were re-suspended in the same medium to give an OD₆₀₀ of 0.790 and 5 serial 10-fold dilutions were prepared for both samples. Equal volumes (5 µl) were plated on DM solid medium containing, ampicillin (100 µg/ml), D-glucose (0.2 %), β-L-arabinose (0.2 %), Tyr and Cys (0.2 mM each) and Hmp (50 µM). Colonies were allowed to grow at 37 °C for 36 h.

7.5.7. Chemical and Enzymatic Reconstitution Experiments

Reconstitution experiments were almost exclusively conducted on ThiGH-His isolated from pRL800/BL21(DE3) (section 7.4.5). These samples were reconstituted in buffers (D or E) already containing 5 mM DTT. However, freshly prepared DTT was routinely added to a final and overall concentration of 10 mM prior to the addition of other components. The ThiGH-His complex (500 µl, 60-130 µM in ThiH-His) was chemically reconstituted by incubation (2-3 h), under anaerobic conditions, with a 5-fold excess of FeCl₃ and Na₂S, added in this order, followed by 30 min incubation with EDTA (2 mM). EDTA-treated samples were then applied to a NAP-10 column equilibrated in buffer D and eluted with 1.5 ml of the same buffer. Reconstituted ThiGH-His samples were analysed for the iron content (section 7.5.4) and by UV-visible spectroscopy (section 7.5.5).

ThiGH-His samples (2-3 ml, 130 µM in ThiH-His) were enzymatically reconstituted by overnight incubation, under anaerobic conditions, with either the

components listed in **Table 7.12** or with just IscS, FeCl₃, and Cys (same concentrations as in **Table 7.12**). IscSUA, HscAB and Fdx were purified by Dr. T. Ziegert (157) in our laboratory.

Component	Final concentration (mM)
HscA	0.61*10 ⁻³
HscB	0.039
IscU	0.012
IscS	1.6*10 ⁻³
Fdx	0.006
DTT	10
ATP	2
Cysteine	4
Fe ³⁺	0.650

Table 7.12. Enzymes and other components used to reconstitute the Fe-S centre of ThiGH-His samples isolate from pRL800/BL21(DE3).

After 30 min incubation with EDTA (2 mM), ThiGH-His (2.5 ml) was applied to a PD-10 column equilibrated in DTT-free buffer D and eluted with the same buffer. The eluate (3.5 ml) was then applied to a nickel-charged Chelating Sepharose column (6 ml) equilibrated in buffer A (section 7.5.2). The column was washed with buffer A (3 column volumes) and proteins were eluted at 1 ml/min with an increasing gradient of buffer C from 0 to 50 % over 1 column volume, followed by isocratic elution with 100 % buffer C (1 column volume). Protein concentration was estimated by the method of Bradford (method 12) and the most concentrated fractions were individually gel filtered onto PD-10 columns equilibrated in buffer D, to remove the imidazole. Eluted fractions were pooled, concentrated to 3 mg/ml by ultrafiltration in buffer E and immediately analysed for the iron content and by UV-visible spectroscopy or stored at -80 °C until analysed.

7.6. Experimental for Chapter 4

7.6.1. Expression of *ThiI*

thiI (1.5 kbp) was amplified by PCR using ThiI1 and ThiI2 as forward and reverse primers, respectively. The PCR product was ligated into pBAD-TOPO and subsequently subcloned on a *NcoI/BamH1* fragment into pET-24d(+). The resultant plasmids were named pRL500 (Figure 7.8) and pRL600, respectively. pRL600 was transformed into BL21(DE3) (method 4). An overnight culture of pRL600/BL21(DE3) was used as 1 % inoculum for a small scale expression experiment (method 13) using duplicate cultures. Cells were induced with IPTG and grown at 37°C for 4h before being harvested and lysed. Cleared lysates and pellets were analysed by SDS-PAGE.

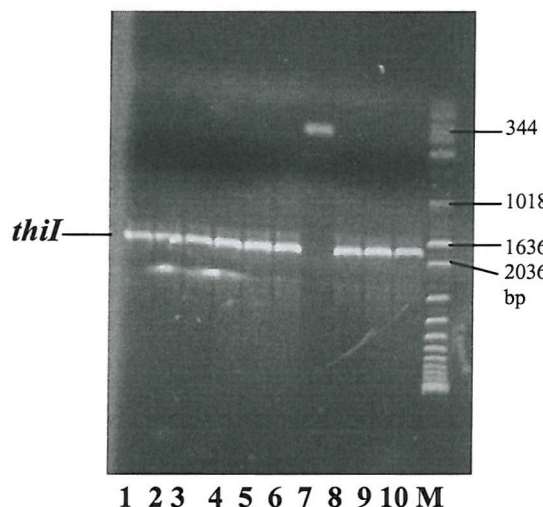


Figure 7.8. PCR screening to identify colonies containing pRL500. Numbers correspond to the colony labels. Apart from colony 7 [the PCR product (0.3 kbp) visible in lane 7 corresponds to the region of the vector amplified between the primers], the remaining 9 colonies contained the insert (expected gene size: 1.5 + 0.3 kbp). M = molecular weight marker.

7.6.2. Expression of *ThiE*

thiE (660 bp) was amplified by PCR using thiE FORWARD and ThiE-His Rev as primers. The A-tailed PCR product (**Figure 7.9 A**) was ligated into pBAD-TOPO, resulting in pRL1900, and subsequently subcloned on a *Nco*1/*Xho*1 fragment into pBAD/HisA, pBAD/His repair and pET-24d(+), resulting in pRL2000 and pRL2020 and pRL2030, respectively. Sequencing of pRL2000 (Eurogentec, Southampton) revealed the existence of a stop codon, left in the sequence of ThiE-His Rev (**Table 7.9**), upstream the (CAC)₆ sequence encoding the hexahistidine tag. This mistake prevented the expression of ThiE as a hexahistidine-tagged protein.

pRL2000 and pRL2020 were transformed into BL21(DE3); pRL2030 was transformed into both BL21(DE3) and C43(DE3). ThiE expression was first investigated from pRL2000/BL21(DE3) (method 13). These cells were grown at 37 °C, induced when the OD₆₀₀ reached ~0.6 and incubated for a further 4 h before being harvested by centrifugation. The cell pellet was then re-suspended in lysis buffer and lysed by sonication. Soluble and insoluble protein fractions were analysed by SDS-PAGE (method 11). The same experiment was repeated with pRL2020/BL21(DE3) (2 x 10 ml cultures) grown and induced in parallel with pBAD/HisA/BL21(DE3) (1 x 10 ml culture). After the induction, one of the pRL2020/BL21(DE3) cultures and pBAD/HisA/BL21(DE3) were grown at 37 °C for 3.5 h before being harvested, whilst the second pRL2020/BL21(DE3) culture was grown at the same temperature overnight. SDS-PAGE analysis revealed no difference between cleared lysate and pellet from pBAD/HisA/BL21(DE3) and the correspondent fractions from both cultures of pRL2020/BL21(DE3). The expression experiment was repeated for the third time with pRL2030/BL21(DE3) and pRL2030/C43(DE3). These cultures were induced and grown at 37 °C for 4 h. Then cells were harvested and lysed by sonication. SDS-PAGE analysis of cleared lysates and pellets revealed the presence of ThiE in the insoluble fractions from both strains.

7.6.3. Expression of *ThiD*

thiD-F and ThiD-His-R were used as primers to amplify *thiD-His* (830 bp) (**Figure 7.9 B**). The PCR product was ligated into pBAD-TOPO (method 4) and then

subcloned on a *Nco*1/*Xho*1 fragment into pBAD-His A and pET-24d(+). The resultant plasmids were named pRL2100, pRL2200 and pRL2220, respectively. pRL2200 and pRL2220 were transformed into BL21(DE3). pRL2200/BL21(DE3) was grown on a small scale (method 13), induced, and cultured for a further 6 h at 37 °C before being harvested. Protein expression in the soluble and insoluble fractions was then analysed by SDS-PAGE. The soluble expression level of ThiD from pRL2220/BL21(DE3) was instead investigated on a medium scale experiment. An overnight culture (10 ml) of pRL2220/BL21(DE3) was used as a 1 % inoculum in 2YT medium (100 ml). When the OD₆₀₀ reached approximately 0.6, cells were induced with IPTG, and cultured for a further 4 h before being harvested (JA-14, 12000 rpm, 10 min, 4 °C). The cell pellet was then transferred to a 1.5 ml eppendorf tube, re-suspended in lysis buffer (1 ml, method 13) and lysed by sonication as described in method 13. The cleared lysate (700 µl, ~8 mg/ml) was applied to a nickel spin column and proteins were eluted as described in method 15. Cleared lysate, pellet and fractions eluted from the spin column were analysed by SDS-PAGE. As the gel showed that ThiD did not bind to the column, pRL2200 was sequenced (Eurogentec, Southampton), and the sequencing analysis revealed a mutation of the fourth histidine of the (His)₆ tag into a proline.

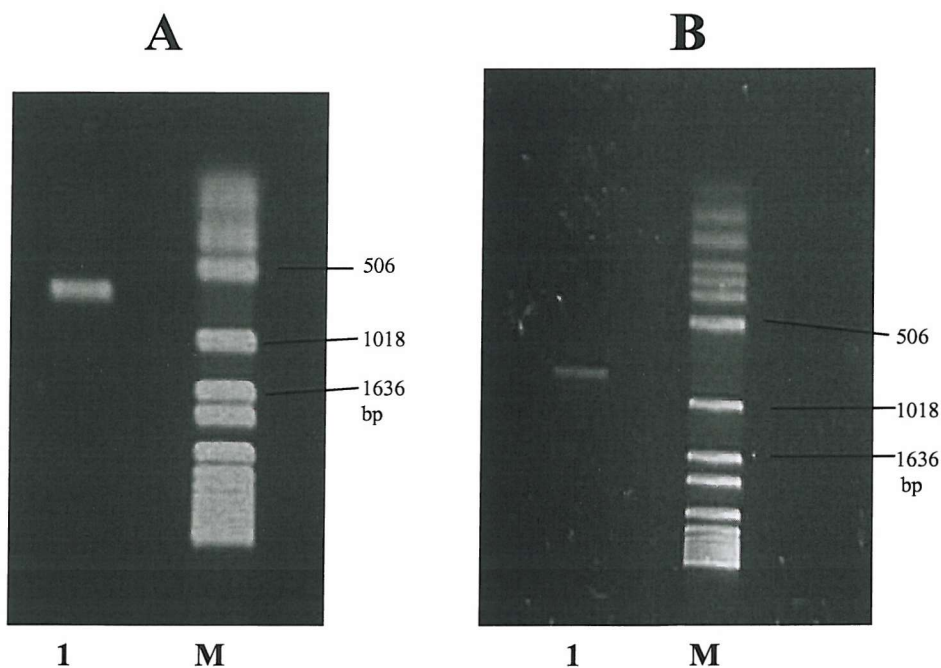


Figure 7.9. Purified *thiE* (660 bp, lane 1, A) and *thiD-His* (830 bp, lane 1, B). M = molecular weight marker.

7.6.4. Expression and Purification of ThiFS from pRL1800/BL21(DE3)

pRL1000 was isolated from pRL1000/XL1-Blue (method 6) and restricted on a preparative scale (method 7) with *Sal*1. The plasmid was cut in two positions producing two fragments of 1.8 and 6.3 kbp. The largest fragment, containing *thiFS*, was isolated (method 8) and its sticky ends joined by ligation (conditions described in method 9 without the insert). The resultant plasmid was named pRL1800 and was transformed into BL21(DE3). To find out whether the temperature could affect the solubility of ThiFS, 2 x 10 ml of 2YT medium were inoculated with pRL1800/BL21(DE3) (method 13); cells were grown, induced with IPTG, then one of the cultures was incubated overnight at 27 °C whilst the other was incubate at 37 °C. Cells were harvested, lysed and cleared lysates and pellets analysed by SDS-PAGE (method 11).

ThiFS was routinely expressed on a large scale (method 14) at 27 °C overnight, yielding 35-45 g of cell paste. The two proteins were purified at 4 °C as described by Taylor *et al.* (71), with only slight variations. The following buffers were used: buffer A, 50 mM Tris-HCl, pH 8.0, 2 mM EDTA, 2 mM DTT; buffer B, buffer A containing 1 M NaCl; buffer C, 50 mM Tris-HCl, pH 8.0, 2 mM DTT, 12.5 % (w/v) glycerol.

pRL1800/BL21 cell paste (35 g) was re-suspended in buffer A (100 ml) containing lysozyme (0.1 mg/ml), benzonase (5 U/ml) and PMSF (1 mM) stirring continuously for 30-40 min, then lysed by sonication (20 bursts of 30 sec with 30 second rest) cooled on ice. The cell debris was removed by centrifugation (JA-14, 12000 rpm, 30 min at 4 °C) and the cleared lysate (104 ml) adjusted to 20 % saturation with solid (NH₄)₂SO₄ (12 g), slowly added over 45 min at 4 °C. The cloudy suspension was centrifuged (JA-14, 12000 rpm, 10 min at 4 °C) and the pellet discarded. The supernatant was adjusted to 50 % of saturation of (NH₄)₂SO₄ (19.7 g) over 45 min at 4 °C and the precipitate recovered by centrifugation (JA-14, 12000 rpm, 10 min at 4 °C). The pellet was re-dissolved in 35 ml of buffer A and dialysed against the same buffer (6 l) overnight at 4 °C. The dialysed protein fraction (45 ml, 7.5 mg/ml, as estimated by Bradford assay) was diluted with buffer A to 110 ml and applied to the Q-Sepharose column (190 ml). The column was washed with buffer A (2 column volumes) before eluting the proteins at 5 ml/min with an increasing concentration of buffer B from 0 to 100 % over 6 column volumes, collecting 15 ml fractions. The protein concentration in the fractions was estimated by the Bradford assay (method 12) and the most

concentrated fractions were analysed by SDS-PAGE on 18 % gels. ThiS was eluted with ~230 mM NaCl and ThiF with ~ 330 mM NaCl.

The ThiS containing fractions (30 ml) were pooled, concentrated to 10 ml by ultrafiltration (3 kDa MWCO) and applied to a S-75 column (744 ml, 3.4 I.D. x 82 cm) equilibrated in buffer C (3 column volumes). Proteins were eluted at 3 ml/min discarding the first 250 ml before collecting 12 ml fractions. The most concentrated fractions were analysed on an 18 % SDS-PAGE gel and ThiS identified in fractions 18-20, with a purity of ~ 80-90 %. These fractions were pooled and concentrated by ultrafiltration to 10 mg/ml. To analyse the protein by ESI-MS, ThiS (2 mg/ml) was applied to a NAP-10 column equilibrated in H₂O and eluted at a final concentration of 0.8 mg/ml. The protein was diluted 100 times and to this solution (500 µl) CH₃CN (200 µl) and HCOOH 1 % (v/v) were added.

The ThiF containing fractions (45 ml) were pooled, concentrated to 10 ml by ultrafiltration (10 kDa MWCO) and applied to the same S-75 column that had been used to purify ThiS, equilibrated in buffer C (1 l). Proteins were eluted at 3 ml/min with buffer C, collecting 12 ml fractions (after having discarded the first 225 ml). The protein concentration was estimated by the Bradford assay and the most concentrated fractions were analysed on an 18 % SDS-PAGE gel. ThiF was present in all the fractions but only fractions 1 and 2 appeared relatively pure. ThiF was purified in the same way from other 42 g of cells, and fractions 1 and 2 from the two purifications were pooled (20 mg, overall) and concentrated to 3 mg/ml by ultrafiltration. ThiF was characterised by ESI-MS after desalting onto a NAP-10 column equilibrated with H₂O; the protein concentration in the sample [400 µl H₂O + 200 µl CH₃CN, HCOOH 1 % (v/v)] was 0.2 mg/ml.

7.6.5. Expression and Purification of Dxs-His

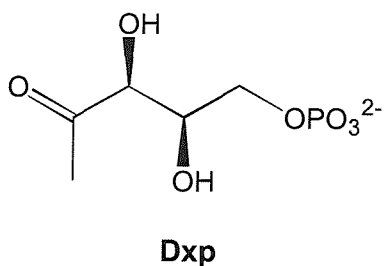
BL21(DE3) cells transformed with a pET-23b-derived plasmid encoding Dxs-His were received as liquid culture. These cells (10 µl) were plated on selective 2YT solid medium containing ampicillin and incubated at 37 °C overnight. A single colony was then used to inoculate 2YT medium (10 ml), and cells were grown at 37 °C (method 13), induced with IPTG and harvested after 5 h at 22°C. The cell pellet was re-

suspended in lysis buffer, lysed and cleared lysate and pellet were analysed by SDS-PAGE on a 15 % gel (method 11). After having ascertained the size and therefore the integrity of the protein, the culture was used to prepare glycerol freezes of the Dxs-His producing strain (method 10). These freezes were subsequently used for a large scale growth (method 14) experiment which yielded 19 g of biomass.

Dxs-His was aerobically purified at 4°C using the following buffers: buffer A, 50 mM Tris-HCl, pH 8.0, 0.5 M NaCl, 2.5 mM TPP; buffer B, 50 mM Tris-HCl, pH 8.0, 0.5 M NaCl, 0.5 M imidazole.

Cell paste (19 g) was re-suspended in buffer A (80 ml) containing lysozyme (0.1 mg/ml) and benzonase (10 U/ml), stirring continuously for ~30 min. Cells were then lysed by sonication (15-20 times 30 sec bursts with 30 sec rest between each burst), in a glass beaker cooled with crushed ice, PEI was added [0.1-0.2 % (v/v)] and the cell debris precipitated by centrifugation (JA-14 rotor, 12000 rpm for 30-40 min at 4°C). The cleared lysate was applied to a Chelating Sepharose column (40 ml) previously charged with NiSO₄ (40 ml, 0.2 M), and the column was washed with buffer A (4 column volumes). Proteins were eluted at 5 ml/min with an increasing gradient of buffer B from 0 to 50 % over 2 column volumes, followed by isocratic elution with 50 % buffer B (2 column volumes). Fractions (10 ml) were collected and the protein concentration estimated by Bradford assay (method 12). Meanwhile proteins had begun to precipitate in fractions 4 and 5 (**Figure 4.13**, Chapter 4), so without running a SDS-PAGE gel to check the purity, fractions 7-12 were pooled (60 ml, 3-6 mg/ml) and diluted to 80 ml with Tris-HCl 50 mM, pH 8.0 to decrease the NaCl and imidazole concentration. This volume was reduced to 35 ml (7 mg/ml) by ultrafiltration (30 kDa MWCO) and applied to a S-75 gel filtration column (3 cm I.D. x 15 cm) previously equilibrated with Tris-HCl 50 mM, pH 8.0. Proteins were eluted at 2 ml/min with the same buffer. The purest fractions, as judged by SDS-PAGE analysis, were pooled, concentrated to 12 mg/ml by ultrafiltration and stored at -80 °C.

7.6.6. Enzymatic Synthesis of 1-deoxy-D-xylulose-5-phosphate (Dxp)



Aldolase and triose phosphate isomerase were purchased as ammonium sulphate suspensions and desalted prior to use. In particular, the aldolase suspension (0.7 ml, 21 mg/ml, 14 U/mg) was divided into two 350 μ l aliquots and the volume of each aliquot adjusted to 950 μ l with reaction buffer: 50 mM Tris-HCl, pH 8.0, 1 mM DTT, 0.5 mM TPP, 5 mM MgCl₂. The protein dissolved rapidly and the combined solutions were applied at 4°C to a PD-10 column previously equilibrated with the same buffer. Aldolase was eluted in 3 ml (13 mg overall), aliquoted and stored at -80 °C. The TPI suspension (0.6 ml, 10 mg/ml, 9500 U/mg) received similar treatment, but it re-dissolved with gentle agitation over 30 min. TPI was eluted from the PD-10 column in 3 ml (4.6 mg overall), aliquoted and stored at -80°C.

1-deoxy-D-xylulose-5-phosphate was enzymatically synthesized as described by Taylor *et al.* (158). Briefly, fructose 1,6-diphosphate (13) (340 mg, 0.8 mmol) and sodium pyruvate (2) (231 mg, 2 mmol) were transferred to a dark vessel (a 50 ml Falcon tube wrapped in foil) and dissolved in reaction buffer (36 ml), before adding Dxs-His (0.5 ml, 6 mg), aldolase (40 U) and TPI (200 U) in a total volume of 4 ml. The reaction mixture was incubated overnight at 37 °C in an orbital shaker (100 rpm), and the progress of the reaction monitored by thin layer chromatography (159) using aluminium backed silica plates developed in isopropanol/ethyl acetate/water (6:1:3). The plates were dried, stained with *p*-anisaldehyde: sulphuric acid and heated to 100°C, revealing the product as a blue spot (R_f = 0.65, **Figure 7.10**). When the reaction was judged to be complete, the proteins were removed by ultrafiltration (10 kDa MWCO), and the filtrate was freeze-dried yielding 450 mg of residue mainly consisting of product with TrisH⁺ as the counter ion (1.3 mmol, 81 % yield). The solid was re-dissolved in H₂O (40 ml) and divided into 1.2 ml aliquots stored at -80 °C. Dxp was

purified by semi-preparative HPLC (Perkin Elmer Prep-10 Octyl column, 250 x 10.0 mm) injecting 400 μ l (~ 6 mg of crude) of mixture and eluting with H₂O at 2 ml/min. The elution was monitored at 220 nm and 0.5 ml fractions were collected from t = 6.0 min to t = 8.0 min. The purity of the fractions was checked by TLC, loading not less than 18 μ l per sample and developing in isopropanol/ethyl acetate/water (6:1:3). TLC plates were dried and analysed under the UV lamp or the Gene Genius Bio imaging system to locate the thiamin pyrophosphate, then sprayed with *p*-anisaldehyde/H₂SO₄ and heated at 100 °C to reveal the Dxp. Thiamin pyrophosphate-free fractions were pooled and freeze dried. The resultant white solid was then weighed and dissolved in 1 ml of D₂O containing *tert*-butyl alcohol as internal standard (8 μ l, 85.3 μ mol) to estimate the Dxp concentration by NMR by integration of the signals at 2.2 and 1.1 ppm. The D₂O was then removed by freeze-drying and the solid dissolved in 50 mM Tris-HCl, pH 8.0, 5 mM MgCl₂ to yield a 50 mM stock solution. The absence of contaminating TPP was confirmed with the thiochrome assay (method 16).

Subsequent freeze-drying steps from acidic or neutral Dxp solutions often produced a yellow solid; the addition of 200-400 μ l of 50 mM Tris-HCl, pH 8.0, 5 mM MgCl₂ prior to the freeze-drying helped preventing the formation of this impurity. Dxp was analysed by ¹H and ¹³C NMR and by ESI-MS. The spectroscopic data were consistent with those already published (159,191).

δ _H (300 MHz, D₂O) 4.4 (1H, d, *J* = 1.5 Hz), 4.2 (1H, dt, *J* = 6.6, 1.5 Hz), 3.7 (2H, t, *J* = 6.6 Hz), 2.2 (3H, s).

δ _C (75.5 MHz, D₂O) 215.8 (C), 79.6 (C), 73.4 (C), 66.8 (C), 28.5 (C).

m/z (%) (ESI-MS) 213 ((M-H)⁺, 100), 175 (28).

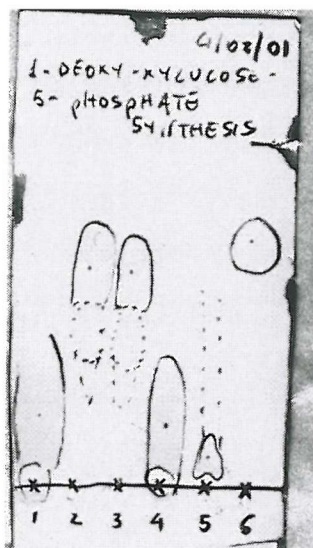
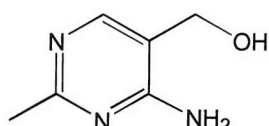


Figure 7.10. Dxp reaction mixture monitored by thin layer chromatography (TLC). The TLC plate was developed in isopropanol:ethyl acetate:water (6:1:3), then dried, stained with *p*-anisaldehyde:sulphuric acid and heated to 100°C. Lane 1: reaction mixture $t = 0$; lane 2: reaction mixture, $t = 15$ h, 25 °C; lane 3: reaction mixture, $t = 15$ h, 37 °C; lane 4: fructose-1,6-diphosphate; lane 5: glyceraldehyde 3-phosphate; lane 6: sodium pyruvate.

7.6.7. *Synthesis of 4-amino-5-hydroxymethyl-2-methylpyrimidine (Hmp)*



Hmp

NaNO_2 (224 mg, 3.2 mmol) was dissolved in H_2O (1.2 ml) and this solution was added dropwise to a stirred solution of compound **15** (400 mg, 2.8 mmol, **Scheme 4.5**, Chapter 4) in HCl (0.48 M, 12 ml, 5.6 mmol). This mixture was stirred at 62°C and the reaction monitored by TLC using silica plates developed with CHCl_3 : MeOH (6:4). The starting material **15** and the major UV visible product showed $R_f = 0.24$ and $R_f = 0.54$, respectively. After 1 h the reaction was judged to have reached the end point (> 70 %) (**Figure 7.11**) and NaOH (1 M) was added to the bright yellow suspension until

the pH became alkaline ($\text{pH} > 7$). The suspension was filtered and the solvent of the filtrate removed *in vacuo*.

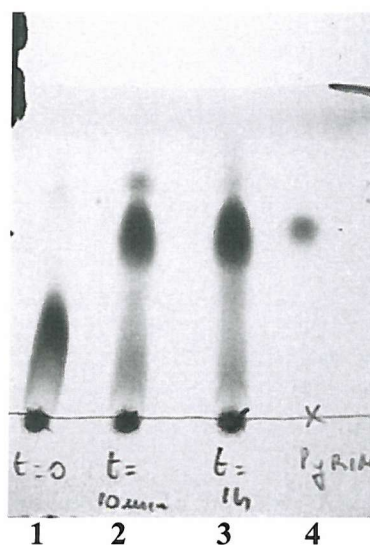


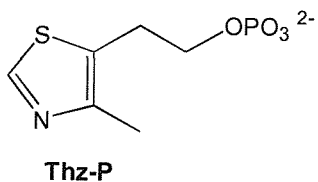
Figure 7.11. Hmp synthesis monitored by thin layer chromatography. The TLC plate was developed in CHCl_3 : MeOH (6:4) and analysed under a UV lamp. Lane 1: reaction mixture $t = 0$; lane 2: reaction mixture $t = 10 \text{ min}$; lane 3: reaction mixture $t = 1 \text{ h}$; lane 4: pure Hmp used as standard.

The yellow solid was re-suspended in MeOH (2-3 ml) to dissolve the product. The supernatant was decanted, leaving behind solid NaCl , and the MeOH removed *in vacuo*. The yellow solid was re-suspended in CHCl_3 : MeOH (90:10) and pure MeOH added, dropwise, until the organic compounds dissolved, separating from solid NaCl ; the supernatant was decanted and purified by silica chromatography (CHCl_3 : MeOH , 90:10) to yield a white solid (238 mg, 60 % yield).

δ_{H} (300 MHz, D_2O) 7.8 (1H, s); 4.4 (2H, s); 2.2 (3H, s).

m/z (%) (ESI-MS) 140 ($(\text{M}+\text{H})^+$, 100), 141 (10).

7.6.8. Synthesis of 4-methyl-5-(β -hydroxyethyl)thiazole phosphate (Thz-P)



Thiamine monophosphate (0.9 g, 2 mmol) was dissolved in water (5 ml) and the pH adjusted to 4.8 adding NaOH (5 M, 2-3 drops). To this solution potassium metabisulphite (2 g, 9 mmol) was added and dissolved by stirring. After 3 h at room temperature a copious amount of white precipitate had formed. The product formation was monitored by thin layer chromatography using silica plates developed with isopropanol:ethyl acetate:water (6:1:3) and the reaction was judged to be > 70 % complete after 36 h. The precipitate was removed by filtration, washed with 0.5 ml of ice-cold water and discarded. The TLC analysis of the filtrate showed a single spot corresponding to the product (R_f = 0.55) and to this filtrate, hydrogen peroxide was added [30 % (v/v), 1 ml] in 250 μ l aliquots allowing 10-15 min between each addition. The solution was then concentrated *in vacuo* to a final volume of ~2 ml and white regular crystals were observed to form. Further precipitation was achieved by storage at 4°C (30 min). The supernatant was then decanted and the white crystalline precipitate re-dissolved in water (25 ml) and freeze-dried to yield a white solid (385 mg, 90 % yield).

δ_H (300 MHz, D₂O) 9.6 (1H, s), 4.0 (2H, q, J = 5.9 Hz), 3.1 (2H, t, J = 5.9 Hz), 2.4 (3H, s).

δ_C (75.5 MHz, D₂O) 157.0 (C), 66.9 (C), 29.4 (C), 13.8 (C).

m/z (%) (ESI-MS) 222 ((M-H)⁻, 100), 212 (30), 129 (70).

7.7. Experimental for Chapter 5

7.7.1. *Effect of the Adenosine Treatment on the Production of TPP by E. coli*

83-1

The following media were used to grow or re-suspend *E. coli* 83-1: DM medium, Davis-Mingioli medium (178) (Appendix B) without glucose; DM1 medium, DM medium supplemented with glucose [0.2 %, (w/v)], Tyr and Phe (0.2 mM each), Trp (0.1 mM), 4-hydroxybenzoic acid, 2,3-dihydroxybenzoic acid and 4-aminobenzoic acid (10 μ M each) (30). Combinations of Tyr (0.2 mM), Hmp (14 μ M) and Thz-P (14 μ M) were added to the DM medium where stated. Stock solutions of the above supplements were prepared as follows: glucose, 20 % (w/v) in H₂O; Tyr, 200 mM in 0.5 M HCl; a mixture of Phe (200 mM) and Trp (100 mM) in 250 mM HCl; a mixture of 4-hydroxybenzoic acid, 2,3-dihydroxybenzoic acid and 4-aminobenzoic acid, 10 mM each in H₂O; Hmp, 2 mg/ml (14 mM) in H₂O; Thz-P, 10 mM in 50 mM Tris-HCl. Amino acid suspensions were heated at low power in a Compact microwave (Sharp) for 10-20 sec and mixed until dissolved.

Prior to use, all solutions were filter sterilised or autoclaved (glucose solution). Experiments were carried out in duplicate to estimate the error associated with the procedure; therefore, due to the large number of samples, data relative to the adenosine de-repression phase and to the thiamine production by de-repressed cells had to be obtained from two separate experiments.

Part 1: time course of the adenosine de-repression. *E. coli* 83-1 was de-repressed in DM1 medium containing adenosine (300 μ g/ml), essentially as described by Estramareix (30). The TPP content was determined in duplicate and expressed as ng of TPP/mg of wet cells. To be able to use the 'wet weight' of the cell pellets in the calculations, the published procedure was slightly modified. Single colonies were used to inoculate DM1 medium (10 ml) and the cells grown for 8-10 hours; the resultant culture was used as a 0.3 % inoculum into fresh DM1 medium (300 ml) and grown overnight at 37 °C. Cells were harvested by centrifugation (JA-14, 12000 rpm, 10 min at 4°C), re-suspended in DM medium (10 ml), transferred to pre-weighed tubes (15 ml) and centrifuged (JA-14 with adaptors, 7000 rpm, 10 min at 4°C). After having drained most of the medium, residual liquid was removed by gently wiping the walls of each

tube with a clean tissue. Tubes were then re-weighed and the 'wet weight' obtained by subtraction. The weighed cell pellets (~ 500 mg) were re-suspended in DM medium to yield 24 mg/ml suspensions, pooled and used as inoculum (1.3 ml) in DM1 medium (100 ml/flask, 12 flasks) to which solid adenosine had been previously added and dissolved (37 °C, 250 rpm for 10 min before the inoculation). Cultures were incubated in an orbital shaker at 37 °C, 200 rpm. A pair of flasks were withdrawn at t = 0 and every 30 min for exactly 2.5 h, rapidly cooled in icy water and the cells harvested by centrifugation. The cell pellets were then re-suspended and washed with sterile 0.9 % NaCl (2 X 10 ml), and the wet weight determined as described above. Cell pellets (27-180 mg) were stored at -80 °C until analysed as described in method 16 A.

Part 2: time course of the thiamine production by de-repressed 83-1 cells.
Cultures of *E. coli* 83-1 (100 ml/flask, 14 flasks) were incubated with adenosine as described above, and samples (2 per time point) withdrawn at t = 0, 1.0 and 2.5 h, to monitor the de-repression phase. At the end of this phase, the cultures were quickly cooled in icy water, and the cells harvested by centrifugation (JA-14, 12000 rpm, 10 min at 4°C). The cell pellets were then washed with sterile 0.9 % NaCl (2 X 10 ml) and transferred to pre-weighed tubes to be weighed. The pellets (700-800 mg) were re-suspended in DM medium to yield 30 mg/ml suspensions, pooled and used as a 10 % inoculum into DM medium (10 ml in 50 ml tubes) containing Hmp and either Tyr or Thz-P, or no supplement. The 10 ml cultures were shaken at 37 °C and the cells harvested every 30 min for 2 h by centrifugation in (pre-weighed) 15 ml tubes. The cell pellets were washed with NaCl solution, weighed and stored at -80 °C until analysed. The TPP content was estimated as described in method 16 A.

7.7.2. Comparison between Adenosine Treated 83-1 and pRL1020/83-1 Cells in the Presence of β-L-arabinose

DM and DM1 media were supplemented with ampicillin (100 µg/ml) in all the experiments with pRL1020/83-1. Experiments were not carried out in duplicate.

pRL1020 was transformed into *E. coli* 83-1 (method 4). pRL1020/83-1 cultures to be de-repressed (100 ml/flask, 14 flasks) were prepared as described in the previous section, but in addition to adenosine (300 µg/ml) also β-L-arabinose [0.2 % (w/v)] was

added. Cultures were incubated at 37 °C and flasks withdrawn every 30 min for 2.5 h. At the end of the de-repression phase, the remaining cultures were harvested by centrifugation, and washed cell suspensions prepared in DM medium (10 ml in 50 ml tubes) containing Hmp (14 µM) and either Tyr (0.2 mM) or Thz-P (14 µM), or no supplement. The 10 ml cultures were incubated at 37 °C and cells harvested every 30 min for 2 h by centrifugation as already described. The thiamine content was estimated by the thiochrome method (method 16 A).

The experiment was repeated with 83-1 cells under identical conditions (except for the ampicillin).

7.7.3. *De-repression Experiments on *E. coli* KG33 Cells*

pBAD/HisA was transformed into *E. coli* KG33 (method 4). An overnight culture of pBAD/HisA/KG33 in Davis-Mingioli medium supplemented with 3 mg/l TPP, was prepared by inoculating 10 ml of this medium with a single colony and incubating for 8-10 h; this culture (10 ml) was then used to inoculate fresh medium (1 l), and cells grown overnight. An overnight culture in 2YT was directly prepared by inoculating the medium (200 ml) with a single colony. Cells from overnight cultures were harvested (JA-14, 12000 rpm, 10 min, 4°C) and re-suspended in DM medium (10 ml, section 7.7.1), then transferred to pre-weighed 15 ml tubes, centrifuged (JA-14 with adaptors, 7000 rpm, 10 min at 4°C), washed (3 x 10 ml) with DM medium and weighed as described in section 7.7.1. The cell pellets (300-800 mg) were re-suspended in DM medium to yield 80 mg/ml suspensions and used (5 ml) to inoculate 2 x 1 l of Davis-Mingioli medium. Cells were incubated at 37 °C and cellular growth monitored by measuring the OD₆₀₀ at t = 0 and every 90 min for 12 h. Samples (100 ml) were withdrawn from the 2 independent cultures at the same time points. Cells were cooled down, harvested, washed and weighed as previously described (section 7.7.1), and the thiamine content estimated by the thiochrome assay (method 16 A).

To obtain enough cells for an *in vitro* complementation experiment, a 2 l overnight culture in TPP-supplemented Davis-Mingioli medium was prepared as described above. Cell were harvested, weighed (2.5 g) and re-suspended in DM medium to yield 160 mg/ml suspensions, which were pooled and used to inoculate (2.5 ml) 4 x 1 l of Davis-Mingioli medium. Cells were incubated at 37 °C and cellular

growth monitored by measuring the OD₆₀₀ at t = 0 and every 2 h for 10 h. Samples (100 ml) were withdrawn at t = 0, 2 and 10 h to determine the thiamine content. After 2 h incubation, half of the cells were cooled down by swirling in icy water and harvested by centrifugation, re-suspended in sterile 0.9 % NaCl (10 ml), transferred to pre-weighed 15 ml tubes and weighed. The remaining half was harvested after 10 h. The large scale growth experiment yielded 1.1 g of cells (from 2 l) after 2 h and 5.0 g of cells (from 2 l) after 10 h.

Reaction mixtures were prepared anaerobically. 850 mg of TPP depleted cells harvested at t = 10 h were introduced, in a 15 ml tube, into the glove box and re-suspended in anaerobic *in vitro* buffer [1.7 ml, 50 mM Tris-HCl, pH 8.0, 20 mM MgCl₂, 5 mM DTT, 12.5 % (w/v) glycerol]. The suspension was then withdrawn from the anaerobic box and rapidly lysed by sonication (4 bursts of 10 sec with 30 second rest), cooled on ice. The lysate was returned to the box and allowed to degas for 10 min, then cleared by centrifugation (JA-14 with appropriate adaptors, 7000 rpm, 15 min at 4°C). The protein concentration in the cleared lysate was estimated to be 34 mg/ml by the Bradford assay (method 12). Reaction mixtures contained the components listed in **Table 7.13**.

Component	Volume, Final Conc.
KG33 lysate (10 h)	100 µl, 13.6 mg/ml
purified ThiGH-His	100 µl, 3.5 mg/ml
Tyr	1.6 mM
Cys	1.6 mM
Dxp	1.0 mM
Hmp	0.6 mM
ATP	20 mM

Table 7.13. Components present in the *in vitro* complementation assays. Tyr, Cys, Dxp, Hmp and ATP were mixed in the appropriate proportions and 50 µl of mixture added to each assay. Total volume: 250 µl.

Stock solutions of the thiazole precursors and ATP were prepared as described in section 7.8.2 and were degassed for 30 min before being added to the reaction mixtures. Thz-P (0.6 mM) was added to positive control assays. Reaction mixtures were immediately stopped or incubated at 37 °C for 4 h. The thiamine content was estimated as described in method 16 B.

7.8. Experimental for Chapter 6

*7.8.1. Large Scale Growth of *E. coli* pRL1020/83-1 in the Presence of Adenosine*

A single colony was used to inoculate DM1 medium (10 ml, section 7.7.1) and cells grown at 37 °C for 8-10 hours. This culture (3 ml) was used to inoculate fresh DM1 medium (800 ml). After overnight incubation at 37 °C, the cells were harvested by centrifugation (2 tubes, JA-14, 12000 rpm, 10 min at 4°C). The cell pellets were weighed as described in section 7.7.1, re-suspended in DM medium to yield 100 mg/ml suspensions which were pooled and used as inocula (5 ml) in DM1 medium (4 X 1.25 l) supplemented by the addition of adenosine (300 mg/l). Cells were grown at 37 °C for 2.5 h, then cooled down by swirling in icy water and harvested. The typical yield of cell paste ranged between 5.5 and 7.5 g from 5 l. The cell paste was stored at -80 °C until used.

7.8.2. General Conditions for the In Vitro Assay

1) Preparation of cell-free extracts under anaerobic conditions. The reaction buffer was obtained from an anaerobic solution of 50 mM Tris-HCl, pH 8.0, 20 mM MgCl₂, 12.5 % (w/v) glycerol, by adding freshly prepared DTT (250 mM) to a final concentration of 5 mM (800 µl in 40 ml). The DTT stock solution was prepared inside the glove box, by introducing a weighed amount of powder subsequently dissolved in anaerobic buffer.

Cell-free extracts from de-repressed *E. coli* pRL1020/83-1 or pRL1020/BL21(DE3) were prepared by introducing weighed amounts of cell paste

(0.8-1.0 g) into the glove box and resuspending it in anaerobic reaction buffer (1.6-2.0 ml). The suspensions were then withdrawn from the anaerobic box and rapidly lysed by sonication (4 x 30 sec bursts, with 30 sec rest), cooled on ice. The lysates were returned to the box and allowed to degas for 10 min, then cleared by centrifugation (JA-14 with appropriate adaptors, 7000 rpm, 15 min at 4°C) in gas-tight tubes. The protein concentration in these lysates was typically 35-45 mg/ml, as estimated by the method of Bradford (method 12). The cleared lysate prepared from pRL1020/BL21(DE3) cells (grown in 2YT medium) was routinely gel filtered through a NAP-10 column, equilibrated in anaerobic reaction buffer, to remove nearly all of the low molecular weight molecules, including TP and TPP. This gel filtration step was carefully carried out under the following standard conditions: 800 µl of lysate were applied to the NAP-10 column, followed by 200 µl of buffer; proteins were eluted with 1.3 ml of buffer discarding the first 3 drops. The protein fraction obtained from pRL1020/BL21(DE3) is referred to as 'ThiGH-enriched protein fraction'. Cell free lysates and desalted protein fractions were prepared by similar methods from de-repressed pRL1020/83-1 cells, and are termed 'de-repressed 83-1 lysate' and 'de-repressed 83-1 proteins', respectively. The typical protein concentration in gel filtered lysates varied between 15 and 25 mg/ml.

2) Preparation of reaction mixtures. Stock solutions of Tyr, Cys, Dxp, Hmp and ATP were prepared as follows: 40 mM Tyr in 100 mM HCl; 80 mM Cys in reaction buffer, freshly prepared in the glove box; 50 mM Dxp in 50 mM Tris-HCl, pH 8.0, 5 mM MgCl₂; 14 mM Hmp in reaction buffer or H₂O; 250 mM ATP in 300 mM Tris-HCl pH 8.8. The ATP solution (final pH 6.5) was freshly prepared from a 500 mM stock solution in H₂O (250 µl), by adding of 1.5 M Tris-HCl, pH 8.8 (100 µl) and H₂O (150 µl). Apart from Cys, all the other stock solutions were stored in aliquots (\leq 1 ml) at -20 °C, defrosted and allowed to degas for at least 30 min inside the box before being added to the reaction mixtures. Tyr stock solutions were carefully inspected for precipitate before use.

The thiazole precursors, Hmp and ATP were not individually added but mixed inside the box, just before addition to the reaction mixtures, as indicated in **Table 7.14**:

Component	Stock Solution (mM)	Volume (μl)	Final Conc. in 250 μl
			Assays (mM)
ATP	250	400	20
Tyr	40	200	1.6
Hmp	14	200	0.6
Cys	80	100	1.6
Dxp	50	100	1

Table 7.14. Mixture of low molecular weight components added to *in vitro* assays.
Total volume: 1 ml; added 50 μl/assay.

50 μl of mixture were added to each assay. Cys and Dxp were replaced with reaction buffer in all the experiments in which these thiazole precursors were omitted.

Unless otherwise specified, experiments were carried out in duplicate. Typical reaction mixtures contained 100 μl of de-repressed 83-1 lysate or protein fraction, 100 μl of ThiGH-enriched protein fraction or purified ThiGH-His (8.0-10.0 mg/ml, total protein concentration) and 50 μl of low molecular weight components (Table 7.14). Depending on the experiment, the total volume varied between 250 and 350 μl, as required. Anaerobic MgCl₂ (40 μl, 500 mM in H₂O) was added to samples of ThiGH-His (1 ml) in buffer E (section 7.5.2) to a final concentration of 20 mM. Reaction mixtures were immediately analysed or incubated for 4 h at 37 °C. *De novo* production of thiamine mono and pyrophosphate was estimated by the thiochrome method using the chromatographic system 1 (method 16 B), unless otherwise indicated. For each set of conditions, the amounts of TP and TPP were estimated separately, the respective background levels subtracted, and the results expressed as pmol/mg of protein/h.

Please refer to Chapter 6 for pathnames to the HPLC files where the original data are stored.

7.8.3. Thiazole Synthase Activity in *E. coli* Cleared Cell Lysates

pRL1020/83-1 was de-repressed as described in section 7.8.1 and pRL1020/BL21(DE3) was cultured and induced as described in method 14. The ThiGH-enriched protein fraction (25 mg/ml) and the de-repressed pRL1020/83-1 lysate (46 mg/ml) were prepared as described in the previous section. Reaction mixtures were prepared in 250 μ l adopting the conditions reported in **Table 7.15**.

Sample	ThiGH-enriched prot. fraction	De-repressed pRL1020/83-1 lysate	Precursor	Buffer
			Mix	
1,2,3,4	-	100	50	100
5,6,7,8	25	100	50	75
9,10,11,12	50	100	50	50
13,14,15,16	100	100	50	-
17,18,19,20	100	-	50	100
21,22,23,24	100	25	50	75
25,26,27,28	100	50	50	50

Table 7.15. Conditions for experiment 6.2.2, Chapter 6.

7.8.4. Comparing the Effect of the ThiGH-Enriched Protein Fraction and Purified ThiFS and ThiGH-His

Thz-P (15 μ l, 10 mM in 50 mM Tris-HCl), ThiGH-enriched protein fraction (100 μ l, 20 mg/ml), purified ThiGH-His (100 μ l, 7.0 mg/ml), ThiFS (100 μ l, 1 mg/ml in ThiS and 2.7 mg/ml in ThiF) or buffer (100 μ l) were added to the de-repressed pRL1020/83-1 lysate (100 μ l, 33 mg/ml) in the presence of the thiazole precursors, ATP and Hmp. The ThiFS mixture (1:1.4 ThiF:ThiS molar ratio) was prepared from partially purified ThiF (450 μ l, 3 mg/ml, section 7.6.4) and purified ThiS (50 μ l, 10 mg/ml).

In a separate experiment, pRL1020/83-1 was grown on a large scale as described in section 7.8.1 with or without adenosine. The repressed and de-repressed

pRL1020/83-1 lysates were prepared as described in section 7.8.2, mixed with the thiazole precursors, ATP and Hmp, adjusting the volume to 250 µl with reaction buffer, and the *de novo* production of TP and TPP estimated as described in method 16 B (chromatographic system 2).

7.8.5. Thiazole Synthase Activity Dependency on the Concentration of the Precursors

Reaction mixtures contained de-repressed pRL1020/83-1 proteins (100 µl, 23–26 mg/ml), purified ThiGH-His (100 µl, 10 mg/ml) and the low molecular weight component mixture (50 µl) lacking the specific thiazole precursor whose concentration was varied. Dxp (2.5 or 50 mM stock solutions), Cys and Tyr solutions were then added as indicated in Tables 7.16 and 7.17, and the volume of the reaction mixtures adjusted to 270 µl with buffer. The Tyr concentration was varied in the same way as the Cys concentration.

Sample	50 mM Dxp (µl)	Buffer	Final Dxp Conc. (mM) in 270 µl
1,2,3,4	-	20	0
5,6	10 (2.5 mM)	10	0.09
7,8	1	19	0.19
9,10	2.5	17.5	0.46
11,12	3.8	16.2	0.70
13, 14	5	15	0.93
15, 16	10	10	1.9
17, 18	15	5	2.8
19, 20	20	-	3.7

Table 7.16. Conditions adopted to vary the Dxp concentration in reaction mixtures containing the de-repressed pRL1020/83-1 proteins, purified ThiGH-His, Cys, Tyr, Hmp and ATP in a total volume of 270 µl.

Sample	50 mM Cys (μ l)	Buffer	Final Conc. (mM) in 270 μ l
1,2,3,4	-	20	0
5,6	10 (2.5 mM)	10	0.09
7,8	20 (2.5 mM)	-	0.19
9,10	2.5	17.5	0.46
11,12	3.8	16.2	0.70
13,14	5	15	0.93
15,16	10	10	1.9

Table 7.17. Conditions adopted to vary the Cys (or Tyr) concentration in reaction mixtures containing the de-repressed pRL1020/83-1 proteins, purified ThiGH-His, Dxp, Tyr (or Cys), Hmp and ATP in a total volume of 270 μ l.

7.8.6. Thiazole Synthase Activity: Effect of *ThiF* and *ThiS*

1) Investigation of the effect exerted by the addition of a ThiFS mixture (section 7.8.4) on the thiazole synthase activity. Reaction mixtures were prepared in a total volume of 350 μ l by mixing the de-repressed pRL1020/83-1 proteins (100 μ l, 25 mg/ml) with one of the following: purified ThiGH-His (100 μ l, 8.2 mg/ml), ThiFS (100 μ l, 1.0 mg/ml in ThiS and 2.7 mg/ml in ThiF), ThiGH-His plus ThiFS. Two low molecular weight component mixtures were prepared: one containing all the thiazole precursors, ATP and Hmp and the other containing just Tyr, ATP and Hmp.

2) Investigation of the effect exerted by the addition of ThiF and ThiS, individually, on the thiazole synthase activity. Reaction mixtures contained de-repressed pRL1020/83-1 proteins (100 μ l, 25 mg/ml), purified ThiGH-His (85 μ l, 9.4 mg/ml) and one of the following: ThiF (100 μ l, 3 mg/ml), ThiS (100 μ l, 1.0 mg/ml), ThiF plus ThiS, in a total volume of 350 μ l. In this experiment, two low molecular weight component mixtures were prepared: one containing all the thiazole precursors, ATP and Hmp and the other containing just Tyr, ATP and Hmp.

7.8.7. Time Course and Effect of the Concentration of ThiGH-His

To monitor the production of TP and TPP in time, assays containing de-repressed 83-1 proteins (100 µl, 24 mg/ml), purified ThiGH-His (85 µl, 9.4 mg/ml), Hmp, ATP and Tyr, in a total volume of 250 µl, were prepared. Reaction mixtures were stopped and analysed every hour from t = 0 to t = 6 h. In one of the assays, BSA was added (5 µl, 100 mg/ml) and the reaction mixture incubated overnight. BSA did not prevent protein precipitation, which occurred after approximately 2 h incubation, but analysis of this reaction mixture provided evidence of the stability of the products for at least 24 h. In another assay, SAM (5 µl, 50 mM, 1 mM final concentration) was added and the reaction mixture incubated for 4 h, before being analysed.

The dependency of the thiazole forming activity on the concentration of the ThiGH-His complex was investigated in 350 µl reaction mixtures containing the de-repressed pRL1020/83-1 proteins (16 mg/ml), Tyr, ATP and Hmp and an increasing amount of purified ThiGH-His (8.2 mg/ml): 0, 20, 50, 100, 150 and 200 µl.

7.8.8. Preliminary Fractionation Experiments on the De-repressed pRL1020/83-1 Cleared Lysate

Analytical scale. The de-repressed pRL1020/83-1 lysate was fractionated aerobically at 19 °C. Cell paste (2 g) was re-suspended in 50 mM Tris-HCl, pH 8.0, 2 mM DTT and 25 mM MgCl₂ (3 ml), lysed by sonication (5 x 15 sec burst with 30 sec rest) cooled on ice, and cleared by centrifugation (JA-14 with inserts to fit 15 ml tubes, 7500 rpm, 30 min, 4 °C). The cleared lysate was aliquoted (600 µl) in 1.5 ml eppendorf tubes and further centrifuged (13000 rpm, 10 min, 4 °C), then an aliquot (475 µl) was applied to a Superdex 200 HR 10/30 column equilibrated in lysis buffer, and proteins were eluted at 0.5 ml/min with the same buffer. 7 fractions were collected (5 ml each); these were analysed by SDS-PAGE (method 11) and the protein concentration estimated by the method of Bradford (method 12). Fractions were stored at -80 °C until used. Before testing their activity, fractions 3-7 (2 ml) were concentrated by using MWCO membrane filters (5 kDa) to 100-300 µl (final protein concentration varied between 0 and 12 mg/ml) and degassed for at least 30 min inside the glove box. Assays (280 µl) were prepared as follows: de-repressed pRL1020/83-1 lysate (50 µl, 27

mg/ml), purified ThiGH-His (80 μ l, 8.2 mg/ml), Tyr, Hmp and ATP, and 50 μ l of one of the fractions to analyse (3-7). Before being added to the reaction mixtures fractions (200 μ l aliquots) were degassed for 30 min inside the glove box.

Preparative scale. The de-repressed pRL1020/83-1 lysate was fractionated aerobically at 4°C. Cell paste (7 g) was re-suspended in lysis buffer (14 ml, 50 mM Tris-HCl, pH 8.0, 2 mM DTT and 25 mM MgCl₂) containing lysozyme (0.1 mg/ml) and benzonase (10 U/ml), stirring for 1 h. Cell were lysed by sonication (15 x 15 sec burst with 30 sec rest) cooled on ice, and cleared by centrifugation (JA-20, 15000 rpm, 30 min, 4 °C). The cleared lysate (18 ml, 30 mg/ml) was applied to a S-200 column (3.4 cm I.D. x 85 cm) equilibrated in lysis buffer and proteins were isocratically eluted at 3 ml/min with the same buffer. After having discarded the first 150 ml of eluate, 10 ml fractions were collected. Fractions 8, 11, 14, 17, 20, 23, 26, 29, 32, 35, 39, 41 and 44 were analysed by SDS-PAGE, and the protein concentration estimated by the method of Bradford (0-4 mg/ml). Apart from fraction 8, all the above mentioned fractions were tested for activity, without further concentration, under the following conditions: de-repressed pRL1020/83-1 lysate (50 μ l, 32 mg/ml), purified ThiGH-His (85 μ l, 9.4 mg/ml), Tyr, Hmp, ATP and 65 μ l of one of the fractions to analyse, in a total volume of 250 μ l. Before being added to the reaction mixtures fractions (200 μ l aliquots) were degassed for 30 min inside the glove box.

7.8.9. Thiazole Synthase Activity: Preliminary Experiments on the Effect of SAM and Reducing Agents

ThiGH-His (500 μ l, 130 μ M in ThiH-His) was incubated for 2 hours with a 5-fold molar excess of FeCl₃ and Na₂S, in the presence of freshly prepared DTT (5 mM), under anaerobic conditions. A sample of reconstituted ThiGH-His (250 μ l) was then further incubated at room temperature (19 °C) with freshly prepared dithionite (2.5 μ l, 100 mM in anaerobic buffer) for 30 min (88), during which the colour of the complex was observed to fade. Reconstituted samples were neither treated with EDTA nor gel filtered. Reconstituted ThiGH-His (100 μ l) was added to reaction mixtures containing the de-repressed pRL1020/83-1 lysate (100 μ l, 16 mg/ml), Tyr, ATP, Hmp, SAM (5 μ l, 50 mM, 1 mM final concentration) and NADPH (5 μ l, 50 mM, 1 mM final

concentration); dithionite-reduced ThiGH-His was added to the same reaction mixtures lacking NADPH. After 4 h incubation, the thiamine content in the assays (250 µl) was estimated by the thiochrome method (method 16 B, chromatographic system 2).

Data relative to the effect of SAM alone were obtained from the experiment described in section 7.8.7 (method 16 B, chromatographic system 1).

Appendix A

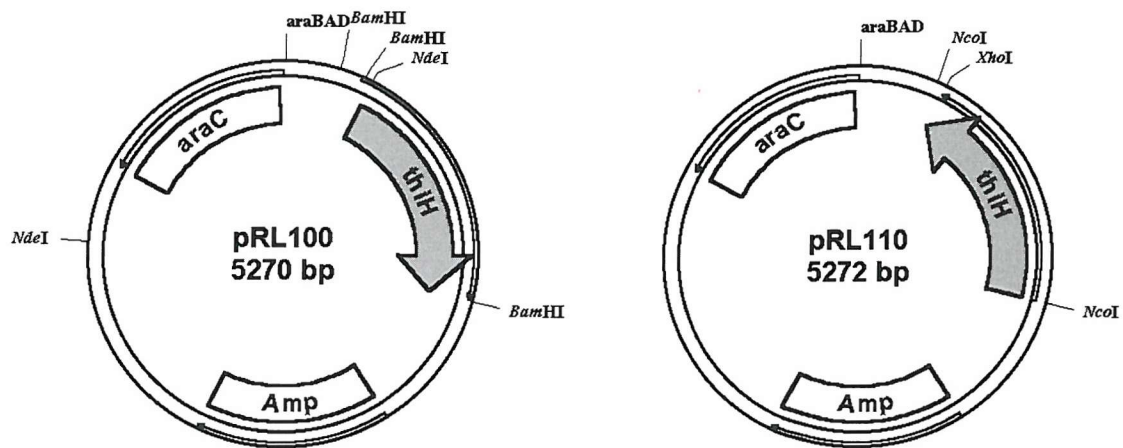
List of Assembled Plasmids

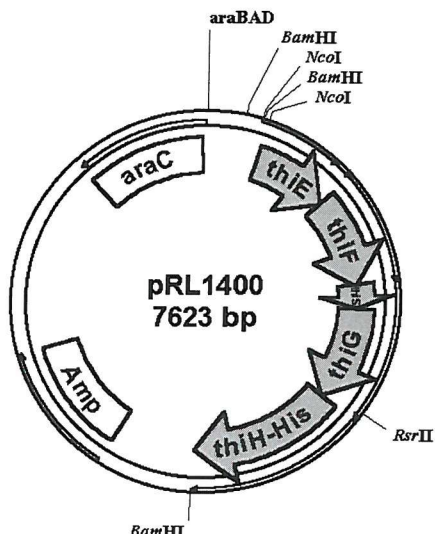
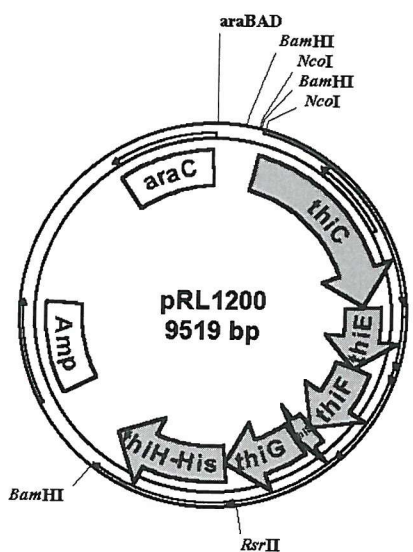
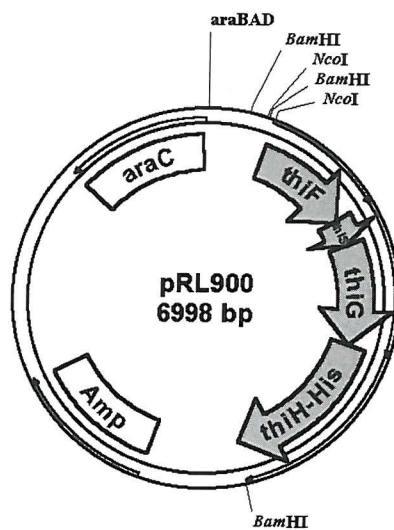
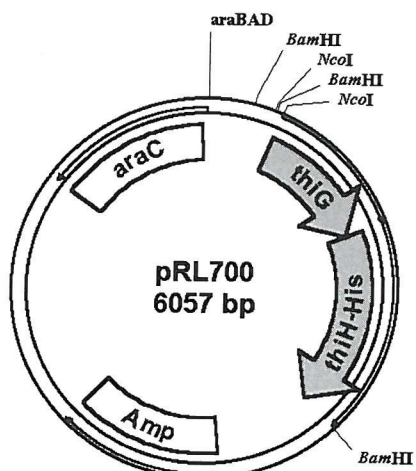
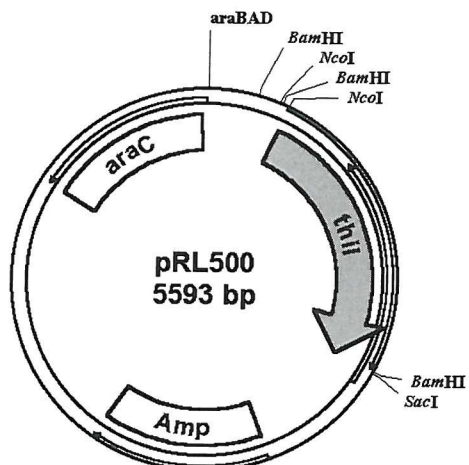
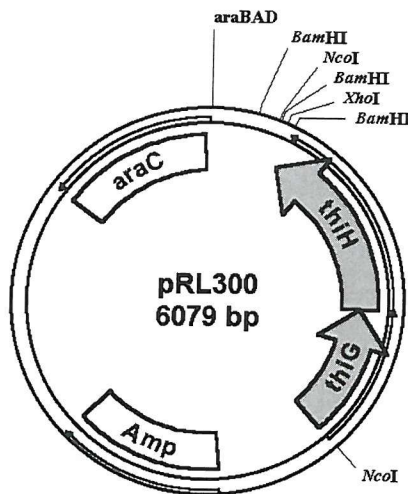
Name	Insert	Parental	Resistance
		Plasmid	Marker
pRL100	<i>Nde</i> 1/ <i>Bam</i> H1 <i>thiH</i>	pBAD-TOPO	Ampicillin
pRL110	<i>Nco</i> 1/ <i>Xho</i> 1 <i>thiH</i>	pBAD-TOPO	Ampicillin
pRL200	<i>Nde</i> 1/ <i>Bam</i> H1 <i>thiH</i>	pET-24a(+)*	Kanamycin
pRL220, pRL220*	<i>Nco</i> 1/ <i>Xho</i> 1 <i>thiH</i>	pBAD/HisA°	Ampicillin
pRL221	<i>Nco</i> 1/ <i>Xho</i> 1 <i>thiH</i> , <i>Xho</i> 1/ <i>Eco</i> R1 <i>GroELS</i>	pBAD/HisA°	Ampicillin
pRL222	<i>Nco</i> 1/ <i>Xho</i> 1 <i>thiH</i> , <i>Xho</i> 1/ <i>Eco</i> R1 <i>trxA</i>	pBAD/HisA°	Ampicillin
pRL300	<i>Nco</i> 1/ <i>Bam</i> H1 <i>thiGH</i>	pBAD-TOPO	Ampicillin
pRL400	<i>Nco</i> 1/ <i>Bam</i> H1 <i>thiGH</i>	pET-24d(+)*	Kanamycin
pRL500	<i>Nco</i> 1/ <i>Bam</i> H1, <i>Sac</i> 1 <i>thiI</i>	pBAD-TOPO	Ampicillin
pRL600	<i>Nco</i> 1/ <i>Bam</i> H1, <i>Sac</i> 1 <i>thiI</i>	pET-24d(+)*	Kanamycin
pRL700	<i>Nco</i> 1/ <i>Bam</i> H1 <i>thiGH-His</i>	pBAD-TOPO	Ampicillin
pRL800	<i>Nco</i> 1/ <i>Bam</i> H1 <i>thiGH-His</i>	pET-24d(+)*	Kanamycin
pRL820	<i>Nco</i> 1/ <i>Xho</i> 1 <i>thiGH-His</i>	pBAD/HisA°	Ampicillin
pRL821	<i>Nco</i> 1/ <i>Xho</i> 1 <i>thiGH-His</i> , <i>Xho</i> 1/ <i>Eco</i> R1 <i>iscSUA-hscBA-</i> <i>fdx</i>	pBAD/HisA°	Ampicillin
pRL900	<i>Nco</i> 1/ <i>Bam</i> H1 <i>thiFSGH-His</i>	pBAD-TOPO	Ampicillin
pRL1000	<i>Nco</i> 1/ <i>Bam</i> H1 <i>thiFSGH-His</i>	pET-24d(+)*	Kanamycin
pRL1020	<i>Nco</i> 1/ <i>Xho</i> 1 <i>thiFSGH-His</i>	pBAD/HisA°	Ampicillin
pRL1021	<i>Nco</i> 1/ <i>Xho</i> 1 <i>thiFSGH-His</i> , <i>Xho</i> 1/ <i>Eco</i> R1 <i>iscSUA-hscBA-</i> <i>fdx</i>	pBAD/HisA°	Ampicillin

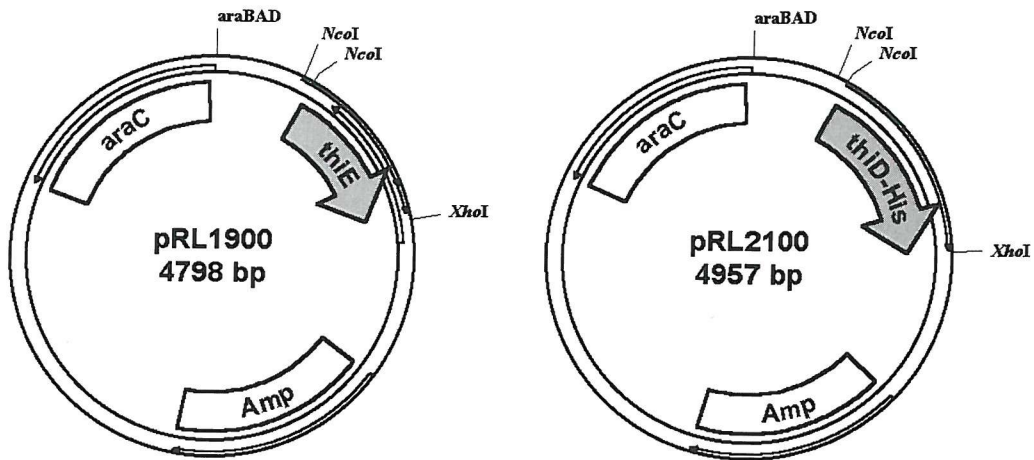
pRL1200	<i>Nco</i> 1/ <i>Bam</i> H1 <i>thiCEFSGH-His</i>	pBAD-TOPO	Ampicillin
pRL1300	<i>Nco</i> 1/ <i>Xho</i> 1 <i>thiCEFSGH-His</i>	pBAD/HisA°	Ampicillin
pRL1400	<i>Nco</i> 1/ <i>Bam</i> H1 <i>thiEFSGH-His</i>	pBAD-TOPO	Ampicillin
pRL1500	<i>Nco</i> 1/ <i>Xho</i> 1 <i>thiEFSGH-His</i>	pBAD/HisA°	Ampicillin
pRL1800	<i>Nco</i> 1/ <i>Sal</i> 1 <i>thiFS</i>	pET-24d(+)*	Kanamycin
pRL1900	<i>Nco</i> 1/ <i>Xho</i> 1 <i>thiE</i>	pBAD-TOPO	Ampicillin
pRL2000	<i>Nco</i> 1/ <i>Xho</i> 1 <i>thiE</i>	pBAD/HisA°	Ampicillin
pRL2020	<i>Nco</i> 1/ <i>Xho</i> 1 <i>thiE</i>	pBADHisRepair°	Ampicillin
pRL2030	<i>Nco</i> 1/ <i>Xho</i> 1 <i>thiE</i>	pET-24d(+)*	Kanamycin
pRL2100	<i>Nco</i> 1/ <i>Xho</i> 1 <i>thiD-His</i>	pBAD-TOPO	Ampicillin
pRL2200	<i>Nco</i> 1/ <i>Xho</i> 1 <i>thiD-His</i>	pBAD/HisA°	Ampicillin
pRL2220	<i>Nco</i> 1/ <i>Xho</i> 1 <i>thiD-His</i>	pET-24d(+)*	Kanamycin

Protein expression was induced with IPTG (*) or β-L-arabinose (°).

Maps of Cloning Plasmids (pBAD-TOPO Derivatives)







Appendix B

B.1. Agarose gel electrophoresis

- 50 X Running buffer solution, 50 X TAE

Per litre:

Tris base	242 g
Glacial acetic acid	57.1 ml
0.5 M EDTA	100 ml

Adjusted to pH 8.0 with HCl.

- 1 % Agarose gel

Per gel:

Agarose	0.4 g
TAE buffer, 1 X	40 ml

The suspension was heated at top power rating in a Compact microwave (Sharp) until the agarose had dissolved, poured and allowed to solidify at 4 °C.

- 6 X Gel electrophoresis loading buffer

Glycerol	30 % (v/v)
Bromophenol blue	0.25 % (w/v)

- Electrophoresis gel stain

Ethidium bromide	1 µg/ml
------------------	---------

B.2. Sodium Dodecyl Sulphate Polyacrylamide Gel Electrophoresis (SDS-PAGE)

- 5 X Running buffer

Per litre:

Tris base	15 g
Glycine	94 g
SDS	5 g

- SDS-PAGE gel

Per gel (5 ml)

15 % resolving gel:

H ₂ O	1.1 ml
30 % (w/v) Acrylamide/bis-acrylamide (37.5:1)	2.5 ml
1.5 M Tris-HCl, pH 8.8	1.3 ml
10 % (w/v) SDS	50 µl
10 % (w/v) Ammonium persulphate,	50 µl
TEMED	2 µl

Per gel (5 ml)

18 % resolving gel:

H ₂ O	0.6 ml
30 % (w/v) Acrylamide/bis-acrylamide (37.5:1)	3.0 ml
1.5 M Tris-HCl, pH 8.8	1.3 ml
10 % (w/v) SDS	50 µl
10 % (w/v) Ammonium persulphate,	50 µl
TEMED	2 µl

Per gel (2 ml)

3 % stacking gel:

H ₂ O	1.4 ml
30 % (w/v) Acrylamide/bis-acrylamide (37.5:1)	0.33 ml
1.0 M Tris, pH 6.8	0.25 ml
10 % (w/v) SDS	20 µl
10 % (w/v) Ammonium persulphate	20 µl
TEMED	2 µl

Freshly prepared ammonium persulphate and TEMED were added just prior to pouring the gels.

- 2 X SDS-PAGE loading buffer

Tris-HCl	50 mM, pH 6.5
Bromophenol Blue	0.1 % (w/v)
SDS	2 % (w/v)
Glycerol	10 % (w/v)
DTT	100 mM

- SDS-PAGE gel stain

Per litre

Acetic acid	100 ml
Methanol	450 ml
H ₂ O	450 ml
Coomassie Brilliant Blue	2.5 g

- SDS-PAGE gel destain

Per litre

Acetic acid	100 ml
Methanol	300 ml
H ₂ O	600 ml

B.3. Bradford Assay

- Bradford Reagent

Per litre:

88 % Phosphoric acid	100 ml
Ethanol	50 ml
Coomassie Brilliant Blue	100 mg
H ₂ O	850 ml

Coomassie Brilliant Blue was first dissolved in ethanol, then phosphoric acid and H₂O were added and the solution filtered.

B.4. Growth Media

- 2 X Tryptone/Yeast extract (2YT)

Per litre:

Bacto tryptone	16 g
Yeast extract	10 g
NaCl	5 g

- SOC medium

Per litre:

Bacto tryptone	20 g
Yeast extract	5 g
NaCl	0.6 g

The medium (970 ml) was autoclaved, allowed to cool down and the following sterile solutions added:

1M MgCl ₂	10 ml
1M MgSO ₄	10 ml
2M Glucose	10 ml

MgCl₂ and MgSO₄ were filter sterilised.

- Davis-Mingioli Medium

Per litre:

K ₂ HPO ₄	7 g
KH ₂ PO ₄	3 g
Na ₃ -citrate·3H ₂ O	0.5 g
MgSO ₄ ·7H ₂ O	0.1 g
(NH ₄) ₂ SO ₄	1 g
H ₂ O	1 l

The medium was autoclaved and stored at room temperature until used. Prior to use, sterilised 20 % (w/v) glucose was added to a final concentration of 0.2 % (w/v).

- 2YT agar plates

Per litre:

Bacto tryptone	16 g
Yeast extract	10 g
NaCl	5 g
Agar	15 g

The solution was autoclaved and allowed to cool down to 50 °C before adding ampicillin or kanamycin to a final concentration of 100 µg/ml and 30 µg/ml, respectively. This medium was poured into petri dishes, allowed to harden and stored at 4 °C.

- DM1 agar plates

Per litre:

K ₂ HPO ₄	7 g
KH ₂ PO ₄	3 g
Na ₃ -citrate·3H ₂ O	0.5 g

MgSO ₄ ·7H ₂ O	0.1 g
(NH ₄) ₂ SO ₄	1 g
Agar	15 g
H ₂ O	1 l

The solution was autoclaved and allowed to cool down to 50 °C before adding ampicillin (100 µg/ml), glucose [0.2 % (w/v)], Tyr and Phe (0.2 mM each), Trp (0.1 mM), 4-hydroxybenzoic acid, 2,3-dihydroxybenzoic acid and 4-aminobenzoic acid (10 µM each). This medium was poured into petri dishes, allowed to harden and stored at 4 °C.

Bibliography

1. Bender, D. A. (1999) *Proceedings of the Nutrition Society* **58**, 427-433
2. Singleton, C. K., and Martin, P. R. (2001) *Current Molecular Medicine* **1**, 197-207
3. Metzler, D. E. (1977) in *Biochemistry- The Chemical Reactions of Living Cells*, pp. 430-431, Academic Press, London
4. Friedrich, W. (1988) in *Vitamins*, pp. 341-401, de Gruyter
5. Spenser, I. D., and White, R. L. (1997) *Angewandte Chemie-International Edition in English* **36**(10), 1033-1046
6. Bordwell, F. G., and Satish, A. V. (1991) *Journal of the American Chemical Society* **113**, 985-990
7. Page, M., and Williams, A. (1997) in *Organic and Bio-organic Mechanisms*, pp. 169-171, Addison Wesley Longman, Harlow
8. Stryer, L. (1996) Trans. Pessino, A., and Sparatore, B. in *Biochimica* (Zanichelli, ed), fourth Ed., pp. 598-606, Bologna
9. Sprenger, G. A., Schorken, U., Wiegert, T., Grolle, S., deGraaf, A. A., Taylor, S. V., Begley, T. P., BringerMeyer, S., and Sahm, H. (1997) *Proceedings of the National Academy of Sciences of the United States of America* **94**(24), 12857-12862
10. Lois, L. M., Campos, N., Putra, S. R., Danielsen, K., Rohmer, M., and Boronat, A. (1998) *Proceedings of the National Academy of Sciences of the United States of America* **95**(5), 2105-2110
11. Rohmer, M., Seemann, M., Horbach, S., Bringer-Meyer, S., and Sahm, H. (1996) *Journal of the American Chemical Society* **118**, 2564-2566
12. Fuchs, G. (1999) in *Biology of the Prokaryotes* (Lengeler, J. W., Drews, G., and Schlegel, H. G., eds), pp. 130-131, Blackwell Science, Stuttgart
13. Begley, T. P., Downs, D. M., Ealick, S. E., McLafferty, F. W., Van Loon, A., Taylor, S., Campobasso, N., Chiu, H. J., Kinsland, C., Reddick, J. J., and Xi, J. (1999) *Archives of Microbiology* **171**(5), 293-300

14. White, R. L., and Spenser, D. (1996) in *Escherichia coli and Salmonella typhimurium: Cellular and Molecular Biology* (Neidhardt, F. C., Curtiss, R. R., Ingraham, J. L., Lin, E. C., Low, K. B., Magasanik, B., Reznikoff, W. S., Riley, M., Schaechter, M., and Umbarger, H. E., eds) Vol. 1, pp. 1175-1209, American Society for Microbiology, Washington, D.C.
15. Estramareix, B., and Therisod, M. (1984) *Journal of the American Chemical Society* **106**, 3857-3860
16. Estramareix, B., and David, S. (1990) *Biochimica et Biophysica Acta* **1035**, 154-160
17. Zalkin, H., and Nygaard, P. (1996) in *Escherichia coli and Salmonella typhimurium: Cellular and Molecular Biology* (Neidhardt, F. C., Curtiss, R. R., Ingraham, J. L., Lin, E. C., Low, K. B., Magasanik, B., Reznikoff, W. S., Riley, M., Schaechter, M., and Umbarger, H. E., eds) Vol. 1, pp. 561-579, American Society for Microbiology, Washington, D.C.
18. Newell, P. C., and Tucker, R. G. (1968) *Biochemical Journal* **106**, 279-287
19. Kozluk, T., and Spenser, I. D. (1987) *Journal of the American Chemical Society* **109**, 4698-4702
20. Tazuya, K., Yamada, K., and Kumaoka, H. (1989) *Biochimica et Biophysica Acta* **990**, 73-79
21. Tazuya, K., Azumi, C., Yamada, K., and Kumaoka, H. (1994) *Biochemistry and Molecular Biology International* **33**(4), 769-774
22. Zeidler, J., Ullah, N., Nath Gupta, R., Pauloski, R. M., Sayer, B. G., and Spenser, I. D. (2002) *Journal of the American Chemical Society* **124**, 4542-4543
23. Kumaoka, H., and Brown, G. M. (1967) *Archives of Biochemistry and Biophysics* **122**, 378-384
24. Yamada, K., Morisaki, M., and Kumaoka, H. (1983) *Biochimica et Biophysica Acta* **756**, 41-48
25. David, S., Estramareix, B., and Hirshfeld, H. (1967) *Biochimica et Biophysica Acta* **148**, 11-21
26. Grue-Sorensen, G., White, R. L., and Spenser, I. D. (1986) *Journal of the American Chemical Society* **108**, 146-158

27. Himmeldirk, K., Sayer, B. G., and Spenser, I. D. (1998) *Journal of the American Chemical Society* **120**(15), 3581-3589
28. Himmeldirk, K., Kennedy, I. A., Hill, R. E., Sayer, B. G., and Spenser, I. D. (1996) *Chemical Communications* (10), 1187-1188
29. David, S., Estramareix, B., Fischer, J.-C., and Therisod, M. (1982) *Journal of the Chemical Society Perkin Transactions 1*, 2131-2137
30. Estramareix, B., and Therisod, M. (1972) *Biochimica et Biophysica Acta* **192**, 375-380
31. Bellion, E., Kirkley, D. H., and Faust, J. R. (1976) *Biochimica et Biophysica Acta* **437**, 229-237
32. White, R. H., and Rudolph, F. B. (1978) *Biochimica et Biophysica Acta* **542**, 340-347
33. Tazuya, K., Yamada, K., Nakamura, K., and Kumaoka, H. (1987) *Biochimica et Biophysica Acta* **924**, 210-215
34. White, R. H. (1979) *Biochimica et Biophysica Acta* **583**, 55-62
35. Julliard, J. H., and R., D. (1991) *Proceedings of the National Academy of Sciences of the United States of America* **88**, 2042-2045
36. Tazuya, K., Morisaki, M., Yamada, K., Kumaoka, H., and Saiki, K. (1987) *Biochemistry International* **14**, 153-160
37. Yamada, K. (1992) *Bitamin* **66**, 1-24
38. Xi, J., Ge, Y., Kinsland, C., McLafferty, F. W., and Begley, T. P. (2001) *Proceedings of the National Academy of Sciences of the United States of America* **98**(15), 8513-8518
39. Vanderhorn, P. B., Backstrom, A. D., Stewart, V., and Begley, T. P. (1993) *Journal of Bacteriology* **175**(4), 982-992
40. Kelleher, N. L., Taylor, S. V., Grannis, D., Kinsland, C., Chiu, H. J., Begley, T. P., and McLafferty, F. W. (1998) *Protein Science* **7**(8), 1796-1801
41. Webb, E., Febres, F., and Downs, D. M. (1996) *Journal of Bacteriology* **178**(9), 2533-2538
42. Mizote, T., Tsuda, M., Nakazawa, T., and Nakayama, H. (1996) *Microbiology-UK* **142**, 2969-2974

43. Petersen, L. A., and Downs, D. M. (1997) *Journal of Bacteriology* **179**(15), 4894-4900
44. Webb, E., Claas, K., and Downs, D. (1998) *Journal of Biological Chemistry* **273**(15), 8946-8950
45. Webb, E., Claas, K., and Downs, D. M. (1997) *Journal of Bacteriology* **179**(13), 4399-4402
46. Imamura, N., and Nakayama, H. (1982) *Journal of Bacteriology* **151**, 708-717
47. Webb, E., and Downs, D. (1997) *Journal of Biological Chemistry* **272**(25), 15702-15707
48. Skovran, E., and Downs, D. M. (2000) *Journal of Bacteriology* **182**(14), 3896-3903
49. Lauhon, C. T., and Kambampati, R. (2000) *Journal of Biological Chemistry* **275**(26), 20096-20103
50. Reddick, J. J., Kinsland, C., Nicewonger, R., Christian, T., Downs, D. M., Winkler, M. E., and Begley, T. P. (1998) *Tetrahedron* **54**(52), 15983-15991
51. Kambampati, R., and Lauhon, C. T. (1999) *Biochemistry* **38**(50), 16561-16568
52. Kambampati, R., and Lauhon, C. T. (2000) *Journal of Biological Chemistry* **275**(15), 10727-10730
53. Zheng, L. M., Cash, V. L., Flint, D. H., and Dean, D. R. (1998) *Journal of Biological Chemistry* **273**(21), 13264-13272
54. Schwartz, C. J., Djaman, O., Imlay, J. A., and Kiley, P. J. (2000) *Proceedings of the National Academy of Sciences of the United States of America* **97**(16), 9009-9014
55. Mizote, T., Tsuda, M., Smith, D. D. S., Nakayama, H., and Nakazawa, T. (1999) *Microbiology-UK* **145**, 495-501
56. Backstrom, A. D., McMordie, R. A. S., and Begley, T. P. (1995) *Journal of the American Chemical Society* **117**(8), 2351-2352
57. Chiu, H. J., Reddick, J. J., Begley, T. P., and Ealick, S. E. (1999) *Biochemistry* **38**(20), 6460-6470
58. Reddick, J. J., Nicewonger, R., and Begley, T. P. (2001) *Biochemistry* **40**(34), 10095-10102

59. Peapus, D. H., Chiu, H. J., Campobasso, N., Reddick, J. J., Begley, T. P., and Ealick, S. E. (2001) *Biochemistry* **40**(34), 10103-10114

60. Newell, P. C., and Tucker, R. G. (1966) *Biochemical Journal* **100**, 517-524

61. Kawasaki, T., Iwashima, A., and Nose, Y. (1969) *The Journal of Biochemistry* **65**, 407-416

62. Rodionov, D. A., Vitreschak, A. G., Mironov, A. A., and Gelfand, M. S. (2002) *Journal of Biological Chemistry* **277**(50), 48949-48959

63. Miranda-Rios, J., Navarro, M., and Soberon, M. (2001) *Proceedings of the National Academy of Sciences of the United States of America* **98**(17), 9736-9741

64. Winkler, W., Nahvi, A., and Breaker, R. R. (2002) *Nature* **419**, 952-956

65. Hesselberth, J. R., and Ellington, A. D. (2002) *Nature Structural Biology* **9**, 891-893

66. Szostak, J. W. (2002) *Nature* **419**, 890-891

67. Newell, P. C., and Tucker, R. G. (1968) *Biochemical Journal* **106**, 271-277

68. Newell, P. C., and Tucker, R. G. (1966) *Biochemical Journal* **100**, 512-516

69. Wang, C. Y., Xi, J., Begley, T. P., and Nicholson, L. K. (2001) *Nature Structural Biology* **8**(1), 47-51

70. Hochstrasser, M. (2000) *Nature Cell Biology* **2**(8), E153-E157

71. Taylor, S. V., Kelleher, N. L., Kinsland, C., Chiu, H. J., Costello, C. K., Backstrom, A. D., McLafferty, F. W., and Begley, T. P. (1998) *Journal of Biological Chemistry* **273**(26), 16555-16560

72. Leimkuhler, S., Wuebbens, M. M., and Rajagopalan, K. V. (2001) *Journal of Biological Chemistry* **276**(37), 34695-34701

73. Marquet, A. (2001) *Current Opinion in Chemical Biology* **5**(5), 541-549

74. Rudolph, M. J., Wuebbens, M. M., Rajagopalan, K. V., and Schindelin, H. (2001) *Nature Structural Biology* **8**(1), 42-46

75. Mihara, H., and Esaki, N. (2002) *Applied Microbiology and Biotechnology* **60**(1-2), 12-23

76. Gralnick, J., Webb, E., Beck, B., and Downs, D. (2000) *Journal of Bacteriology* **182**(18), 5180-5187

77. Palenchar, P. M., Buck, C. J., Cheng, H., Larson, T. J., and Mueller, E. G. (2000) *Journal of Biological Chemistry* **275**(12), 8283-8286

78. Wright, C. M., Palenchar, P. M., and Mueller, E. G. (2002) *Chemical Communications* (22), 2708-2709

79. Rieder, G., Merrick, M. J., Castorph, H., and Kleiner, D. (1994) *Journal of Biological Chemistry* **269**(20), 14386-14390

80. Chaudhuri, B. N., Lange, S. C., Myers, R. S., Davisson, V. J., and Smith, J. L. (2003) *Biochemistry* **42**(23), 7003-7012

81. Park, J. H., Dorrestein, P. C., Zhai, H., Kinsland, C., McLafferty, F. W., and Begley, T. P. (2003) *Biochemistry* **42**, 12430-12438

82. Settembre, E. C., Dorrestein, P. C., Park, J. H., Augustine, A. M., Begley, T. P., and Ealick, S. E. (2003) *Biochemistry* **42**(10), 2971-2981

83. Leonardi, R., Fairhurst, S. A., Kriek, M., Lowe, D. J., and Roach, P. L. (2003) *Febs Letters* **539**, 95-99

84. Sofia, H. J., Chen, G., Hetzler, B. G., Reyes-Spindola, J. F., and Miller, N. E. (2001) *Nucleic Acids Research* **29**(5), 1097-1106

85. Cheek, J., and Broderick, J. B. (2001) *Journal of Biological Inorganic Chemistry* **6**(3), 209-226

86. Frey, P. A., and Reed, G. H. (2000) *Archives of Biochemistry and Biophysics* **382**, 6-14

87. Ollagnier-de-Choudens, S., Sanakis, Y., Hewitson, K. S., Roach, P. L., Baldwin, J. E., Munck, E., and Fontecave, M. (2000) *Biochemistry* **39**(14), 4165-4173

88. Miller, J. R., Busby, R. W., Jordan, S. W., Cheek, J., Henshaw, T. F., Ashley, G. W., Broderick, J. B., Cronan, J. E., and Marletta, M. A. (2000) *Biochemistry* **39**(49), 15166-15178

89. McIver, L., Baxter, R. L., and Campopiano, D. J. (2000) *Journal of Biological Chemistry* **275**(18), 13888-13894

90. Hewitson, K. S., Baldwin, J. E., Shaw, N. M., and Roach, P. L. (2000) *Febs Letters* **466**(2-3), 372-376

91. Kulzer, R., Pils, T., Kappl, R., Huttermann, J., and Knappe, J. (1998) *Journal of Biological Chemistry* **273**(9), 4897-4903

92. Tamarit, J., Gerez, C., Meier, C., Mulliez, E., Trautwein, A., and Fontecave, M. (2000) *Journal of Biological Chemistry* **275**(21), 15669-15675

93. Fontecave, M., Mulliez, E., and Ollagnier-de-Choudens, S. (2001) *Current Opinion in Chemical Biology* **5**(5), 506-511

94. Jarrett, J. T. (2003) *Current Opinion in Chemical Biology* **7**, 174-182

95. Frey, M., Rothe, M., Wagner, A. F. V., and Knappe, J. (1994) *Journal of Biological Chemistry* **269**(17), 12432-12437

96. Sun, X. Y., Eliasson, R., Pontis, E., Andersson, J., Buist, G., Sjoberg, B. M., and Reichard, P. (1995) *Journal of Biological Chemistry* **270**(6), 2443-2446

97. Henshaw, T. F., Cheek, J., and Broderick, J. B. (2000) *Journal of the American Chemical Society* **122**(34), 8331-8332

98. Sun, X. Y., Ollagnier, S., Schmidt, P. P., Atta, M., Mulliez, E., Lepape, L., Eliasson, R., Graslund, A., Fontecave, M., Reichard, P., and Sjoberg, B. M. (1996) *Journal of Biological Chemistry* **271**(12), 6827-6831

99. Ollagnier, S., Mulliez, E., Schmidt, P. P., Eliasson, R., Gaillard, J., Deronzier, C., Bergman, T., Graslund, A., Reichard, P., and Fontecave, M. (1997) *Journal of Biological Chemistry* **272**(39), 24216-24223

100. Escalettes, F., Florentin, D., Bui, B. T. S., Lesage, D., and Marquet, A. (1999) *Journal of the American Chemical Society* **121**(15), 3571-3578

101. Ugulava, N. B., Gibney, B. R., and Jarrett, J. T. (2001) *Biochemistry* **40**(28), 8343-8351

102. Bui, B. T. S., Florentin, D., Fournier, F., Ploux, O., Mejean, A., and Marquet, A. (1998) *Febs Letters* **440**(1-2), 226-230

103. Gibson, K. J., Pelletier, D. A., and Turner, I. M. (1999) *Biochemical and Biophysical Research Communications* **254**(3), 632-635

104. Lieder, K. W., Booker, S., Ruzicka, F. J., Beinert, H., Reed, G. H., and Frey, P. A. (1998) *Biochemistry* **37**(8), 2578-2585

105. Flint, D. H., Tuminello, J. F., and Emptage, M. H. (1993) *Journal of Biological Chemistry* **268**, 22369-22376

106. Ollagnier, S., Mulliez, E., Gaillard, J., Eliasson, R., Fontecave, M., and Reichard, P. (1996) *Journal of Biological Chemistry* **271**(16), 9410-9416

107. Ugulava, N. B., Gibney, B. R., and Jarrett, J. T. (2000) *Biochemistry* **39**(17), 5206-5214
108. Birch, O. M., Fuhrmann, M., and Shaw, N. M. (1995) *Journal of Biological Chemistry* **270**(32), 19158-19165
109. Bianchi, V., Eliasson, R., Fontecave, M., Mulliez, E., Hoover, D. M., Matthews, R. G., and Reichard, P. (1993) *Biochemical and Biophysical Research Communications* **197**(2), 792-797
110. Mulliez, E., Padovani, D., Atta, M., Alcouffe, C., and Fontecave, M. (2001) *Biochemistry* **40**(12), 3730-3736
111. Duin, E. C., Lafferty, M. E., Crouse, B. R., Allen, R. M., Sanyal, I., Flint, D. H., and Johnson, M. K. (1997) *Biochemistry* **36**(39), 11811-11820
112. Walsby, C. J., Hong, W., Broderick, W. E., Cheek, J., Ortillo, D., Broderick, J. B., and Hoffman, B. M. (2002) *Journal of the American Chemical Society* **124**(12), 3143-3151
113. Cosper, N. J., Booker, S. J., Ruzicka, F., Frey, P. A., and Scott, R. A. (2000) *Biochemistry* **39**(51), 15668-15673
114. Walsby, C. J., Ortillo, D., Broderick, W. E., Broderick, J. B., and Hoffman, B. M. (2002) *Journal of the American Chemical Society* **124**(38), 11270-11271
115. Kohda, J., Endo, Y., Okumura, N., Kurokawa, Y., Nishihara, K., Yanagi, H., Yura, T., Fukuda, H., and Kondo, A. (2002) *Biochemical Engineering Journal* **10**(1), 39-45
116. Hartl, F. U., and Hayer-Hartl, M. (2002) *Science* **295**(5561), 1852-1858
117. Baneyx, F. (1999) *Current Opinion in Biotechnology* **10**(5), 411-421
118. Yasukawa, T., Kaneiishii, C., Maekawa, T., Fujimoto, J., Yamamoto, T., and Ishii, S. (1995) *Journal of Biological Chemistry* **270**(43), 25328-25331
119. Sareen, D., Sharma, R., and Vohra, R. M. (2001) *Protein Expression and Purification* **23**(3), 374-379
120. Goenka, S., and Rao, C. M. (2001) *Protein Expression and Purification* **21**(2), 260-267
121. Nakamura, M., Saeki, K., and Takahashi, Y. (1999) *Journal of Biochemistry* **126**(1), 10-18

122. Takahashi, Y., and Nakamura, M. (1999) *Journal of Biochemistry* **126**(5), 917-926

123. Kriek, M., Peters, L., Takahashi, Y., and Roach, P. L. (2003) *Protein Expression and Purification* **28**(2), 241-245

124. Miyazaki, T., Yoshimi, T., Furutsu, Y., Hongo, K., Mizobata, T., Kanemori, M., and Kawata, Y. (2002) *Journal of Biological Chemistry* **277**(52), 50621-50628

125. Bessette, P. H., Aslund, F., Beckwith, J., and Georgiou, G. (1999) *Proceedings of the National Academy of Science* **96**, 13703-13708

126. Prinz, W. A., Aslund, F., Holmgren, A., and Beckwith, J. (1997) *Journal of Biological Chemistry* **272**(25), 15661-15667

127. Aslund, F., and Beckwith, J. (1999) *Journal of Bacteriology* **181**(5), 1375-1379

128. Missiakas, D., and Raina, S. (1997) *Journal of Bacteriology* **179**(8), 2465-2471

129. Frazzon, J., and Dean, D. R. (2001) *Proceedings of the National Academy of Sciences of the United States of America* **98**, 14751-53

130. Schwartz, C. J., Giel, J. L., Patschkowski, T., Luther, C., Ruzicka, F. J., Beinert, H., and Kiley, P. J. (2001) *Proceedings of the National Academy of Sciences of the United States of America* **98**(26), 14895-14900

131. Agar, J. N., Krebs, C., Frazzon, J., Huynh, B. H., Dean, D. R., and Johnson, M. K. (2000) *Biochemistry* **39**(27), 7856-7862

132. Smith, A. D., Agar, J. N., Johnson, K. A., Frazzon, J., Amster, I. J., Dean, D. R., and Johnson, M. K. (2001) *Journal of the American Chemical Society* **123**(44), 11103-11104

133. Krebs, C., Agar, J. N., Smith, A. D., Frazzon, J., Dean, D. R., Huynh, B. H., and Johnson, M. K. (2001) *Biochemistry* **40**(46), 14069-14080

134. Ollagnier-de-Choudens, S., Mattioli, T., Tagahashi, Y., and Fontecave, M. (2001) *Journal of Biological Chemistry* **276**(25), 22604-22607

135. Silberg, J. J., Hoff, K. G., and Vickery, L. E. (1998) *Journal of Bacteriology* **180**(24), 6617-6624

136. Hoff, K. G., Silberg, J. J., and Vickery, L. E. (2000) *Proceedings of the National Academy of Sciences of the United States of America* **97**(14), 7790-7795

137. Silberg, J. J., Hoff, K. G., Tapley, T. L., and Vickery, L. E. (2001) *Journal of Biological Chemistry* **276**(3), 1696-1700

138. Tokumoto, U., Nomura, S., Minami, Y., Mihara, H., Kato, S., Kurihara, T., Esaki, N., Kanazawa, H., Matsubara, H., and Takahashi, Y. (2002) *Journal of Biochemistry* **131**, 713-9

139. Kakuta, Y., Horio, T., Takahashi, Y., and Fukuyama, K. (2001) *Biochemistry* **40**, 11007-12

140. Rebeil, R., Sun, Y. B., Chooback, L., Pedraza-Reyes, M., Kinsland, C., Begley, T. P., and Nicholson, W. L. (1998) *Journal of Bacteriology* **180**(18), 4879-4885

141. Pierrel, F., Bjork, G. R., Fontecave, M., and Atta, M. (2002) *Journal of Biological Chemistry* **277**(16), 13367-13370

142. Johnson, M. K., Spiro, T. G., and Mortenson, L. E. (1982) *Journal of Biological Chemistry* **257**, 2447-2452

143. Ollagnier-de-Choudens, S., and Fontecave, M. (1999) *Febs Letters* **453**(1-2), 25-28

144. Broderick, J. B., Henshaw, T. F., Cheek, J., Wojtuszewski, K., Smith, S. R., Trojan, M. R., McGhan, R. M., Kopf, A., Kibbey, M., and Broderick, W. E. (2000) *Biochemical and Biophysical Research Communications* **269**(2), 451-456

145. Kiley, P. J., and Beinert, H. (1999) *Fems Microbiology Reviews* **22**, 341-352

146. Vollmer, S. J., Switzer, R., and Debrunner, P. G. (1983) *Journal of Biological Chemistry* **258**, 14284-14293

147. Fish, W. W. (1988) *Methods in Enzymology* **158**, 357-364

148. Beinert, H. (1983) *Analytical Biochemistry* **131**(2), 373-378

149. Wong, K. K., Murray, B. W., Lewisch, S. A., Baxter, M. K., Ridky, T. W., Ulissi-DeMario, L., and Kozarich, J. W. (1993) *Biochemistry* **32**, 14102-14110

150. Ollagnier-de Choudens, S., Sanakis, Y., Hewitson, K. S., Roach, P., Baldwin, J. E., Munck, E., and Fontecave, M. (2000) *Biochemistry* **39**(14), 4165-4173

151. Rebeil, R., and Nicholson, L. W. (2001) *Proceedings of the National Academy of Sciences of the United States of America* **98**, 9038-9043

152. Liu, A., and Graslund, A. (2000) *Journal of Biological Chemistry* **275**(17), 12367-12373

153. Ugulava, N. B., Sacanell, C. J., and Jarrett, J. T. (2001) *Biochemistry* **40**(28), 8352-8.

154. Emptage, M. H., Dreyers, J., Kennedy, M. C., and Beinert, H. (1983) *Journal of Biological Chemistry* **258**, 11106-11111

155. Rabinowitz, J. (1971) *Methods in Enzymology* **24**, 431-446

156. Ollagnier, S., Meier, C., Mulliez, E., Gaillard, J., Schuenemann, V., Trautwein, A., Mattioli, T., Lutz, M., and Fontecave, M. (1999) *Journal of the American Chemical Society* **121**(27), 6344-6350

157. Ziegert, T. (2003) *Ph.D thesis*, University of Southampton, Southampton

158. Taylor, S. V., Vu, L. D., Begley, T. P., Schorken, U., Grolle, S., Sprenger, G. A., Bringer-Meyer, S., and Sahm, H. (1998) *Journal of Organic Chemistry* **63**(7), 2375-2377

159. Hecht, S., Kis, K., Eisenreich, W., Amslinger, S., Wungsintaweekul, J., Herz, S., Rohdich, F., and Bacher, A. (2001) *Journal of Organic Chemistry* **66**, 3948-3952

160. Andersag, H., and Westphal, K. (1937) *Chemische Berichte* **70**, 2035-2044

161. Leder, I. G. (1970) *Methods in Enzymology* **18**, 166-7

162. Kawasaki, T., and Nose, Y. (1969) *The Journal of Biochemistry* **65**, 417-425

163. Moyed, H. S. (1964) *Journal of Bacteriology* **88**, 1024-1029

164. Nierlich, D. P., and Magasanik, B. (1971) *Biochimica et Biophysica Acta* **230**, 349-361

165. Levine, R. A., and Taylor, M. W. (1982) *Journal of Bacteriology* **149**, 1041-1049

166. Downs, D. M. (1992) *Journal of Bacteriology* **174**(5), 1515-1521

167. Downs, D. M., and Petersen, L. (1994) *Journal of Bacteriology* **176**(16), 4858-4864

168. Petersen, L., Enos-Berlage, J., and Downs, D. M. (1996) *Genetics* **143**(1), 37-44

169. Enos-Berlage, J. L., and Downs, D. M. (1999) *Journal of Bacteriology* **181**(3), 841-848

170. Hoffmeyer, J., and Neuhard, J. (1971) *Journal of Bacteriology* **106**, 14-24

171. Manse, R. J., and Koch, A. L. (1960) *Journal of Biological Chemistry* **235**, 450-456

172. Houlberg, U., and Jensen, K. F. (1983) *Journal of Bacteriology* **153**, 837-845

173. Rolfes, R. J., and Zalkin, H. (1988) *Journal of Biological Chemistry* **263**, 19653-19661

174. Gerrits, J., Eindhoven, H., Brunnekreeft, J. W. I., and Hessels, J. (1997) *Methods in Enzymology* **279**, 74-82

175. Therisod, M., Gaudry, D., and Estramareix, B. (1977) *Nouveau Journal de Chimie* **2**, 119-121

176. Fuchs, G., and Kroger, A. (1999) in *Biology of the Prokaryotes* (Lengeler, J. W., Drews, G., and Schlegel, H. G., eds), pp. 100, Blackwell Science, Stuttgart

177. Guzman, L. M., Belin, D., Carson, M. J., and Beckwith, J. (1995) *Journal of Bacteriology* **177**(14), 4121-4130

178. Davis, B. D., and Mingoli, E. S. (1950) *Journal of Bacteriology* **60**, 17-27

179. Flint, D. H. (1996) *Journal of Biological Chemistry* **271**(27), 16068-16074

180. Begley, T. P., Xi, J., Kinsland, C., Taylor, S., and McLafferty, F. (1999) *Current Opinion in Chemical Biology* **3**(5), 623-629

181. Baxter, R. L., Hanley, A. B., and Chan, H. W. S. (1990) *Journal of the Chemical Society Perkin Transactions 1*, 2963-2966

182. Fujiwara, M., and Matsui, K. (1948) *Analytical Chemistry* **25**, 811

183. Skovran, E., and Downs, D. M. (2003) *Journal of Bacteriology* **185**(1), 98-106

184. Padovani, D., Thomas, F., Trautwein, A. X., Mulliez, E., and Fontecave, M. (2001) *Biochemistry* **40**(23), 6713-6719

185. Taylor, J. C., and Markham, G. D. (1999) *Journal of Biological Chemistry* **274**, 32909-32914

186. Cosper, M. M., Cosper, N. J., Hong, W., Shokes, J. E., Broderick, W. E., Broderick, J. B., Johnson, M. K., and Scott, R. A. (2003) *Protein Science* **12**(7), 1573-1577

187. Layer, G., Moser, J., Heinz, D. W., Jahn, D., and Schubert, W. D. (2003) *EMBO Journal* **22**, 6214-24

188. Sambrook, J., Fritsch, E. F., and Maniatis, T. (1989) *Molecular Cloning: A Laboratory Manual*, 2nd Ed., Cold Spring Harbor Laboratory Press, Cold Spring Harbor, NY

189. Laemmli, U. K. (1970) *Nature* **227**, 680-685

190. Bradford, M. M. (1976) *Analytical Biochemistry* **72**, 248-54
191. Feurle, J., Jomaa, H., Wilhelm, M., Gutsche, B., and Herderich, M. (1998) *Journal of Chromatography A* **803**(1-2), 111-119